

An unexpected new red-bellied *Stumpffia* (Microhylidae) from forest fragments in central Madagascar highlights remaining cryptic diversity

Katherine E. Mullin¹, Manoa G. Rakotomanga², Jeff Dawson³, Frank Glaw⁴,
Andolalao Rakotoarison^{5,6}, Pablo Orozco-terWengel¹, Mark D. Scherz⁷

1 Cardiff University, School of Biosciences, Sir Martin Evans Building, Museum Avenue, Cardiff, CF10 3AX, UK **2** Conservation Action Plan for Madagascar ('C.A.P. Mada'), Antananarivo, Madagascar **3** Durrell Wildlife Conservation Trust, Les Augrès Manor, La Profonde Rue, Trinity, Jersey, JE3 5BP, Channel Islands, UK **4** Zoologische Staatssammlung München (ZSM-SNSB), Münchhausenstr. 21, 81247 München, Germany **5** Department of Animal Biology, University of Antananarivo, Madagascar **6** School for International Training, VN 41A Bis Ambohitsoa Ankazolava, 101 Antananarivo, Madagascar **7** Natural History Museum of Denmark, University of Copenhagen, Universitetsparken 15, 2100, Copenhagen Ø, Denmark

Corresponding authors: Pablo Orozco-terWengel (orozco-terwengelpa@cardiff.ac.uk),
Katherine E. Mullin (mullink@cardiff.ac.uk)

Academic editor: Angelica Crottini | Received 17 February 2022 | Accepted 5 May 2022 | Published 6 June 2022

<https://zoobank.org/66A42A6D-DE56-4C17-9D18-3DE0EDE489C0>

Citation: Mullin KE, Rakotomanga MG, Dawson J, Glaw F, Rakotoarison A, Orozco-terWengel P, Scherz MD (2022) An unexpected new red-bellied *Stumpffia* (Microhylidae) from forest fragments in central Madagascar highlights remaining cryptic diversity. ZooKeys 1104: 1–28. <https://doi.org/10.3897/zookeys.1104.82396>

Abstract

The Madagascan endemic subfamily Cophylinae in the family Microhylidae, is an example of a taxonomic group for which much is still to be discovered. Indeed, the cophyline frogs present a large portion of Madagascar's cryptic and microendemic amphibian diversity, yet they remain understudied. A new red-bellied species of the microhylid frog genus *Stumpffia* is described from the central plateau of Madagascar. Visual encounter surveys in Ambohitantely and Anjozorobe in 2019 and 2020 identified this previously unknown *Stumpffia* species, which closely resembles *Stumpffia kibomena* known from Andasibe in the east. *Stumpffia lynnae* **sp. nov.** adds another species to the red-bellied species complex, differing from *S. kibomena* by genetic differentiation in the mitochondrial 16S rRNA gene (3.6–3.9%) and distinct nuclear RAG1 haplotypes, as well as strongly by its advertisement call. The new species is known from across Ambohitantely Special Reserve and Anjozorobe Angavo protected area, but is known only from one complete specimen and eight individual tissue samples. Based on the rarity of the species, the small number of locations in which it has been found, and its disappearing forest habitat, its IUCN Red List

classification is suggested as “Endangered”. This species is the first *Stumpffia* described from Madagascar’s central plateau, highlighting the importance of conserving the remnant forest fragments in this area and the ongoing need to survey and protect this threatened habitat type.

Keywords

Amphibian, cophyline, DNA barcoding, phylogeny, taxonomy

Introduction

Madagascar is one of the world’s top biodiversity hotspots for conservation priority (Myers et al. 2000) and is home to a predicted 500+ species of endemic amphibians (Perl et al. 2014), although only 375 have been described so far (Frost 2022). Despite intensive studies in the last 30 years, there are still significant gaps in the taxonomic inventory of anurans (Vieites et al. 2009). Meanwhile, much of the island’s forest is now reduced to remnant forest fragments with data from 2014 showing that 46% of Madagascar’s forest is within 100 m of a forest edge (Vieilledent et al. 2018). The loss and fragmentation of this key amphibian habitat puts its endemic species at risk of extinction, making full inventories necessary to understand the island’s extant biodiversity, and to guide conservation efforts of these environments.

The three Madagascan endemic subfamilies of Microhylidae Günther, 1858; Dycophinae Boulenger, 1882, Scaphiophryninae Laurent, 1946, and Cophylinae Cope, 1889; are examples of taxonomic groups for which much is still to be discovered. Indeed, the cophyline frogs present a large proportion of Madagascar’s cryptic and microendemic amphibian diversity (Rakotoarison et al. 2017); however they are understudied. The subfamily Cophylinae is a morphologically diverse group comprising arboreal, terrestrial, fossorial, and rupicolous species (Glaw et al. 2007). Within this subfamily, *Stumpffia* Boettger, 1881 are the most diverse of the eight recognized genera, with currently 44 recognised species (Frost 2022) and several species still to be described (Rakotoarison et al. 2017).

Stumpffia contains most of the smallest cophyline frogs (Rakotoarison et al. 2017), some of which are among the smallest vertebrates in the world, with adults generally having a snout–vent length (SVL) under 20 mm and some species reaching only 9 mm SVL (Glaw and Vences 2007; Klages et al. 2013; Rakotoarison et al. 2017). The genus is found across much of the humid parts of the island, but most species are found in northern Madagascar. Several species of *Stumpffia* are micro-endemic (Wollenberg et al. 2008; Köhler et al. 2010) with many species restricted to very small ranges, sometimes restricted to single mountaintops (Rakotoarison et al. 2017).

Prior to surveys in 2018 no *Stumpffia* species were known from Madagascar’s central plateau (Ambohitantely Special Reserve and surrounding forest fragments). *Anilany helenae* Vallan, 2000 from Ambohitantely Special Reserve was originally described as *Stumpffia helenae* (Vallan, 2000a), before a comprehensive revision of the Cophylinae determined this species to be in its own genus (Scherz et al. 2016), leaving the central plateau again without any *Stumpffia*.

Visual encounter surveys in late 2018 (Razafindraibe et al. 2021), early 2019, and 2020, however, discovered a *Stumpffia* species of uncertain affinities that had a bright red belly. According to general morphological similarities to *Stumpffia kibomena* Glaw et al. 2015, this species was called *Stumpffia* cf. *kibomena* by Razafindraibe et al. (2021). During the same surveys in 2020 an apparently similar *Stumpffia* was also recorded 70 km east of Ambohitantely in the Anjozorobe-Angavo protected area, an area containing more continuous forest than Ambohitantely, and which was until relatively recently connected to Madagascar's eastern rainforest block. The only other *Stumpffia* record for this site was *Stumpffia roseifemoralis* Guibé, 1973 which was found in a 2007 inventory (Wilme et al. 2007) and was reported as scarce, found in just one of seven surveyed locations. In a more recent review inventory, this one *Stumpffia* species record was listed as *Stumpffia* sp., not *S. roseifemoralis* (Goodman et al. 2018). The identification of this species originally as *S. roseifemoralis* was probably based on the red colouration of its legs, but its identity as *S. roseifemoralis* can be ruled out because this species has been shown to be restricted to north-eastern Madagascar (Rakotoarison et al. 2017) and is morphologically different to the individuals found in the 2020 surveys.

Bright red colour on the venter is an interesting feature that has recently been highlighted as occurring in several different clades of frogs in Madagascar (Glaw et al. 2020). In *Stumpffia*, several species are known to have red or reddish colouration over their posterior abdomen and ventral surfaces of legs: *Stumpffia be* Köhler et al., 2010, *S. kibomena*, *S. meikeae* Rakotoarison et al., 2017, *S. miovaova* Rakotoarison et al., 2017, *S. nigrorubra* Rakotoarison et al., 2017 and *S. roseifemoralis* (Rakotoarison et al. 2017). These species belong to several different clades, and such colouration must have evolved independently in this genus, and assignment to any one species, or even clade, solely based on the red colour is not possible.

Geographically, the nearest occurring species of *Stumpffia* with a red belly is *S. kibomena*, described by Glaw et al. (2015) from the Andasibe region in central-eastern Madagascar. It is known from two areas in the Andasibe vicinity, but is rarely seen and few specimens are available, leading to the assumption that this species has a secretive lifestyle, is seasonal, or is indeed rare and restricted to a small range. *Stumpffia kibomena* belongs to a diverse clade of frogs of moderately large body size (14.4–23.7 mm), called Clade C2 by Rakotoarison et al. (2017), which includes several lineages with red bellies (*S. miovaova* and *S. kibomena*, and several deep lineages considered conspecific with *S. kibomena* by Rakotoarison et al., (2017)), but others with no remarkable ventral colour (*Stumpffia achillei* Rakotoarison et al., 2017, *S. analanjirofo* Rakotoarison et al., 2017, *S. fusca* Rakotoarison et al., 2017) and one species with stark white and black ventral colouration (*S. grandis* Guibé, 1973). These species are all distributed in rainforests of eastern and northeastern Madagascar.

Here, we provide new data on the red-bellied *Stumpffia* species that has been found in both Ambohitantely and Anjozorobe. We find that it is morphologically and genetically most similar to *Stumpffia kibomena*, but that it differs substantially from that species genetically and especially in the male advertisement call. We therefore describe it as a new species, which represents the first species of the genus in the central highlands of Madagascar.

Materials and methods

Specimen collection and morphological measurement

Visual encounter surveys (**VES**) were conducted during the day and evening throughout March – May 2019 and January – March 2020 in some of the last remaining forest blocks in Madagascar's central highlands. Locations included six forest fragments in Ambohitantely Special Reserve (18.1960°S, 47.2865°E, elevation ~ 1600 m a.s.l.), the two forest fragments in Ankafoibe protected area (18.1089°S, 47.1932°E, elevation 1475 m a.s.l.), forest at Anjozorobe (18.4095°S, 47.9447°E, elevation ~ 1350 m a.s.l.), and at Andasibe Mitsinjo (18.9335°S, 48.4129°E, elevation ~ 900 m a.s.l.) (Fig. 1). VES were conducted along 200 m transects to allow sampling across the different microhabitats and biotypes present in the forest fragments, and quadrat samplings (4 m²) were also conducted randomly along the transects to target leaf litter species (Bell et al. 2006). Our survey methods followed the 'intermediate intensity' of VES, returning all objects to their original position and not destroying any habitat features, reducing impact on the environment (Crump and Scott 1994).

DNA was sampled from each individual using the less invasive buccal swab sampling technique, following the method of Pidancier et al. (2003). Fine tip rayon swabs (Medical Wire & Equipment Co. #MW113) were used, and stored in 0.5–0.75 mL of Longmire Lysis buffer (Longmire et al. 1997). When individuals were too small to buccal swab, skin swabs were taken instead. Field numbers used were **KAMU**, **KAMUS**, referring to the collections of Katherine Mullin, specimen and swabs respectively. Institutional acronyms are as follows: **ZFMK**, Zoologische Forschungsmuseum Alexander Koenig, Bonn; **NMBE**, Naturhistorisches Museum Bern; and **ZSM**, Zoologische Staatssammlung München. The snout–vent length (SVL) measurement was taken of all individuals in situ, and all individuals were photographed in life. One specimen from Ambohitantely (field number KAMU2) was collected on 21 January 2020. It was euthanised using Benzocaine, fixed in 100% ethanol, and stored in 70% ethanol for long-term preservation. Tissue was removed from the right thigh and stored in 100% ethanol. The specimen was deposited in the ZSM. The following measurements of the preserved specimen were taken by KM using precision callipers, as in Rakotoarison et al. (2017): snout–vent length (**SVL**), maximum head width (**HW**), head length (**HL**), horizontal tympanum diameter (**TD**), horizontal eye diameter (**ED**), eye–nostril distance (**END**), nostril–snout tip distance (**NSD**), nostril–nostril distance (**NND**), forelimb length (**FORL**), hand length (**HAL**), hindlimb length (**HIL**), foot length including tarsus (**FOTL**), foot length (**FOL**), tibia length (**TIBL**), and tibio-tarsal articulation (**RHL**).

Molecular datasets

DNA was extracted from the buccal swabs and storage lysis buffer using the Qiagen DNeasy kits following manufacturer's protocol. We assembled phylogenies based on two mitochondrial gene fragments to assess the phylogenetic relationship between the

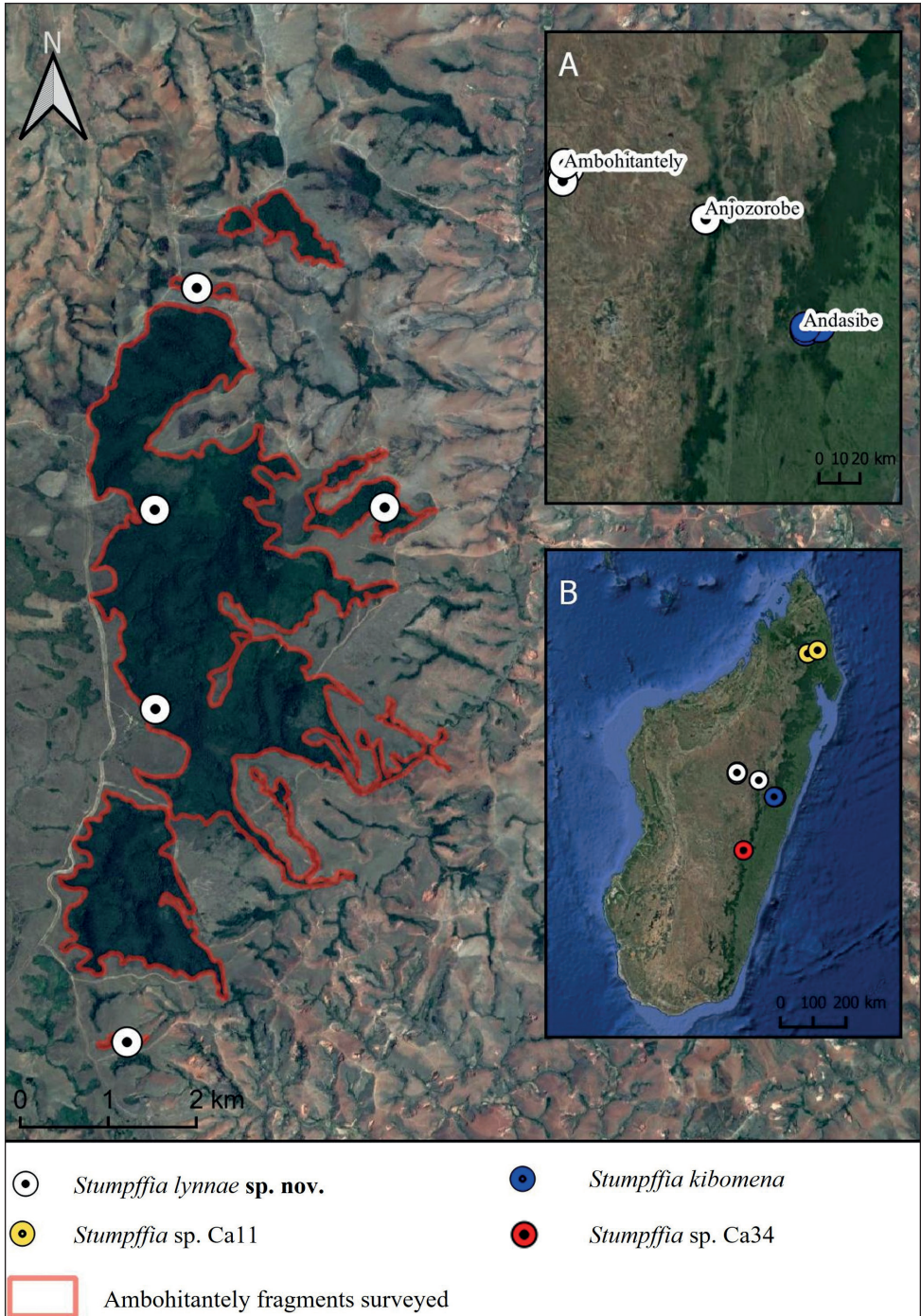


Figure 1. Map of Ambohitantely Special Reserve showing known *Stumpffia lymnae* sp. nov. distribution. **A** Ambohitantely, Anjozorobe, and Andasibe relative to one another **B** map of Madagascar showing the wider distribution of *Stumpffia lymnae* sp. nov. and its sister species *Stumpffia kibomena*, *Stumpffia* sp. Ca11 and *Stumpffia* sp. Ca34. Satellite imagery Google Earth (2015).

newly collected material and other *Stumpffia* species, and built a haplotype network using one nuclear gene.

The 5' fragment of 16S rRNA (~ 630 base pairs) was amplified using the 16SL3 and 16SAH primers as in Vences et al. (2003). A 12.5 µl PCR reaction volume was used including 2 µl of DNA (concentration not quantified), 1 µl of 5 × Green GoTaq Flexi reaction buffer (Promega), 1.5 µl of MgCl₂ (25 mM), 0.6 µl of deoxynucleotides (dNTPs 10mM/each), 0.3 µl of each primer (10pmol), 0.06 µl of 5U/µl GoTaq G2 Flexi DNA Polymerase (Promega), and molecular biology-grade deionised H₂O. PCR thermo-cycling conditions were as follows: denaturation for 90 s at 94 °C, followed by 33 cycles of denaturation at 94 °C for 45 s, primer annealing at 55 °C for 45 s and PCR product extension at 72 °C for 90 s, finishing with an elongation step of 72 °C for 10 min. This region is not the usual 16S rRNA region used for barcoding frogs in Madagascar, but has previously been used to assess mitochondrial differentiation in *Stumpffia* (Rakotoarison et al. 2017), enabling comparisons to be made. PCR products were sequenced at Eurofins Genomics and the sequences viewed and edited in Geneious Prime. Published sequences of 27 other *Stumpffia* species were downloaded from GenBank and aligned with our new sequences using the MUSCLE alignment algorithm in MEGAX (Kumar et al. 2018). These species included representatives from all major clades of *Stumpffia* (12 in Clade A, one in Clade B, four in Clade C1, and ten in Clade C2). Model testing was also conducted in MEGAX and the most suitable DNA evolution model was selected with the AIC criterion. A Maximum Likelihood phylogeny was constructed, also in MEGAX, using the GTR+G model, using all sites, and Subtree-Pruning and Regrafting (SPR) Level 5 that carries out an extensive search of the tree space. Uncorrected pairwise distances (p-distance) were calculated between the species used in the phylogeny using the TaxI2 tool in the iTaxoTools toolkit (Vences et al. 2021), which is based on the original TaxI (Steinke et al. 2005).

The recombination-activating gene 1 (**RAG1**) was used as a nuclear marker as it is known to show distinct haplotypes for closely related *Stumpffia* species (Klages et al. 2013; Rakotoarison et al. 2017). These sequences were analysed separately from the mitochondrial DNA in order to obtain further support of their status as a distinct species, as it provides evidence for genetic differentiation of lineages from an unlinked locus (Vences et al. 2018). The primers CophF1 and CophF2 were used to amplify a region of RAG1 (~ 503 bp), using the same reaction volume and concentrations as above, and with PCR thermo-cycling conditions of 120 s of denaturation at 94 °C, followed by 35 cycles of denaturation at 94 °C for 20 s, primer annealing at 53 °C for 50 s and PCR product extension at 72 °C for 180 s, finishing with a final PCR product elongation step of 72 °C for 10 min, as in Rakotoarison et al. (2019). PCR products were sequenced in both directions to enable the reliable identification of heterozygote sites. Sequences were checked and heterozygote positions inferred in Geneious Prime. The novel sequences were aligned with those of closely related species in Clade C2 of Rakotoarison et al. (2017) monograph using MUSCLE, ensuring all sequences were on the same reading frame. Sequences were not available for *Stumpffia* sp. Ca11 and *S. betampona* Rakotoarison et al. 2017. The final alignment, and that used for the haplotype network, was 338 bp in length due to the length of the sequences available for comparison.

Haplotypes were phased in DNAsp (Rozas et al. 2017) using the PHASE algorithm (Stephens, et al. 2001). A Neighbour-Joining tree based on uncorrected pairwise differences was constructed in MEGAX and visualised as a haplotype network using Haploviewer (<http://www.cibiv.at/~greg/haploviewer>).

A fragment of mitochondrial Cytochrome Oxidase 1 (COI) was also amplified and sequenced, however given there is limited reference material from closely related species (1 sequence from *Stumpffia* sp. Ca34 and none from *Stumpffia* sp. Ca11 or *S. kibomena*), it was not analysed in detail here. The primers Chmf4 and Chmr4 were used to amplify a region of ~ 658 bp, using the same reaction volume and concentrations as above, and with PCR thermo-cycling conditions as in Che et al. (2012) with the exception of a higher annealing temperature at 58 °C. To add support of the placement of this putative new species in the *Stumpffia* phylogeny a Maximum Likelihood phylogeny was constructed using the HKY+G+I model with 1000 bootstrap replicates. The same *Stumpffia* species as those in the 16S tree were used, but fewer species have COI sequences available, and hence the dataset is smaller.

Where possible the sequences of the same individual within each species were used throughout the 16S, RAG1 and COI analysis for consistency. All newly obtained sequences were deposited into GenBank (accession numbers are provided in Suppl. material 3: Table S1). To contribute toward the growing reference barcoding database for Malagasy amphibians, we also amplified the 3' fragment of 16S rRNA using the 16SA-L and 16SB-H primers (Palumbi et al. 1991).

Bioacoustic analysis

One advertisement call recording was made of a male observed with an inflated vocal sac in Anjozorobe. The call recording was made using the application RecForge II on a Samsung Galaxy A5 smartphone using its internal microphone, the file was saved as a .wav sound file. This male was swabbed, and DNA sequenced. Air temperature at the time of the call was recorded with a Kestrel 2500 weather meter. Call analysis was conducted in Audacity v. 2.3.3, following a call-centred approach, defining a call as the main coherent sound unit, separated from other such units by a distinct period of silence, with multiple calls strung together into a call series (Köhler et al. 2017). Temporal call parameters are given in milliseconds (**ms**) and the number of calls analysed (***n***) in parentheses. Recordings were re-sampled at 44.1 kHz and 32-bit resolution for analysis. The call file contained at least two individuals calling, but only the target specimen (the loudest calls) was included in our analysis. We silenced the inter-call intervals between the eight calls, amplified the calls by 10 decibels, and carried out one round of noise reduction. Spectrograms were obtained with a Hanning window function at 1024 bands FFT resolution. The frequency analysis tool in Audacity was used to check for the most dominant energy peak, and this was repeated for each call in the call series. This analysis was also conducted with a Hanning window function at 1024 bands. We also measured the *Stumpffia kibomena* calls from Vences et al. (2006) (CD 3, track 52) to ensure the calls were measured in the same way. The original call measurements from the *S. kibomena* species description (Glaw et al. 2015) were also collated for comparison.

Results

Throughout 880-person survey hours during both day and evening surveys, only eight individuals of the putative new *Stumpffia* species were observed, six from Ambohitantely and two from Anjozorobe (Table 1). Morphologically they strongly resemble *S. kibomena* and two candidate species; *Stumpffia* sp. Ca11 from Marojejy and Ambolokopatrika in north-eastern Madagascar, and *Stumpffia* sp. Ca34 from Ranomafana National Park.

Molecular species delimitation

Maximum Likelihood analysis of the 5' fragment of the mitochondrial 16S rRNA gene of the species included in the analysis yielded a phylogeny which reflected that seen in the comprehensive integrative taxonomy conducted by Rakotoarison et al. (2017) (Fig. 2). The new specimens from Anjozorobe and Ambohitantely formed a well-supported clade (97% bootstrap; Fig. 2), divided into two subclades by locality also well supported statistically (98% Ambohitantely clade and 99% Anjozorobe clade). As predicted based on their morphology, the putative new species seems to share a common ancestor with *Stumpffia* sp. Ca11 and *S. kibomena*, although support for the clade including these three species was low (51%).

Uncorrected pairwise distances (p-distances) estimated for the 16S sequences between specimens from Anjozorobe and Ambohitantely was 1.3%, while the within groups distances were 0.0% and 0.12%, respectively. The mean p-distance between the Ambohitantely individuals and the *S. kibomena* sequences was 3.9%, and between the Anjozorobe individuals and *S. kibomena* sequences was 3.6% (Suppl. material 4: Table S2). This exceeds the threshold of 3% used to consider a candidate species in Neotropical and Malagasy frogs (Fouquet et al. 2007; Vieites et al. 2009). Similar levels of divergence were found between *Stumpffia* sp. Ca11 and the putative new species; *Stumpffia* sp. Ca11 is 4.2% divergent with respect to the Anjozorobe samples, 4.6% with respect to the Ambohitantely sequences, and 4.5% from *S. kibomena*. Meanwhile *Stumpffia* sp. Ca34 had larger p-distances, being 7.0–7.2% divergent from the putative new species (no difference between Ambohitantely and Anjozorobe individuals), 6.0% from *S. kibomena*, and 7.2–8.0% from *Stumpffia* sp. Ca11. There are currently a lack of specimens and knowledge available for the descriptions of *Stumpffia* sp. Ca11 and *Stumpffia* sp. Ca34 (Rakotoarison et al. 2019).

Within the 16S alignment there are five differences that are unique to the putative new species (Suppl. material 2: Fig. S2). These include (1) one position where all eight specimens have a C while all other *Stumpffia* in the alignment have a T (position 480 in the alignment), and (2) another position where all eight specimens have a T and all other included species have a C with the exception of *S. betampona* which has an A (position 545). The other three differences vary between the specimens from Ambohitantely and those from Anjozorobe; (3) one position, which is a T in the six

Table 1. Details of all *Stumpffia lynnae* sp. nov. samples from Ambohitantely (Amb) and Anjozorobe (Anj). ND: Not Determined.

Sample ID	Date	Location	Time	Coordinates	Elevation (m)	Forest type	Distance from water (m)	Substrate	Sex	SVL (mm)	Call	COI	5' 16S rRNA	RAG1
KAMUS60	13/04/19	Amb	10:15	S18.1969, E47.2842	1586	Slope	10	Leaf litter	Juvenile	8.3	–	X	X	X
KAMUS74	16/04/19	Amb	19:29	S18.1753, E47.3088	1408	Riparian	1	Leaf litter	ND	15.5	–	X	X	–
KAMUS167	12/05/19	Amb	11:10	S18.2328, E47.2811	1522	Slope	5	Soil under large rock	ND	19.8	–	X	X	X
KAMUS200	16/05/19	Amb	08:50	S18.1517, E47.2886	1532	Slope	5	Leaf litter	ND	11.3	–	X	X	X
ZSM 1/2022 holotype	24/01/20	Amb	09:00	S18.1517, E47.2886	1540	Riparian	5	Leaf litter under pandans	ND	20.9	–	X	X	X
KAMUS256	24/01/20	Amb	09:53	S18.1517, E47.2886	1528	Riparian	5	Leaf litter	ND	16.0	–	X	X	X
KAMUS370	15/02/20	Anj	19:00	S18.4116, E47.9501	1432	Slope	ND	Leaf litter	F – gravid	22.2	–	X	X	X
KAMUS371	15/02/20	Anj	19:00	S18.4116, E47.9501	1432	Slope	ND	Leaf litter	M – calling	20.1	X	X	X	X
Razafindraibe et al. (2021)	12/19	Amb	08:30-11:00	S18.1755, E47.2841	1560	ND	ND	Bamboo node	ND	–15-20	–	–	–	–

Ambohitantely specimens but is a C in all other species and the Anjozorobe specimens (position 141), (4) a two base pair deletion in the two individuals from Anjozorobe (CC or CT depending on the species they are compared to; positions 196–197), and (5) the insertion of an A in the six Ambohitantely individuals that is not present in any other species or the specimens of Anjozorobe (position 456).

The RAG-1 sequence (504 bp) was successfully obtained for seven out of the eight individuals from Ambohitantely and Anjozorobe. The sequences obtained show segregating genetic variation (five haplotypes) and one haplotype shared between Ambohitantely and Anjozorobe (Fig. 3). Neither of these localities shared haplotypes with individuals of *S. kibomena* or the other species, and they differed from them by at least three mutational steps.

The COI phylogeny mirrors that of the 16S marker, and also forms a well-supported clade of the putative new species (100% bootstrap), with the Anjozorobe individuals divided into a well-supported subclade (99%). The putative new species is sister to *Stumpffia* sp. Ca34 (81% support). The phylogeny can be seen in Suppl. material 1: Fig. S1.

In summary, there is concordant evidence from two mitochondrial markers and a nuclear DNA fragment to support the species-level genetic distinction of the specimens from Anjozorobe and Ambohitantely, not just from Clade C2 species but also from all 27 described species of *Stumpffia* included in the analysis, as well as from the nearest currently known candidate species, *Stumpffia* sp. Ca11 and *Stumpffia* sp. Ca34.

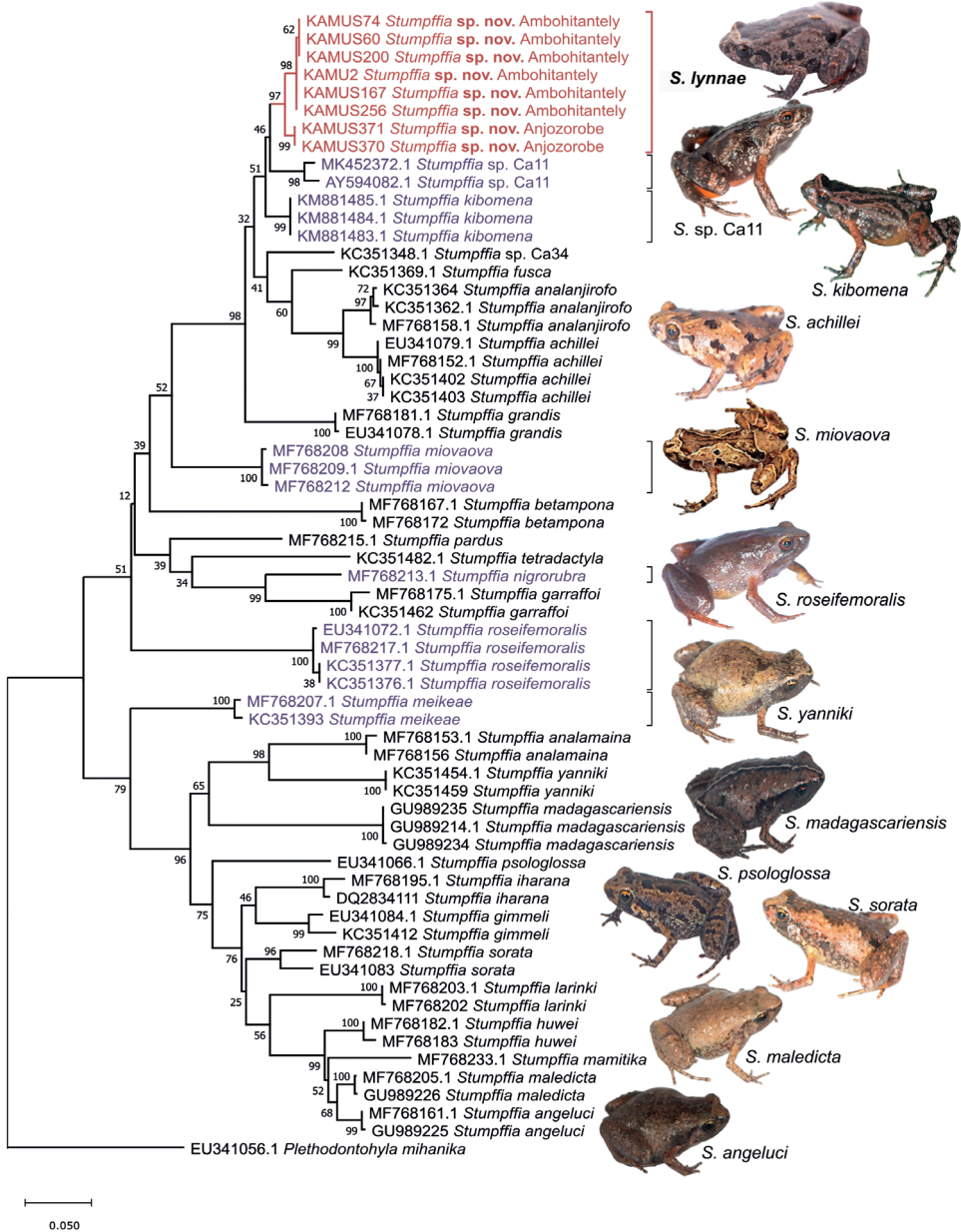


Figure 2. Maximum Likelihood tree of *Stumpffia* spp. based on analysis of a 621 bp fragment of the mitochondrial 16S rRNA gene. MUSCLE alignment, General Time Reversible model plus Gamma distribution, all sites used, × 1000 bootstraps, SPR level 5, no variant sites. Purple labels mark the other red-bellied *Stumpffia* species. Photographs Mark D. Scherz and Frank Glaw.

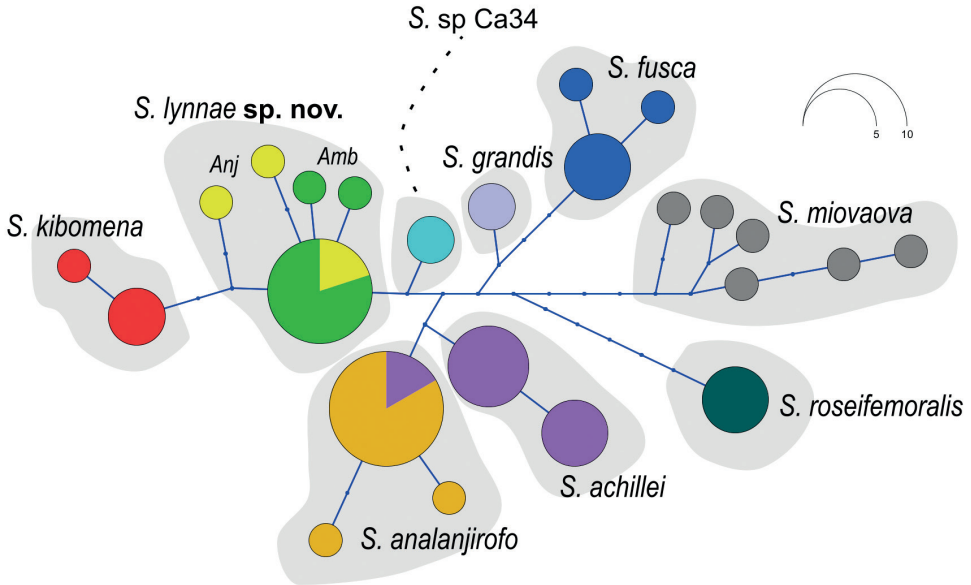


Figure 3. Haplotype network constructed from nuclear RAG-1 gene sequences (338 bp) of seven specimens of *Stumpffia lynnæ* sp. nov. (two from Anjozorobe (Anj; yellow) and five from Ambohitantely (Amb; green)) and eight other closely related *Stumpffia* species from Clade C2 (Rakotoarison et al. 2017). Small dots represent mutational steps.

Acoustic differentiation

The advertisement call of *S. kibomena* was described by Glaw et al. (2015). Here, we reanalysed an available call recording of that species and the calls of one specimen of the putative new species from Anjozorobe (Fig. 4, Table 2; no call voucher available). Distinct differences are recognizable between these calls. Note/call duration and dominant frequency are suitable variables for taxonomic inference (Köhler et al. 2017) and both of these call traits are drastically different from those of calls of *S. kibomena*, as is the duration of intervals between calls in the call series (Fig. 4, Table 2). Call duration (= note duration) was longer in the putative new species than in *S. kibomena* (163–184 ms vs. 68–82 ms ($n = 8$) based on our measurements of the *S. kibomena* calls), and the duration of intervals between calls was also much longer (3498–5581 ms vs. 742–766 ms in *S. kibomena* ($n = 7$)). The dominant frequency range was lower (2027–2044 Hz vs. 3858–3883 Hz in *S. kibomena*). These differences are such that the two calls can easily be distinguished by human ear, providing unambiguous support for the species-level distinction of these two taxa. Regrettably, no calls are available from *Stumpffia* sp. Ca11 or *Stumpffia* sp. Ca34.

Thus, in the following we provide a formal description of this new species, which is morphologically cryptic with respect to *S. kibomena* but genetically and bioacoustically distinct.

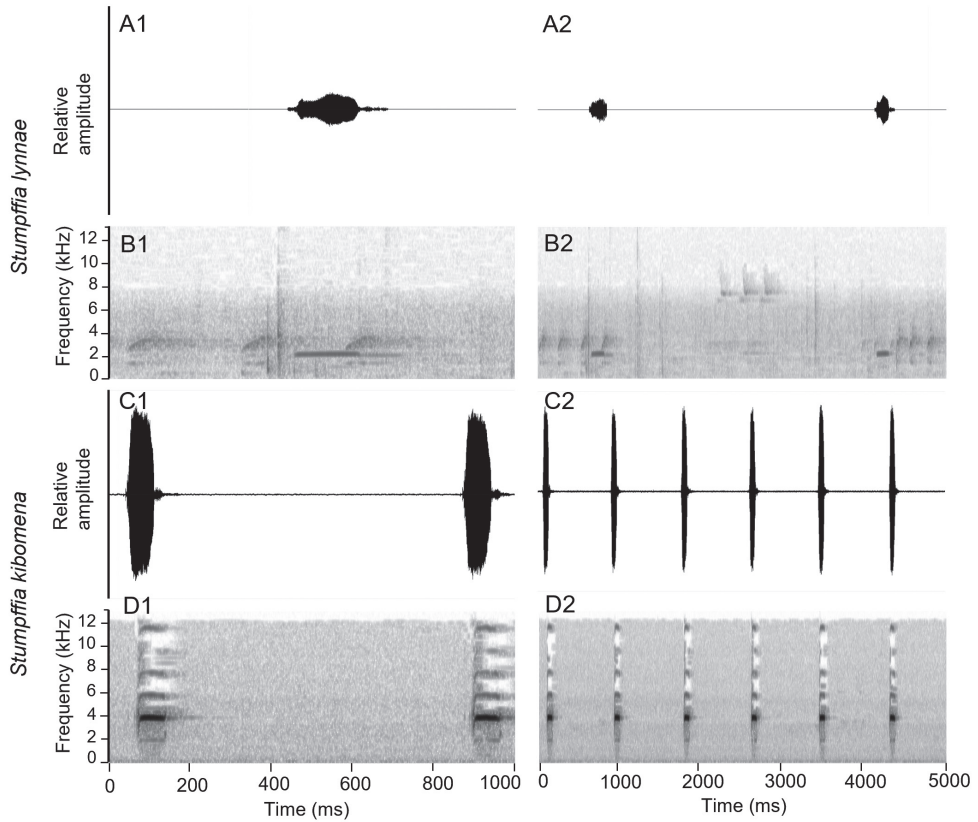


Figure 4. Male advertisement call of *S. lynnæ* sp. nov. **A** oscillogram **B** spectrogram. *S. kibomena* **C** oscillogram **D** spectrogram over a one-second interval (column 1) and a five-second time interval (column 2).

Table 2. Acoustic traits of *Stumpffia kibomena* in comparison to those of *S. lynnæ* sp. nov.

Species and source	Number of calls in series	Call – repetition rate (number calls/second)	Call duration (= note duration) (ms)	Duration of interval between calls (end-start) (ms)	Dominant frequency range (Hz)
<i>S. kibomena</i> (Glaw et al. 2015)	11–22 ($n = 5$)	1.2–1.3	70–76 (73 ± 2 , $n = 9$)	770–813 (797 ± 15 , $n = 9$)	3900–4300
<i>S. kibomena</i> (CD track measured by KM)	21	1.2	68–82 (74.3 , $n = 8$)	742–766 (757 , $n = 7$)	3858–3883
<i>Stumpffia lynnæ</i> sp. nov. (KM original recording)	8	0.25	163–184 (174 , $n = 8$)	3498–5581 (4357 , $n = 7$)	2027–2044

Stumpffia lynnæ sp. nov.

<http://zoobank.org/C5DD7133-3EC6-46D9-A895-48864C56EB61>

Holotype. ZSM 1/2022 (field number KAMU2), an unsexed adult, collected by K. Mullin, M. G. Rakotomanga, M. L. C. Razafiarimanana and T. Raditra, on 21 January 2020, in one of the northern fragments in Ambohitantely Special Reserve (18.1517°S, 47.2886°E, 1540 m a.s.l.), Analamanga Region, central Madagascar (Fig. 5).

Diagnosis. The new species is assigned to the genus *Stumpffia* based on its morphological and genetic affinities. Within the genus, it is distinguished by the unique combination of the following characters: (1) SVL 15.5–22.2 mm (adults in life), (2) limited digital reduction on the hands and feet such that first finger is reduced; other fingers not reduced and first toe is slightly reduced; other toes not reduced, (3) bright red to orange colouration confined to the ventral surfaces of the legs, posterior abdomen, and ventral arms, (4) absence of red markings on the lower jaw, and advertisement call with (5) inter-call intervals of 3498–5581 ms, (6) call/note duration 163–184 ms, (7) dominant frequency 2027–2044 Hz, and (8) distinct genetic divergence in the mitochondrial and nuclear genome to other known species.

Stumpffia lynnae sp. nov. can be distinguished from all other *Stumpffia* species except *S. be*, *S. kibomena*, *S. meikeae*, *S. miovaova*, *S. nigrorubra*, and *S. roseifemoralis* by the presence of bright red colouration on ventral surfaces of arms, legs, and abdomen. Among these species it can be distinguished from *S. be* by smaller body size (15.5–22.2 mm adults in life vs. 25.2 mm) and less expanded terminal discs on fingers and toes, as well as being in a different major clade of *Stumpffia* (Clade C rather than Clade A; Rakotoarison et al. 2017); from *S. meikeae* by the colour on the belly (bright red to orange vs. fainter more champagne to salmon colouration in *S. meikeae*), by less expanded terminal discs on fingers and toes, as well as being in a different major clade of *Stumpffia* (Clade C rather than Clade B; Rakotoarison et al. 2017); from *S. miovaova* by a larger maximum body size (22.2 vs. 18.2 mm) and colour on the belly (bright red vs. fiery orange); from *S. nigrorubra* by the dorsal colouration and patterns (dark brown dorsolateral bands and pale brown colouration in adult *S. lynnae* vs. darker mottled black and dark iridescent dorsal colouration in *S. miovaova*, and its phylogenetic placement in Clade C2 rather than Clade C1 (Rakotoarison et al. 2017); and finally from *S. roseifemoralis* by a larger maximum body size (22.2 vs. 18.4 mm), more vibrant ventral colouration, rougher dorsal skin in life, and less homogeneous dorsal colouration. Further, *S. lynnae* sp. nov. differs from all the above, other than *S. kibomena*, by the presence of dense blackish pigmentation on the throat, and different dorsal patterns.

Stumpffia lynnae sp. nov. is morphologically almost indistinguishable from *S. kibomena* (Table 3). However, an elongated red marking on each side of the lower jaw is absent from all observed specimens, but can be present in *S. kibomena* (Glaw et al. 2015), and the upper arms of *S. lynnae* are usually brown versus usually red in *S. kibomena*. Direct comparison of these features can be seen in Fig. 6, with additional ‘in life’ images of the *S. lynnae* individuals sampled and *S. kibomena* specimens in Figs 7, 8, respectively, for further comparison. The new species also strongly differs from *S. kibomena* in bioacoustics (see Table 2 and the comparison of the two species in the previous section). It differs specifically from *S. kibomena* by the following base pair differences in the analysed 5’ fragment of the 16S rRNA gene: position 385 T vs. C and 547 A vs. T. It further differs from *S. kibomena* and all other *Stumpffia* species in our alignment by the base pair differences as listed above: position 480 C vs. T; 545 T vs. C or A; 141 T (Ambohitantely specimens) vs. C; 196–197 CC/CT deletion (Anjozorobe specimens); and 456 A insertion (Ambohitantely specimens).

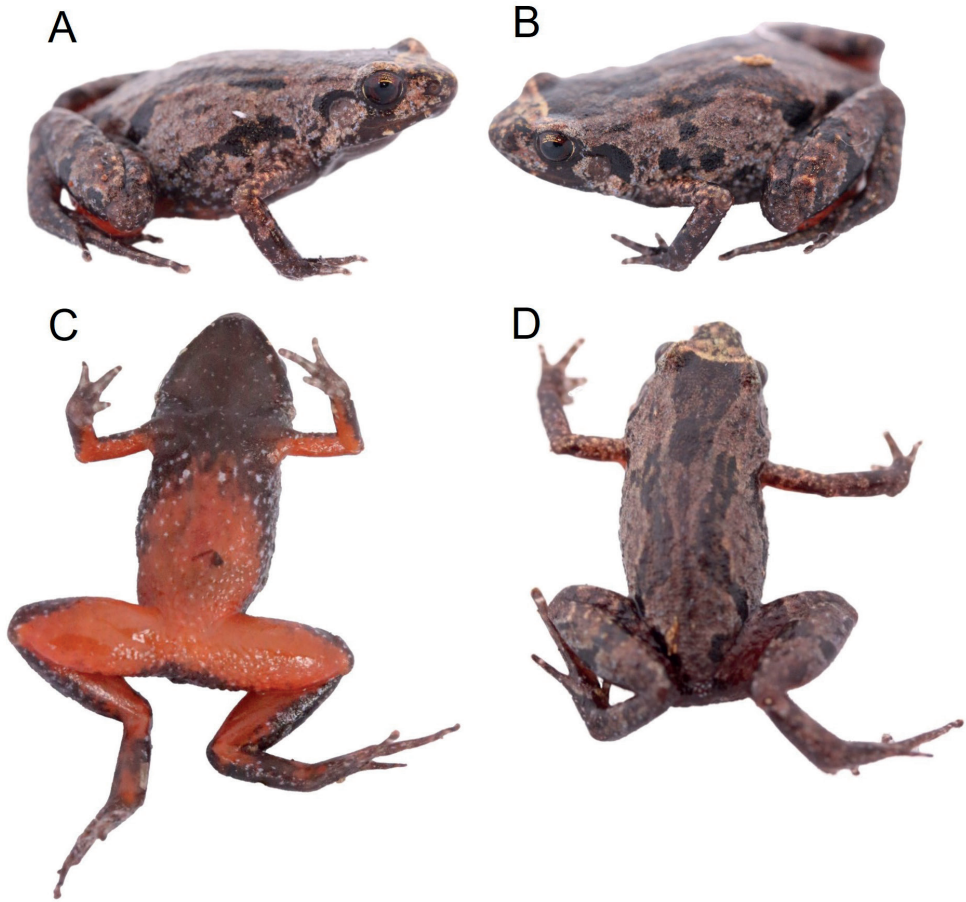


Figure 5. Images of the holotype ZSM 1/2022 (KAMU2) from Ambohitantly Special Reserve in life **A, B** dorsal lateral view **C** ventral view **D** dorsal view.

Table 3. Morphological data of *Stumpffia lynnae* sp. nov. and *Stumpffia kibomena* (data for latter species from Glaw et al. (2015), and the proportion of the SVL (/SVL).

Measurements (mm)	<i>S. lynnae</i> sp. nov. Holotype ZSM 1/2022	/SVL	<i>S. kibomena</i> holotype ZFMK 60007	/SVL	<i>S. kibomena</i> NMBE 1044940	/SVL	<i>S. kibomena</i> NMBE 1034211	/SVL
1 SVL	20.5		21.2		19.8		17.1	
2 HW	6.5	0.32	6.7	0.32	6.9	0.35	6.2	0.36
3 HL	5.0	0.24	5.1	0.24	4.9	0.25	4.3	0.25
4 TD	1.5	0.07	1.2	0.06	1.4	0.07	1.3	0.08
5 ED	2.0	0.10	1.9	0.09	1.6	0.08	1.6	0.09
6 END	1.5	0.07	1.9	0.09	1.7	0.09	1.3	0.08
7 NSD	0.5	0.02	1.1	0.05	0.8	0.04	0.8	0.05
8 NND	2.0	0.10	2.4	0.11	2.4	0.12	2.3	0.13
9 FORL	12.0	0.59	12.5	0.59	12.1	0.61	11.5	0.67
10 HAL	4.0	0.20	5.0	0.24	4.5	0.23	4.4	0.26
11 HIL	32.0	1.56	35.5	1.67	32	1.62	29.5	1.73
12 FOTL	14.5	0.71	15.3	0.72	14.7	0.74	14.8	0.87
13 FOL	8.5	0.41	10.0	0.47	8.9	0.45	9.2	0.54
14 TIBL	9.0	0.44	10.6	0.50	9.6	0.48	9.3	0.54
15 RHL	Eye		Eye		Eye		Eye	



Figure 6. Direct comparison between the holotype of *S. lynnae* ZSM 1/2022 (KAMU2) and a female *S. kibomena* specimen from An'ala (photo Frank Glaw). Boxes highlight the morphological differences highlighted; elongated red marking on each side of the lower jaw on *S. kibomena*, absent on the observed *S. lynnae*, and the red arms on *S. kibomena* compared to the brown arms on *S. lynnae*.

Holotype description. A specimen in a good state of preservation, except for skin loss where left thigh tissue muscle was removed for tissue sample. The body is elongated with the head wider than long, but not wider than the body. The snout is roughly rounded in both dorsal and lateral views. The nostrils are not protuberant and are closer to the tip of the snout than the eye. The tympanum is distinct and large (75% of eye diameter), and the supratympanic fold is indistinct. First finger short, others not reduced (Fig. 9). Inner metacarpal tubercle low, without a distinct prepollex, outer metacarpal tubercle indistinct and pale. Forelimbs are slender, the hand is without webbing, presents a relative finger length $1 < 2 < 4 < 3$ with the fourth finger slightly longer than the second; and fingertips are not expanded into discs. First finger reduced; other fingers not reduced. The hind limbs are slender and the tibiotarsal articulation reaches the eye when the hind limb is addressed along the body. There is no webbing between toes, and the relative toe length is $1 < 2 < 5 < 3 < 4$ with the fifth toe slightly shorter than the third. First toe slightly reduced; other toes not reduced. Inner metatarsal tubercle oblong and indistinct, and outer metatarsal tubercle absent, lateral metatarsalia connected. The dorsal skin was slightly bumpy in life, without distinct dorsolateral folds, and the ventral skin was granular on the abdomen but smooth on the throat. The tongue is long, broadening posteriorly, attached anteriorly, not notched. Maxillary teeth and vomerine odontophores are absent, and the choanae are large and oval shaped.

Measurements (in mm). Snout-vent length 20.5, maximum head width 6.5, head length from tip of snout to posterior edge of snout opening 5.0, horizontal tympanum diameter 1.5, horizontal eye diameter 2.0, distance between anterior edge of eye and nostril 1.5, distance between nostril and tip of snout 0.5, internarial distance 2.0, forelimb length (from limb insertion to tip of longest finger) 12.0, hand length, to the tip of the longest finger 4.0, hind limb length (from the cloaca to the tip of the longest toe) 32.0, tibia length 9.0, foot length including tarsus 14.5, foot length 8.5 (Table 3).

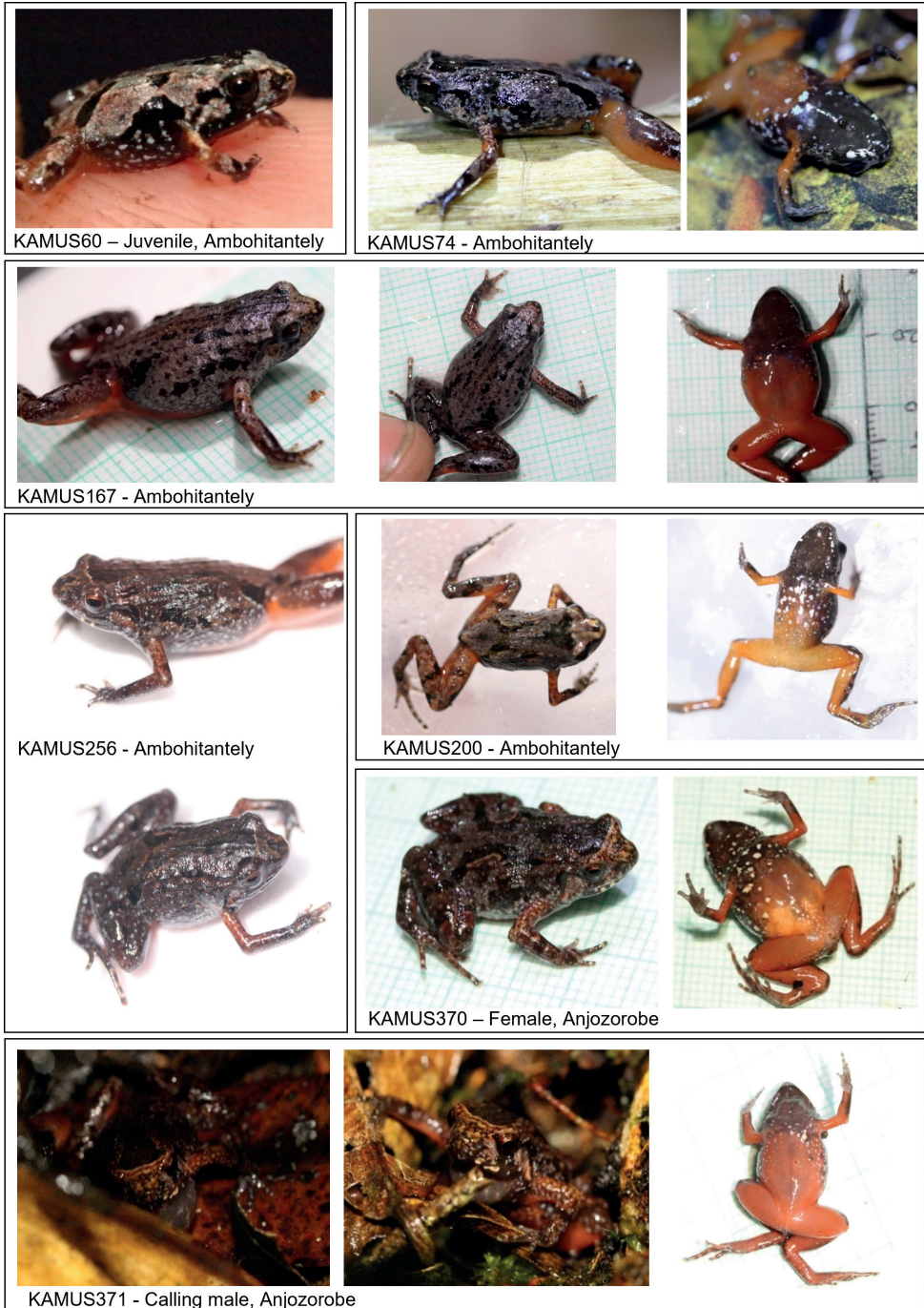


Figure 7. Images of the additional observed specimens of *Stumpffia lynnae* sp. nov. including the calling male (KAMUS371).



Figure 8. Images of *Stumpffia kibomena* (top row from the species description of Glaw et al. (2015) and the bottom row from inaturalist.org taken by Leonard Bolte and Jordan Broadhead, used with permission). Note the red marking on the lower lips and the red arms which differ from *S. lynnae* sp. nov.



Figure 9. Holotype hands and feet of *S. lynnae* (row **A**) and *S. kibomena* (row **B**). Not to scale.

In life the dorsum was pale brown, with dark brown markings (Fig. 5). These markings include a dark brown triangular marking between the eyes which extends posteriorly. A beige coloured band runs between the eyes at the base of the triangular marking. As in the *S. kibomena* holotype, two continuous narrow black bands extend posteriorly from level of the arms' insertion, converging towards the mid-dorsum and then diverging posteriorly without touching towards the inguinal region (referred herein as dorsolateral bands). The throat is black with few scattered white spots and these white spots continue as the ventral side becomes bright red. The pupil is black with a copper iris and golden colouration at the top. All four limbs are coloured red on the ventral sides. After two years in preservative, the red ventral colouration has faded.

Variation. Seven additional frogs were sampled for DNA and basic measurements were taken. Details of these frogs and their collection sites are shown in Table 1 and images in Fig. 7. There is some variation in colour/patterns with some individuals being greyer on the dorsal side (rather than brown) (KAMUS60 and KAMUS74), also with dark brown markings. The markings of the juvenile are black. The dorsolateral bands are not always present, for example KAMUS167 has speckled markings. This individual also did not have the beige band across the head between the eyes. The female from Anjozorobe (KAMUS370), KAMUS256 and KAMUS200 from Ambohitantely had pale brown markings outlining the dark brown dorsolateral bands. All specimens have the same ventral colouration and markings (black throat, red belly, and white spots), though the tone of the belly varies from orange, dark orange to red (KAMUS167; see Fig. 7).

Call description. The calls were recorded from a male (KAMUS371) at Anjozorobe during heavy rainfall on the 15th of February 2020, at 19:30, at an air temperature of 20.5 °C. The male was calling while sitting on the leaf litter on a slope in primary forest close to a female. The male was not collected as a specimen due to lack of permits to allow this, but swabs for DNA analysis were collected. The advertisement call of *S. lynnae* sp. nov. is structurally similar to that of other *Stumpffia* species in that it is a single melodious note that is repeated at regular intervals in call series. The call is simple, with the call composed of a slightly amplitude-modulated single tonal note, with multiple calls repeated in series at regular intervals. The calls are evenly spaced across the call series with silent intervals between calls. A definitive number of calls per call series cannot be determined given the sample size of one recording. Frequency is distributed across one band for each note, and frequency modulation is relatively equal across the note. No harmonics were seen in this call recording. The individual emitted eight calls, with a call-repetition rate of 0.25 calls per second. Call/note duration was 163–184 ms, and the duration of intervals between calls was 3498–5581 ms ($n = 7$). The dominant frequency range was 2027–2044 Hz (Table 2).

Etymology. This species name is a matronym honouring Lynne Mullin, to whom we are pleased to dedicate this attractively colourful species in recognition of the unconditional support she has provided to the first author. The origin of Lynn/e is from Celtic language, with the meaning waterfall, pond, and lake. Given the popular waterfall in the centre of Ambohitantely Special Reserve where this species was first found, this name seems appropriate. The name has further relevance to this beautiful red-bel-

lied frog with the Spanish meaning of the feminine name ‘pretty’. The species epithet is defined as a genitive noun with the ‘e’ removed for easier pronunciation.

Distribution. While just eight individuals were recorded, the six at Ambohitantely were distributed across four fragments (three in addition to the core forest block) including a very small (3.5 ha) fragment at the southern end of the reserve (Fig. 1). This suggests that they are widely distributed across the protected area. Surveys in the two forest fragments at Ankafobe did not detect the species, but this is not surprising given the size of the fragments and the reduced diversity at Ankafobe compared to Ambohitantely (Mullin et al. 2021). However, it cannot be ruled out that this species may exist in relict forest fragments in the area surrounding Ambohitantely Special Reserve, and between Ambohitantely and Anjozorobe. This species’ elevational range (1432–1586 m) is greater than *S. kibomena*’s range at Andasibe (900–950 m).

Natural history. The encounters of the nine frogs (including the one individual found by Razafindraibe et al. 2021) were during both morning and evening surveys from December to May, suggesting they are active throughout the day and the wet season. No surveys have been undertaken outside of this wet season window, so their activity during the dry season is unknown. The holotype was resting on top of the leaf litter under a *Pandanus* sp. screwpalm in riparian habitat at an elevation of 1540 m a.s.l. All eight frogs from this study were found in slope or riparian forest, between 1 and 10 metres from a water source. All individuals were found on the forest floor; seven were on leaf litter and one was found on bare soil under a large rock. The individual recorded by Razafindraibe et al. (2021) was found guarding eggs in a water filled bamboo node. This was the first record of a *Stumpffia* laying eggs in a bamboo hole but supports evidence that closely related *Stumpffia* may reproduce opportunistically in water-filled cavities close to the forest floor (Razafindraibe et al. 2021). The advertisement call was recorded during heavy rain in the evening during February. Combined with the eggs observed in December, this suggests that this species may be reproductively active throughout the wet season. Given the low number of individuals found across the high number of survey hours, we conclude that this species either has cryptic habitats, or is indeed rare.

Conservation. This species is known to occur in two locations with different conservation situations. Ambohitantely Special Reserve, currently managed by Madagascar National Parks is highly fragmented, and is threatened by cattle grazing, illegal logging and forest activities, forest burning for charcoal, and forest fires and fire suppression activities (Goodman, Raherilalao and Wohlauser 2018 pp 1338–1340). The number of forest fragments surrounding the Reserve boundary has substantially declined since 1996 (Vallan 2000b), as has the forest cover inside the reserve, having decline 6.3% from 1996–2016 (Goodman et al. 2018). Reforestation efforts within the Reserve have been blighted by fires (KM pers. obs.). Further, an invasive caterpillar is currently causing canopy leaf loss across the Reserve (S. Goodman pers. comms) which has been noted to dry out the leaf litter which could be devastating for amphibians (KM pers. obs.). Meanwhile, Anjozorobe is still connected to large expanses of continuous forest, and is managed by the local-led Association Fanamby; however, it is subject to similar threats and lost 33.2% of its forest between 1996 and 2016 (Goodman et al. 2018:

1362–1365). Stricter conservation actions and management are required at both sites. We can assume that the populations of *S. lynnae* are declining due to the ongoing habitat loss and severe fragmentation of the populations. Given the very low numbers of individuals found during surveys we assume this species is naturally rare.

Under the IUCN Red List criterion B (Geographic range), we believe this species should be listed as Endangered for both B1, extent of occurrence (EOO), and B2, area of occupancy (AOO) (IUCN 2012). Its EOO is $< 5,000 \text{ km}^2$ at 530 km^2 ; however, much of this area is inhospitable savannah grasslands and farmland between Ambohitantely and Anjozorobe. More relevant is its AOO, which is $< 500 \text{ km}^2$, estimated to be $\sim 100 \text{ km}^2$. The species fulfils two further criteria to be considered Endangered. B(a) ‘severely fragmented OR number of locations’ as it exists in severely fragmented locations/populations with no connectivity between the fragments at Ambohitantely, or between Ambohitantely and Anjozorobe. It was found in two locations across five forest fragments, one of which was just 3.5 hectares in size. Given that all the forest fragments it was found in are frequently burned and logged, they are predicted to reduce in size, with some disappearing in the near future. This degradation will influence all of the subcriteria within B(b) ‘continuing decline observed, estimated, inferred or projected in any of; (i) extent of occurrence; (ii) area of occupancy; (iii) area, extent and/or quality of habitat; (iv) number of locations or subpopulations; and (v) number of mature individuals.’ This suggested Red List status is in line with two microendemic amphibian species that are found at Ambohitantely, *Anilany helenae* and *Anodonthyla vallani*, which are both listed as Critically Endangered given they are found in just Ambohitantely Special Reserve (*A. vallani*) (IUCN 2020a) and Ambohitantely and surrounding isolated forest fragments (*A. helenae*) (IUCN 2016, 2020b; Mullin et al. 2021).

Discussion

Stumpffia lynnae is genetically and bioacoustically different to its close relative *S. kibomena*, to which it is morphologically very similar. This new species of *Stumpffia* brings the total number of known *Stumpffia* to 45, but given the similarity to *S. kibomena*, *Stumpffia* sp. Ca11, and *Stumpffia* sp. Ca34, also highlights the cryptic diversity that exists within the genus.

Razafindraibe et al. (2021) and this study were the first to report this species from Ambohitantely despite surveys by Vallan (2000b) and regular surveys by field courses led by the Association Vahatra. This highlights the cryptic diversity that remains to be found in Ambohitantely and the surrounding forest fragments in the central highlands, and the importance of this area in Madagascar for amphibian diversity. It affirms the importance of continuing to survey these areas to understand the diversity present, and the addition of another potentially Endangered species supports the need to protect these areas from ongoing deforestation and forest exploitation. This delayed finding following previous surveys suggests that this species is rare and/or cryptic and elusive.

Madagascar presents high levels of amphibian micro-endemism (Wollenberg et al. 2008; Vences et al. 2009, 2010; Brown et al. 2016) and this is notable in the genus

Stumpffia (Rakotoarison et al. 2017). There is no comprehensive hypothesis explaining why this occurs on the island across taxa, but the patterns have been explored on the basis of river catchments, bioregions, and previous climatic events causing forest contraction (Wilme et al. 2006). In terms of anurans, the correlation of body size and micro-endemism has been explored (Wollenberg et al. 2011), as has the influence of the bioclimatic zones (Brown et al. 2016). However, the relationship is still unclear given that many range to body size relationships are understudied with a lack of records and range maps. Ongoing surveys of understudied areas, such as those that facilitated our findings, will further help add to species range maps and contribute towards understanding micro-endemism, and whether for some species their small range is the result of habitat loss or understudied locations, as opposed to true micro-endemism.

The presence of *S. lynnae* in both Ambohitantely and Anjozorobe may provide evidence that these two forests were once connected. If these forests were once connected and the species existed across a larger range, this species may not have formerly exhibited micro-endemism. Its current AOO fits within the range of most *Stumpffia*, between 50 to 100 km² (Rakotoarison et al. 2017), however if forest previously existed between the two sites, its range would have been much larger. When *Stumpffia* are known from more than one locality, they often present distinct mitochondrial haplotypes between the locations (Rakotoarison et al. 2017), as seen in *S. lynnae*. This pattern may be due to their small body size and limited dispersal ability, which contributes to facilitating lineage sorting (Orozco-Terwengel et al. 2011; Pabijan et al. 2012; Crottini et al. 2019). However, this genetic differentiation may also be due to forest isolation if it has persisted for a long time.

A study of endemism in the Mantellidae family found that many sister species pairs did not have overlapping ranges, but there were some examples of young micro-endemic sister species occurring in full sympatry (Wollenberg et al. 2011). The former reflects the relationship between *S. lynnae* and *Stumpffia* sp. Ca11, which may be more closely related than *S. lynnae* and *S. kibomena*, yet they are hundreds of kilometres apart, with *Stumpffia* sp. Ca11 distantly in the north of the island and probably having never had overlapping ranges. Future studies need to verify the status of this candidate species, as well as the poorly known *Stumpffia* sp. Ca34 from Ranomena.

On the contrary, however, the latter finding of Wollenberg et al. (2011) could mirror the case of *S. lynnae* sp. nov. and *S. kibomena*, which may have evolved in sympatry or parapatry, given the likely recent connectivity between Anjozorobe and Andasibe. Satellite imagery from the year 2000 shows much more forest between Anjozorobe and Mantadia National Park, close to Andasibe (Global Forest Watch 2021), and the forest cover shown in 1953 was greater still (Vieilledent et al. 2018). If these two species (*S. lynnae* and *S. kibomena*) did at some point occur in sympatry, this may explain the extreme difference in their male advertisement calls, which are the basis for sexual selection and mate recognition, and consequently often differ substantially between closely related sympatric taxa (Köhler et al. 2017). Meanwhile, elevation may have been a cause of allopatric divergence with respect to *S. kibomena* given that the species exists at ~ 900 m a.s.l (Glaw et al. 2015) while *S. lynnae* was found at higher elevation of ~ 1400–1600 m a.s.l. Conversely, the species may not have had overlapping

ranges and the different calls may have simply been selected in different directions in isolation. More research is required to understand fully when these forests, and that at Ambohitantely, were separated, e.g., using population genetic approaches and genomic data (e.g., ddRAD-seq) from multiple species distributed in this region.

This species adds another to the list of those with red markings, which occur in many different groups of frogs in Madagascar (Glaw et al. 2020). The function of such markings is unknown and may indeed vary by clade. For example, in the mantellid frogs like *Mantella madagascariensis*, it serves as aposematism, but in other species it may serve in antipredator behaviour or intraspecific communication (Glaw et al. 2020). In the Cophylinae, where it occurs in species of *Platypelis*, a few *Rhombophryne* species, and several independent clades of *Stumpffia*, the function is not known (Glaw et al. 2020). In this new species and in other *Stumpffia* the colour is rapidly lost when stored in 70% ethanol, whereas it is not lost in *Platypelis ranjomena* Glaw et al., 2020 even after years in ethanol. This difference suggests that distinct chemical basis may underpin what otherwise may seem to be the same or similar phenotypes, as seen for *Mantella madagascariensis* Grandidier, 1872 species group (Crottini et al. 2019). Future research could be conducted to understand the origins of this colouration.

This new *Stumpffia* highlights the importance of continued survey effort in the central highlands, and adds another endemic species to the area, highlighting the need to protect the rapidly dwindling forest fragments. It also highlights the taxonomic research that is still required to fully understand the *Stumpffia* genus, with this species alone still requiring more knowledge. More individuals should be surveyed to understand more about their population size, distribution, and population trends as well as their life history and ecology.

Acknowledgements

We thank Cardiff University for ethical approval and the Madagascar Ministry of the Environment and Sustainable Development (MEDD) for providing our research permit No332/19/MEDD/SG/DGEF/DGRNE, and export permit No046N-EA03/MG20. We thank the Department of Animal Biology, University of Antananarivo for supporting the permits and larger project. We could not have conducted fieldwork without field guides Tovo Raditra from Madagascar National Parks and Shecene from Anjozorobe, and research assistants Minosoa L. C. Razafiarimanana (2020) and Malalaitiana Rasoazanany (2019). We thank Durrell Wildlife Conservation Trust for providing financial and logistical support in the field. The UK Natural Environment Research Council supported this work through the GW4+ Doctoral Training Partnership NE/L002434/1. MDS was supported by a grant from the German Research Foundation (Deutsche Forschungs Gemeinschaft) SCHE 2181/1-1. The sequence data underlying this article are available in the GenBank Nucleotide Database at <https://www.ncbi.nlm.nih.gov/genbank/>, and can be accessed with accession numbers 5' 16S rRNA ON314863–ON314871, 3'16S ON332822–ON332828, COI ON313699–ON313706, RAG1 ON323575–ON323581 (details in Suppl. material 3: Table S1).

KM and MGR conducted the field work. KM conducted the laboratory work, data analysis and morphometric measurements. KM wrote the manuscript. MDS provided guidance throughout data analysis and manuscript preparation. All authors contributed toward the final manuscript.

References

- Bell KE, Donnelly MA, Rica DC (2006) Influence of forest fragmentation on community structure of frogs and lizards in northeastern Costa Rica. *Conservation Biology* 20(6): 1750–1760. <https://doi.org/10.1111/j.1523-1739.2006.00522.x>
- Boettger O (1881) Diagnoses reptilium et batrachiorum novorum ab ill. In: A Stumff (Ed.) *Insula Nossi-Bé Madagascariensis lectorum*. *Zoologischer Anzeiger* 4: 358–361.
- Boulenger GA (1882) *Catalogue of the Batrachia Salientias*. Ecaudata in the Collection of the British Museum, 2nd edn. Taylor and Francis, London, 588 pp. [pp 180–182, 473–475]
- Brown JL, Sillero N, Glaw F, Bora P, Vieites DR, Vences M (2016) Spatial biodiversity patterns of Madagascar's amphibians and reptiles. *PLoS ONE* 11(1): 1–26. <https://doi.org/10.1371/journal.pone.0144076>
- Che J, Chen H, Yang J, Jin J, Jiang KE, Murphy RW, Zhang Y (2012) Universal COI primers for DNA barcoding amphibians. *Molecular Ecology Resources* 12(2): 247–258. <https://doi.org/10.1111/j.1755-0998.2011.03090.x>
- Cope ED (1889) *Batrachia of North America*. *Bulletin of the United States National Museum* 34: 5–525. <https://doi.org/10.5962/bhl.title.38254>
- Crottini A, Orozco-Terwengel P, Rabemananjara FCE, Hauswaldt SJ, Vences M (2019) Mitochondrial introgression, color pattern variation, and severe demographic bottlenecks in three species of Malagasy poison frogs, genus *Mantella*. *Genes* 10(4): 1–25. <https://doi.org/10.3390/genes10040317>
- Crump ML, Scott NJ (1994) Chapter 2 Visual encounter surveys. In: Heyer WR, Donnelly MA, McDiarmid RW, Hayek LC, Foster MS (Eds) *Measuring and monitoring biological diversity: Standard methods for amphibians*. Smithsonian Institution Press, Washington, 84–92.
- Fouquet A, Gilles A, Vences M, Marty C, Blanc M, Gemmell NJ (2007) Underestimation of species richness in neotropical frogs revealed by mtDNA analyses. *PLoS ONE* 2(10): e1109. <https://doi.org/10.1371/journal.pone.0001109>
- Frost DR (2022) *Amphibians Species of the World*. <https://amphibiansoftheworld.amnh.org/> [accessed 22 Apr 2022]
- Glaw F, Vences M (2007) *A Field Guide to the Amphibians and Reptiles of Madagascar*. 3rd edn. Vences & Glaw Verlag, Cologne, 494 pp. [pp 118–142]
- Glaw F, Vallan D, Andreone F, Edmonds D, Dolch R, Vences M (2015) Beautiful bright belly: A distinctive new microhylid frog (Amphibia: *Stumpffia*) from eastern Madagascar. *Zootaxa* 3925(1): 120–128. <https://doi.org/10.11646/zootaxa.3925.1.8>
- Glaw F, Scherz MD, Rakotoarison A, Crottini A, Raselimanana AP, Andreone F, Köhler J, Vences M (2020) Genetic variability and partial integrative revision of *Platypelis* frogs (Microhylidae) with red flash marks from eastern Madagascar. *Vertebrate Zoology* 70(2): 141–156. <https://doi.org/10.26049/VZ70-2-2020-04>

- Global Forest Watch (2021) Global Forest Watch map. <https://www.globalforestwatch.org/map/> [accessed 9 Dec 2021]
- Goodman SM, Raherilalao MJ, Wohlauser S (2018) The Terrestrial Protected Areas of Madagascar: Their History, Description and Biota. Association Vahatra, Antananarivo.
- Grandidier MA (1872) Description de quelques reptiles nouveaux, découverts à Madagascar en 1870. *Annales des Sciences Naturelles (Zoologie)* 15(5): 6–11.
- Guibé J (1973) Batraciens nouveaux de Madagascar. *Bulletin du Museum National d'Histoire Naturelle. Zoologie* 171: 1169–1192.
- Günther ACLG (1858) On the systematic arrangement of the tailless batrachians and the structure of *Rhinophrynus dorsalis*. *Proceedings of the Zoological Society of London* 1858(1): 339–352. <https://doi.org/10.1111/j.1469-7998.1858.tb06387.x>
- IUCN (2012) IUCN Red List Categories and Criteria: Version 3.1. 2nd edn.. IUCN, Gland, Switzerland and Cambridge, UK, [iv +] 32 pp.
- IUCN SSC Amphibian Specialist Group (2016) *Rhombophryne helenae*. The IUCN Red List of Threatened Species 2016: e.T58010A84183331. <https://doi.org/10.2305/IUCN.UK.2016-1.RLTS.T58010A84183331.en> [accessed 10 Dec 2021]
- IUCN SSC Amphibian Specialist Group (2020a) *Anodonthyla vallani* (amended version of 2016 assessment). The IUCN Red List of Threatened Species 2020: e.T190944A176030045. <https://doi.org/10.2305/IUCN.UK.2020-3.RLTS.T190944A176030045.en> [accessed 10 Dec 2021]
- IUCN SSC Amphibian Specialist Group (2020b) *Rhombophryne kibomena* (amended version of 2016 assessment). The IUCN Red List of Threatened Species 2020: e.T79680110A177167158. <https://doi.org/10.2305/IUCN.UK.2020-3.RLTS.T79680110A177167158.en> [accessed 19 Nov 2021]
- Klages J, Glaw F, Köhler J, Müller J, Hipsley CA, Vences M (2013) Molecular, morphological and osteological differentiation of a new species of microhylid frog of the genus *Stumpffia* from northwestern Madagascar. *Zootaxa* 3717(2): 280–300. <https://doi.org/10.11646/zootaxa.3717.2.8>
- Köhler J, Vences M, D’Cruze N, Glaw F (2010) Giant dwarfs: Discovery of a radiation of large-bodied ‘stump-toed frogs’ from karstic cave environments of northern Madagascar. *Journal of Zoology* 282(1): 21–38. <https://doi.org/10.1111/j.1469-7998.2010.00708.x>
- Köhler J, Jansen M, Rodríguez A, Kok PJR, Toledo LF, Emmrich M, Glaw F, Haddad CFB, Rödel MO, Vences M (2017) The use of bioacoustics in anuran taxonomy: Theory, terminology, methods and recommendations for best practice. *Zootaxa* 4251(1): 1–124. <https://doi.org/10.11646/zootaxa.4251.1.1>
- Kumar S, Stecher G, Li M, Knyaz C, Tamura K (2018) Molecular Evolutionary Genetics Analysis across computing platforms. *Molecular Biology and Evolution* 35(6): 1547–1549. <https://doi.org/10.1093/molbev/msy096>
- Laurent RF (1946) Mises au point dans la taxonomie des ranides, *Revue de Zoologie et de Botanique Africaines*. Tervuren 39: 336–338.
- Longmire JL, Maltbie M, Baker RJ (1997) Use of ‘Lysis Buffer’ in DNA Isolation and its Implication for Museum Collections. *Occasional Papers, Museum of Texas Tech University* 163: 1–3. <https://doi.org/10.5962/bhl.title.143318>

- Mullin K, Rakotomanga M, Razafarimanana M, Barata I, Dawson J, Hailer F, Orozco ter Wengel P (2021) First amphibian inventory of one of Madagascar's smallest protected areas, Ankafoabe, extends the range of the Critically Endangered *Anilany helenae* (Vallan, 2000) and the Endangered *Boophis andrangoloaka* (Ahl, 1928). *Herpetology Notes* 14: 521–531.
- Myers N, Mittermeyer RA, Mittermeier CG, Da Fonseca GAB, Kent J (2000) Biodiversity hotspots for conservation priorities. *Nature* 403(6772): 853–858. <https://doi.org/10.1038/35002501>
- Orozco-Terwengel P, Corander J, Schlötterer C (2011) Genealogical lineage sorting leads to significant, but incorrect Bayesian multilocus inference of population structure. *Molecular Ecology* 20(6): 1108–1121. <https://doi.org/10.1111/j.1365-294X.2010.04990.x>
- Pabijan M, Wollenberg KC, Vences M (2012) Small body size increases the regional differentiation of populations of tropical mantellid frogs (Anura: Mantellidae). *Journal of Evolutionary Biology* 25(11): 2310–2324. <https://doi.org/10.1111/j.1420-9101.2012.02613.x>
- Palumbi S, et al. (1991) *The simple fool's guide to PCR*. Version 2. Honolulu: University of Hawaii: Honolulu, HI: Dept. of Zoology and Kewalo Marine Laboratory, University of Hawaii.
- Perl RGB, Nagy ZT, Sonet G, Glaw F, Wollenberg KC, Vences M (2014) DNA barcoding Madagascar's amphibian fauna. *Amphibia-Reptilia* 35(2): 197–206. <https://doi.org/10.1163/15685381-00002942>
- Pidancier N, Miquel C, Miaud C (2003) Buccal swabs as a non-destructive tissue sampling method for DNA analysis in amphibians. *The Herpetological Journal* 13(4): 175–178. <https://doi.org/10.1016/j.patcog.2015.07.013>
- Rakotoarison A, Scherz MD, Glaw F, Köhler J, Andreone F, Franzen M, Glos J, Hawlitschek O, Jono T, Mori A, Ndriantsoa SH, Rasoamam N, Riemann JC, Rödel MO, Gonçalves M, Vieites DR, Crottini A, Vences M (2017) Describing the smaller majority: Integrative taxonomy reveals twenty-six new species of tiny microhylid frogs (genus *Stumpffia*) from Madagascar. *Vertebrate Zoology* 67(3): 271–398. <https://doi.org/10.5281/zenodo.3338100>
- Rakotoarison A, Scherz MD, Bletz MC, Razafindraibe JH, Glaw F, Vences M (2019) Diversity, elevational variation, and phylogeographic origin of stump-toed frogs (Microhylidae: Cophylinae: *Stumpffia*) on the Marojejy massif, northern Madagascar. *Salamandra* (Frankfurt) 55(2): 115–123. <https://doi.org/10.5281/zenodo.2840366>
- Razafindraibe JH, Scherz MD, Dawson JS, Vences M, Rakotoarison A (2021) First record and probable reproductive mode of a true *Stumpffia* from Ambohitantly Special Reserve in the central highlands of Madagascar. *Herpetology Notes* 14: 493–495.
- Rozas J, Ferrer-Mata A, Sánchez-DelBarrio JC, Guirao-Rico S, Librado P, Ramos-Onsins SE, Sánchez-Gracia A (2017) DnaSP v6: DNA Sequence Polymorphism Analysis of Large Datasets. *Molecular Biology and Evolution* 34(12): 3299–3302. <https://doi.org/10.1093/molbev/msx248>
- Scherz MD, Vences M, Rakotoarison A, Andreone F, Köhler J, Glaw F, Crottini A (2016) Reconciling molecular phylogeny, morphological divergence and classification of Madagascar narrow-mouthed frogs (Amphibia: Microhylidae). *Molecular Phylogenetics and Evolution* 100: 372–381. <https://doi.org/10.1016/j.ympev.2016.04.019>

- Steinke D, Salzburger W, Vences M, Meyer A (2005) TaxI - A software tool for DNA barcoding using distance methods. *Philosophical Transactions of the Royal Society of London. Series B, Biological Sciences* 360(1462): 1975–1980. <https://doi.org/10.1098/rstb.2005.1729>
- Stephens M, Smith NJ, Donnelly P (2001) A new statistical method for haplotype reconstruction from population data. *American Journal of Human Genetics* 68(4): 978–989. <https://doi.org/10.1086/319501>
- Vallan D (2000a) A new species of the genus *Stumpffia* (Amphibia: Anura: Microhylidae) from a small forest remnant of the central high plateau of Madagascar. *Revue Suisse de Zoologie* 107(4): 835–841. <https://doi.org/10.5962/bhl.part.80150>
- Vallan D (2000b) Influence of forest fragmentation on amphibian diversity in the nature reserve of Ambohitantely, highland Madagascar. *Biological Conservation* 96(1): 31–43. [https://doi.org/10.1016/S0006-3207\(00\)00041-0](https://doi.org/10.1016/S0006-3207(00)00041-0)
- Vences M, Kosuch J, Glaw F, Böhme W, Veith M (2003) Molecular phylogeny of hyperoliid treefrogs: Biogeographic origin of Malagasy and Seychellean taxa and re-analysis of familial parafly. *Journal of Zoological Systematics and Evolutionary Research* 41(3): 205–215. <https://doi.org/10.1046/j.1439-0469.2003.00205.x>
- Vences M, Glaw F, Marquez R (2006) The Calls of the Frogs of Madagascar. 3 Audio CD's and booklet. Fonoteca Zoológica, Madrid.
- Vences M, Wollenberg KC, Vieites DR, Lees DC (2009) Madagascar as a model region of species diversification. *Trends in Ecology & Evolution* 24(8): 456–465. <https://doi.org/10.1016/j.tree.2009.03.011>
- Vences M, Köhler J, Pabijan M, Glaw F (2010) Two syntopic and microendemic new frogs of the genus *Blommersia* from the east coast of Madagascar. *African Journal of Herpetology* 59(2): 133–156. <https://doi.org/10.1080/21564574.2010.512961>
- Vences M, Hildenbrand A, Warmuth KM, Andreone F, Glaw F (2018) A new riparian *Mantidactylus* (*Brygoomantis*) frog from the Tsaratanana and Manongarivo Massifs in northern Madagascar. *Zootaxa* 4486(4): 575–588. <https://doi.org/10.11646/zootaxa.4486.4.10>
- Vences M, Miralles A, Brouillet S, Ducasse J, Fedosov A, Kharchev V, Kumari S, Patmanidis S, Puillandre N, Scherz MD, Kostadinov I, Renner S (2021) iTaxoTools 0.1: Kickstarting a specimen-based software toolkit for taxonomists. *Megataxa* 6(2): 77–92. <https://doi.org/10.11646/megataxa.6.2.1>
- Vieilledent G, Grinand C, Rakotomalala FA, Ranaivosoa R, Rakotoarijaona JR, Allnutt TF, Achard F (2018) Combining global tree cover loss data with historical national forest cover maps to look at six decades of deforestation and forest fragmentation in Madagascar. *Biological Conservation* 222: 189–197. <https://doi.org/10.1016/j.biocon.2018.04.008>
- Vieites DR, Wollenberg KC, Andreone F, Köhler J, Glaw F, Vences M (2009) Vast underestimation of Madagascar's biodiversity evidenced by an integrative amphibian inventory. *Proceedings of the National Academy of Sciences of the United States of America* 106(20): 8267–8272. <https://doi.org/10.1073/pnas.0810821106>
- Wilme L, Goodman SM, Ganzhorn JU (2006) Biogeographic evolution of Madagascar's microendemic biota. *Science* 312(5776): 1063–1066. <https://doi.org/10.1126/science.1122806>

- Wilme L, Goodman SM, Raselimanana AP (2007) Inventaires de la faune et de la flore du couloir forestier d'Anjozorobe – Angavo, Recherches pour le développement Série Sciences Biologiques 24: 111–135.
- Wollenberg KC, Vieites DR, van der Meijden A, Glaw F, Cannatella DC, Vences M (2008) Patterns of endemism and species richness in Malagasy cophyline frogs support a key role of mountainous areas for speciation. *Evolution* 62(8): 1890–1907. <https://doi.org/10.1111/j.1558-5646.2008.00420.x>
- Wollenberg KC, Vieites DR, Glaw F, Vences M (2011) Speciation in little: The role of range and body size in the diversification of Malagasy mantellid frogs. *BMC Evolutionary Biology* 11(1): e217. <https://doi.org/10.1186/1471-2148-11-217>

Supplementary material 1

Figure S1

Authors: Katherine E. Mullin, Manoa G. Rakotomanga, Jeff Dawson, Frank Glaw, Andolalao Rakotoarison, Pablo Orozco-terWengel, Mark D. Scherz

Data type: docx file

Explanation note: Maximum Likelihood phylogeny of selected *Stumpffia* species using a 624 bp region of the COI mitochondrial marker, using the HKY+G+I model with 1000 bootstrap replicates.

Copyright notice: This dataset is made available under the Open Database License (<http://opendatacommons.org/licenses/odbl/1.0/>). The Open Database License (ODbL) is a license agreement intended to allow users to freely share, modify, and use this Dataset while maintaining this same freedom for others, provided that the original source and author(s) are credited.

Link: <https://doi.org/10.3897/zookeys.1104.82396.suppl1>

Supplementary material 2

Figure S2

Authors: Katherine E. Mullin, Manoa G. Rakotomanga, Jeff Dawson, Frank Glaw, Andolalao Rakotoarison, Pablo Orozco-terWengel, Mark D. Scherz

Data type: docx file

Explanation note: Sections of the 16S rRNA gene alignment, showing the differences of *Stumpffia lynnae* sp. nov. in comparison to 27 other *Stumpffia* species from across the *Stumpffia* phylogeny.

Copyright notice: This dataset is made available under the Open Database License (<http://opendatacommons.org/licenses/odbl/1.0/>). The Open Database License (ODbL) is a license agreement intended to allow users to freely share, modify, and use this Dataset while maintaining this same freedom for others, provided that the original source and author(s) are credited.

Link: <https://doi.org/10.3897/zookeys.1104.82396.suppl2>

Supplementary material 3

Table S1

Authors: Katherine E. Mullin, Manoa G. Rakotomanga, Jeff Dawson, Frank Glaw, Andolalao Rakotoarison, Pablo Orozco-terWengel, Mark D. Scherz

Data type: docx file

Explanation note: GenBank accession numbers.

Copyright notice: This dataset is made available under the Open Database License (<http://opendatacommons.org/licenses/odbl/1.0/>). The Open Database License (ODbL) is a license agreement intended to allow users to freely share, modify, and use this Dataset while maintaining this same freedom for others, provided that the original source and author(s) are credited.

Link: <https://doi.org/10.3897/zookeys.1104.82396.suppl3>

Supplementary material 4

Table S2

Authors: Katherine E. Mullin, Manoa G. Rakotomanga, Jeff Dawson, Frank Glaw, Andolalao Rakotoarison, Pablo Orozco-terWengel, Mark D. Scherz

Data type: docx file

Explanation note: Pairwise uncorrected distances between the 27 *Stumpffia* species used in the 16S phylogeny.

Copyright notice: This dataset is made available under the Open Database License (<http://opendatacommons.org/licenses/odbl/1.0/>). The Open Database License (ODbL) is a license agreement intended to allow users to freely share, modify, and use this Dataset while maintaining this same freedom for others, provided that the original source and author(s) are credited.

Link: <https://doi.org/10.3897/zookeys.1104.82396.suppl4>

Life cycle and description of the immature stages of a terrestrial firefly endemic to Mexico: *Photinus extensus* Gorham (Coleoptera, Lampyridae)

Martín L. Zurita-García¹, Daniel Edwin Domínguez-León^{1,2}, Viridiana Vega-Badillo^{1,2},
Mireya González-Ramírez^{1,2}, Ishwari Giovanni Gutiérrez-Carranza¹,
Geovanni M. Rodríguez-Mirón³, Sara López-Pérez³, Paulina Cifuentes-Ruiz¹,
Miriam Aquino-Romero¹, Santiago Zaragoza-Caballero¹

1 Departamento de Zoología, Instituto de Biología, Universidad Nacional Autónoma de México, Apartado Postal 70-153, 04510, Mexico City, Mexico **2** Posgrado en Ciencias Biológicas, Universidad Nacional Autónoma de México, Edificio D, 1° Piso. Circuito de Posgrados, Ciudad Universitaria, 04510, Mexico City, Mexico **3** Colección Coleopterológica, Museo de Zoología, Facultad de Estudios Superiores Zaragoza, Universidad Nacional Autónoma de México, Av. Guelatao 66, Col. Ejército de Oriente, Alcaldía Iztapalapa, 09230, Mexico City, Mexico

Corresponding author: Daniel Edwin Domínguez-León (biologiaunamedwin@gmail.com)

Academic editor: Vinicius S. Ferreira | Received 16 January 2022 | Accepted 19 May 2022 | Published 7 June 2022

<http://zoobank.org/68CE42A1-3B99-441B-B15D-8E163C06A40B>

Citation: Zurita-García ML, Domínguez-León DE, Vega-Badillo V, González-Ramírez M, Gutiérrez-Carranza IG, Rodríguez-Mirón GM, López-Pérez S, Cifuentes-Ruiz P, Aquino-Romero M, Zaragoza-Caballero S (2022) Life cycle and description of the immature stages of a terrestrial firefly endemic to Mexico: *Photinus extensus* Gorham (Coleoptera, Lampyridae). ZooKeys 1104: 29–54. <https://doi.org/10.3897/zookeys.1104.80624>

Abstract

The life cycle, morphology, and bionomy of *Photinus extensus* Gorham, 1881, an endemic species of Mexico, are described. Redescriptions of adults (male and female) are also presented. Larvae were reared to the adult stage from eggs laid by females collected at the El Pedregal de San Ángel Ecological Reserve, south of Mexico City. The activity period of adults of *P. extensus* begins at the end of July and finishes by the end of August. Females lay between 3 and 198 eggs. Larvae hatch from the eggs after a period of 11 to 71 days, undergo 6 larval instars and a pupal stage in an annual cycle. Morphological characters of the sixth larval instar of *P. extensus* are compared with those of several other genera assigned to the tribe Photinini. Knowledge of the natural history of firefly larvae is relevant since most species do not feed as adults and therefore depend on resources acquired during the larval stage.

Keywords

Bionomics, egg, larva, Photinini, pupa, redescription

Introduction

Fireflies belong to the family Lampyridae Rafinesque, 1815, and show a wide-ranging phenotypic and ecological diversity (Riley et al. 2021). Currently, there are more than 2400 described species with a worldwide distribution (Martin et al. 2019; Ferreira et al. 2020; Zaragoza-Caballero et al. 2020; Riley et al. 2021; Silveira et al. 2022). The highest species diversity is found in the Neotropical region (Costa 2000). Fireflies include nonluminous and luminous adults, luminous larvae and the females of some taxa are flightless (Branham 2010; Lewis et al. 2020). They inhabit wetlands, grasslands, forests, agricultural fields and urban parks (Lewis et al. 2020). Many fireflies are strongly associated with particular habitats and vegetation types (Faust 2017).

Firefly species can be either diurnally or nocturnally active. Diurnal species generally do not have light organs as adults and rely on pheromonal and visual cues (Ohba 2004; Branham 2010). Luminous species are nocturnal or crepuscular, with bioluminescent signals produced from photic organs of various shapes and sizes located on abdominal ventrites. These visual signals are typically used in sexual signaling to communicate species identity and facilitate pair formation (Branham 2010).

Firefly larvae can be aquatic, semiaquatic or terrestrial and can be found along the margins of streams and ponds as well as in leaf litter or rotten logs (Branham 2010). All known larvae are luminous and emit glows of varying duration. They are predatory on snails, earthworms and other soft-bodied prey (Lewis et al. 2020). The adults of most species do not feed and therefore rely on resources gathered during the larval stages (Lloyd 2002; Vaz et al. 2020). Multiple genera endemic to the Neotropical region have no larval or pupal descriptions. The few species that have been studied have different life histories (Vaz et al. 2020).

Currently, only the morphology of a small percentage of lampyrid larvae, at the generic or specific levels, of the approximately 144 genera and 2400 species, is known (Archangelsky 2010; Madruga and Branham 2020; Vaz et al. 2020; Zaragoza-Caballero et al. 2020; Riley et al. 2021; Silveira et al. 2022). There are a few studies describing the immature stages in the tribe Photinini. However, most of them have poorly detailed descriptions, composed only by the last larval stage (Riley et al. 2021). Besides, no tools to compare microstructures have been implemented. Of the 29 genera belonging to Photinini (Martin et al. 2019; Zaragoza-Caballero et al. 2020), there are detailed descriptions only for some species of *Pyraclonema* Solier in Gay, 1849, *Pyropyga*, Motschulsky, 1852 *Lucidina* Gorham, 1883, *Lucidota* Laporte, 1833, *Phosphaenus* Laporte 1833 (Bugnion 1929; Beutel 1995; Branham and Archangelsky 2000; Archangelsky and Branham 2001; Archangelsky 2010, Kawashima 2017; Novák 2018b).

Photinus Laporte, 1833 is the most diverse genus of the subfamily Lampyrinae with more than 300 described species (McDermott 1964; Zaragoza-Caballero et al. 2020). Members of this genus live in a variety of habitats (from tropical dry forests to temperate and tropical montane cloud forests). Species range from the United States to Argentina. One species, recently collected in Spain, was described as new (Zaragoza-Caballero and Viñolas 2018) but then synonymized with the South American species *Photinus signaticollis* (Blanchard, 1846) (Koken et al. 2022).

In the past 20 years the number of known *Photinus* species has increased due to the description of new species from Mexico (Zaragoza-Caballero 2000, 2005, 2007, 2015, 2017; Zaragoza-Caballero et al. 2020). This fact contrasts with the lack of knowledge of the larval stages and the natural history of these organisms. Until now, no study has accurately documented the life cycle duration of a *Photinus* species. This lack of knowledge is the result of the difficulty of collecting mated females, as well as challenges associated with rearing larvae under laboratory conditions. Moreover, some species are known to spend several years in the larval stage, and the time fireflies need to complete their life cycle depends on the geographical region and the availability of larval food (Buschman 2017).

As for most genera in the family Lampyridae, *Photinus* larvae are poorly studied. Buschman (2017) observed that the first instars of this genus are smaller compared to those of *Photuris* Dejean, 1833, but no descriptions are provided. Most research documenting the natural history of *Photinus* focuses on the adult stage. These studies include courtship in males (flash communication) (Wing 1991; Viviani 2001; Faust and Weston 2009; Faust 2010), nuptial gifts (Lewis et al. 2004a, 2004b), the utilization of ejaculate-derived proteins to nourish developing oocytes in certain species (Demary 2005) and the size of signal detection and emission organs (López-Palafox et al. 2020).

This paper documents the life cycle and larval morphology of a *Photinus* species for the first time. *Photinus extensus* Gorham, 1881 is an endemic species of Mexico. Its known distribution includes the state of Chiapas, Hidalgo, Mexico, Morelos and Mexico City (Zaragoza-Caballero et al. 2020). A reduced population of this firefly was also found in El Pedregal de San Ángel Ecological Reserve, South of Mexico City. The life cycle of *P. extensus* is herein presented, with descriptions of larval instar 6. Some characteristics of instars 1 and 3 are mentioned; the adult was described as well.

Methods

Collection

Adults of *P. extensus* were collected in the buffer zone of the El Pedregal de San Ángel Ecological Reserve (19°19'28.82"N, 99°11'20.95"W); this zone is between the core zone and the urban area of Mexico City, it is totally in the territory of the Universidad Nacional Autónoma de México. El Pedregal de San Ángel Ecological Reserve is located at the Southeast of Mexico City in the central Campus of the (UNAM) (Fig. 1). This community developed on a basaltic lava substrate approximately 1,670 years ago (Lot and Camarena 2009); the type of vegetation corresponds to a xerophytic shrub (Rzedowski 1978). The climate is sub-humid tempered with summer rains and an annual average precipitation of 833 mm; the annual average temperature is 15.5 °C (Orozco-Segovia et al. 2009). Fourteen adult females and 70 adult males of *P. extensus* were collected on August the 3rd, 8th, and 10th of 2018, between 19:30 and 21 h. Adult specimens were located by their bioluminescence in the undergrowth, where

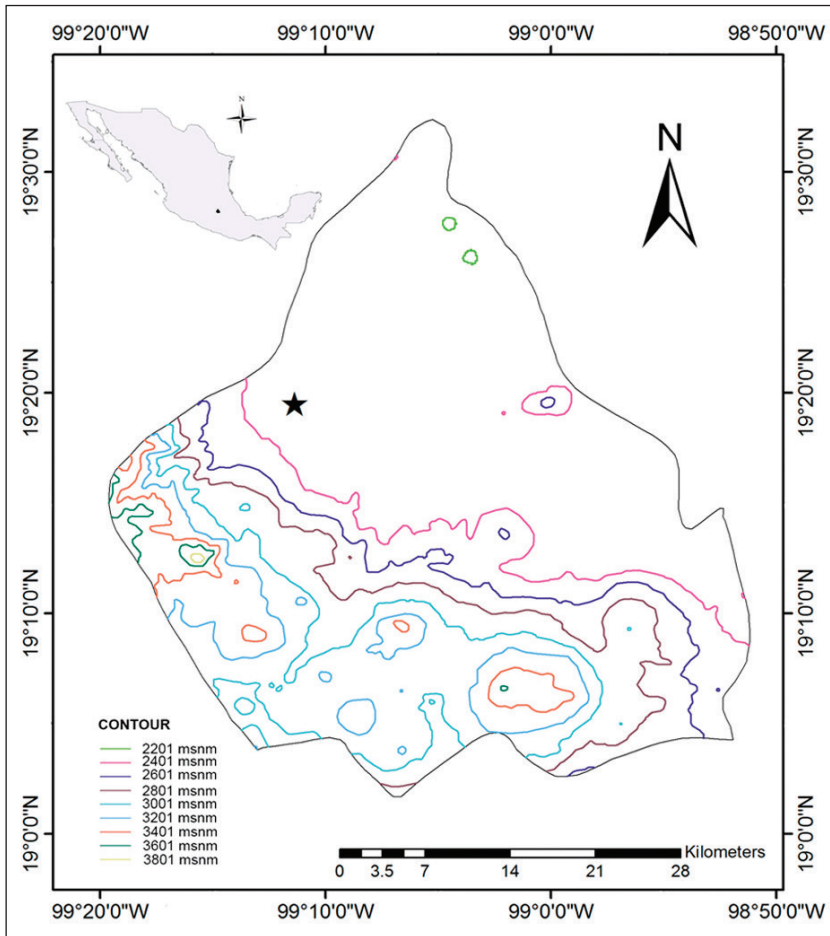


Figure 1. Map of Mexico City. Location of the study area where adults of *P. extensus* were collected (indicated with a star).

the dominant plant species is *Pittocaulon praecox* (Cav.) H. Rob. & Brettel (Asterales: Asteraceae). Other collections were made at the same site between June and July 2019, and five larvae were obtained. These developed into two female pupae and three males. Larvae, pupae, and adults were fixed in 70% ethanol for their preservation.

Rearing in the laboratory

To observe the reproductive activity of *P. extensus*, adult specimens collected were divided into 14 groups consisting of five males and one female were placed in an 8 × 15 cm plastic container; peat moss substrate was added to simulate their natural environment. After oviposition, eggs were placed over a gauze patch in a 50 × 100 mm

Petri dish, and moistened every 48 hours with an antimycotic solution based on Nistatine diluted in water (1/10). After eclosion, larvae were partitioned into groups of five in separate Petri dishes (5×10 mm). To avoid dehydration, a filter paper layer was added and moistened every two days. This filter paper was replaced every week. Starting with the fourth larval instar, each larva was placed in a separate Petri dish (5×10 mm), with half of the dish covered with the filter paper, and the other half filled with sterilized dry sawdust. Following previous studies (Archangelsky and Branham 2001; Archangelsky 2010), larvae were fed small pieces of earthworm *Eisenia fetida* (Savigny, 1826) (Haplotaxida: Lumbricidae). Dead or partially consumed prey were removed from the Petri dishes every two days to keep containers clean. Pupae were maintained in Petri dishes (5×10 mm) at room temperature with sterilized dry sawdust until they completed their development. Specimens representing the different larval instars, pupae, and adults, were preserved in 70% ethanol for reference and subsequent study.

Morphological study

Adults were identified using original descriptions, literature (Zaragoza-Caballero et al. 2000), and by comparison with photographs of type specimens (Natural History Museum of London, **BMNH**) (Fig. 2A–F) and specimens identified by experts deposited at the Colección Nacional de Insectos (**CNIN**), Instituto de Biología, UNAM, terminology of internal genitalia of females followed Silveira et al. (2022). Juvenile stages and adults of *P. extensus* were examined under a Zeiss stereoscopic microscope (Discovery V8) with a 1× objective lens coupled with 16× eyepieces. Larval heads of each instar were separated from the body and immersed in 10% KOH solution, the mouthparts were dissected under a stereoscopic microscope and placed in glycerin on slides for observation. Description of the distribution of the setae was made for the last instar larva following Branham and Archangelsky (2000) and Archangelsky (2010). Pygopodial structure for the last instar larva was interpreted using Fu et al. (2012). Redescription of the adult of *P. extensus* was made based on collected material. For the morphological description of larval instars, we followed the terminology of Novák (2018a) and Fu et al. (2012). A table 1 was made to compare morphological larval characters of Photinini (*Pyractonema*, *Pyropyga*, *Lucidota*, *Lucidina*, *Phosphaenus* and *Photinus*) (Branham and Archangelsky 2000; Archangelsky and Branham 2001; Archangelsky 2010; Novák 2018b), after Archangelsky (2010) and Kawashima (2017).

Images were taken with an AxiocamMRC5 camera attached to a Zeiss Axio Zoom V16 microscope with an objective lens Plan NeoFluar Z, 1×10.25 FWD 56 at the Laboratorio de Microscopía y Fotografía de la Biodiversidad II, Instituto de Biología, UNAM. Larvae were examined and imaged with a Hitachi SU1015 scanning electron microscope at the Laboratorio de Microscopía y Fotografía de la Biodiversidad I, Instituto de Biología, UNAM.

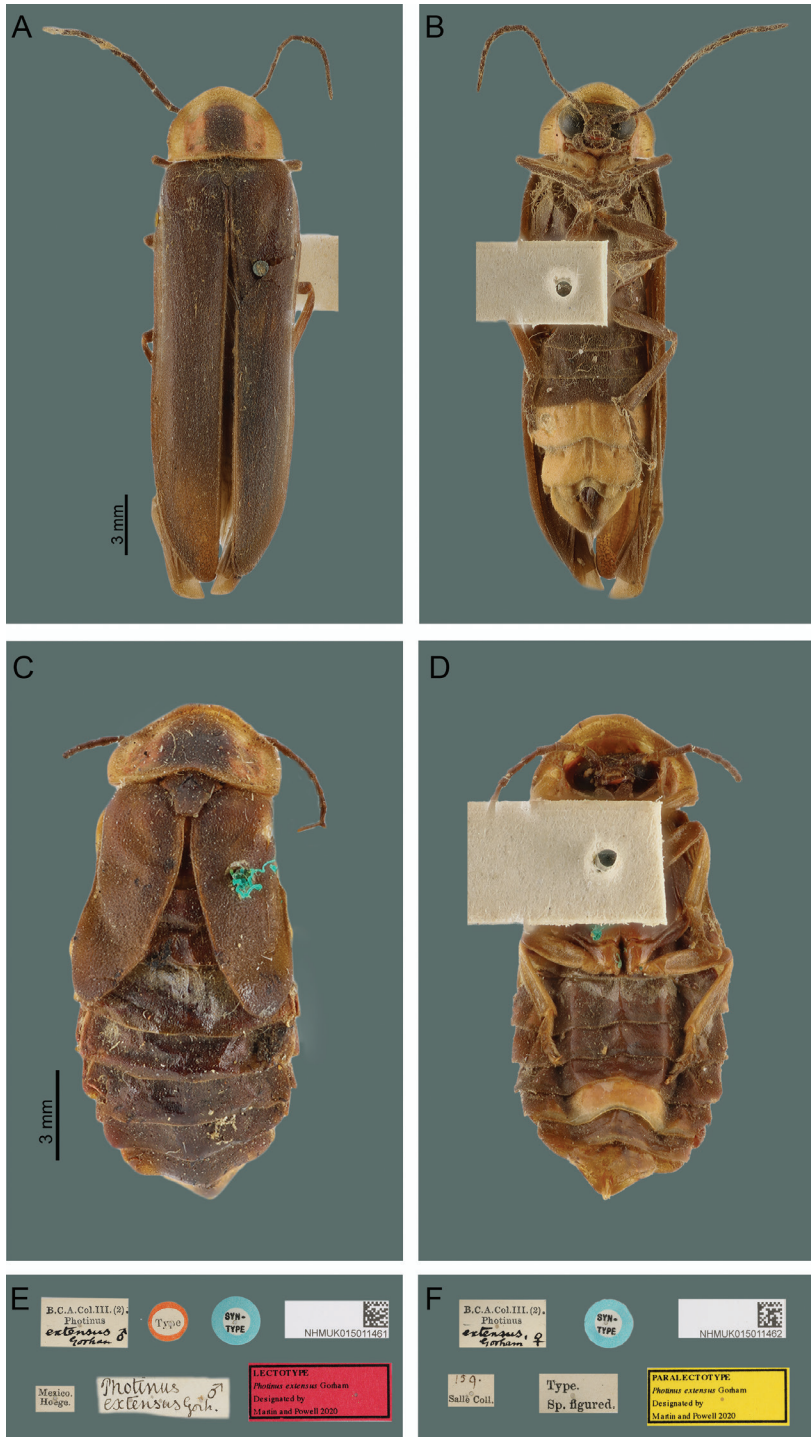


Figure 2. *Photinus extensus* Gorham, type specimens NHM-London **A** general habitus of the adult male in dorsal view **B** ventral view **C** general habitus of the adult female in dorsal view **D** ventral view **E** male labels (lectotype) **F** female labels (paralectotype). Photos: Keita Matsumoto.

Results

Photinus extensus Gorham, 1881

Figs 3A–E, 4A–E [Adults]

Redescription. Adult male (Fig. 3A, B) (n = 70). Length of body 16.1–20.3 mm; width 3.7–4.2 mm. Body brownish, except the pronotal disk with a central black spot and two red spots at the sides; prothorax, coxae, seventh and eighth ventrites yellowish; light organ in sternites 5–6 and 7th sternite with diminished light spots.

Head. Interocular space flat, almost parallel, shagreen-like integument, brilliant and pilose; frons vertical, interantennal distance (0.17–0.22 mm; 0.2 ± 0.01 mm) slightly wider than the antennal fossae (0.23–0.32 mm; 0.28 ± 0.04 mm); eyes finely faceted, semispherical, prominent, longer (1.1–1.18 mm; 1.17 ± 0.03 mm) than wide (0.62–0.98 mm; 0.9 ± 0.08 mm); antennae filiform, long (5.7–7.11 mm; 7.0 ± 0.11 mm), one-and-a half times longer than pronotum, extending beyond the posterior coxae, scape claviform reaching a length of (0.69–0.98 mm; 0.79 ± 0.10 mm), as long as the next two antennomeres together, the second short (0.19–0.79 mm; 0.28 ± 0.05 mm), the third to the tenth (0.54–0.71 mm; 0.66 ± 0.07 mm), the eleventh reaches (0.51–0.73 mm; 0.77 ± 0.03 mm); frontoclypeal suture membranous, almost straight; clypeus trapezoidal, anterior margin concave, with setae along the margin; mandibles falcate, robust, with setae on the external base; maxillar palpomere ogival and robust, labial palpomere securiform.

Thorax. Pronotum wider (3.95–4.4 mm; 4.04 ± 0.08 mm) than long (2.8–3.4 mm; 3.01 ± 0.27 mm), semicircular, with a longitudinal groove indistinct in the basal half, anterior margin rounded, posterior sinuate, posterior angles straight, sides narrowly explanate, with irregular glandular pores at the front and ordered on the posterior and lateral margins, surface brilliant, abundant pilosity, decumbent; scutellum spatulate, with the posterior margin rounded, surface brilliant, punctate and decumbent pilosity; long elytra, parallel, four and a half times longer (12–13.5 mm; 12.6 ± 0.57 mm) than wide (2.4–2.8 mm; 2.58 ± 0.19 mm), surface rugose, opaque, with two types of pilosity, one relatively long and erect, the other small and procumbent; mesothoracic respiratory spiracles not tubular; long legs, pro, meso and metalegs similar to each other, femurs fusiform, tibiae channeled, a little dilated at the apex, external margin crenulate, two symmetric tibial spurs present in pro, meso and meta legs, tarsomeres laterally compressed, first metatarsomere longer (0.6–0.76 mm; 0.73 ± 0.03 mm) than the next two metatarsomeres together (0.51–0.68 mm; 0.63 ± 0.08 mm), fourth bifid, covering the fifth, claws simple.

Abdomen. Sternites 5–6 longer than the preceding, with stigmatiform pores, posterior margin of sternite six cleaved, the seventh concave, the eighth ojival; posterior margin of pygidium convex; aedeagus short, robust, with symmetrical basal piece (0.67–0.7 mm; 0.68 ± 0.05 mm), as long as lateral lobes (0.66–0.7 mm; 0.67 ± 0.45 mm), with posterior margin concave, lateral lobes apically acute and convergent, median lobe cylindrical, with dorsal part membranous and ventral part with sclerosed base and apical half membranous, dorso-basal excrescences as long, oblique lobes, median orifice apical, lateral lobes narrowing towards the apex, apex blunt and wide (Fig. 3C, D, E).

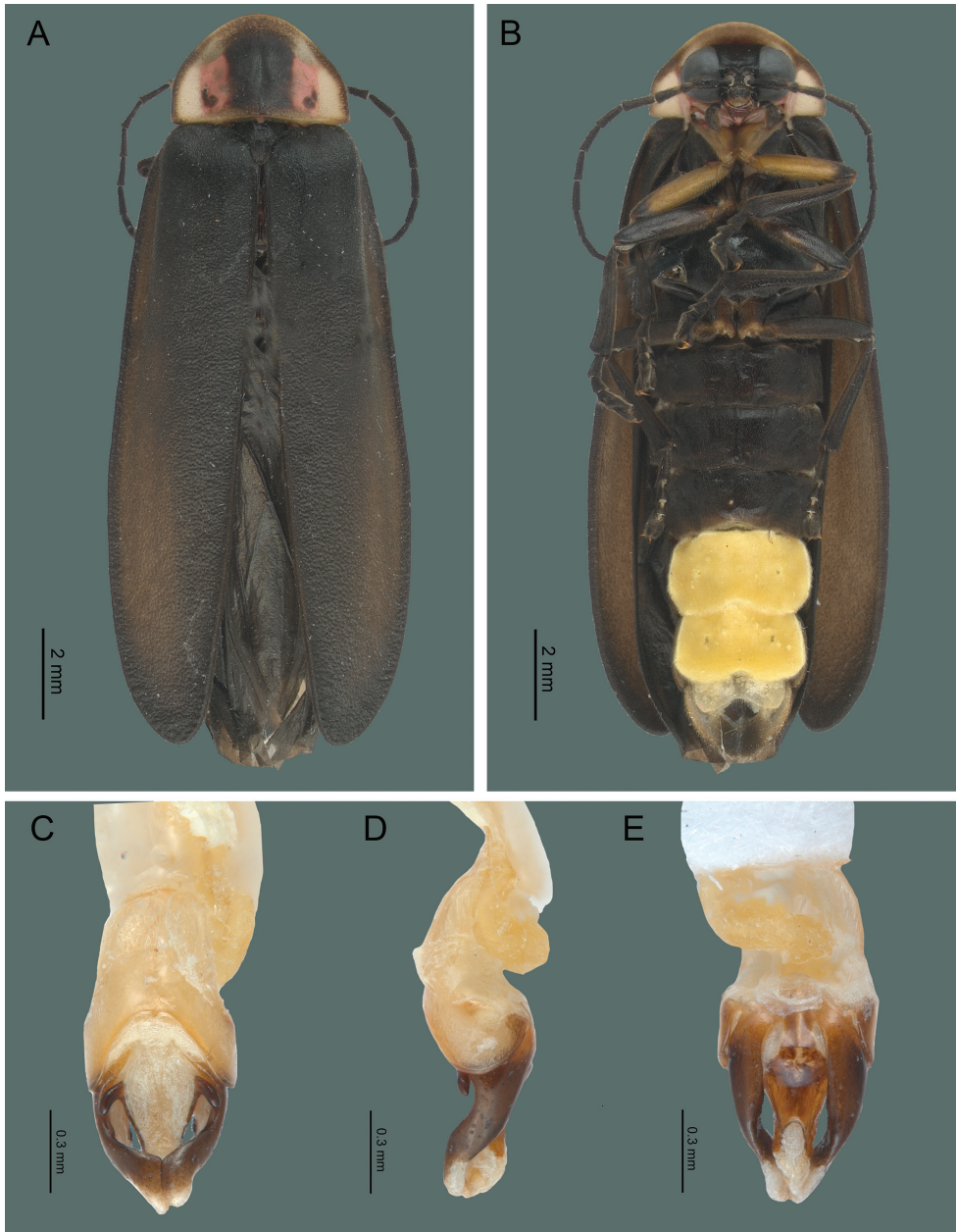


Figure 3. *Photinus extensus* Gorham **A** general habitus of the adult male in dorsal view **B** ventral view; Aedeagus: **C** dorsal view **D** lateral view **E** ventral view.

Adult female (Fig. 4A, B) (n = 14). Length: 11.1–20.3 mm; width: 3.2–6.5 mm. Body brownish, except the pronotal disk with a central black spot and two red spots at the sides; procoxae, protrochanters, meso-coxae, meta-coxae, seventh and eighth sternites yellowish; light organ in fifth sternite.

Head. Interocular space flat, more or less parallel, shagreen integument, brilliant and pilose, frons vertical, interantennal distance (0.16–0.37 mm; 0.25 ± 0.10 mm) wider than antennal fossae (0.16–0.37 mm; 0.44 ± 0.16 mm); eyes small, finely faceted, semispherical, longer (0.65–0.94 mm; 0.67 ± 0.25 mm) than wide (0.45–0.76 mm; 0.54 ± 0.15 mm), antennae filiform, short (4.16–5.52 mm; 5.23 ± 0.96 mm), as long as the length of pronotum, without extending beyond the posterior margin of metasternum; scape reaching a length of (0.57–0.64 mm; 0.58 ± 0.34 mm), longer than the two next antennomeres together, the second short (0.2–0.39 mm; 0.37 ± 0.06 mm), from the third to the tenth (0.35–0.58 mm; 0.44 ± 0.07 mm), the eleventh reaches (0.54–0.69 mm; 0.68 ± 0.05 mm); frontoclypeal suture membranous, almost straight; clypeus trapezoidal, anterior margin concave, with setae along the margin; mandibles falcate, robust with setae on the external base; maxillar palpomere ogival and robust, labial palpomere securiform.

Thorax. Pronotum wider (3.27–4.97 mm; 4.21 ± 0.86 mm) than long (2.21–2.6 mm; 2.2 ± 0.2 mm), semicircular, with a longitudinal groove indistinct on the basal half, anterior margin rounded, posterior margin straight, posterior angles straight, sides narrowly explanate, with glandular pores irregular at the front and ordered on the posterior and lateral margins, surface brilliant, pilosity abundant, decumbent, scutellum spatulate, with the posterior margin rounded, surface brilliant, punctate and pilosity decumbent; elytra short, without covering the abdomen, two-and-a-half times longer (4.62–6.5 mm; 5.2 ± 0.62 mm) than wide (1.91–2.71 mm; 2.22 ± 0.42 mm), surface rugose, opaque, pilosity decumbent; divergent in the median margin, epipleura reduced, mesothoracic respiratory spiracles not tubular; legs similar to each other; tibiae and femurs flat, fusiform, tibiae channeled, a little dilated at the apex, external margin crenulate, tarsomeres laterally compressed, first metatarsomere (0.41–0.64 mm; 0.62 ± 0.22 mm) slightly longer than the next two together (0.46–0.58 mm; 0.53 ± 0.06 mm), the fourth bifid, covering part of the fifth, claws simple.

Abdomen. Sternites 5–6 longer than the preceding, without stigmatiform pores, posterior margin of sternite six almost straight, the seventh cleaved, the eighth with a notched; posterior margin of pygidium convex. Internal genitalia with a short and rounded spermatophore-digesting gland, longer than spermatheca, bursa copulatrix with an elongated and weakly sclerotized plate. Ovipositor with valvifers free, two-and-a-half times longer (2.41–3.10 mm; 2.75 ± 0.48 mm) than coxites (1–1.12 mm; 1.06 ± 0.08 mm); coxites divergent posteriorly; styli minute, sclerotized; proctigerplate short with rounded posterior margin, well-sclerotized (Fig. 4C, D, E).

Description of pre-imaginal stages.

Egg (Fig. 5A, B). Semispherical shape, whitish, with a diameter of approximately 290–300 μm (Fig. 5A). Surface with concavities that differ in size and shape (4–10 μm), evenly distributed, some present in aggregations (Fig. 5B). As time elapsed, the surface of the eggs became more transparent, allowing the observation of the larvae before hatching.

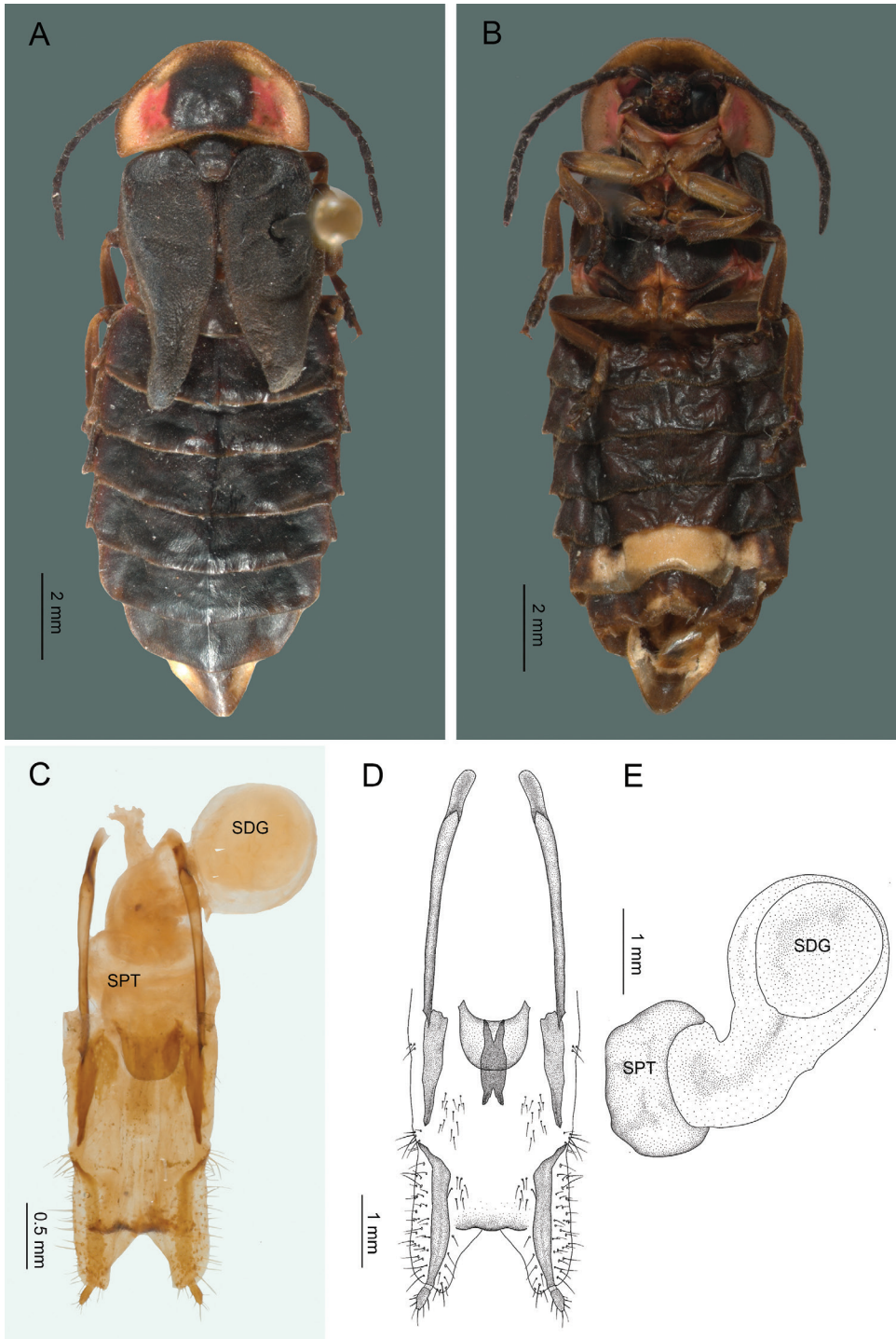


Figure 4. *Photinus extensus* Gorham **A** general habitus of the adult female in dorsal view **B** ventral view **C** internal genitalia **D** ovipositor dorsal view **E** internal anatomy of the reproductive tract: spermatophore digesting (SDG) and spermateca (SPT).

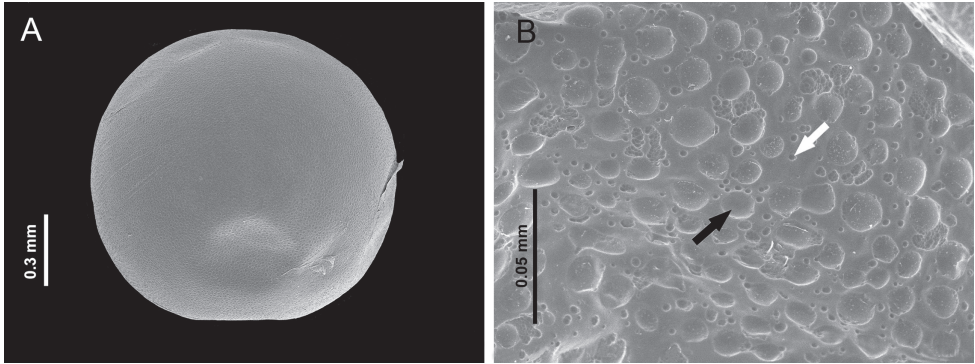


Figure 5. **A** Egg of *Photinus extensus* Gorham **B** surface with concavities that differ in size and shape (4–10 μm), evenly distributed, some present in aggregations.

Sixth instar larva (Figs 6A, B, 7A–H, 8A–G, 9A–F). **Description.** Elongate, tapering body, dorso-ventrally flattened, length 12.27–18.18 mm; integument of granular appearance; tergites from protergum to abdominal segment IX divided by sagittal line in dorsal view. Tergites with two lateral pale stripes that run throughout the body to the VIII segment, more sclerotized than the sternites, with clearly visible setae on the posterior margin of tergites VII to X; the last tergum completely dark except the lateral margins paler; anterior margin of the first head segment with two fossae (sensorial or glandular) paler and bigger than the rest of the punctations of the segment. Membranous pleura except for a dark sclerotized area around the spiracles, without apparent setae. The ventral surface is flexible due to the intersegmental membranes. Mesothoracic and abdominal pleural areas of segments I–VIII with bilabiate spiracles.

Head capsule. Prognathous; slightly visible when retracted into prothorax due to the transparency of the protergum; extensible neck membrane covered in extremely short spines forms a two-layer envelope around the head; partially retractable within the prothorax; completely sclerotized, small, wider (0.88–1.54 mm; 1.2 ± 0.27 mm) than long (0.68–1.09 mm; 0.92 ± 0.17 mm), flat, sides almost parallel; stemmata on each side, with an almost transparent spot located posteriorly to the stemmata; clypeus and labrum fused forming the clypeo-labrum covering base of the mandibles in dorsal view; maxillae and labium connate forming maxillolabial complex covering most of the ventral cephalic area; epicranial suture dark, U-shaped, with a very short epicranial stem, frontal arms V-shaped (Figs 7A, 8A). Epipharynx formed by two oval plates, without setae, that project centrally beyond the anterior margin of the head. Hypopharynx with short setation.

Antenna. Trimerous, located on the distal margin of the epicranial plate; partially retractable into the antennal socket; three-segmented, basal antennomere and second antennomere (0.42–0.55 mm; 0.48 ± 0.05 mm) elongated, and a third segment (the flagellum) short (0.24–0.31 mm; 0.26 ± 0.03 mm); adjacent sensorial cone present; basal antennomere with two long setae in the anterior mid, almost entirely covered by moderately dense, second antennomere with long setae close to apex and entirely covered by dense smaller finer setae, third antennomere with long setae from base to apex, with short setae on the anterior margin (Fig. 7B, 8B).

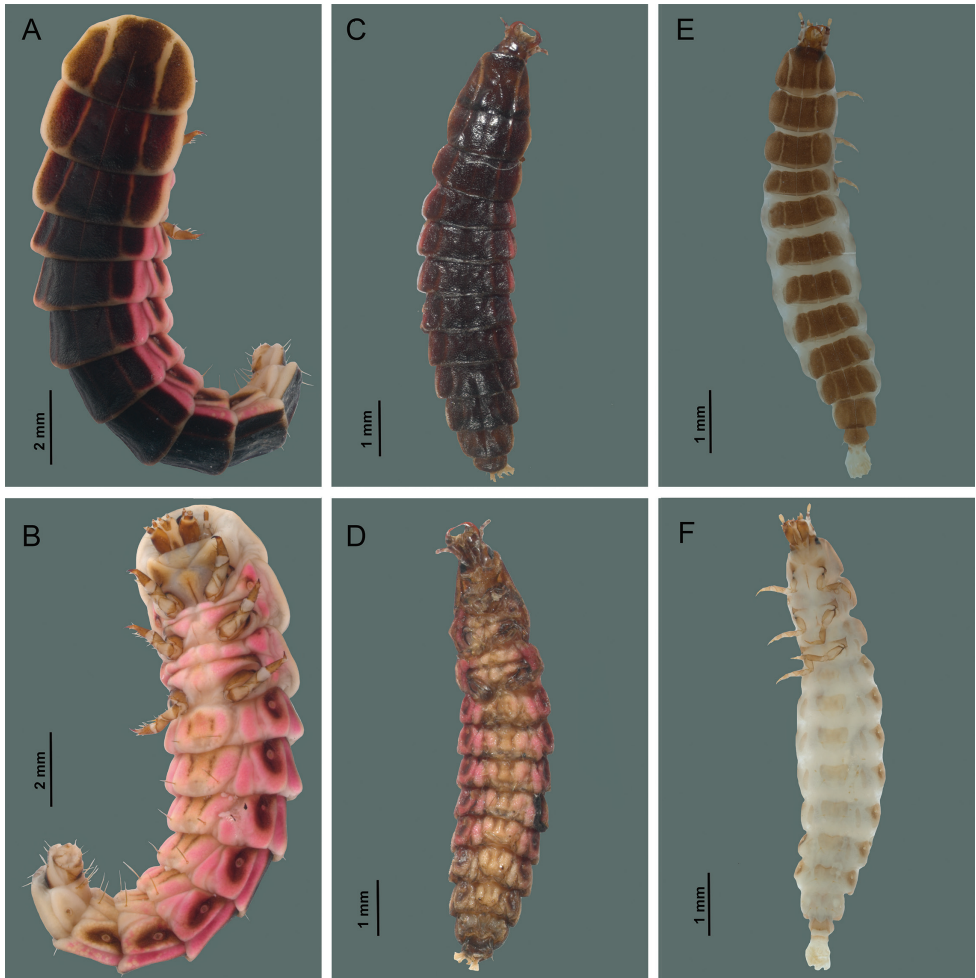


Figure 6. *Photinus extensus* Gorham **A** instar 6 in dorsal view **B** instar 6 in ventral view **C** instar 3 in dorsal view **D** instar 3 in ventral view **E** instar 1 in dorsal view **F** instar 1 in ventral view.

Maxilla. Consisting of five parts, attached to lateral margins labium forming a maxillo-labial complex. Cardo elongate, irregular shape, with four setae in ventral surface, on long setae in posterior margin. Stipes elongated, ventrally covered with erect setae, with three long stout setae placed radially on the ventral apical region. Galea present, with two segments, the first longer and stouter than the apical, which is triangular (Fig. 7C, D). Lacinia covered with brush of long setae on outer lateral margin. Maxillae with three-segmented palpi, basal segment long (0.57–0.71 mm; 0.66 ± 0.06 mm) covered by setae in mid-region, segment II wider (0.30–0.40 mm; 0.35 ± 0.04 mm) than long (0.12–0.16 mm; 0.14 ± 0.01 mm); apical segment cylindrical (0.10–0.14 mm; 0.12 ± 0.01 mm) with numerous setae from base to mid region; (Figs 7E, F, 8C, D).

Labium. Closely attached to maxilla, formed by prementum, mentum and postmentum. Prementum heart-shaped, surface covered with numerous short setae and two long setae close apex; labial palpi with two segments, basal palp subquadrate with few setae in mid-region, distal palp conical without setae; mentum with one pair of setae on anterior third and one pair of setae on posterior third; postmentum elongate, slightly sclerotized at the medial base, laterally united by membranes to the cardines; with a setae on each side near the base.

Mandible. Symmetrical, falcate, strongly sclerotized, with an internal channel opening subapically on outer edge. Penicillus well-developed. Retinaculum short and rounded, present only as a blunt protuberance on basal third of the mandible. Densely covered by fine setae on the external margins basely, basal half on inner margin of mandible covered with a brush of stout setae, being longest on the retinaculous protuberance (8E, F); mesal margin serrate.

Thorax. Protergum wider (2.43–3.81 mm; 3.14 ± 0.57 mm) than long (1.54–2.59 mm; 2.11 ± 0.43 mm), subsemicircular, wider posteriorly, rounded at posterolateral corners, covering the retracted head. Meso- and metatergum subrectangular three times wider than long, delimited by a pleural suture elongate barely evident from the laterotergites. Lateral areas of meso and metathorax scarcely sclerotized, composed of two laterotergites, the anterior with a well-developed spiracle on the mesothorax. Episterna extending from the anterior part to the lateral part of the coxae; epimeron forming a little sclerotized stripe, parallel to the coxae.

Legs. Pentamerous, the first pair of forelegs slightly shorter than the second and third. Coxae short (0.76–1.16 mm; 0.98 ± 0.18 mm), cylindrical, widely separated at the base, decumbent; coxal-trochanteric membrane reaching about 1/3 of the coxal length. Trochanters pentagonal, joining the femur obliquely (0.51–0.82 mm; 0.71 ± 0.13 mm). Femur narrow and cylindrical in lateral view. Tibiotarsus narrowing distally with stout setae. All legs with a double row of long setae in the inner margin, numerous short setae in the outer margin; pretarsus claw-like with two setae at base (Figs 7G, H, 8G).

Abdomen. Tergites III–IX of similar length (0.86–1.36 mm; 1.09 ± 0.17 mm), width almost constant; segments I–VIII (or I–VII) wider than long, bearing a pair of long stout setae posterolaterally, with laterotergites at each side, with sclerotized plates containing the spiracles; ventral area of segments I–VIII with sternal areas almost squared, slightly pigmented, sternites with two long setae in mid-region; sternal medial area margined by laterosternites – sometimes pigmented, elongate, narrow, and paired, delimited by laterotergites dorsally, and ventrally by a medial sternal plate; ventral area of segment IX with a simple plate, without area differentiation; light organ present and segment VIII indistinct; abdomen ending with a series of eversible filaments (pygopodia) bifurcate at the apex, at least 30 pygopodia arise from 12 basal stalks which may branch more than once (the dorso and ventrolateral stalks branch into three); densely packed recurved hooks occur on the ventrolateral surface of each exerted pygopod and completely covering at apex, with toothed scales on the dorsolateral surface only on anterior half. (Fig. 9A–G).

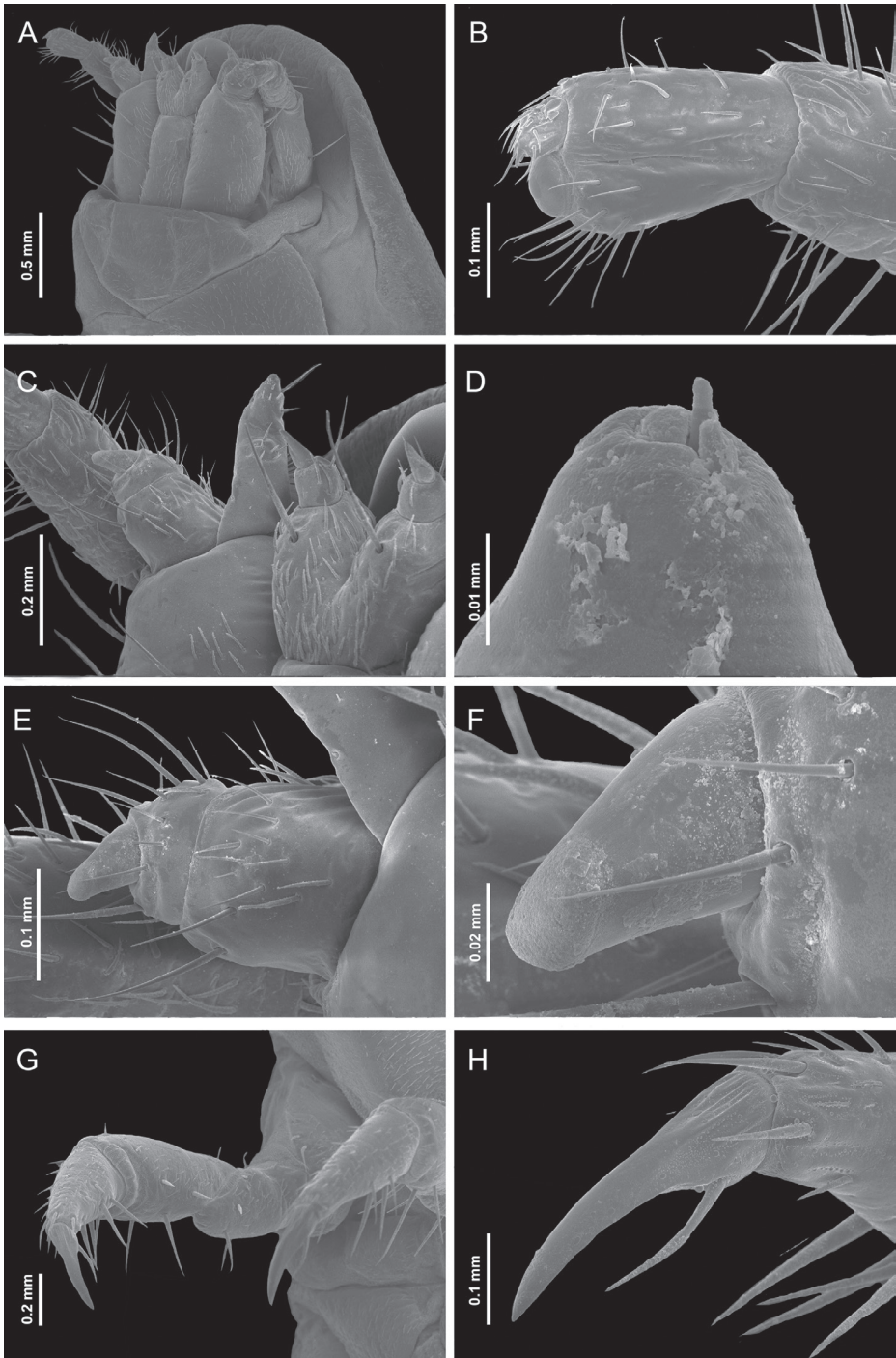


Figure 7. Sixth instar of *Photinus extensus* Gorham **A** SEM image of the head retracted and anterior part of prothorax in lateroanterior view **B** antennae **C** prementum, maxillary palpus and galea (lateroventral) **D** distal part of galea **E, F** maxillary palpi in ventrolateral view **G** right metathoracic leg in ventrolateral view **H** pretarsus.

Third instar larva (Fig. 6C, D). Description. Similar to sixth instar. Length 11.45–13.78 mm. **Head capsule.** Wider (0.82–0.96 mm; 0.92 ± 0.05 mm) than long (0.57–0.85 mm; 0.71 ± 0.12 mm). **Antenna.** Basal antennomere and second antennomere (0.28–0.35 mm; 0.32 ± 0.02 mm), and a third segment (the flagellum) (0.15–0.21 mm; 0.18 ± 0.02 mm). **Maxilla.** Maxillae with three-segmented palpi, basal segment long (0.34–0.54 mm; 0.43 ± 0.07 mm) covered by setae in mid region, segment II wider (0.30–0.43 mm; 0.36 ± 0.06 mm) than long (0.12–0.17 mm; 0.14 ± 0.02 mm); apical segment cylindrical (0.10–0.13 mm; 0.11 ± 0.01 mm). **Thorax.** Protergum wider (1.36–1.53 mm; 1.4 ± 0.06 mm) than long (1.18–1.68 mm; 1.3 ± 0.20 mm), trapezoidal. **Legs.** Coxae short (0.77–0.97 mm; 0.86 ± 0.08 mm), femur obliquely (0.43–0.60 mm; 0.52 ± 0.07 mm). **Abdomen.** Tergites III–IX (0.68–0.85 mm; 0.77 ± 0.045 mm) ventral area of segments I–VIII with sternal areas almost squared, slightly pigmented, sternites with two long setae in mid-region.

First instar larva (Fig. 6E, F). Description. Similar to sixth instar. Length 3.72–8.80 mm; after hatching, the first instar body does not appear sclerotized to the degree found in later instars. **Head capsule.** Wider (0.48–0.72 mm; 0.6 ± 0.10 mm) than long (0.24–0.51 mm; 0.38 ± 0.12 mm), s (Figs 6A and 7A).

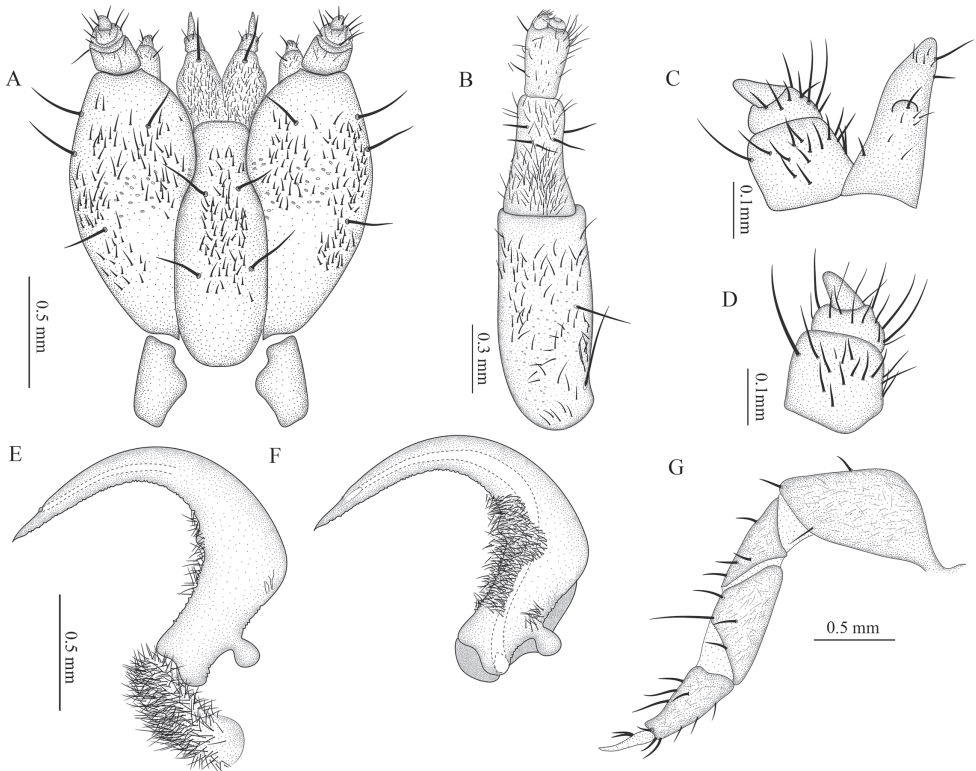


Figure 8. *Photinus extensus* Gorham, head structures of sixth instar larva **A** head capsule ventral view **B** right antenna, dorsal view **C** maxillary palpus and galea, ventral view **D** maxillary palpus, ventral view **E** mandible dorsal view **F** mandible ventral view and **G** leg dorsal view.

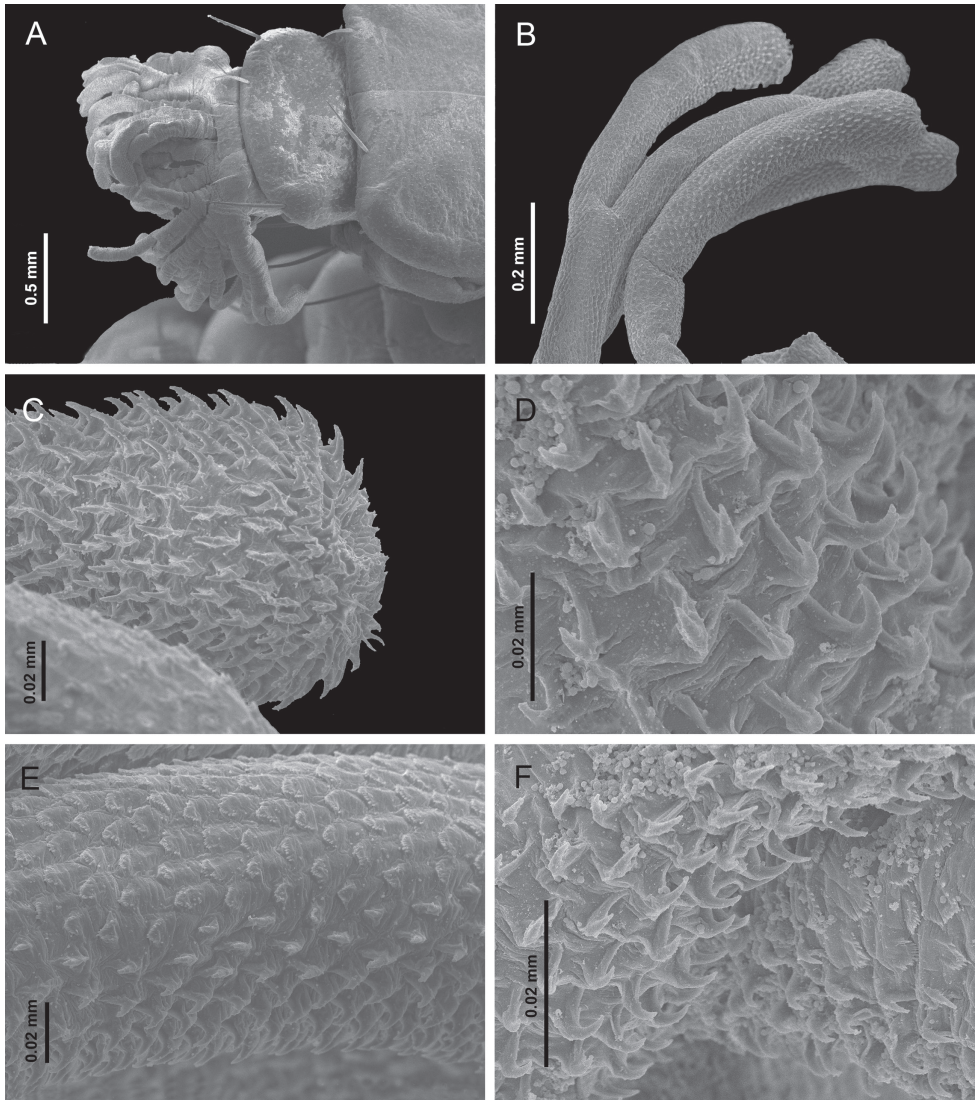


Figure 9. Sixth instar of *Photinus extensus* Gorham **A, B** SEM image of pygopodium in general view and detailed **C–F** detail of the surface of pygopodium.

Antenna. Basal antennomere and second antennomere (0.12–0.28 mm; 0.19 ± 0.06 mm) elongated, and a third segment (the flagellum) short (0.08–0.17 mm; 0.12 ± 0.03 mm). **Maxilla.** Maxillae with three-segmented palpi; basal segment long 0.24–0.47 mm; 0.31 ± 0.08 mm) and well-defined, segment II wider (0.12–0.17 mm; 0.15 ± 0.01 mm) than long (0.05–0.07 mm; 0.06 ± 0.007 mm); apical segment (0.03–0.047 mm; 0.037 ± 0.007 mm). **Labium.** Postmentum elongate, slightly sclerotized at the medial base, laterally united by membranes to the cardines; with a setae on each side near the base.

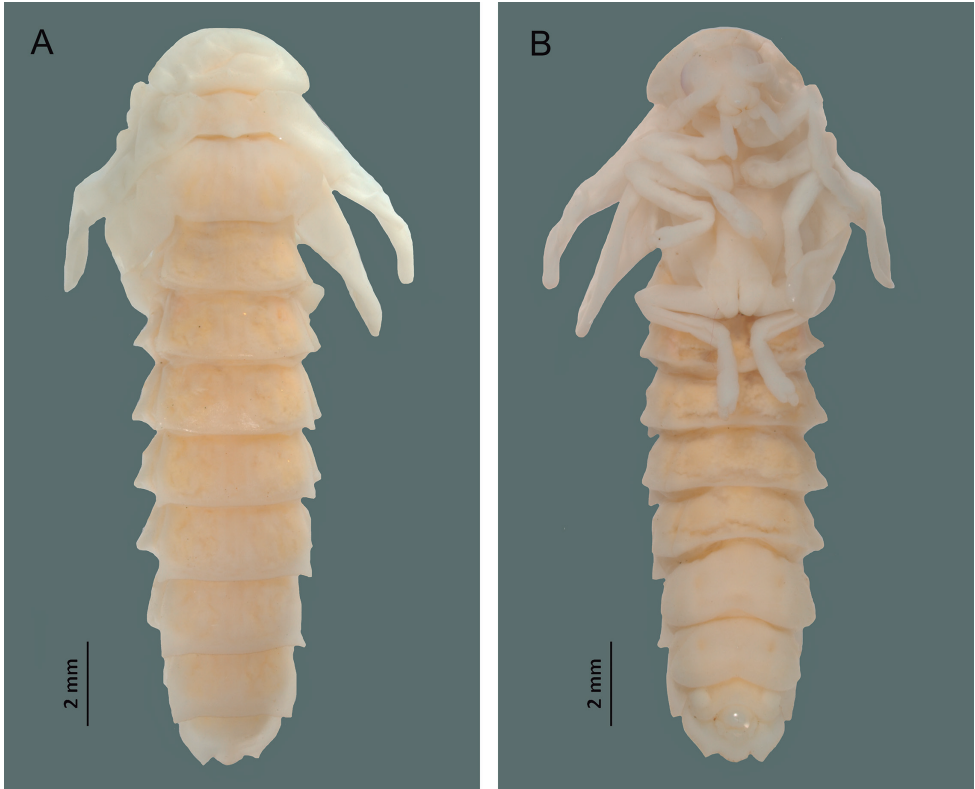


Figure 10. *Photinus extensus* Gorham **A** pupa in dorsal view **B** pupa in ventral view.

Thorax. Protergum wider (0.73–1.47 mm; 0.94 ± 0.21 mm) than long (0.51–0.75 mm; 0.53 ± 0.09 mm). **Legs.** Coxae short (0.44–0.65 mm; 0.53 ± 0.08 mm), femur obliquely (0.21–0.34 mm; 0.27 ± 0.05 mm). **Abdomen.** Tergites III–IX (0.31–1.2 mm; 0.74 ± 0.28 mm).

Pupa, male (Fig. 10A, B). Length 17–23 mm; width 6–7 mm. Body elongate, curved, ventrally concave, pale yellowish (sternites I–VIII slightly pigmented at the ends).

Head. Totally covered by the pronotum in dorsal view. Large eyes, located at the sides of the head; antennae in front of the eyes, nearer the frontal center, mouthparts visible in ventral view.

Thorax. Pronotum wider than long, semicircular, totally covering the head. Meso and metanotum shorter, subrectangular, bearing the elytra sideways. All pairs of legs free, visible in ventral view. Spiracles present in the pleural areas of mesothorax.

Abdomen. Abdominal segments subrectangular, wider than long, spiracles present on abdominal pleural areas of segments I–VIII. Light organ on sternites V–VI.

Life cycle (Fig. 11). In their natural habitat, adults of *P. extensus* are active from early July, when the first males can be observed. Bioluminescent activity begins at dusk,

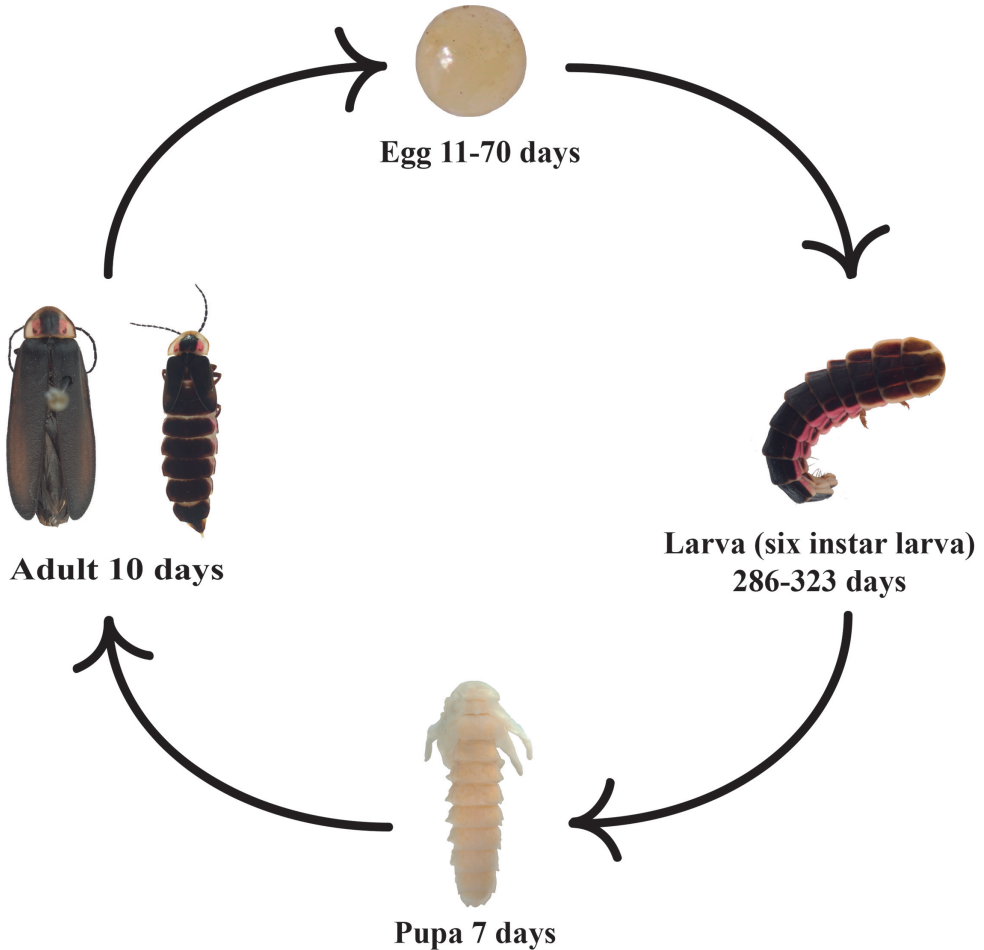


Figure 11. Life cycle of *Photinus extensus* Gorham.

at approximately 20:00 h, and diminishes considerably an hour later. Male flight does not exceed 2 m in height. Females are brachypterous and perch in the undergrowth approximately 50 cm from the ground. Males flash every 4.5 seconds, flying in an arc when illuminated. When males detect a female, they wait for an intense flash as a response, which is brief. The flash intervals are of 10 to 20 seconds. Males react by flying lower and towards the female. Groups of 3 to 5 males commonly compete with each other to get the female first, to mate with her. Two types of competition were observed among males: 1) a mating ball: four or more males cover the copulating pair and try to dislodge the copulating male to gain access to the female, and 2) males using their pronotum as a lever to pry a copulating male from the female. In the laboratory, copulation was observed to last from between 2 to more than 4 hours.

During oviposition, females bend their abdomen and place the apical part of it on the substrate. Eggs are laid superficially or buried, randomly distributed, individually,

or in groups (up to aggregates of 50). The number of eggs deposited by each female varied from three to 198. Eggs emit a faint bioluminescence since they are oviposited, which is only perceptible to the human eye in complete darkness. In total, 956 eggs from 13 females were obtained.

Under lab condition *P. extensus* completed its development in approximately 12 months, from oviposition to imago. The egg stage under laboratory conditions had a duration of 11 to 70 days, with mortality of $n = 144$ eggs (15%).

Photinus extensus undergoes six similar larval instars that differ in both size and color (Fig. 4). Cannibalism among larvae during rearing was not observed. The only food larvae consumed was the earthworms provided. There was no synchronization among larvae during the progression of larval instars, which started at the end of August until the beginning of July. In captive conditions, the process of ecdysis from one stage to the other varied among individuals. The first larval instar had a duration of 14 to 153 days, where mortality was 60% ($n = 491$) among the eggs that hatched. The second larval instar had a duration of 14 to 172 days, with mortality of 61% ($n = 199$). The third larval instar had a duration of 15 to 140 days; mortality was 71% ($n = 87$). The fourth larval instar had a duration of 17 to 140 days, with a mortality of 52% ($n = 20$). The fifth larval instar had a duration of 24 to 192 days ($n = 18$) and the last larval instar had a duration of 53 days ($n = 8$). Pupation had a duration of 7 days in July, and according to the observations in the field, pupae were found under pyroclastic rocks.

Discussion

Photinus extensus has six instars; they are very similar and only differ in size, color and the degree of the body sclerotized and presence of setae. Instar III differs from I and VI by a trapezoidal pronotum (Fig. 5) and an exposed head. The periods of time of the instar I–V are variable in different specimens, ranging from 14 and 192 days; the last instar period in different specimens is constant, approximately 50 days; the pupa is completely developed in seven days.

Frequently, the identification and description of larvae in the tribe Photinini is based on the characters present in the final larval instar, mostly body shape, color pattern, head capsule features, and the morphology of mouthparts (Archangelsky 2010). There are both similarities and differences between larvae belonging to the tribe Photinini, including *P. extensus* (see Table 1). The larval character suite found in *P. extensus* is most similar to those found in *Pyraconema*, *Lucidota*, and *Pyropyga*. The major exception to this is the number of segments in the maxillary palp. Although this last character is shared with the genus *Phosphaneus*, it differs in the opening of the mandible channel. *P. extensus* differs from *Lucidina* in the number of segments in the maxillary palp, and the number of retinacula of the mandible. There are some patterns among the larvae described in Photinini; the shape of the body is narrow and parallel and the pronotal shape is semicircular or semioval and the opening of the mandible channel is at the inner margin subapical.

Table 1. Morphological larval characters of known Photinini genera (after Archangelsky 2010, Kawashima 2017 and Novák 2018b).

Character	<i>Pyrractonema nigripennis</i> Solier	<i>Pyropyga nigricans</i> (Say)	<i>Lucidota atra</i> Olivier	<i>Lucidina accensa</i> Gorham	<i>Phosphaenus hemipterus</i> (Goeze)	<i>Photinus extensus</i> Gorham
Body shape	Narrow, parallel 5.7–6.1× longer than narrow	Narrow, parallel	Narrow, parallel	Wide, suboval 4.2× longer than narrow	Oblong and narrow ~4.5× longer than narrow	Narrow, parallel ~5× longer than narrow
Ratio: body length/thoracic length	2.8–3.1	3.4–3.7	3.4–3.7	2.6	3.14	2.9
Cephalic capsule	Short and wide, retractable into the thorax	Short and wide, retractable into the thorax	Short and wide, retractable into the thorax	Subquadrate, moderately flattened dorso-ventrally.	Rectangular, retractable into the thorax	Short and wide, retractable into the thorax
Antennae	Wide, partially retracted into the head	Wide, partially retracted into the head	Wide, partially retracted into the head	Long and thin, completely retracted into the head	Long and thin, partially retracted into the head	Long and thin, partially retracted into the head
Opening of the mandible channel	At the exterior margin, subapical	At the exterior margin, subapical	At the exterior margin, subapical	At the exterior margin, subapical	At the exterior margin, subapical	At the exterior margin, subapical
Number of retinacula of the mandible	1	1	2	4	1	1
Maxillar palp	Three palpomere	Three palpomere	Three palpomere	Two palpomere	Two palpomere	Four palpomere
Shape of pronotum	subcircular	subcircular	subcircular	subcircular	subcircular	suboval
Shape of mesonotum	sub oval	sub oval	sub oval	trapezoidal	sub oval	rectangular
Shape of metanotum	sub oval	sub oval	sub oval	rectangular	sub oval	rectangular
Thorax color	Dark with three pale, longitudinal, and subparallel lines	Dark with three pale, longitudinal and subparallel lines	Dark with three pale, longitudinal and subparallel lines	Almost blackish brown, lateral and hind margins more or less paler than the ground Subrectangular	dorsally dark reddish-brown, ventrally pink/ochre/light brown with darker plates on laterotergites and sternum	Dark, with pale stripes
Shape of the abdominal tergites	Subrectangular, except VII–IX subsquared	Suboval	Suboval, posterior margin of tergites V–VIII straight	Subrectangular	I–VII, IX subrectangular, VIII suboval	Subrectangular
Abdomen color	With a clear line on each side. Dark segments VII–IX.	Dark with pale lateral areas (segments I–VIII)	Dark with three pale longitudinal and subparallel lines, at the inner interior margin	Almost blackish brown, lateral and hind margins more or less paler than the ground I–VI, segments VII–X pale yellowish to milky white	pink/ochre/light brown	Pale with a little pink stripe in the second third in segments I–V, the rest of them pale

The distribution of the setae is different between genera (Table 2), chaetotaxy will be useful in Lampyridae as a tool to distinguish between immatures, also as a source of informative phylogenetic characters (Ballantyne et al. 2019; Riley et al. 2021; Vaz et al. 2021). However, the few studies on the morphology of immatures in Lampyridae and the lack of knowledge of chaetotaxy hinder comparison between fireflies and makes the elaboration of more detailed hypotheses very difficult.

Table 2. Chaetotaxy larval characters.

	<i>Photinus extensus</i> Gorham	<i>Pyrractonema nigripennis</i> Solier	<i>Lucidota atra</i> Olivier
Hypopharynx	Margin covered by dense pubescence.	Surface covered by dense pubescence.	No information.
Mandible	With patches of dense pubescence in the basal part in ventral Margin covered by dense pubescence. With patches of dense pubescence in the basal part in ventral view. Mid-region covered by a single row of long setae.	With patches of dense pubescence in ventral view. Mid-region covered by only one row of setae.	Mid-region covered by only one row of long setae. One long seta close to the apex.
Cardo	With 4 long setae in ventral surface and one long seta in the posterior margin.	With 13–15 setae in ventral surface.	Without setae.
Maxillary palpomeres	Basal palp covered by setae in the mid region. Distal palp with setae from base to mid region.	Basal palp covered by setae. Palp II with some setae. Last palp without setae.	Basal palp with long setae from the mid region to the apex. Palp II with shorter setae. Distal palp without setae.
Labial palpomeres	Basal palp with few setae in mid region. Distal palp without setae.	Basal palp with some setae. Distal palp without setae.	Basal palp with few long setae. Distal palp with one long seta.
Prementum	Surface with many setae. Two long setae close to apex.	Dorsal and ventral surface with many setae.	With two basal regions of very fine setae, with longer setae on the palp segment.
Submentum	With two long setae in mid region.	With two long setae in the basal middle.	No information.
Antennomeres	Apex with two long setae. Antennomere III with long setae from base to apex.	All antennomeres covered by setae. Antennomere III with many short setae.	Basal antennomer with mid region covered by setae. Anterior region with longer setae. Antennomere II covered evenly by long setae. Antennomere III with short setae.
Legs	With a double row of long setae in the inner margin. Outer margin with many setae. Pretarsus with two setae at the base.	With a double row of long setae in the inner margin. Pretarsus with two setae at the base.	With a double row of long setae in the inner margin. Pretarsus with two setae at the base.
Abdomen	Sternites with two long setae in mid-region.	Sternites with two long setae in mid-region.	No information.

The larval characters have shown to be important to clarify the phylogenetic relationships as Archangelsky (2010) mentioned. However, it seems to be a difficult task to get a good dataset of larval characters of Lampyridae.

The life cycle, morphology, and behavior of the species of *Photinus* are similar. *Photinus carolinus* Green, 1956, *P. ignitus* Fall, 1927, *P. marginellus* LeConte, 1852, *P. pyralis* (Linnaeus, 1767), *P. greeni* Lloyd, 1969, and *P. extensus* are the known species that produce spermatophores due to the prolonged time of copulation (Cratsley et al. 2003; South and Lewis 2012).

The length of the pupal stage varies slightly in *Photinus*. The pupal stage of *P. extensus* and *P. carolinus* has a duration of six days (Faust 2010). Nevertheless, the pupa of *P. carolinus* is present during May, while that of *P. extensus* is present in July. Another difference is that the pupae of *P. extensus* observed in the field were found under pyroclastic rocks, in contrast with *P. carolinus*, which has been reported to occur under leaf-litter, near rotten logs, or moss (Faust 2010). Until now, little information has come to light about the pupae in other genera of Photinini (Archangelsky and Branham 2001). In other genera like *Aspisoma* Laporte, 1833, of Cratomorphini, the pupal stage is similar, occurring during a short period between six and ten days (Costa et al. 1988; Archangelsky 2004).

Conclusion

The complete life cycle of *Photinus extensus*, including descriptions of egg, larvae, and pupa, was documented for the first time. Larvae were reared in laboratory conditions to the adult stage from eggs. The six instar of *P. extensus* are very similar; they differ only in size and in the sclerotized degree.

Among Photinini larvae there are not many differences, differing in the number of segments in the maxillary palp and in the number of retinacula of the mandible; the shape of the body and pronotum, and the opening of the mandible channel follow a similar pattern. Life cycle information is essential to carry out protection and conservation actions for insects that are very sensitive to environmental changes, like fireflies. For example, the species that do not produce light are easily overlooked and the information about their life cycle is deficient. This results in “Data Deficient” categorization in evaluations of extinction risk. Thus, more studies are needed in which the life history, habitat associations, and microhabitat are detailed (Fallon et al. 2021). Also, it is necessary to understand that requirements of larvae are different to those of adults to have an integral vision in the actions of protection of the fireflies.

Acknowledgements

We thank Susana Guzmán (IBUNAM) for help with the use of the Zeiss equipment, and Berenit Mendoza (IBUNAM) for the electron micrographs. We are grateful to Marc A. Branham and Sarah Sander Lower for their work correcting the English text in the manuscript and their valuable comments. We also thank Simone Policena Rosa, Luiz Silveira and Oliver Keller for helping to improve the manuscript. We thank the Natural History Museum of London, Michael Geiser and Keita Matsumoto for providing photographs of the lectotype. MLZG, DEDL, PCR and IGGC field work; IGGC and DEDL designed the breeding method; DEDL, IGGC, MGR and VVB laboratory work; SZC and IGGC identified the species; VVB, MGR, GMRM and MAR produced the photographs. SLP and DEDL constructed tables 1 and 2. All authors wrote the manuscript, revised it, and discussed the data.

References

- Archangelsky M (2004) Description of the last larval instar and pupa of *Aspisoma fenestrata* Blanchard, 1837 (Coleoptera: Lampyridae) with brief notes on its biology. *Tijdschrift voor Entomologie* 147(1): 49–55. <https://doi.org/10.1163/22119434-900000138>
- Archangelsky M (2010) Larval and pupal morphology of *Pyraclonema nigripennis* Solier (Coleoptera: Lampyridae: Photinini) and comparative notes with other Photinini larvae. *Zootaxa* 2601(1): 37–44. <https://doi.org/10.11646/zootaxa.2601.1.3>

- Archangelsky M, Branham MA (2001) Description of last instar and pupa of *Pyropyga nigricans* (Coleoptera: Lampyridae, Photinini) and comparison with larvae of other Photinini genera. *Canadian Entomologist* 133(2): 155–164. <https://doi.org/10.4039/Ent133155-2>
- Ballantyne LA, Lambkin CL, Ho J-Z, Jusoh WFA, Nada B, Nak-Eiam S, Thancharoen A, Wattana-chaiyingcharoen W, Yiu V (2019) The Luciolinae of S. E. Asia and the Australopacific region: a revisionary checklist (Coleoptera: Lampyridae) including description of three new genera and 13 new species. *Zootaxa* 4687(1): 1174. <https://doi.org/10.11646/zootaxa.4687.1.1>
- Beutel RG (1995) Phylogenetic analysis of Elateriformia (Coleoptera: Polyphaga) based on larval characters. *Journal of Zoological Systematics and Evolutionary Research* 33(3–4): 145–171. <https://doi.org/10.1111/j.1439-0469.1995.tb00969.x>
- Branham MA (2010) Lampyridae Latreille, 1817. In: Leschen RAB, Beutel GR, Lawrence JF (Eds) *Coleoptera, Beetles. Volume 2: Morphology and Systematics (Elateroidea, Bostrichiformia, Cucujiformia partim)*. Walter de Gruyter, Berlin, Germany, 141–149. <https://doi.org/10.1515/9783110911213.141>
- Branham MA, Archangelsky M (2000) Description of the last larval instar and pupa of *Lucidota atra* (G.A.Olivier, 1790) (Coleoptera: Lampyridae), with a discussion of abdominal segment homology across life stages. *Proceedings of the Entomological Society of Washington* 102(4): 869–877.
- Bugnion E (1929) Le ver-luisant provençal et la Luciole nicoise. *Association des Naturalistes de Nice et des Alpes-Maritimes; Memoire Supplement au "Riviera Scientifique"*, 131 pp.
- Buschman LL (2017) Analysis of courtship flash behaviour in two *Photuris* fireflies (Coleoptera: Lampyridae) with field validation and rearing notes. In: Day JC (Ed.) *Lampyrid: The Journal of Bioluminescent Beetle Research*. Abingdon, CreateSpace Independent Publishing Platform, 1–19.
- Costa C (2000) Estado de conocimiento de los Coleoptera neotropicales. In: Martín-Piera F, Morrone JJ, Melic A (Eds) *Hacia un proyecto CYTED para el inventario y estimación de la diversidad entomológica en iberoamérica: Pribes 2000*. Sociedad Entomológica Aragonesa, Zaragoza, 99–114.
- Costa C, Vanin SA, Casari-Chen SA (1988) *Larvas de Coleoptera do Brasil*. Museu de Zoologia, Universidad de Sao Paulo, Brazil, 282 pp. <https://doi.org/10.5962/bhl.title.100233>
- Cratsley CK, Rooney JA, Lewis SM (2003) Limits to nuptial gift production by male fireflies, *Photinus ignitus*. *Journal of Insect Behavior* 16(3): 361–370. <https://doi.org/10.1023/A:1024876009281>
- Demary K (2005) Sperm storage and viability in *Photinus* fireflies. *The Journal of Physiology* 7: 837–841. <https://doi.org/10.1016/j.jinsphys.2005.04.001>
- Fallon CE, Walker AC, Lewis S, Cicero J, Faust L, Heckscher CM, Pérez-Hernández CX, Pfeiffer B, Jepsen S (2021) Evaluating firefly extinction risk: Initial red list assessments for North America. *PLoS ONE* 16(11): 1–18. <https://doi.org/10.1371/journal.pone.0259379>
- Faust LF (2010) Natural history and flash repertoire of the synchronous firefly *Photinus carolinus* (Coleoptera: Lampyridae) in the great Smoky Mountains National Park. *The Florida Entomologist* 93(2): 208–217. <https://doi.org/10.1653/024.093.0210>

- Faust LF (2017) Fireflies, glow-worms, and lightning bugs: identification and natural history of the fireflies of the Eastern and Central United States and Canada. Athens (GA), University of Georgia Press, USA, 356 pp.
- Faust LF, Weston PA (2009) Degree-day prediction of adult emergence of *Photinus carolinus* (Coleoptera: Lampyridae). *Environmental Entomology* 38(5): 1505–1512. <https://doi.org/10.1603/022.038.0519>
- Ferreira VS, Keller O, Branham MA (2020) Multilocus phylogeny support the nonbioluminescent firefly Chespirito as a new subfamily in the Lampyridae (Coleoptera: Elateroidea). *Insect Systematics and Diversity* 4(6): 1–13. <https://doi.org/10.1093/isd/ixaa014>
- Fu X, Ballantyne LA, Lambkin CL (2012) The external larval morphology of aquatic and terrestrial Luciolinae fireflies (Coleoptera: Lampyridae). *Zootaxa* 3405(1): 1–34. <https://doi.org/10.11646/zootaxa.3405.1.1>
- Kawashima I (2017) Larval morphology of the lampyrine species, *Lucidina accensa* Gorham (Coleoptera: Lampyridae: Lampyrinae) from Honshū, Japan. *Japanese journal of systematic entomology = 日本昆虫分類学会会報*, 23(1): 129–134.
- Koken M, Guzmán-Álvarez JR, Gil-Tapetado D, Romo Bedate MA, Laurent G, Rubio L, Rovira Comas S, Wolfler N, Verfaillie F, De Cock R (2022) Quick spreading of populations of an exotic firefly throughout Spain and their recent arrival in the french Pyrenees. *Insects* 13(2): e148. <https://doi.org/10.3390/insects13020148>
- Lewis SM, Cratsley CK, Demary K (2004a) Mate recognition and choice in *Photinus* fireflies. *Annales Zoologici Fennici* 41: 809–821.
- Lewis SM, Crastley CK, Rooney JA (2004b) Nuptial Gifts and Sexual Selection in *Photinus* Fireflies. *Integrative and Comparative Biology* 44(3): 234–237. <https://doi.org/10.1093/icb/44.3.234>
- Lewis SM, Wong CH, Owens A, Fallon C, Jepsen S, Thancharoen A, Wu C, De Cock R, Novák M, López-Palafox T, Khoo V, Reed JM (2020) A Global Perspective on Firefly Extinction Threats. *Bioscience* 70(2): 157–167. <https://doi.org/10.1093/biosci/biz157>
- Lloyd JE (2002) Family 62. Lampyridae. In: Arnett Jr RH, Thomas MC, Skelley PE, Frank JH (Eds) *American Beetles vol. 2: Polyphaga: Scarabaeoidea through Curculionoidea*. CRC Press, Boca Raton, Florida, 187–196.
- López-Palafox T, Macías-Ordóñez R, Cordero CR (2020) The size of signal detection and emission organs in a synchronous firefly: Sexual dimorphism, allometry and assortative mating. *PeerJ* 8: e10127. <https://doi.org/10.7717/peerj.10127>
- Lot A, Camarena P (2009) El Pedregal de San Ángel de la ciudad de México: reserva ecológica urbana de la Universidad Nacional. In: Lot A, Cano-Santana Z (Eds) *Biodiversidad del ecosistema del Pedregal de San Ángel. Libro conmemorativo del 25*, 19–25.
- Madruga O, Branham MA (2020) Description of life cycle and preimaginal stages of *Alecton discoidalis* Laporte, 1833 (Coleoptera: Lampyridae) under laboratory conditions. *Zootaxa* 4816(1): 81–91. <https://doi.org/10.11646/zootaxa.4816.1.4>
- Martin GJ, Stanger-Hall KF, Branham MA, Da Silveira LFL, Lower SE, Hall DW, Li XY, Lemmon AR, Lemmon EM, Bybee SM (2019) Higher-Level Phylogeny and Reclassification of Lampyridae (Coleoptera: Elateroidea). *Insect Systematics and Diversity* 3(6): 1–15. <https://doi.org/10.1093/isd/ixz024>

- McDermott FA (1964) The taxonomy of the Lampyridae. *Transactions of the American Entomological Society* 90: 1–72.
- Novák M (2018a) Redescription of immature stages of central European fireflies, Part 2: *Lamprohiza splendididula* (Linnaeus, 1767) larva, pupa and notes on its life cycle and behaviour (Coleoptera: Lampyridae). *Zootaxa* 4378(4): 516–532. <https://doi.org/10.11646/zootaxa.4378.4.4>
- Novák M (2018b) Redescription of immature stages of central European fireflies, Part 3: *Phosphaenus emipterus* (Goeze, 1777) larva, pupa and notes on its life cycle and behavior, with a key to three Central European lampyrid larvae (Coleoptera: Lampyridae). *Zootaxa* 4382(3): 450–464. <https://doi.org/10.11646/zootaxa.4382.3.2>
- Ohba N (2004) Flash communication systems of Japanese fireflies. *Integrative and Comparative Biology* 44(3): 225–233. <https://doi.org/10.1093/icb/44.3.225>
- Orozco-Segovia A, Gamboa de Buen A, Barrandas-Miranda VL (2009) La diversidad funcional de los ecosistemas. In: Lot A, Cano-Zantana Z (Eds) *Biodiversidad del Ecosistema en el Pedregal del San Ángel*. Universidad Nacional Autónoma de México, México, 295–316.
- Riley WB, Rosa SP, Lima da Silveira LF (2021) A comprehensive review and call for studies on firefly larvae. *PeerJ* 9: 1–24. <https://doi.org/10.7717/peerj.12121>
- Rzedowski J (1978) *Vegetación de México*, Limusa, México, 247–273.
- Silveira LFLd, Lima W, Fonseca CRVd, McHugh J (2022) *Haplocauda*, a new genus of fireflies endemic to the Amazon rainforest (Coleoptera: Lampyridae). *Insects* 13(1): e58. <https://doi.org/10.3390/insects13010058>
- South A, Lewis SM (2012) Effects of male ejaculate on female reproductive output and longevity in *Photinus* fireflies. *Canadian Journal of Zoology* 90(5): 677–681. <https://doi.org/10.1139/z2012-031>
- Vaz S, Lima da Silveira LF, Policena RS (2020) Morphology and life cycle of a new species of *Psilocladus* Blanchard, 1846 (Coleoptera, Lampyridae, Psilocladinae), the first known bromeliad-inhabiting firefly. *Papéis Avulsos de Zoologia* 24(special issue): 1–15. <https://doi.org/10.11606/1807-0205/2020.60.special-issue.24>
- Vaz SNC, Guerrazzi MC, Rocha M, Faust LF, Gabriel Khattar G, Mermudes JRM, Silveira LFL (2021) On the intertidal firefly genus *Micronaspis* Green, 1948, with a new species and a phylogeny of Cratomorphini based on adult and larval traits (Coleoptera: Lampyridae). *Zoologischer Anzeiger* 292: 64–91. <https://doi.org/10.1016/j.jcz.2021.01.002>
- Viviani VR (2001) Fireflies (Coleoptera: Lampyridae) from Southeastern Brazil: habitats, life history, and bioluminescence. *Annals of the Entomological Society of America* 94(1): 129–145. [https://doi.org/10.1603/0013-8746\(2001\)094\[0129:FCLFSB\]2.0.CO;2](https://doi.org/10.1603/0013-8746(2001)094[0129:FCLFSB]2.0.CO;2)
- Wing SR (1991) Timing of *Photinus collustrans* reproductive activity: finding a mate in time (Coleoptera: Lampyridae). *Coleopterists Bulletin* 45: 57–74.
- Zaragoza-Caballero S (2000) Cantharoidea (Coleoptera) de México. IV. Nuevos *Photinus* (Lampyridae) del estado de Morelos. *Dugesiana* 7(1): 1–17.
- Zaragoza-Caballero S (2005) Nuevas especies de *Photinus* (Coleoptera: Lampyridae: Photinini) de Jalisco, México. *Folia Entomologica Mexicana* 44(1): 75–82.
- Zaragoza-Caballero S (2007) A new species of *Photinus* (Coleoptera: Lampyridae: Photinini) from Jalisco, Mexico, with comments on intraspecific aedeagal variability and a key to the species of the subgenus *Paraphotinus*. *Zootaxa* 1437(1): 61–67.

- Zaragoza-Caballero S (2015) Nuevas especies de *Photinus* (Coleoptera: Lampyridae: Photinini) del bosque tropical caducifolio de Pacífico mexicano. *Revista Mexicana de Biodiversidad* 86(3): 638–651. <https://doi.org/10.1016/j.rmb.2015.08.001>
- Zaragoza-Caballero S (2017) Nuevos *Photinus* Laporte, 1832 (Coleoptera: Lampyridae: Photinini). *Dugesiana* 24(2): 221–230. <https://doi.org/10.32870/dugesiana.v28i2.7161>
- Zaragoza-Caballero S, Viñolas A (2018) *Photinus immigrans* sp. nov. (Coleoptera: Lampyridae: Photinini): Primer registro del género *Photinus* en Cataluña, España. *Revista gaditana de Entomología* 9(1): 273–286.
- Zaragoza-Caballero S, López-Pérez S, Vega-Badillo V, Domínguez-León DE, Rodríguez-Mirón GM, González-Ramírez M, Gutiérrez-Carranza IG, Cifuentes-Ruiz P, Zurita-García ML (2020) Luciérnagas del centro de México (Coleoptera: Lampyridae): descripción de 37 especies nuevas. *Revista Mexicana de Biodiversidad* 91(0): 1–70. <https://doi.org/10.22201/ib.20078706e.2020.91.3104>

Reconnecting research and natural history museums in Italy and the need of a national collection biorepository

Franco Andreone¹, Ferdinando Boero², Marco A. Bologna³,
Giuseppe M. Carpaneto³, Riccardo Castiglia⁴, Spartaco Gippoliti⁵,
Bruno Massa⁶, Alessandro Minelli⁷

1 Museo Regionale di Scienze Naturali, Via G. Giolitti, 36, I-10123 Torino, Italy **2** Università di Napoli Federico II, CNR-IAS, Stazione Zoologica Anton Dohrn, Villa Comunale, I-80121 Napoli, Italy **3** Dipartimento di Scienze, Università Roma Tre, Viale G. Marconi, 446, I-00146 Roma, Italy **4** Dipartimento di Biologia e Biotecnologie “Charles Darwin”, Università “La Sapienza” di Roma, Via A. Borelli, 50, I-00161 Roma, Italy **5** Società Italiana per la Storia della Fauna “Giuseppe Altobello”, Viale Liegi, 48A, I-00198 Roma, Italy **6** Dipartimento di Scienze agrarie, alimentari e forestali, Università di Palermo, Viale Scienze, 13, I-90128 Palermo, Italy **7** Dipartimento di Biologia, Università di Padova, Via Ugo Bassi, 58B, I-35131 Padova, Italy

Corresponding author: Franco Andreone (franco.andreone@regione.piemonte.it)

Academic editor: Pavel Stoev | Received 28 December 2021 | Accepted 18 May 2022 | Published 8 June 2022

<http://zoobank.org/2340A96C-380F-439E-8C79-CE28C322D0EE>

Citation: Andreone F, Boero F, Bologna MA, Carpaneto GM, Castiglia R, Gippoliti S, Massa B, Minelli A (2022) Reconnecting research and natural history museums in Italy and the need of a national collection biorepository. ZooKeys 1104: 55–68. <https://doi.org/10.3897/zookeys.1104.79823>

Abstract

In Italy, differently from other countries, a national museum of natural history is not present. This absence is due, among other reasons, to its historical political fragmentation up to 1870, which led to the establishment of medium-sized museums, mostly managed by local administrations or universities. Moreover, a change of paradigm in biological research, at the beginning of the 20th century, contributed to privilege experimental studies in universities and facilitated the dismissal of descriptive and exploratory biology, which formed the basis of the taxonomic research carried out by natural history museums. Consequently, only a few museums have a provision of curatorial staff, space and material resources adequate to maintain their original mission of discovering the natural world, by conducting a regular research activity accompanied by field campaigns. The creation of a national research centre for the study of biodiversity, facilitating interconnections among the existing natural history museums could be a solution and is here supported, together with a centralised biorepository to host collections and vouchers, to the benefit of current and future taxonomic research and environmental conservation. Such an institution should find place and

realisation within the recently proposed National Biodiversity Future Center (NBFC) planned within the National Plan of Recovery and Resilience (PNRR). Pending upon the creation of this new national centre, a network among the existing museums should coordinate their activities.

Keywords

Biodiversity, biogeography, biorepository, collections, conservation, national natural history museum, taxonomy

Natural history museums (hereafter “museums”) played and still play a crucial role in the discovery and description of the natural world (Davis 1996; Bakker et al. 2020). Their genesis and development vary largely across countries, mostly depending on a heterogeneous array of historical constraints and geopolitical aspects.

Current museums’ core missions include pivotal activities, among which: (a) gathering, preserving, digitalizing, and implementing scientific collections of natural objects, organisms, and parts of them; (b) exploring and monitoring biodiversity, discovering living beings, describing and interpreting wildlife in taxonomic, biogeographical, and ecological terms; and (c) disseminating scientific knowledge. In particular, museums are prominent hubs of taxonomic studies: with an estimate of eight million eukaryotic species present on Earth—of which barely two million are described today—intensive field surveys and taxonomic assessments are badly needed to fill the gap in the knowledge of our planet’s biodiversity, and, finally, to promote its conservation (Dubois 2003; Boero 2010; Costello et al. 2013). Museums share the primary mission of hosting natural history collections: these often include type series (specimens upon which taxa are described) and voucher series, which are useful to support the knowledge of species, including morphology, distribution, ecology, and evolution.

Many existing scientific collections were assembled by naturalists in the 18th and 19th centuries and, thus, also have a historical importance (Clemann et al. 2014; Camacho et al. 2018). As a general trait, collections form a sound scientific reference for present and future research, including studies to understand and interpret the geographic and genetic variation of the species and populations, as well as the changes in their distribution range. Beside this, museums have the commitment to conserve biodiversity, an objective representing a recent complement to the traditional ones and highlighting how biological conservation can profit from taxonomy, faunal and floral studies, and biogeography (Butler et al. 1998; McCarter et al. 2001; Dubois 2010; Engel et al. 2021). For all these aspects, museums can also be considered true “Alexandrine libraries”, where the knowledge of the natural world is made available to future generations (Funk et al. 2005; Rocha et al. 2014; Salick et al. 2014; Schilthuizen et al. 2015; Dubois 2017; Rohwer et al. 2022).

Sadly, although terms as “biodiversity” and “ecology” are frequently used in daily narrations and political programs, many museums—which should be the places where these ideas and programs are emphasised and made relevant (Massa, 2021)—are currently facing critical difficulties, in particular in assuring a constant census of the

planetary diversity and in warranting science dissemination (Alberch et al. 1994). Italy, in particular, is facing serious problems associated with the management of museums, as already highlighted by Andreone et al. (2014).

We believe that the absence of a national institution is particularly critical and associated to the absence of a relevant research activity. We strongly believe that Italy needs a national repository and/or a national centre to assure that taxonomic studies are pursued, together with voucher-collecting activity. In this contribution we provide a historical overview of the Italian situation and make some operative proposals.

The birth of Italian natural history museums and the historical background

We here summarise the historical aspects behind the formation of Italian museums, since probably not all readers are aware of the fluid geopolitical subdivision of the Italian territory from the period in which the first natural history collections appeared until Italian unification in 1870.

After the Congress of Vienna (1815), Italy was still divided into several dynastic territories belonging to foreign kingdoms or powerful local houses. Most of northern Italy was split between the Kingdom of Savoy-Sardinia (Piedmont, Liguria, and Sardinia) and Lombardy-Venetia (under the rule of the Austrian Empire), with minor entities such as the Duchy of Parma and Piacenza and the Duchy of Modena and Reggio (both under the rule of the Austrian Empire). Most of central Italy belonged to the State of the Church (from Romagna to Latium) or to the ancient Grand Duchy of Tuscany, while southern Italy was unified under the Kingdom of the Two Sicilies, ruled by the Hispanic branch of the Bourbon dynasty. The official birth of united Italy is dated 1861 but the almost complete union occurred only in 1870 after the Third Independence War and the occupation of Rome and Latium; Rome became the capital in 1871. After the First World War (1918), other north-eastern Italian territories were joined in the Kingdom of Italy.

The long-lasting fragmentation into small states and the lack of a political centralisation until 1870 was accompanied by the birth and affirmation of small to medium-sized natural history museums, together with the evident absence of a large, national museum. Some of the small museums were nevertheless precious for the study of natural diversity at regional level, for example, the natural history museum of Francesco Minà Palumbo (a collection of Sicilian animals, plants, minerals, and fossils he collected and the splendid drawings he painted on the Madonie Mountains from 1837 to 1899), the Royal Mineralogical Museum of Naples (established in 1801), and further collections that gave successively rise to larger natural history museums. Other museums, such as the one in Genoa, or those in Turin and Florence, reached an international importance in the last decades of the 19th century and contributed largely to the advancement of descriptive zoology and botany. In any case, the lack of a unified and independent nation hindered the appearance of a centralised institution for the high-level study of geo- and biodiversity and hampered the development of a nation-wide

natural history culture, rarely considered at the same level of humanities, likely also due to the scholastic “Croce-Gentile” reform of around a century ago (Tognon 2016).

Despite this structural deficiency, Italy was the first European country to complete a checklist of its fauna in 1995 (more than 55,000 species listed excluding protozoa; Minelli et al. 1993–1995), with numerous amendments and additions since then (Stoch et al. 2004) showing how provisional our knowledge of biodiversity is. A new online “Checklist” of Metazoa, including some 60,000 species, is now under construction (Bologna et al. 2022).

In other European countries (e.g., Austria, Belgium, Denmark, France, Spain, Sweden, and the United Kingdom), the existing national natural history museums always maintained relevant scientific activities. Other institutions, like the Naturalis Biodiversity Center in Leiden and the Museum für Naturkunde in Berlin, upgraded to new-concept popularization and biodiversity research hubs. In the New World too, the task of making collections and having care of them remained crucial for scientific research in museums. For instance, in the USA (and the whole Western Hemisphere) the American Mammalogical Society, through a Systematic Collections Committee, maintains a census of mammal specimens in qualified institutions to keep high standards of curation (Phillips et al. 2019), standards that are very far from the present Italian situation (Gippoliti et al. 2014). A similar situation is also present in Brazil, where the natural history collections are concentrated in three main national repositories (Museu Nacional - Universidade Federal do Rio de Janeiro, Museu de Zoologia da Universidade de São Paulo, and Museu Paraense Emílio Goeldi), but there are dozens of other natural history collections, mainly associated to universities (Bezerra 2012).

Whereas in the 19th century many Italian natural history museums propelled activities worldwide in the wake of positivism, the inspiration for taxonomic and exploratory studies suddenly faded at the beginning of the new century, despite the colonial research undertaken especially by museums in Genoa, Florence, and Milan (Gippoliti 2005; Chiozzi 2013; Poggi 2017). Thus, museums were increasingly seen as places for science education and outreach, but less as independent research centres. Furthermore, being mostly managed by local administrations (municipalities, regions) or universities, they did not benefit from autonomy and had difficulties in accessing national or international funds. University institutes too often forgot their connections with natural history museums and collections, and/or considered them as useless for modern experimental research. Due to this lack of interest, many universities also failed to care for the maintenance of systematic collections, often seen as obsolete forms of science.

Within this scenario we may already spot some of the difficulties experienced by Italian museums and herbaria in the new millennium: unable to coalesce into larger institutional networks, they were increasingly constrained by limited budgets, lack of space, and reduced personnel. For these reasons, biological surveys, voucher collecting, and collection purchase (which were instead priorities in museums of the 19th century) became rarer. At best museums survived as places where to preserve historical collections; when space was available, a few private collections were also accepted after their owners’ death. In some cases, the historical scientific collections were neglected or abandoned, a circumstance sadly shared by other European countries too (Krištufek et al. 2015; Ceríaco et al. 2021).

Research is a major engine for natural history museums

Due to the above-mentioned causes many Italian museums have difficulties playing the role of scientific institutions. In this aspect they differ from larger European museums, which are dedicated biodiversity centres and actively support research in their country or in biodiversity hotspots. Indeed, collection-based research is crucial to perform taxonomic studies, to confirm the presence of a species at well-defined sites, and to assess conservation status or the dynamics of a species' range, as well as to provide material for the study of some biological traits, such as fecundity and longevity (Tessa et al. 2009). The study of collections also serves to document and unveil life-history parameters and temporal patterns in evolutionary and ecological studies (Wandeler et al. 2007; English et al. 2018). This is, for example, evident when DNA analysis or X-ray CT scans are used to unveil taxonomic and functional aspects (Betz et al. 2007; Broeckhoven and du Plessis 2018). Unfortunately, in Italy almost none of the existing museums have resources to conduct such activities independently and, thus, usually rely on collaborations with other institutions.

The fact that many Italian museums do not have research as a topic mission and do not have a national breadth is also one of the causes for their absence from the European Commission-funded SYNTHESYS+ project, a program creating an integrated European infrastructure for natural history collections (Bartolozzi 2013). In recent times, collections were also used as useful tools to investigate pollution and epidemiology: frozen tissues housed in museums allowed for the discovery of many new hantaviruses in rodents worldwide (Yanagihara et al. 2014; Dunnum et al. 2017) and were used to elucidate the taxonomy of species involved in zoonoses, including the recently widespread SARS-Cov-2 (Colella et al. 2021).

Italy's quest for a national museum

The historical reasons for the lack of a national museum in Italy have already been addressed by Ruffo (2006) and, more recently, by Canadelli (2015), among others, showing that these are mostly associated with Italy's past political fragmentation. As we saw, only a few pre-unitarian states were able to build sufficiently large museums carrying out regular research activity (Bologna 2015). In Germany, a country with a similar history of political fragmentation, museums generally followed another path. From the beginning, they were classified as research centres and usually collaborated with universities acting as scientific centres or featured a good level of autonomy. Differently from what happened in the Netherlands with the Naturalis Biodiversity Center, which centralised all the country natural history collections, several German museums became associated within the Senckenberg Gesellschaft für Naturforschung and operate as a geographically distributed system of collections.

Sadly, while Italian museums in the 19th century were also highly productive in the context of their educational and/or scientific aims, and often produced prestigious

taxonomic and biogeographical schools, they were not able to upgrade later on. Moreover, a strong connection with their hosting town often resulted in a general difficulty and/or unwillingness to give birth to a large institution with national and international scope.

Despite these difficulties, the project of a national museum and/or the implementation of national collections was never forgotten. Many naturalists of the past considered this an important step towards a satisfactory level of natural history studies. In many cases there were concurrent attempts to develop national repositories for natural history collections. As an example, the botanist Filippo Parlatore sent a letter from London on the occasion of the “Terza Riunione degli Scienziati italiani” (Third Meeting of the Italian Scientists, Florence, 15–29 September 1841), suggesting the creation of a “General Herbarium for the Italian Peninsula”, as done by other European countries, proposing Florence as the seat of the “Erbario centrale Italiano” (Capanna 2011). In 1861, just after the unification of Italy, the zoologist Enrico Hyllier Giglioli did his best to put together the first cell of a national museum by establishing in 1877 (again in Florence) the “Collezione Nazionale dei Vertebrati” (National Vertebrate Collection). In 1913, a royal decree established the “Collezione elmintologica centrale italiana e Laboratorio di Elmintologia” (Central Italian helminthological collection and helminthology laboratory) at the Zoological Museum of Naples “Federico II” University. The helminthological collection was set up together with the material assembled by Corrado Parona, Michele Stossich, and Francesco Saverio Monticelli (at that time director, as university professor, of the Zoological Museum), and specifically received financial support from the government to support a curator job position. As a last project of “nationalization” of biological collections, we mention the “Istituto Nazionale di Entomologia” (National Entomological Institute), founded in 1940 by Federico Hartig (1900–1980) and established in Rome, destined to become in 1977 an important part of a new museum of zoology at “La Sapienza” University (Vigna Taglianti and Zilli 2008).

A proposal for a centralised biorepository

It is, therefore, remarkable that in the last 80 years, while biodiversity has increasingly become a global scientific issue, no real attempt has yet been made to foster collection-based biodiversity research, except for a failed attempt in the 1980s to organize a national museum in Florence, pursued by the Accademia Nazionale dei Lincei (Canadelli 2015).

The position of the Italian Peninsula—at the centre of the Mediterranean region, acting as a geographic bridge between Europe and Africa, and having complex palaeogeographic history—and its importance as repeated glacial refuges make research on Italian marine and land ecosystems of international importance (Giaccone et al. 2008), given also that Italy has the richest biodiversity in the European Union (Bologna et al. 2022). In addition, Italian museums host important collections from all over the world, a precious heritage of travellers and scientists who had a global impact on biodiversity research (Pichi-Sermolli 1988; Gippoliti 2005). Aside from those collected in former Italian colonies in Africa, we also mention the rich zoological collections from Borneo (Peters 1872) and New Guinea (Peters and Doria 1878), both housed in the

Genoa Museum; the collections from Latin America collected in the 19th century by Alfredo Borelli and Enrico Festa, and in the 20th century by Josè M. Cei in the Turin Museum (Lavilla et al. 2008). Yet, the present fragmentation of museums and associated collections does not allow for an effective participation of Italy to global models of aggregated natural history databases, such as the VertNet for vertebrates (<http://www.vertnet.org>), the Integrated Digitized Biocollections (iDigBio, <https://www.idigbio.org/>), and the Global Biodiversity Information Facility (GBIF, <https://www.gbif.org/>), toward which museums are moving worldwide (Minelli 2015).

In the light of the difficulties experienced in the past to build a national museum in Italy, we wonder whether there is still room for such a proposal, or, instead, we need to develop a new concept of centralisation and connection. The “Centro Nazionale per la Biodiversità” (NBFC: National Biodiversity Future Centre) planned within the initiatives of the Italian “Piano Nazionale di Ripresa e Resilienza” (PNRR: National Plan of Recovery and Resilience) has the great potential to offer a unique occasion to boost the establishment of a national institution dedicated to biodiversity, taxonomy, and conservation (Ferrari 2022).

Given the crucial role played nowadays by museums for the study, popularisation, and conservation of biodiversity, the realization of a centralised repository is an urgent logical step, especially in the light of a novel awareness of the importance of both biodiversity and ecosystems, as recognized by the European Initiative on Biodiversity, the European Green Deal, and emphasised by the Intergovernmental Science-Policy Platform on Biodiversity and Ecosystem Services (IPBES, <https://ipbes.net/>), the Convention on Biological Diversity (CBD, <https://www.cbd.int/>), and COP15. This was recently echoed also by the PNRR, which aims at realizing an ecological transition in Italy.

Following Minelli's (2013) vision, such a repository should primarily focus on the preservation and valorisation of natural history collections, assuring at the same time a role of coordination and service. On the other hand, the activity of science dissemination through exhibition activities could be left to the existing local museums which are closer to citizens. This would help realising an efficient museum network, going from a local to a national level. This would also enable the development of a national strategy in biodiversity research, taking advantage of existing collections, with a particular focus on taxonomic studies, the baseline for any future conservation effort. Here we quote some of the core activities that could be carried out by the repository:

- **Collection preservation.** A repository assures that the preserved material obtained through field surveys, purchases, and salvages of dead animals is not lost. In fact, local museums often privilege the reception of collections with relevant ostensive and historical value and may discard collections with a mere scientific value. Moreover, private collections (particularly of entomology, ornithology, malacology, and herbaria) are often destroyed after the death of the owner: potentially, these collections are a huge treasure of biodiversity that may be acquired by museums free of charge, but they are often refused due to lack of space. Part of the types of newly described taxa (mainly from Italy) could also find space in such a repository, as well as samples collected during ecological studies (Pyke and Ehrlich 2010).

- **Museums coordination.** Minelli (2013, 2015) and Andreone et al. (2014) already highlighted the need of a “metamuseum” or “diffused museum” connecting the small and medium-sized Italian museums. The biorepository hub could also be done under national coordination to assure the management of the existing natural history collections.

- **Collection digitalization.** Most of the Italian collections still need be digitalized. This would contribute to the creation of a “meta-catalogue” to allow rapid check of vouchers. This task would benefit from an accompanying photographic collection, especially of all of type specimens, including CT scans of remarkable specimens (types and rare or extinct species) and other kinds of data, i.e., bio-acoustics.

- **Shared services for taxonomy.** The biorepository could also support specific taxonomic, phylogenetic, and ecological studies, providing services and expertise. It could act as a central storage hub for genetic samples responding to the highest standards of research (e.g., Phillips et al. 2019), by assuring the formation of a scientific staff for a wide range of disciplines and following field-collecting policies based on established priorities. Hired taxonomists could also provide services to local museums, institutions, and other organizations that need biodiversity information. Collections and expertise could be utilised in the monitoring of alien species at the national level and in the identification of traded species (Palandačić et al. 2020).

- **Taxonomic training.** The expertise on taxonomy is fading away (Boero 2010), and the training of new taxonomists mastering both morphological and molecular approaches is crucial to appreciate the state of the natural capital. The organization of courses on biodiversity given by the few remaining specialists might be a crucial enterprise of the NBFC, to revive the Italian expertise in taxonomy, as done by the National Science Foundation of the US with the Partnership to Enhance Expertise in Taxonomy (Boero 2001).

- **Sanitary observatory.** In collaboration with sanitary authorities, the centre would be the ideal place to deal with biosurveillance activities through the storage of critical specimens that, through an efficient tracking system, are associated with identified pathogens of potential health significance (Thompson et al. 2021). The repository would also serve as location not only for primary vouchers but also for secondary and complementary vouchers of, for example, parasites and pathogens (Colella et al. 2021).

A plea for a new model of research centre

Summing up, the historical fragmentation of Italian museums, and the manifest difficulties in managing and promoting the housed scientific collections, call for a novel concept of a centralised research centre. The global ecological crisis, the availability of PNRR funds, and the urgency to realise an ecological transition focusing on the integrity of the natural capital in terms of biodiversity and ecosystems can contribute to the birth of a new model of coordination and a research centre that could make up for the lack of a national museum of natural history. A centralised repository and a new collaboration of the existing museological institutions is necessary and urgent: the NBFC is a unique and unrepeatable occasion for such a development.

The collection of biological vouchers and the easily accessible availability of natural history collections connected in an operative network within Italy, as well as to researchers from all over the world, is also a priority, particularly for future generations (Rohwer et al. 2022). The existing system of museums should work in a coordinated way to develop a web of institutions, with an interaction from the largest museums to the smallest ones, providing shared resources and facilities. In particular, a centralised research centre could coordinate the research activities led by Italian museums, i.e., providing instruments and tools that are currently missing. This technological supply could allow the realisation of a real hub with efficient interconnections with the existing museums managed by disparate institutions and administrations.

The funds from PNRR are vital to recruit curatorial and scientific personnel that makes the hub the national taxonomy focal point, supporting an organic nationwide action of voucher digitalisation, a high-quality photographic catalogue of most of the specimens (with special emphasis to types), and collaborating with all national biodiversity-related initiatives and bodies (the national protected area system, Italian fauna checklist project, invasive species monitoring, etc). The physical location of the repository, if it will be newly realised or obtained by empowering an already existing institution, obviously depends on a series of choices, including economic and political considerations, which are outside the primary scope of the present paper.

The definition and identification of a biorepository and biodiversity hub will also give strength to the international commitments agreed upon by the Italian government under the Convention on Biological Diversity and the upcoming targets of the Post-2020 Global Biodiversity Framework, where knowledge and conservation of each nation's biodiversity will be at the core of the goals. When this happens, Italy will be endowed with a large and efficient institution for the knowledge and conservation of biodiversity, and a crucial structure to assure a true ecological transition.

Acknowledgements

We thank our colleagues who provided useful information and discussions over the years on the critical situation of natural history collections and museums in Italy. Among these colleagues are E. Canadelli, L. Latella, N. Maio, C. Marangoni, S. Mazzotti, P. Nicolosi, and V. Vomero. Their opinions and suggestions were useful to shape this paper and to solicit our attention on the theme of national museum and national biorepository in Italy. Finally, we give special thanks to A. Antonelli for the useful advice and the critical reading of a first draft of this paper, and to U. Fritz for having acted as a reviewer.

References

- Alberch P, Zavala L, Miles R (1994) The identity crisis of natural history museums at the end of the twentieth century. In: Miles R, Zavala L (Eds) *Towards the museum of the future. New European perspectives*. Routledge, London, 195–200.

- Andreone F, Bartolozzi L, Boano G, Boero F, Bologna M, Bon M, Bressi N, Capula M, Casale A, Casiraghi M, Chiozzi G, Delfino M, Doria G, Durante A, Ferrari M, Gippoliti S, Lanzinger M, Latella L, Maio N, Marangoni C, Mazzotti S, Minelli A, Muscio G, Nicolosi P, Pievani T, Razzetti E, Sabella G, Valle M, Vomero V, Zilli A (2014) Italian natural history museums on the verge of collapse? *ZooKeys* 456: 139–146. <https://doi.org/10.3897/zookeys.456.8862>
- Bakker FT, Antonelli A, Clarke JA, Cook JA, Edwards SV, Ericson PGP, Faurby S, Ferrand N, Gelang M, Gillespie RG, Irestedt M, Lundin K, Larsson E, Matos-Maraví P, Müller J, von Proschwitz T, Roderick GK, Schliep A, Wahlberg N, Wiedenhoeft J, Källersjö M (2020) The Global Museum: natural history collections and the future of evolutionary science and public education. *PeerJ* 8: e8225. <https://doi.org/10.7717/peerj.8225>
- Bartolozzi L (2013) I musei naturalistici italiani nel contesto delle iniziative internazionali sulla biodiversità. *Museologia Scientifica* 9: 17–20.
- Betz O, Wegst U, Weide D, Heethoff M, Helfen L, Lee WK, Cloetens P (2007) Imaging applications of synchrotron X-ray phase-contrast microtomography in biological morphology and biomaterials science. I. General aspects of the technique and its advantages in the analysis of millimetre-sized arthropod structure. *Journal of Microscopy* 227(1): 51–71. <https://doi.org/10.1111/j.1365-2818.2007.01785.x>
- Bezerra AMR (2012) Coleções científicas de mamíferos. I - Brasil. *Boletim da Sociedade Brasileira de Mastozoologia* 65: 19–25.
- Boero F (2001) Light after dark: the partnership for enhancing expertise in taxonomy. *Trends in Ecology and Evolution* 16(5): 266–266. [https://doi.org/10.1016/s0169-5347\(01\)02133-4](https://doi.org/10.1016/s0169-5347(01)02133-4)
- Boero F (2010) The study of species in the era of biodiversity: A tale of stupidity. *Diversity* 2(1): 115–126. <https://doi.org/10.3390/d2010115>
- Bologna MA (2015) Le collezioni zoologiche universitarie: dall'analisi della situazione a proposte per l'inserimento in una rete museologica nazionale. *Rendiconti Accademia Nazionale delle Scienze detta dei XL. Memorie di Scienze Fisiche e Naturali* 132, 38(2): 155–166.
- Bologna MA, Bonato L, Cianferoni F, Minelli A, Oliverio M, Stoch F, Zapparoli M (2022) The new Checklist of the Italian Fauna. *Biogeographia. The Journal of Integrative Biogeography* 37: ucl002. <https://doi.org/10.21426/B637156506>
- Broeckhoven C, du Plessis A (2018) X-ray microtomography in herpetological research: A review. *Amphibia-Reptilia* 39(4): 377–401. <https://doi.org/10.1163/15685381-20181102>
- Butler D, Gee H, MacIlwain C (1998) Museum research comes off list of endangered species. *Nature* 394(6689): 115–117. <https://doi.org/10.1038/28009>
- Camacho MA, Salgado JM, Burneo SF (2018) An accounting approach to calculate the financial value of a natural history collection of mammals in Ecuador. *Museum Management and Curatorship* 33(3): 279–296. <https://doi.org/10.1080/09647775.2018.1466191>
- Canadelli E (2015) Il Museo nazionale italiano di storia naturale. Storia di un'idea. *Rendiconti Accademia Nazionale delle Scienze detta dei XL. Memorie di Scienze Fisiche e Naturali* 132, 38(2): 121–154.
- Capanna E (2011) Eran quattrocento. Le riunioni degli scienziati italiani (1839–1847). CEULS, Roma and CLUEB, Bologna, 244 pp.
- Cerfáco LMP, Parrinha D, Marques MP (2021) Saving collections: taxonomic revisions of the herpetological collection of the Instituto de Investigação Científica Tropical, Lisbon

- (Portugal) with a protocol to rescue abandoned collections. *ZooKeys* 1052: 85–156. <https://doi.org/10.3897/zookeys.1052.64607>
- Chiozzi G (2013) Il contributo del Museo di Storia Naturale di Milano all'esplorazione zoologica dell'Africa. *Natura* 103: 159–186.
- Clemann N, Rowe KMC, Rowe KC, Raadik T, Gomom M, Menkhorst P, Sumner J, Bray D, Norman M, Melville J (2014) Value and impacts of collecting vertebrate voucher specimens, with guidelines for ethical collection. *Memoirs of the Museum of Victoria* 72: 141–151. <https://doi.org/10.24199/j.mmv.2014.72.09>
- Colella JP, Bates J, Burneo SF, Camacho MA, Carrion Bonilla C, Constable I, D'Elía G, Dunnum JL, Greiman S, Hoberg EP, Lessa E, Liphardt SW, Londoño-Gaviria M, Losos E, Lutz HL, Ordóñez Garza N, Peterson AT, Martin ML, Ribas CC, Struminger B, Torres-Pérez F, Thompson CW, Weksler M, Cook JA (2021) Leveraging natural history biorepositories as a global, decentralized, pathogen surveillance network. *PLoS Pathogens* 17(6): e1009583. <https://doi.org/10.1371/journal.ppat.1009583>
- Costello MJ, May RM, Stork NE (2013) Can we name Earth's species before they go extinct? *Science* 339(6118): 413–416. <https://doi.org/10.1126/science.1230318>
- Davis P (1996) *Museums and the Natural Environment. The role of natural history museums in biological conservation.* Leicester University Press, London, 286 pp.
- Dubois A (2003) The relationships between taxonomy and conservation biology in the century of extinctions. *Comptes Rendus Biologies* 326(Supplement 1): e94121. [https://doi.org/10.1016/S1631-0691\(03\)00022-2](https://doi.org/10.1016/S1631-0691(03)00022-2)
- Dubois A (2010) Zoological nomenclature in the century of extinctions: Priority vs. usage. *Organisms, Diversity & Evolution* 10(3): 259–274. <https://doi.org/10.1007/s13127-010-0021-3>
- Dubois A (2017) The need for reference specimens in zoological taxonomy and nomenclature. *Bionomina* 12(1): 4–38. <https://doi.org/10.11646/bionomina.12.1.2>
- Dunnum JL, Yanagihara R, Johnson KM, Armien B, Batsaikhan N, Morgan L, Cook JA (2017) Biospecimen repositories and integrated database as critical infrastructure for pathogen discovery and pathobiology research. *PLoS Neglected Tropical Diseases* 11(1): e0005133. <https://doi.org/10.1371/journal.pntd.0005133>
- Engel MS, Ceríaco LMP, Daniel GM, Dellapé PM, Löbl I, Marinov M, Reis RE, Young MT, Dubois A, Agarwal I, Lehmann P, Alvarado M, Alvarez N, Andreone F, Araujo-Vieira K, Ascher JS, Baêta D, Baldo D, Bandeira SA, Barden P, Barrasso DA, Bendifallah L, Bockmann FA, Böhme W, Borkent A, Brandão CRF, Busack SD, Bybee SM, Channing A, Chatzimanolis S, Christenhusz MJM, Crisci JV, D'elía G, Da Costa LM, Davis SR, De Lucena CAS, Deuve T, Elizalde FS, Faivovich J, Farooq H, Ferguson AW, Gippoliti S, Gonçalves FMP, Gonzalez VH, Greenbaum E, Hinojosa-Díaz IA, Ineich I, Jiang J, Kahono S, Kury AB, Lucinda PHF, Lynch JD, Malécot V, Marques MP, Marris JWM, Mckellar RC, Mendes LF, Nihei SS, Nishikawa K, Ohler A, Orrico VGD, Ota H, Paiva J, Parrinha D, Pauwels OSG, Pereyra MO, Pestana LB, Pinheiro PDP, Prendini L, Prokop J, Rasmussen C, Rödel M-O, Trefaut Rodrigues M, Rodríguez SM, Salatnaya H, Sampaio I, Sánchez-García A, Shebl MA, Santos BS, Solórzano-Kraemer MM, Sousa ACA, Stoev P, Teta P, Trape J-F, Van-Dúnem Dos Santos C, Vasudevan K, Vink CJ, Vogel G, Wagner P, Wappler T, Ware JL, Wedmann S, Zacharie CK (2021) The taxonomic impediment: A

- shortage of taxonomists, not the lack of technical approaches. *Zoological Journal of the Linnean Society* 193(2): 381–387. <https://doi.org/10.1093/zoolinnean/zlab072>
- English PA, Green DJ, Nocera JJ (2018) Stable isotopes from museum specimens may provide evidence of long-term change in the trophic ecology of a migratory aerial insectivore. *Frontiers in Ecology and Evolution* 6: e14. <https://doi.org/10.3389/fevo.2018.00014>
- Ferrari M (2022) La straordinaria varietà italiana. *Le Scienze* 644: 44–51.
- Funk VA, Hoch PC, Prather LA, Wagner WL (2005) The importance of vouchers. *Taxon* 54(1): 127–129. <https://doi.org/10.2307/25065309>
- Giaccone T, Catra M, Serio D, Giaccone G (2008) A review of Mediterranean macrophytobenthos collections present in Italy: A contribution to the Mediterranean Initiative on Taxonomy. *Chemistry and Ecology* 24(sup1): 175–184. <https://doi.org/10.1080/02757540801966355>
- Gippoliti S (2005) Historical museology meets biodiversity conservation. *Biodiversity and Conservation* 14(13): 3127–3134. <https://doi.org/10.1007/s10531-004-0381-0>
- Gippoliti S, Amori G, Castiglia R, Colangelo P, Capanna E (2014) The relevance of Italian museum collections for research and conservation: The case of mammals. *Rendiconti Lincei. Scienze Fisiche e Naturali* 25(3): 351–357. <https://doi.org/10.1007/s12210-014-0304-2>
- Krištufek B, Abramson N, Kotrošan D (2015) Rescue eastern Europe's collections. *Nature* 518(7539): e303. <https://doi.org/10.1038/518303b>
- Lavilla EO, Sclaro JA, Videla F, Adler K (2008) Obituaries: José Miguel Cei (1918–2007). *Herpetological Review* 39(1): 9–10.
- Massa B (2021) Biodiversità, sostantivo singolare femminile. *Il Naturalista Siciliano* 45(1–2): 275–278.
- McCarter J, Boge G, Darlow G (2001) Safeguarding the world's natural treasures. *Science* 294(5549): 2100–2101. <https://doi.org/10.1126/science.1067223>
- Minelli A (2013) Il Museo virtuoso. Proposte per un archivio responsabile della biodiversità globale. In: *I musei delle scienze e la biodiversità*. In: Mazzotti S, Malerba G (Eds) *Atti del XX Congresso ANMS, Ferrara, 17–19 novembre 2010, Museologia Scientifica, Memorie* 9: 41–43.
- Minelli A (2015) Le collezioni dei musei italiani di storia naturale nel quadro della ricerca scientifica nazionale e internazionale. *Rendiconti Accademia Nazionale delle Scienze detta dei XL. Memorie di Scienze Fisiche e Naturali* 132: 105–113.
- Minelli A, Ruffo S, La Posta S [Eds] (1993–1995) *Checklist delle specie della Fauna d'Italia*. Ministero dell'Ambiente, Comitato Scientifico per la Fauna d'Italia. Calderini Editore.
- Palandačić A, Kruckenhauser L, Ahnelt H, Mikschi E (2020) European minnows through time: museum collections aid genetic assessment of species introductions in freshwater fishes (Cyprinidae: *Phoxinus* species complex). *Heredity* 124(3): 410–422. <https://doi.org/10.1038/s41437-019-0292-1>
- Peters W (1872) Übersicht der von den Herren M.se G. Doria und Dr. O. Beccari in Sarawak auf Borneo von 1865 bis 1868 gesammelten Amphibien. *Annali del Museo Civico di Storia Naturale Giacomo Doria* 3: 27–45.
- Peters W, Doria G (1878) Catalogo dei Rettili e dei Batraci raccolti da O. Beccari, L. M. D'Albertis e A. A. Bruijn nella sotto-regione Austro-Malese. *Annali del Museo Civico di Storia Naturale Giacomo Doria* 13: 321–450.

- Phillips CD, Dunnun JL, Dowler RC, Bradley Lisa C, Garner Heath J, MacDonald KA, Lim BK, Revelez MA, Campbell ML, Lutz HL, Ordóñez Garza N, Cook JA, Bradley RD (2019) Curatorial guidelines and standards of the American Society of Mammalogists for collections of genetic resources. *Journal of Mammalogy* 100(5): 1690–1694. <https://doi.org/10.1093/jmammal/gyz111>
- Pichi-Sermolli REG (1988) Il contributo degli italiani alla conoscenza delle flore extra-europee (Pteridophyta e Spermatophyta). I. Note introduttive, Africa. In: Pedrotti F (Ed.) 100 anni di ricerche botaniche in Italia (1888–1988) 2. Società Botanica Italiana, Firenze, 1013–1044.
- Poggi R (2017) 150 years of scientific activity. Notes on the foundation and development of the Museo Civico di Storia Naturale “Giacomo Doria” of Genoa (1867–2017). *Annali del Museo Civico di Storia Naturale "Giacomo Doria" di Genova* 109: 1–272.
- Pyke GH, Ehrlich PR (2010) Biological collections and ecological/environmental research: A review, some observations and a look to the future. *Biological Reviews of the Cambridge Philosophical Society* 85(2): 247–266. <https://doi.org/10.1111/j.1469-185X.2009.00098.x>
- Rocha LA, Aleixo A, Allen G, Almeda F, Baldwin CC, Barclay MVL, Bates JM, Bauer AM, Benzoni F, Berns CM, Berumen ML, Blackburn DC, Blum S, Bolaños F, Bowie RCK, Britz R, Brown RM, Cadena CD, Carpenter K, Ceríaco LM, Chakrabarty P, Chaves G, Choat JH, Clements KD, Collette BB, Collins A, Coyne J, Cracraft J, Daniel T, de Carvalho MR, de Queiroz K, Di Dario F, Drewes R, Dumbacher JP, Engilis Jr A, Erdmann MV, Eschmeyer W, Feldman CR, Fisher BL, Fjeldså J, Fritsch PW, Fuchs J, Getahun A, Gill A, Gomon M, Gosliner T, Graves GR, Griswold CE, Guralnick R, Hartel K, Helgen KM, Ho H, Iskandar DT, Iwamoto T, Jaafar Z, James HF, Johnson D, Kavanaugh D, Knowlton N, Lacey E, Larson HK, Last P, Leis JM, Lessios H, Liebherr J, Lowman M, Mahler DL, Mamonekene V, Matsuura K, Mayer GC, Mays Jr H, McCosker J, McDiarmid RW, McGuire J, Miller MJ, Mooi R, Mooi RD, Moritz C, Myers P, Nachman MW, Nussbaum RA, Foighil DÓ, Parenti LR, Parham JF, Paul E, Paulay G, Pérez-Emán J, Pérez-Matus A, Poe S, Pogonoski J, Rabosky DL, Randall JE, Reimer JD, Robertson DR, Rödel M-O, Rodrigues MT, Roopnarine P, Rüber L, Ryan MJ, Sheldon F, Shinohara G, Short A, Simison WB, Smith-Vaniz WF, Springer VG, Stiassny M, Tello JG, Thompson CW, Trnski T, Tucker P, Valqui T, Vecchione M, Verheyen E, Wainwright PC, Wheeler TA, White WT, Will K, Williams JT, Williams G, Wilson EO, Winker K, Winterbottom R, Witt CC (2014) Specimen collection: An essential tool. *Science* 344(6186): 814–815. <https://doi.org/10.1126/science.344.6186.814>
- Rohwer VG, Rohwer Y, Dillman CB (2022) Declining growth of natural history collections fails future generations. *PLoS Biology* 20(4): e3001613. <https://doi.org/10.1371/journal.pbio.3001613>
- Ruffo S (2006) Montalenti e la proposta di un museo naturalistico nazionale. *Atti dei Convegni Lincei* 228: 69–74.
- Salick J, Konchar K, Nesbitt M (2014) Curating biocultural collections. A handbook. Kew Publishing, Royal Botanical Gardens in association with Missouri Botanical Garden, Kew and St. Louis, 406 pp.
- Schilthuizen M, Vairappan CS, Slade EM, Mann DJ, Miller JA (2015) Specimens as primary data: museums and open science. *Trends in Ecology & Evolution* 30(5): 237–238. <https://doi.org/10.1016/j.tree.2015.03.002>

- Stoch F, Zoia S, Minelli A, Ruffo S, La Posta A, Vigna Taglianti A (2004) Aggiornamenti alla checklist delle specie della fauna italiana. *Bollettino della Società Entomologica Italiana* 136: 251–256.
- Tessa G, Mattioli F, Mercurio V, Andreone F (2009) Egg numbers and fecundity traits in nine species of *Mantella* poison frogs from arid grasslands and rainforests of Madagascar (Anura: Mantellidae). *Madagascar Conservation and Development* 4(2): 113–119. <https://doi.org/10.4314/mcd.v4i2.48651>
- Thompson CW, Phelps KL, Allard MW, Cook JA, Dunnum JL, Ferguson AW, Gelang M, Khan FAA, Paul DL, Reeder DM, Simmons NB, Vanhove MPM, Webala PW, Weksler M, Kilpatrick CW (2021) Preserve a voucher specimen! The critical need for integrating natural history collections in infectious disease studies. *mBio* 12(1): e02698–e20. <https://doi.org/10.1128/mBio.02698-20>
- Tognon G (2016) La riforma Gentile. In: Croce e Gentile: la cultura italiana e l'Europa. Istituto della Enciclopedia Italiana, Roma. https://www.treccani.it/enciclopedia/la-riforma-gentile_%28Croce-e-Gentile%29/ [Accessed on: 2022-5-24]
- Vigna-Taglianti A, Zilli A (2008) *Il Conte e le farfalle. Omaggio a Federico Hartig*. Edizioni Belvedere, Latina, 76 pp.
- Wandeler P, Hoeck PE, Keller LF (2007) Back to the future: museum specimens in population genetics. *Trends in Ecology & Evolution* 22(12): 634–642. <https://doi.org/10.1016/j.tree.2007.08.017>
- Yanagihara R, Gu SH, Arai S, Kang HJ, Song J-W (2014) Hantaviruses: rediscovery and new beginnings. *Virus Research* 187: 6–14. <https://doi.org/10.1016/j.virusres.2013.12.038>

On the verge of extinction – revision of a highly endangered Swiss alpine snail with description of a new genus, *Raeticella* gen. nov. (Gastropoda, Eupulmonata, Hygromiidae)

Jeannette Kneubühler^{1,2}, Markus Baggenstos³, Eike Neubert^{1,2}

1 Natural History Museum Bern, 3005 Bern, Switzerland **2** Institute of Ecology and Evolution, University of Bern, 3012 Bern, Switzerland **3** Oekologische Beratung Markus Baggenstos, Tottikonstrasse 48, 6370 Stans, Switzerland

Corresponding author: Jeannette Kneubühler (jeannette.kneuebuehler@nmbe.ch)

Academic editor: A. M. de Frias Martins | Received 28 February 2022 | Accepted 12 May 2022 | Published 8 June 2022

<http://zoobank.org/12CD28D8-33FF-44D2-B271-87C11240FA2D>

Citation: Kneubühler J, Baggenstos M, Neubert E (2022) On the verge of extinction – revision of a highly endangered Swiss alpine snail with description of a new genus, *Raeticella* gen. nov. (Gastropoda, Eupulmonata, Hygromiidae). ZooKeys 1104: 69–91. <https://doi.org/10.3897/zookeys.1104.82866>

Abstract

The phylogenetic status of the alpine land snail *Fruticicola biconica* has remained questionable since it was described by Eder in 1917. Considered a microendemic species from mountain tops in Central Switzerland, the shell is specially adapted for life under stones. Herein, we show via molecular and anatomical investigations that *F. biconica* neither belongs to the land snail genus *Trochulus*, nor to any other genus within Trochulini, but rather warrants placement within the newly established genus *Raeticella* Kneubühler, Baggenstos & Neubert, 2022. Phylogenetic analyses reveal that *R. biconica* is clearly separated from *Trochulus*. These findings are supported by morphological investigations of the shell and genitalia.

Keywords

Endemism, integrative taxonomy, LGM, mountains, nunataks, phylogeny, Switzerland, *Trochulus*

Introduction

Discovered in the Bannalp, Nidwalden and known from only a few localities in the Central Swiss Alps, *Fruticicola biconica* was described by the Swiss zoologist Leo Eder in 1917.

Later, *F. biconica*, known as the Nidwaldner hairy snail, was moved to the widely used genus *Trichia* W. Hartmann, 1840 and circulated throughout the European literature under this designation (e.g., Kerney et al. 1983). The generic name, *Trichia*, was subsequently replaced by *Trochulus* Chemnitz, 1786 due to homonymy with *Trichia* De Haan, 1839 (Crustacea, Xanthidae).

Previous studies (Pfenninger et al. 2005; Dépraz et al. 2009; Duda et al. 2014; Kruckenhauser et al. 2014; Proćków et al. 2021) included *T. biconicus* individuals in their genetic analyses of *Trochulus* species. Pfenninger et al. (2005) and Dépraz et al. (2009) used the same sequence of *T. biconicus* collected at the type locality at Bannalp. This sequence clustered within the so far known *Trochulus* species and some newly identified lineages, which were not further described (fig. 2 in Pfenninger et al. 2005; fig. 1 in Dépraz et al. 2009). Most likely, Pfenninger et al. (2005) and Dépraz et al. (2009) used misidentified specimens in their phylogenetic studies, or some samples were mixed. Since these authors did not publish images of the investigated specimens, an unequivocal identification is not possible. Duda et al. (2014) and Kruckenhauser et al. (2014) found that *T. biconicus*, “*T. oreinos oreinos*” (A.J. Wagner, 1915), and “*T. oreinos scheerpeltzi*” (Mikula, 1957) form basal lineages in comparison to specimens of *Trochulus* s. str. The latter two taxa were elevated from subspecies to species level (Bamberger et al. 2020) and are today known to belong to the newly described genus *Noricella* (Neiber et al. 2017). Proćków et al. (2021) found the same phylogenetic pattern as Duda et al. (2014) and Kruckenhauser et al. (2014) and questioned the affiliation of *biconicus* to *Trochulus*. Already Turner et al. (1998) had disputed the phylogenetic position of *T. biconicus*. Until today, the phylogenetic position of *T. biconicus* within the Trochulini remained unclear. Hence, an integrative taxonomic approach is applied in this study to investigate the phylogenetic affiliation of *T. biconicus*.

Materials and methods

Specimens investigated

Living individuals of *T. biconicus* were collected in September 2020 at 11 sites of the known distribution area in Central Switzerland (see Fig. 1 for detailed sampling localities). *Trochulus biconicus* is classified as Vulnerable by Swiss law (Federal Office of Environment) and is protected. It is also considered Endangered by the IUCN (<https://www.iucnredlist.org/species/22107/9360310>). Collecting permits were obtained from the cantonal administrations of Nidwalden, Obwalden, and Uri. At each site, 3–5 snails were collected from large populations (>20 individuals)

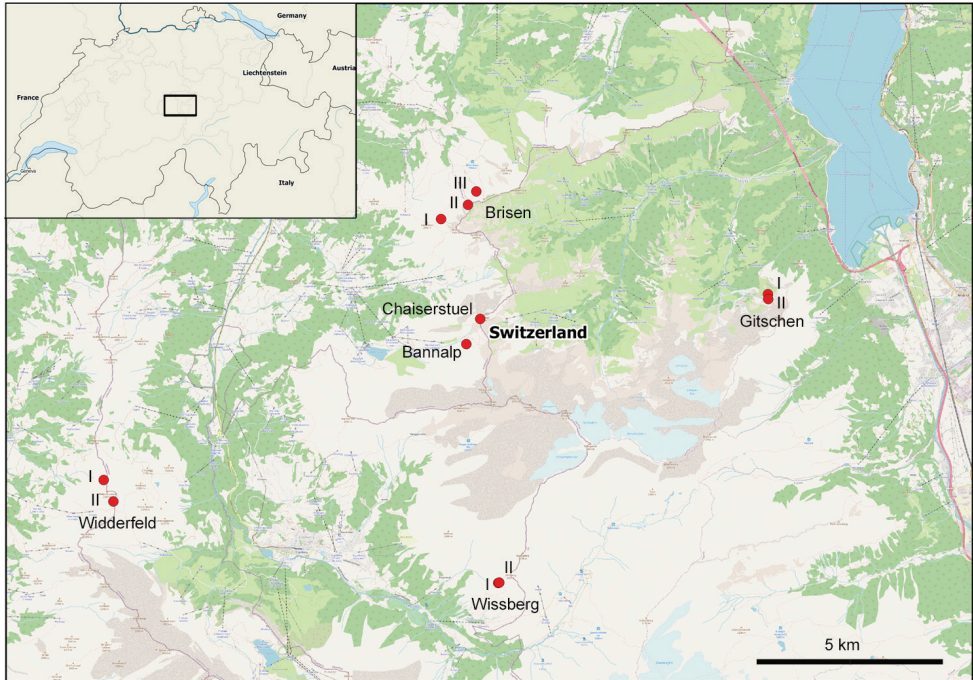


Figure 1. Sampling locations of the investigated individuals of *T. biconicus*.

from under rocks on stony outcrops. The individual snails were preserved in 80% ethanol to keep the body tissue soft for proper anatomical investigations and DNA extraction. In Table 1, sampling localities and GenBank accession numbers are listed for all sequenced specimens of *T. biconicus*, *Trochulus* spp., and *Edentiella edentula*. Usually, two specimens of *T. biconicus* per population were sequenced. Those not destroyed in the extraction process are deposited at the NMBE as voucher material. The map was produced with QGIS (2016, v. 2.18.13) using the Natural Earth data set.

Acronyms of collections

NMBE Natural History Museum Bern, Switzerland;
MNHW Museum of Natural History Wrocław, University of Wrocław, Poland.

Shell morphology and anatomical study of the genitalia

One animal was selected from each population for investigations of the shell morphology and the genital organs. The dissection of the genitalia was performed under a Leica MZ12 stereomicroscope using thin tweezers. The genital organs were removed from the body, spread on a wax-lined bowl and properly pinned with small needles. The

total length of the situs was measured using Mitutoyo callipers. Proportions between different parts of the genitalia were estimated using the total situs length as a reference. Additionally, the inner structures of the penis and the penial papilla were investigated. Pictures of the situs and the shells were taken with a Leica M205 microscope camera using an image-processing program (Leica LAS X v. 3.6.0.20104, Switzerland). The shells were imaged in frontal, lateral, apical, and ventral position. Shell height and shell width were measured using the callipers to assess perpendicularity with the shell axis.

Table 1. Sequenced *T. biconicus* specimens from Central Switzerland. Asterisk (*) marks the type localities of the species studied. Additionally, *Edentiella edentula* (Draparnaud, 1805) and some species of *Trochulus* were sequenced and included for phylogenetic analyses.

Voucher-No.	Species	Locality	Coordinates	Altitude [m]	GenBank accession number COI	GenBank accession number 16S	GenBank accession number ITS2
NMBE 567164	<i>T. biconicus</i>	Bannalp Schonegg*	46.87°N, 8.46°E	2232	MW435154	MW433778	MW433799
NMBE 567165	<i>T. biconicus</i>	Bannalp Schonegg*	46.87°N, 8.46°E	2232	MW435155	MW433779	MW433800
NMBE 567167	<i>T. biconicus</i>	Chaiserstuel	46.87°N, 8.46°E	2263	MW435156	MW433780	MW433801
NMBE 567168	<i>T. biconicus</i>	Chaiserstuel	46.87°N, 8.46°E	2263	MW435157	MW433781	MW433802
NMBE 567149	<i>T. biconicus</i>	Wissberg I	46.81°N, 8.47°E	2335	MW435158	MW433782	MW433803
NMBE 567150	<i>T. biconicus</i>	Wissberg I	46.81°N, 8.47°E	2335	MW435159	MW433783	MW433804
NMBE 567152	<i>T. biconicus</i>	Wissberg II	46.81°N, 8.47°E	2355	MW435160	MW433784	MW433805
NMBE 567153	<i>T. biconicus</i>	Wissberg II	46.81°N, 8.47°E	2355	MW435161	MW433785	MW433806
NMBE 567155	<i>T. biconicus</i>	Widderfeld I	46.83°N, 8.33°E	2120	MW435162	MW433786	MW433807
NMBE 567156	<i>T. biconicus</i>	Widderfeld I	46.83°N, 8.33°E	2120	MW435163	MW433787	MW433808
NMBE 567159	<i>T. biconicus</i>	Widderfeld II	46.83°N, 8.33°E	2290	MW435164	MW433788	MW433809
NMBE 567161	<i>T. biconicus</i>	Brisen I	46.90°N, 8.45°E	2045	MW435165	MW433789	MW433810
NMBE 567137	<i>T. biconicus</i>	Brisen I	46.90°N, 8.45°E	2045	MW435166	MW433790	MW433811
NMBE 567139	<i>T. biconicus</i>	Brisen II	46.90°N, 8.46°E	2130	MW435167	MW433791	MW433812
NMBE 567140	<i>T. biconicus</i>	Brisen II	46.90°N, 8.46°E	2130	MW435168	MW433792	MW433813
NMBE 567142	<i>T. biconicus</i>	Brisen III	46.90°N, 8.46°E	2090	MW435169	MW433793	MW433814
NMBE 567143	<i>T. biconicus</i>	Brisen III	46.90°N, 8.46°E	2090	MW435170	MW433794	MW433815
NMBE 567145	<i>T. biconicus</i>	Gitschen I	46.88°N, 8.57°E	1890	MW435171	MW433795	MW433816
NMBE 567146	<i>T. biconicus</i>	Gitschen I	46.88°N, 8.57°E	1890	MW435172	MW433796	MW433817
NMBE 567148	<i>T. biconicus</i>	Gitschen II	46.88°N, 8.57°E	1970	MW435173	MW433797	MW433818
NMBE 567162	<i>T. biconicus</i>	Gitschen II	46.88°N, 8.57°E	1970	MW435174	MW433798	MW433819
NMBE 568100	<i>T. hispidus</i>	Sweden, prov. Uppland, Uppsala, Linnaeus Garden*	59.8619°N, 17.6342°E		ON477947	–	–
NMBE 568103	<i>T. hispidus</i>	Sweden, Östergötland, Vist	58.3294°N, 15.729°E	70	ON477948	ON479908	ON479901
NMBE 564609	<i>Trochulus</i> sp.	Bullet, Le Chasseron	46.8517°N, 6.5377°E	1606	ON477944	ON479905	ON479898
NMBE 564607	<i>Trochulus</i> sp.	Mervelier, Schelental	47.336°N, 7.5153°E	615	ON477943	ON479904	ON479897
NMBE 543063	<i>Trochulus</i> sp.	St-Cergue, Route de Cuvuloup	46.4487°N, 6.123°E	1208	ON477941	ON479902	ON479895
NMBE 564601	<i>Trochulus</i> sp.	Zernez	46.6998°N, 10.0943°E	1473	ON477942	ON479903	ON479896
NMBE 568094	<i>Trochulus</i> sp.	Lac du Mont d'Orge	46.2321°N, 7.333°E	624	ON477946	ON479907	ON479900
NMBE 565821	<i>T. alpicola</i>	Bannalp Schonegg*	46.8706°N, 8.2491°E	2234	ON477945	ON479906	ON479899
MNHWS_15_29_101	<i>T. villosus</i>	Montagne De Cernier	47.0763°N, 6.8888°E	1385	MW440985	MW447773	MW440678
MNHWS_15_29_02	<i>T. clandestinus</i>	Montagne De Cernier	47.0763°N, 6.8888°E	1385	MW440983	MW447772	MW440676
MNHWS_15_27_12	<i>Trochulus</i> sp.	Gorges de Court	47.2553°N, 7.3439°E	608	MW440984	MW621002	MW440677
MNHWS_15_21_02	<i>T. caelatus</i>	Gorges de Moutier*	47.2856°N, 7.3819°E	477	MW440982	MW621001	MW440675
MNHWS_Er_50	<i>E. edentula</i>	Erschwil	47.3673°N, 7.555°E	459	MW440986	MW621003	MW440679
MNHWS_Er_51	<i>E. edentula</i>	Erschwil	47.3673°N, 7.555°E	459	MW440987	MW621004	MW440680

Abbreviations used in the anatomical descriptions and figures

AG	albumen gland;	Pe	penis;
BC	bursa copulatrix;	PP	penial papilla;
DS	dart sacs;	sh	shell height;
Ep	epiphallus;	sw	shell width;
Fl	flagellum;	Va	vagina;
HD	hermaphroditic duct;	VD	vas deferens.
MG	mucous glands;		

DNA extraction, PCR amplification and sequence determination

For total DNA extraction of the specimens, the Qiagen Blood and Tissue Kit (Qiagen; Hilden, Germany) was used in combination with a QIAcube extraction robot. Circa 0.5 cm³ of tissue was cut and placed in a mixture of 180 µl ATL buffer and 20 µl Proteinase K. It was then incubated for ca. 4 hours at 56 °C in a heater (Labnet, Vortemp 56, witec AG, Littau, Switzerland). For subsequent DNA extraction, the QIAcube extraction robot was used with the Protocol 430 (DNeasy Blood Tissue and Rodent tails Standard). In this study, two mitochondrial markers (COI and 16S) and one nuclear marker (5.8S rRNA+ITS2) were investigated. PCR mixtures consisted of 12.5 µl GoTaq G2 HotStart Green Master Mix (Promega M7423), 4.5 µl ddH₂O, 2 µl forward and reverse primer each, and 4 µl DNA template. The primer pairs implemented for the PCR are listed in Table 2. The following PCR cycles were used: for COI, 2 min at 94 °C, followed by 40 cycles of 1 min at 95 °C, 1 min at 47 °C and 1 min at 72 °C and finally, 5 min at 72 °C; for 16S, 3 min at 96 °C, followed by 40 cycles of 30 s at 94 °C, 30 s at 50 °C and 30 s at 72 °C, and finally, 1 min at 72 °C; and for 5.8S rRNA+ITS2, 3 min at 94 °C, followed by 40 cycles of 30 s at 94 °C, 30 s at 50 °C and 30 s at 72 °C, and finally, 5 min at 72 °C (SensoQuest Tabcyclet and Techne TC-512, witec AG, Littau, Switzerland). The purification and sequencing of the PCR product was performed by LGC (LGC Genomics Berlin, Germany).

Phylogenetic analyses

The phylogenetic analyses were conducted using sequences obtained from GenBank and from this study, which were included as outgroup: *Ichnusotricha berninii* Giusti & Manganeli, 1987, *Plicuteria lubomirskii* (Ślósarski, 1881), *Petasina unidentata* (Draparnaud, 1805), *Noricella oreinos* (A.J. Wagner, 1915), *Noricella scheerpeltzi* (Mikula, 1957) (GenBank numbers and sampling localities published by Neiber et al. 2017), *Edentiella edentula* (Draparnaud, 1805), and several ingroup specimens of *Trochulus* (Table 1). These species were selected to identify the phylogenetic position of *T. biconicus*.

For sequence processing and editing, the software package Geneious v. 9.1.8 (Biomatters Ltd) was used. Topologies were estimated using two different phylogenetic methods: Bayesian Inference (BI) and Maximum Likelihood (ML). Bayesian Inference was performed using Mr. Bayes v. 3.2.6 x64 (Huelsenbeck and Ronquist 2001;

Table 2. Primer pairs used for PCR.

Gene	Primer	Sequence	Sequence length (bp)	Reference
COI	LCO1490	5'-GGTCAACAAATCATAAAGATATTGG-3'	655	Folmer et al. 1994
	HCO2198	5'-TAAACTTCAGGGTGACCAAAAAATCA-3'		
16S	16S cs1	5'-AAACATACCTTTTGCATAATGG-3'	440	Chiba 1999
	16S cs2	5'-AGAAACTGACCTGGCTTACG-3'		
ITS2	ITS2 LSU1	5'-GCTTGC GGAGAATTAATGTGAA-3'	900	Wade and Mordan 2000
	ITS2 LSU3	5'-GGTACCTTGTTTCGCTATCGGA-3'		

Ronquist and Huelsenbeck 2003; Altekar et al. 2004) via the HPC cluster from the University of Bern (<http://www.id.unibe.ch/hpc>). Evolutionary models for each subset were set to mixed models. The Monte Carlo Markov Chain (MCMC) parameter was set as follows: starting with four chains and four separate runs for 20 million generations with a tree sampling frequency of 1000 and a burn in of 25%. RAxML plug-in for Geneious (Stamatakis 2014) was implemented for computing ML inference, using Geneious' plug-in with rapid bootstrapping setting, the search for the best scoring ML tree and 1000 bootstrapping replicates. The model, GTR CAT I was implemented.

Results

Phylogenetic analyses

The BI analysis of the concatenated data set (Fig. 2) shows two major clades within the tribe Trochulini. These two clades are separated with full support. One clade contains representative specimens of *Edentiella* and *Noricella* which form a polytomy. The second major clade within Trochulini contains representatives of *Petasina*, *Trochulus*, and the investigated *T. biconicus* specimens. *Trochulus biconicus* is the sister lineage to the selected *Trochulus* specimens. This node has full posterior probability support. *Trochulus hispidus* from the type locality in Sweden clusters together with a second specimen from Sweden and forms the sister group to two Swiss *Trochulus* specimens from Zerneze and Lac du Mont d'Orge. The resolution within the *T. biconicus* clade is moderate because the investigated individuals differ in only few nucleotides in all three investigated markers.

The ML analysis of the concatenated data set (Fig. 3) shows a similar topology as that of the BI analysis. The difference in the ML and the BI tree is the relationship of *Edentiella* and *Noricella*. In the ML tree, *E. edentula* clusters together with *N. scheerpeltzi*. This node has low support value (bootstrap support of 51 in Fig. 3), whereas in the BI analysis (Fig. 2), *Edentiella* and *Noricella* show a polytomy. In both analyses, *T. biconicus* forms the sister lineage to the selected *Trochulus* species. This node has full ML support. The support values within the *Trochulus* clade are moderate to high.

The *p*-distance, which shows the number of base differences per site from between sequences (Kumar et al. 2018) for the COI was calculated using MEGA

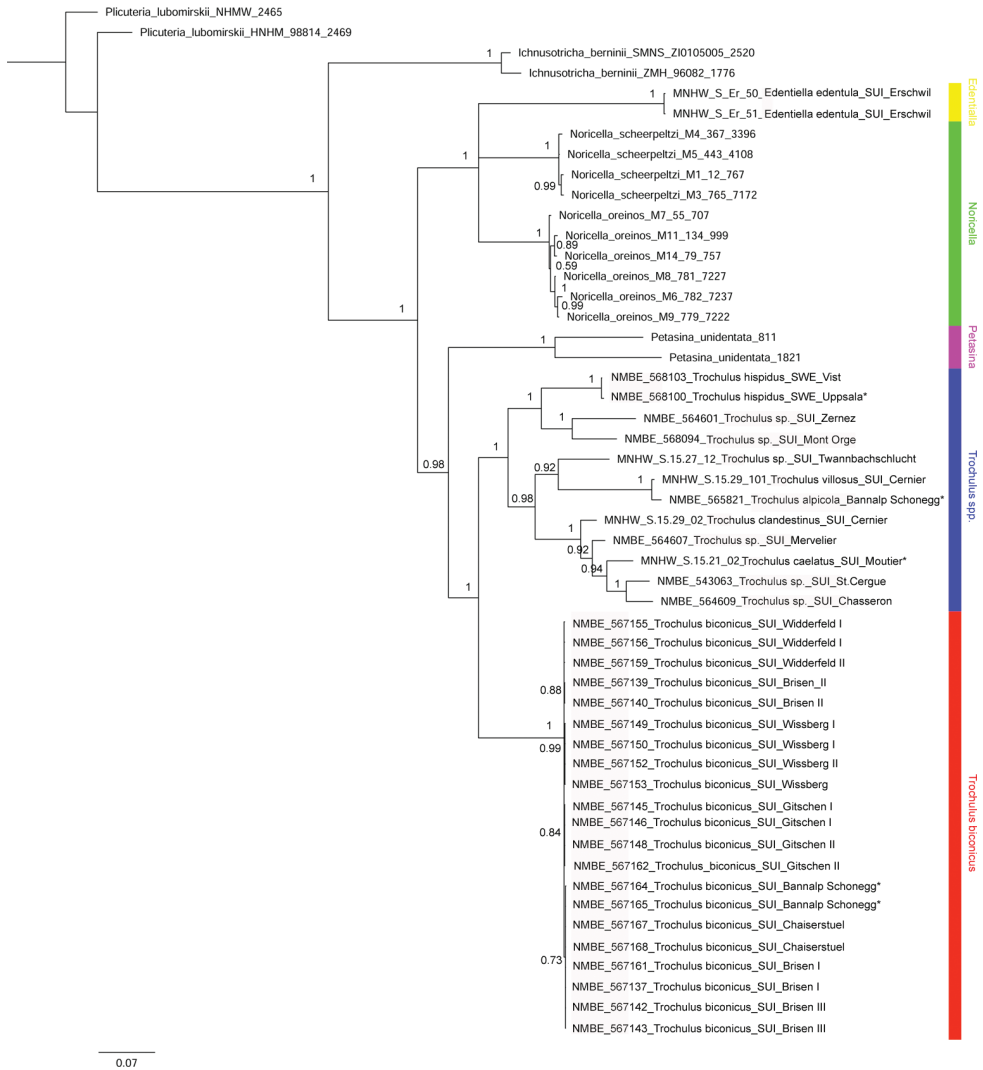


Figure 2. Bayesian Inference (BI) tree based on the concatenated data set of COI, 16S, and 5.8S rRNA+ITS2. Numbers represent Bayesian posterior probabilities.

v. 10.1.8 (<https://www.megasoftware.net/>). The p -distance for *T. biconicus* and the remaining investigated *Trochulus* species ranges from 0.153–0.189, for *T. biconicus* and *E. edentula* from 0.183–0.189, for *T. biconicus* and *Noricella* species from 0.128–0.166, for *T. biconicus* and *P. unidentata* from 0.171–0.176, for *T. biconicus* and *I. berninii* from 0.142–0.147 and for *T. biconicus* and *P. lubomirskii* from 0.177–0.188 (see Suppl. material 1). The genetic investigations in this study clearly show that *T. biconicus* is neither a member of the *Trochulus* clade nor does it belong to another known genus in the Trochulini. It thus, warrants designation in a separate new genus.

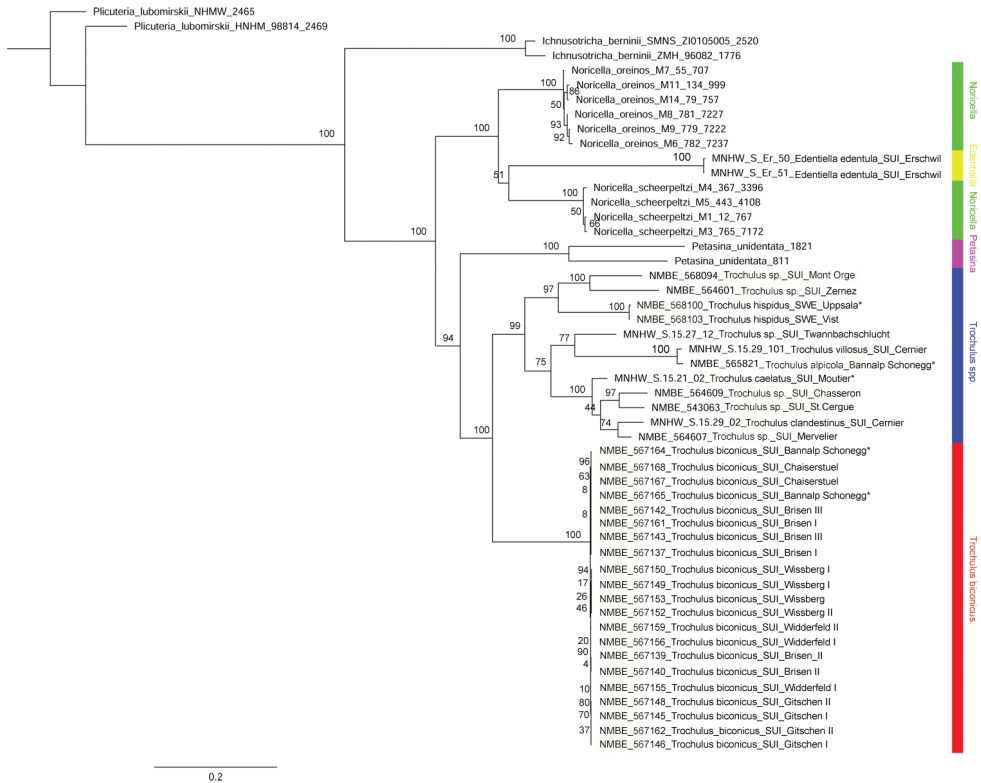


Figure 3. Maximum Likelihood (RAxML) tree based on the concatenated data set of COI, 16S, and 5.8S rRNA+ITS2. Numbers represent bootstrap support values from the ML analysis.

Shell morphology

The shell of *T. biconicus* is flattened, tightly coiled, and beige to brownish. The mean shell width of the investigated individuals ($N = 13$) is 5.63 mm (range: 5.3–6.1 mm; SD = 0.23 mm) with mean shell height reaching 2.67 mm (range: 2.34–2.9 mm; SD = 0.17 mm) (Table 3). The shell bears 5.5–6 whorls which increase only slightly in width towards the perimeter. The umbilicus is entirely open and wide. The crescent-shaped aperture contains a white, poorly developed lip. Neither juveniles nor adults show hairs on the shell (Figs 4–10).

Morphology of the genitalia

The genitalia are characterised by four stylophores, symmetrically placed in two pairs on both sides of the vagina (see fig. 11 in Proćków 2009). The inner dart sacs are somewhat longer and slenderer than the outer sacs. The outer stylophores contain the love darts (see also Proćków 2009). The mucous glands consist of four simple and thin tubes branching off the free oviduct directly above the dart sacs. The vagina is a rather long tube, which is

almost smooth inside or shows some faint elongate tissue folds that connect to the atrium (not shown in the figures). The bursa copulatrix branches off from the free oviduct above the dart sacs and the mucous glands and is terminated by an elongated vesicle.

The penis is fusiform and contains a club-shaped penial papilla which points into the lumen of the penial chamber. The epiphallus is as long as the penis; the penis retractor muscle inserts at the transition zone between epiphallus and penis. The flagellum is about 1.5× the length of the penis and epiphallus each. The epiphallial lumen contains longitudinal tissue ridges (e.g., Fig. 4C). The penial chamber is characterised by smooth walls. The penial papilla contains a lateral subapical pore. The cross section of the penial papilla (Figs 4D, 5D) reveals a central duct surrounded by small folds.

The anatomy of the genitalia of *T. clandestinus* differs from *T. biconicus* by having eight long, thin mucous glands (Fig. 11). The inner dart sacs of the investigated *T. clandestinus* are slightly longer in length than the outer dart sacs. The flagellum has about the same length as the bulbous penis, and the epiphallus is slightly longer than the penis. The cross section of the penial papilla differs in *T. clandestinus* by having several tissue layers around the main tube of the penial papilla (Fig. 11D).

Table 3. Morphological analysis: measurements of the shell and genital organs of *T. biconicus* and *T. clandestinus*. Additionally, some collected dry shells from Bannalp Schonegg (NMBE 567170) and Chaiserstuel (NMBE 567171) were included in the analysis. Asterisk (*) marks the type locality of *T. biconicus*. Umbilicus minor diameter is measured according to Proćków (2009). All measurements are in mm.

Voucher No.	Species	Locality	Coordinates	Altitude [m]	shell width	shell height	umbilicus minor diameter	penis length	epiphallus length	flagellum length	Figure number
NMBE 567151	<i>T. biconicus</i>	Wissberg I	46.81°N, 8.47°E	2335	5.56	2.55	0.8	1.81	2.01	5.98	Fig. 4
NMBE 567160	<i>T. biconicus</i>	Widderfeld II	46.83°N, 8.33°E	2290	5.73	2.59	0.88	2.79	3.42	8.13	Fig. 5
NMBE 567138	<i>T. biconicus</i>	Brisen I	46.90°N, 8.45°E	2045	5.61	2.34	0.73	2.86	3.06	7.25	Fig. 6
NMBE 567163	<i>T. biconicus</i>	Gitschen II	46.88°N, 8.57°E	1970	5.67	2.87	0.84	2.23	3.67	6.38	Fig. 7
NMBE 567166	<i>T. biconicus</i>	Bannalp Schonegg*	46.87°N, 8.46°E	2232	5.75	2.76	0.96	1.84	1.98	4.26	Fig. 8
NMBE 567169	<i>T. biconicus</i>	Chaiserstuel	46.87°N, 8.46°E	2263	5.3	2.46	0.99	2.66	3.21	4.1	Fig. 9
NMBE 567170_1	<i>T. biconicus</i>	Bannalp Schonegg*	46.87°N, 8.46°E	2232	5.7	2.82	1.19	–	–	–	Fig. 10A
NMBE 567170_2	<i>T. biconicus</i>	Bannalp Schonegg*	46.87°N, 8.46°E	2232	6.03	2.73	1.08	–	–	–	Fig. 10B
NMBE 567170_3	<i>T. biconicus</i>	Bannalp Schonegg*	46.87°N, 8.46°E	2232	5.39	2.54	0.99	–	–	–	Fig. 10C
NMBE 567170_4	<i>T. biconicus</i>	Bannalp Schonegg*	46.87°N, 8.46°E	2232	6.1	2.9	1.07	–	–	–	Fig. 10D
NMBE 567171_1	<i>T. biconicus</i>	Chaiserstuel	46.87°N, 8.46°E	2263	5.46	2.76	1.08	–	–	–	Fig. 10E
NMBE 567171_2	<i>T. biconicus</i>	Chaiserstuel	46.87°N, 8.46°E	2263	5.41	2.61	0.79	–	–	–	Fig. 10F
NMBE 567171_3	<i>T. biconicus</i>	Chaiserstuel	46.87°N, 8.46°E	2263	5.46	2.83	0.89	–	–	–	Fig. 10G
NMBE 571318	<i>T. clandestinus</i>	Bern, Bümpliz	46.9435°N, 7.3922°E	540	9.64	5.57	1.29	4.24	5.79	4.69	Fig. 11

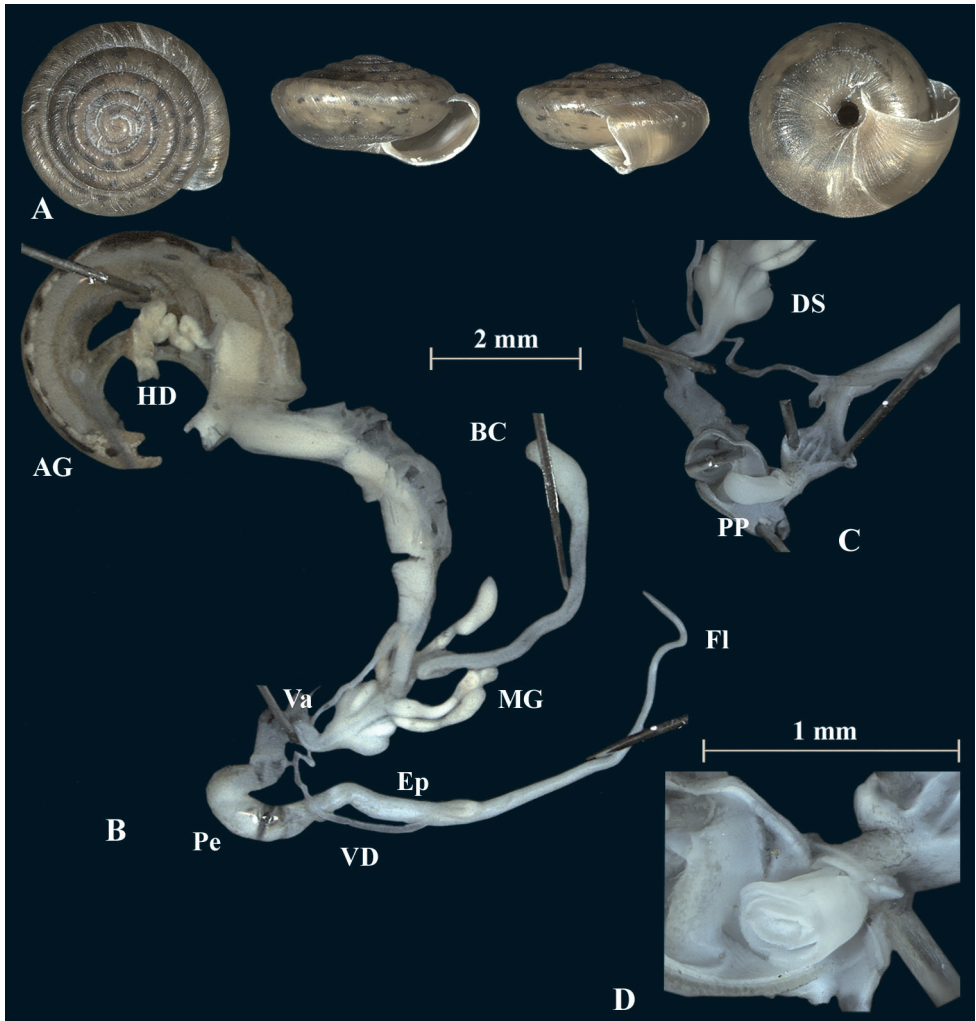


Figure 4. *Trochulus biconicus* (NMBE 567151) collected from Wissberg I **A** shell, sw = 5.56 mm, sh = 2.55 mm **B** situs **C** penis (Pe) with penial papilla (PP) **D** cross section of the penial papilla. Shell $\times 5$.

Taxonomic and systematic implications

The fully supported split between *T. biconicus* and currently known *Trochulus* species (Figs 2, 3) warrants description of a new genus, *Raeticella* gen. nov., based on *Fruticicola biconica*.

Genus *Raeticella* gen. nov.

<http://zoobank.org/D7620E37-3AA3-45D2-BB3C-B55114AF36F2>

Type species. *Fruticicola biconica* Eder, 1917.

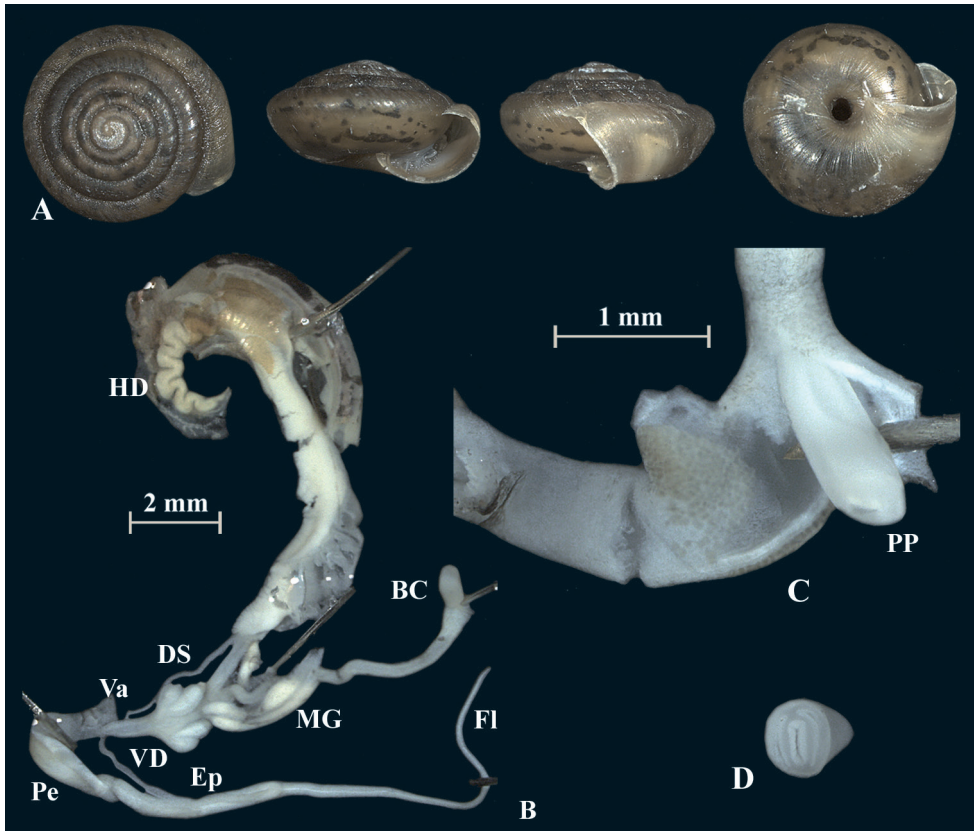


Figure 5. *Trochulus biconicus* (NMBE 567160) collected from Widdersfeld II **A** shell, sw = 5.73 mm, sh = 2.59 mm **B** situs **C** penis (Pe) with penial papilla (PP) **D** cross section of the penial papilla. Shell \times 5.

Genus *Trochulus* Chemnitz, 1786

Trochulus biconicus (Eder, 1917)

Diagnosis. Shell flattened and thin-walled, translucent, compressed in the direction of the axis; no trichome formation; whorls 5.5–6, gradually increasing so that the body whorl is only about twice as wide as the first whorl; the aperture is oblique, narrow, crescent-shaped; lip sharp, whitish and slightly reflexed; the four mucous glands are long, thick and pointed; penis and epiphallus are about the same length; the flagellum is barely separated from the epiphallus.

Differential diagnosis. *Raeticella* gen. nov. differs from *Trochulus* by having a flat, biconical shell, devoid of any periostracal hairs, even in juveniles, and in having only four instead of occasionally six or eight (see Duda et al. 2014) mucous glands. It differs from *Noricella* by lacking a basal tooth, being devoid of any periostracal hairs, the absence of coarse ripples and the absence of an additional fold and bulge in the penial papilla, which occurs in *N. oreinos* (Duda et al. 2014).

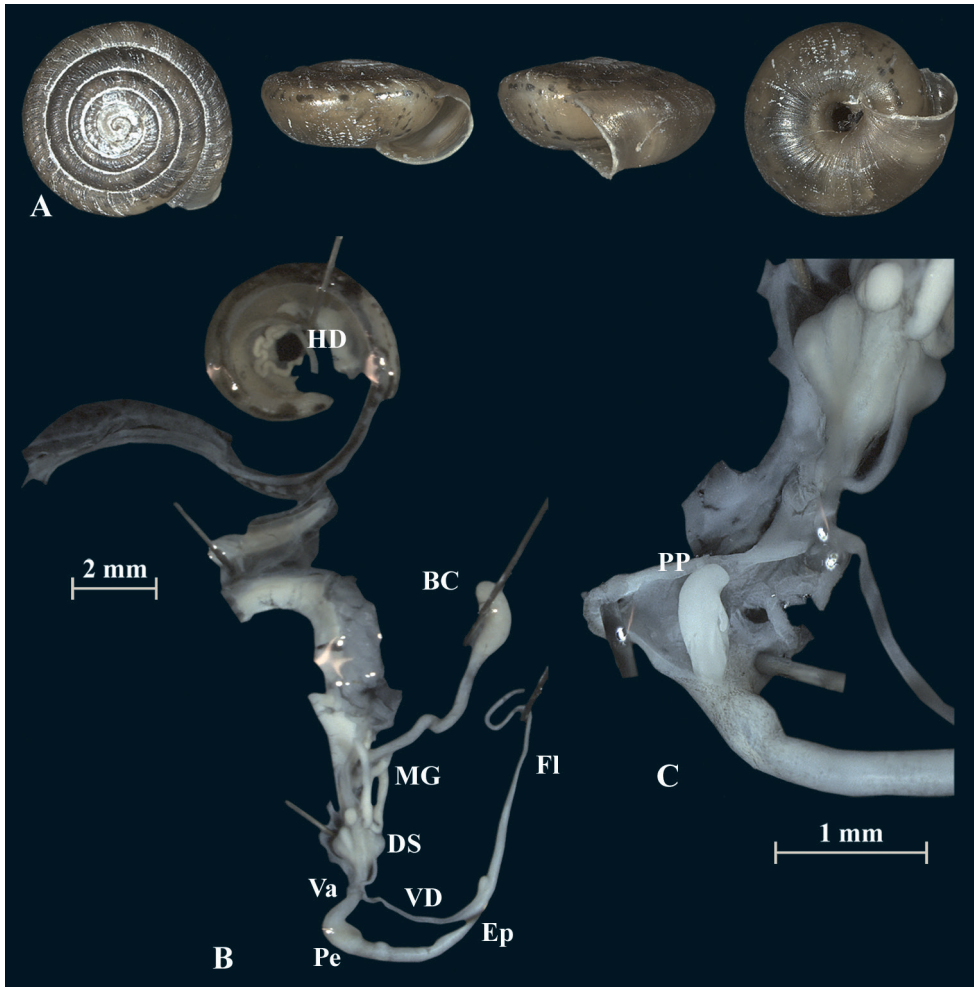


Figure 6. *Trochulus biconicus* (NMBE 567138) collected from Brisen I **A** shell, sw = 5.61 mm, sh = 2.34 mm **B** situs **C** penis (Pe) with penial papilla (PP). Shell $\times 5$.

Etymology. The name is derived from the Roman province of Raetia, which comprised within its larger expansion, the area of what is now known as eastern and central Switzerland. It also refers to the generic name, *Noricella*, which is another recently detected spin-off from *Trochulus* and whose name derives in part from the eastern border province of Raetia (Noricum – now Austria and Slovenia).

Discussion

Neiber et al. (2017) clarified the phylogenetic positions of some species within the Trochulini by establishing the new genus *Noricella* Neiber, Razkin & Hausdorf, 2017. In their study it was proven that *N. oreinos* and *N. scheerpeltzi* differed from the closest

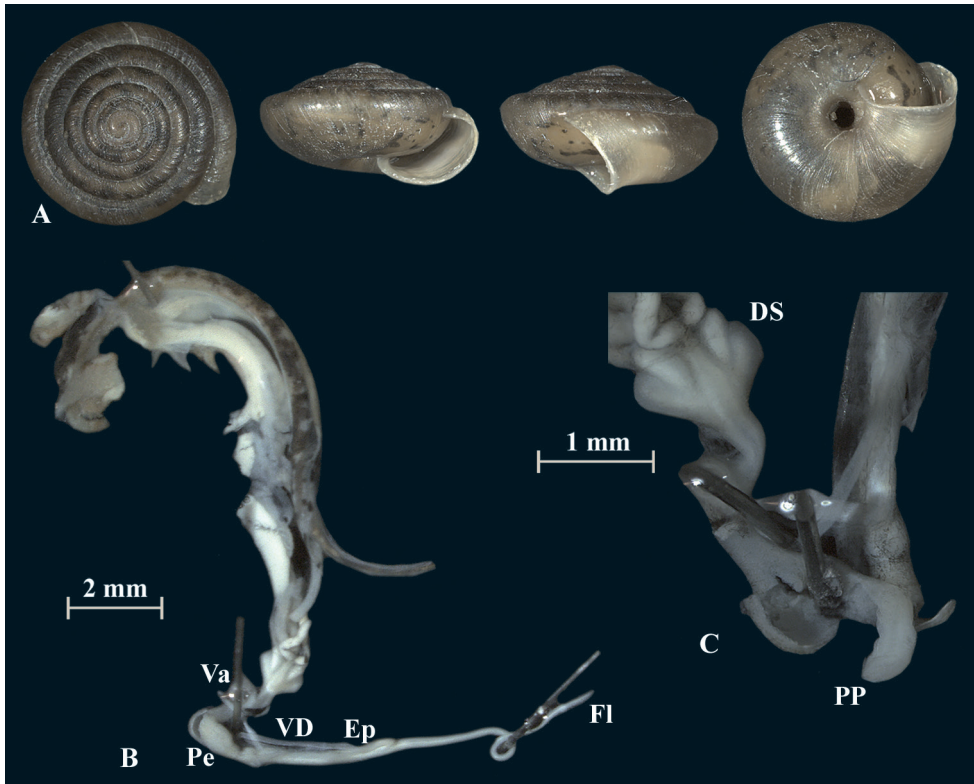


Figure 7. *Trochulus biconicus* (NMBE 567163) collected from Gitschen II **A** shell, sw = 5.67 mm, sh = 2.87 mm **B** situs **C** penis (Pe) with penial papilla (PP). Shell $\times 5$.

related genus *Edentiella* Poliński, 1929 in some apomorphic nucleotide substitutions and by morphological characters. *Edentiella* contains at least one longitudinal septum separating an additional lacuna in the penial papilla which is lacking in *N. oreinos*, in most *Trochulus* species, and in *Petasina* (Neiber et al. 2017). These authors also included some representatives of *Trochulus* but did not have specimens of *R. biconica* available. Turner et al. (1998) had already considered *R. biconica* to be only distantly related to *Trochulus* s. str. because of 1) the lack of periostracal hair even in juveniles, 2) a very long flagellum, and 3) only four instead of six or eight mucous glands. Hence, Turner (1991) suggested to move *R. biconica* into a subgenus of *Trochulus*. The questionable position of *biconicus* in *Trochulus* was recently re-addressed by Proćków et al. (2021). In our analysis, the calculated *p*-distance of *R. biconica* and the investigated *Trochulus* specimens comprises the highest values. The *p*-distance of *R. biconica* and *Noricella* species is lower than for *Trochulus*, which means that *Raeticella* is genetically closer, based on COI, to *Noricella* than to *Trochulus*. Even *Ichmusotricha*, which belongs to the tribe of Ganulini is genetically more similar to *Raeticella* than *Trochulus* is to *Raeticella*.

The shell morphology of *R. biconica* differs from all known *Trochulus* species by having a flat shell with a low spire. The last whorl is bluntly keeled. Adults are always hairless (Proćków 2009). In this regard, it is most like the shells of the two *Noricella*

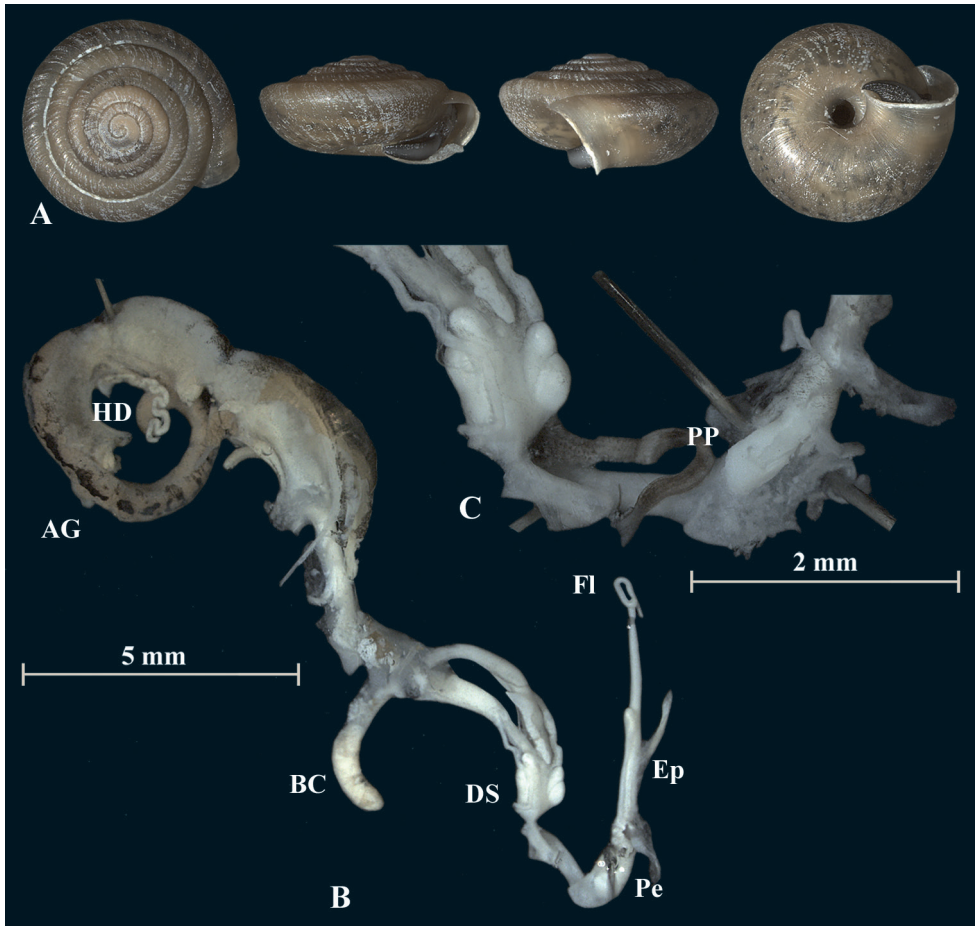


Figure 8. *Trochulus biconicus* (NMBE 567166) collected from Bannalp Schonegg **A** shell, sw = 5.75 mm, sh = 2.76 mm **B** situs **C** penis (Pe) with penial papilla (PP). Shell $\times 5$.

species (Duda et al. 2011, 2014), but the anatomy of the genital organs of these species is different. Both *Noricella* species have four pairs of mucous glands, compared to two pairs in *R. biconica*. *Noricella oreinos* possesses an additional fold and bulge in the penial papilla, which seems to be unique to this species (Duda et al. 2014). The section of the penial papilla in *R. biconica* shows similar internal features as in *T. caelatus* (Proćków 2009), *T. striolatus* (Proćków 2009; Duda et al. 2014; Proćków et al. 2021), and *T. suberectus* (Proćków 2009). *Raeticella biconica* does not possess periostracal hairs, neither as a juvenile nor as an adult. This, however, is considered a typical feature for *Trochulus* species (Proćków 2009).

Hewitt (2004) observed that many taxa in temperate refugial regions in Europe and North America show relatively deep DNA divergence, indicating their presence over several ice ages and suggesting a mode of speciation by repeated allopatry. On the one hand, this possibly explains the deep split between *Raeticella* and *Trochulus* and shifts

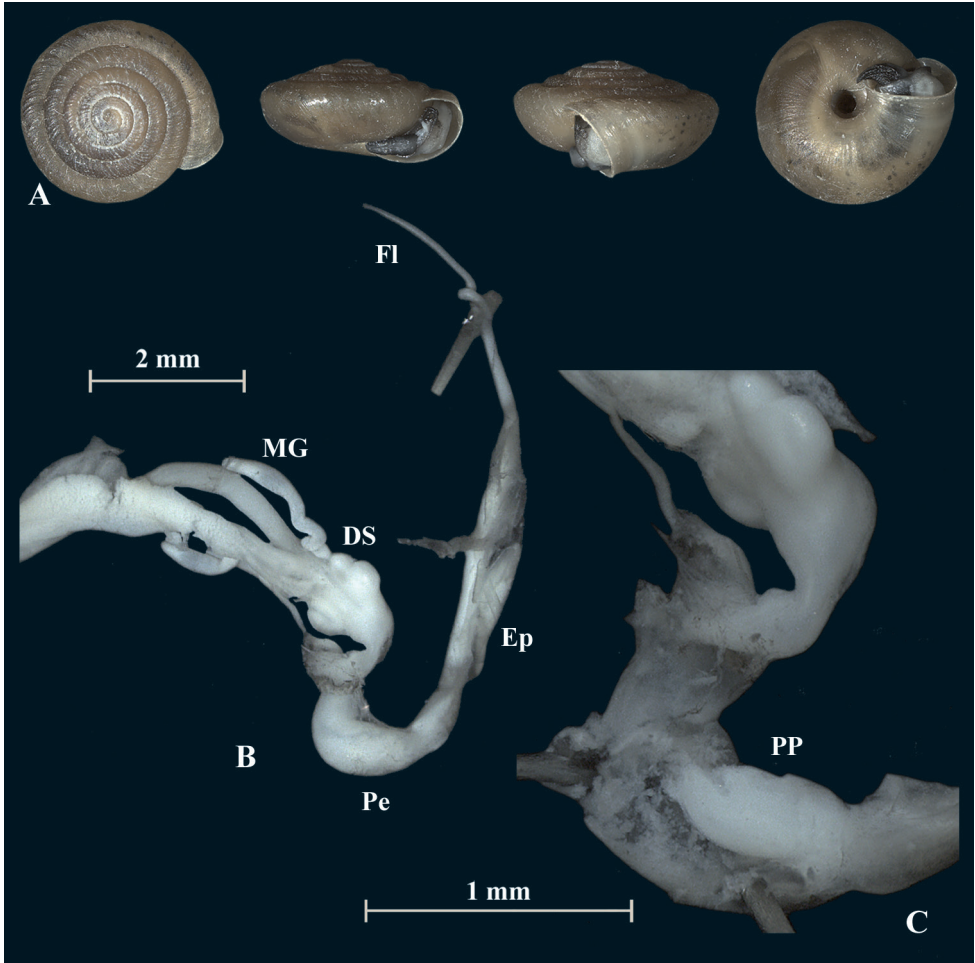


Figure 9. *Trochulus biconicus* (NMBE 567169) collected from Chaiserstuel **A** shell, sw = 5.30 mm, sh = 2.46 mm **B** situs **C** penis (Pe) with penial papilla (PP). Shell $\times 5$.

the splitting event of these groups to the Pliocene. On the other hand, we observed a low genetic diversity within our analysed populations. So, this species probably underwent a bottleneck event during the Pleistocene and the Last Glacial Maximum (LGM). Some isolated populations obviously survived this icy period. The LGM lasted about 30–19 ka in the Alps. During that period, this area was covered by massive ice sheets, and the glaciers reached out to the forelands of both, the northern and southern side of the main alpine chains. However, mountain tops above more than 2000 m were not covered by ice during the LGM. The recession of the glaciers from their maximum extent started around 24 ka (see Ivy-Ochs 2015). We hypothesize that the original distribution area of *R. biconica* was much larger, but only a few individuals survived on neighbouring nunataks (glacial islands) during the LGM. A similar scenario is assumed

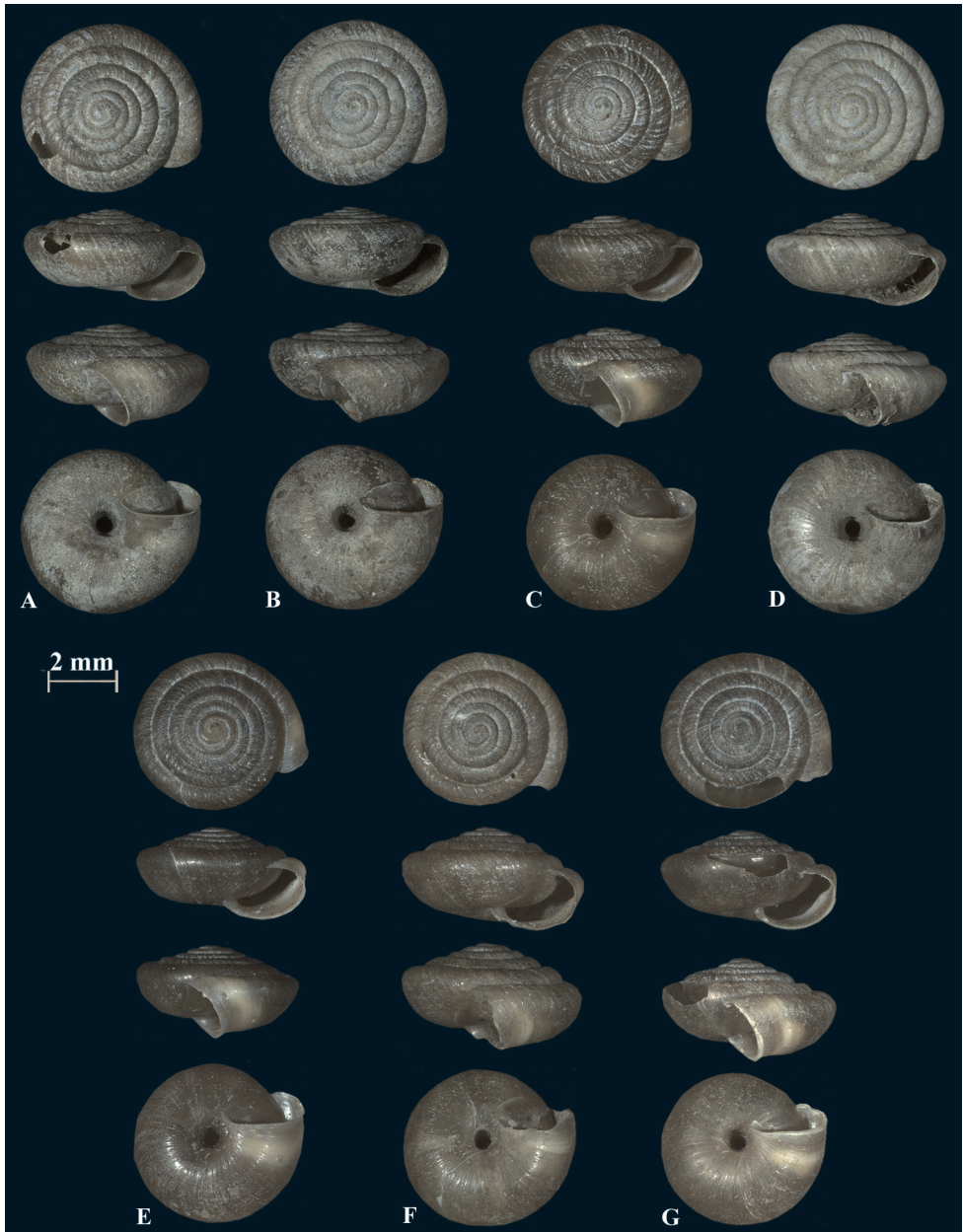


Figure 10. Shells of *Trochulus biconicus* from Bannalp Schonegg (**A–D**) and from Chaiserstuel (**E–G**).

for the evolution of the two *Noricella* species (Duda et al. 2011, 2014; Kruckenhauser et al. 2014). Gittenberger et al. (2004) also hypothesized the survival of *Arianta arbustorum alpicola* (A. Férussac, 1821) on nunataks. A similarly fragmented distribution pattern can be observed in the eastern alpine mollusc species *Cylindrus obtusus* (Draparnaud,

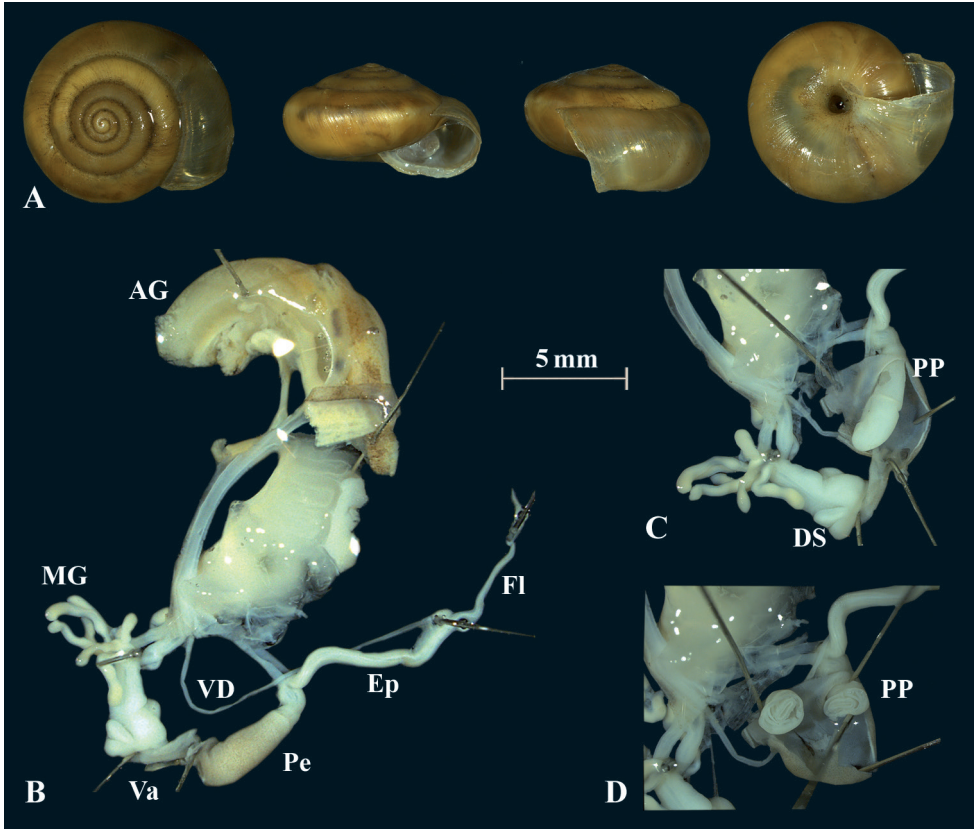


Figure 11. *Trochulus clandestinus* (NMBE 571318) collected from Bümpliz, Bern, Switzerland **A** shell, sw = 9.64 mm, sh = 5.57 mm **B** situs **C** penis (Pe) with penial papilla (PP) **D** cross section of the penial papilla. Shell $\times 3$.

1805) (Schileyko 2012: 95, fig. 2). Schileyko argued that the missing fossil record for this species proves that it was formed at the end of the Würm glaciation approximately 10–12 ka ago. As a species adapted to cold environmental conditions, this species was then assumed to be forced to follow the retreating snow and ice fields, which subsequently lead to habitat fragmentation. This assumption requires an ancestor from interglacials (which is also not found in the fossil record), and has to explain the rapid transformation of an Ariantine species from a globular or even depressed shell to a turritiform shell. This is most unlikely. Based on COI sequences, Cadahía et al. (2014) estimated 1.5–12 mya for the split between *Arianta* and *Cylindrus*. So, we assume that *Raeticella* gen. nov., like the monotypic genus *Cylindrus*, evolved much earlier and survived the Pleistocene by chance on nunatak mountain tops.

The current distribution pattern does not necessarily and strictly reflect the “survivor” populations. ARNAL (2018) found a limited gene flow between the “isolated” populations of *R. biconica*. This shows that dispersal is not completely impossible, but,



Figure 12. Typical habitat of *Raeticella biconica*. This photograph was taken on 25.05.2009 on Chaiserstuel (46.8762°N, 8.4671°E, 2263 m) by Markus Baggenstos.

due to the high-altitude adaptation of the species, it is rather limited to other, hitherto unpopulated high alpine areas. Possible vectors may be large pasturing animals like sheep and goats, but also ibex, chamois, or birds.

In alpine environments, microendemic species with a relict distribution pattern may occur, which were much more widespread in earlier times. They are now restricted to a very small area due to changes in environmental condition (Turner 1991; Cook 2008; Veron et al. 2019). The distribution area of *R. biconica* is currently known to encompass 150 isolated sites on both sides of the Engelberger valley, all situated between 1890 and 2575 m of altitude (Baggenstos 2010).

The habitat of *R. biconica* is very special, and only few other snail species are known to survive in this harsh environment (Eder 1917; Baggenstos 2010). Apart from the occurrence of limestone scree, the snails very much depend on small-scale relief. Slope edges or hilltops, ridges and summits as well as rocky heads and rocky steps are more likely to be colonised by the snail than slope hollows and slope foothills. The highest density of *R. biconica* is reached in areas with more than 50% of rocky scree (Baggenstos 2010). All these sites are covered with snow for a relatively short time in winter. With its flat shell, *R. biconica* is perfectly adapted to live under or between stones (Figs 12, 13). Flatness was interpreted as an adaptation to the cold



Figure 13. Close-up of *Raeticella biconica* crawling on the underside of a stone. This photograph was taken on 09.09.2009 on Chaiserstuel (46.8762°N, 8.4671°E, 2263 m) by Markus Baggenstos.

climate at the top of the mountains and may protect the animals from predators (Baur 1987). When it gets too hot, the snails retreat into the ground. The individuals are mainly active during night (Baggenstos 2010). Almost all known *R. biconica* habitats are blue grass meadows. These are alpine grasslands rich in flowers with a great diversity and a remarkably high proportion of Leguminosae. The prominent structural elements are *Sesleria caerulea* and *Carex sempervirens*. The soil cover is relatively thin, interspersed with gravel and stones and dries out quickly (Delarze et al. 2008). Wigger (2007) observed that *R. biconica* mainly feeds on decaying leaves of blue grass (*Sesleria caerulea*). The landscape of these meadows is strongly influenced by extensive pasturing and hiking tourism. Pasture animals like sheep, goats, and cows can modify the position of large stones and thus create new micro habitats for the snails. However, stronger interventions, such as the removal of stones or a climate-related transfer of the rubble-rich sites into closed meadows or woodland formations would cause the snail to disappear (Turner 1991).

This stenoeccious species is prone to extinction because of climate change. Over the last 100 years temperatures have increased by about 0.12–0.20 °C per decade in the Swiss Alps and the snow seasons have shortened (Kohler et al. 2014). *Raeticella biconica* already reached the summits of the mountains in their vicinity, and there is no more alternative for avoiding unsuitable climate conditions. Considering that global warming is ongoing, *R. biconica* may well become extinct in just a few years.

Conclusion

Long known morphological characteristics in conjunction with our genetic analyses show that *R. biconica* should be assigned to a new genus. Morphologically, the investigated individuals of *R. biconica* strongly resemble *N. oreinos* (Duda et al. 2011). But the genetic analyses of several different species from all genera within Trochulini reveal that *R. biconica* does not belong to any currently known genus. Therefore, a new monotypic genus within Trochulini is introduced.

Acknowledgements

We are indebted to Małgorzata Proćków for providing tissue samples of *E. edentula* and some *Trochulus* specimens, to Ted von Proschwitz for providing *T. hispidus* samples from the Swedish type locality, to Adrienne Jochum for the linguistic revision, to Tom Burri for paleoecological insights, to the Swiss Federal Office of Environment (FOEN) for financial support (contract no. 110010344 / 8T30/00.5147.PZ/0006), and to the cantonal authorities of Nidwalden (Felix Omlin), Obwalden (Andreas Bacher), and Uri (Georges Eich) for providing sampling permits.

References

- Altekar G, Dwarkadas S, Huelsenbeck JP, Ronquist F (2004) Parallel Metropolis-coupled Markov chain Monte Carlo for Bayesian phylogenetic inference. *Bioinformatics* (Oxford, England) 20(3): 407–415. <https://doi.org/10.1093/bioinformatics/btg427>
- ARNAL Büro für Natur und Landschaft AG (2018) Projekt Naturschutzgenetik – Schlussbericht: Methodik und Resultate (Insbeso. «Verbund»). Report, Herisau, 45 pp.
- Baggenstos M (2010) Verbreitung und Biologie der Nidwaldner Haarschnecke (*Trochulus biconicus*). Report, Stans, 45 pp.
- Bamberger S, Duda M, Tribsch A, Haring E, Sattmann H, Macek O, Affenzeller M, Kruckenhauser L (2020) Genome-wide nuclear data confirm two species in the Alpine endemic land snail *Noricella oreinos* s.l. (Gastropoda, Hygromiidae). *Journal of Zoological Systematics and Evolutionary Research* 58(4): 982–1004. <https://doi.org/10.1111/jzs.12362>
- Baur B (1987) Richness of land snail species under isolated stones in a karst area on Öland, Sweden. *Basteria* 51: 129–133.
- Cadahía L, Harl J, Duda M, Sattmann H, Kruckenhauser L, Fehér Z, Zopp L, Haring E (2014) New data on the phylogeny of Ariantinae (Pulmonata, Helicidae) and the systematic position of *Cylindrus obtusus* based on nuclear and mitochondrial DNA marker sequences. *Journal of Zoological Systematics and Evolutionary Research* 52(2): 163–169. <https://doi.org/10.1111/jzs.12044>
- Chemnitz JH (1786) Neues systematisches Conchylien-Cabinet. Neunten Bandes zwote Abtheilung, enthaltend die ausführliche Beschreibung von den Land- und Flußschnecken,

- oder von solchen Conchylien welche nicht im Meer, sondern auf der Erde und in süßen Wassern zu leben pflegen. Mit zwanzig nach der Natur gemalten und durch lebendige Farben erleuchteten. Raspe, Nürnberg, [xxvi +] 194 pp. [pls 117–136] <https://doi.org/10.5962/bhl.title.125416>
- Chiba S (1999) Accelerated evolution of land snails *Mandarina* in the oceanic Bonin Islands: Evidence from mitochondrial DNA sequences. *Evolution; International Journal of Organic Evolution* 53(2): 460–471. <https://doi.org/10.1111/j.1558-5646.1999.tb03781.x>
- Cook LM (2008) Species richness in Madeiran land snails, and its causes. *Journal of Biogeography* 35(4): 647–653. <https://doi.org/10.1111/j.1365-2699.2007.01801.x>
- Delarze R, Gonseth Y, Galland P (2008) Lebensräume der Schweiz: Ökologie, Gefährdung, Kennarten. Ott Verlag, Thun, 424 pp.
- Dépraz A, Hausser J, Pfenninger M (2009) A species delimitation approach in the *Trochulus sericeus/hispidus* complex reveals two cryptic species within a sharp contact zone. *BMC Evolutionary Biology* 9(1): e171. <https://doi.org/10.1186/1471-2148-9-171>
- Duda M, Sattmann H, Haring E, Bartel D, Winkler H, Harl J, Kruckenhauser L (2011) Genetic differentiation and shell morphology of *Trochulus oreinos* (Wagner, 1915) and *T. hispidus* (Linnaeus, 1758) (Pulmonata: Hygromiidae) in the northeastern Alps. *Journal of Molluscan Studies* 77(1): 30–40. <https://doi.org/10.1093/mollus/eyq037>
- Duda M, Kruckenhauser L, Sattmann H, Harl J, Jaksch K, Haring E (2014) Differentiation in the *Trochulus hispidus* complex and related taxa (Pulmonata: Hygromiidae): morphology, ecology and their relation to phylogeography. *Journal of Molluscan Studies* 80(4): 371–387. <https://doi.org/10.1093/mollus/eyu023>
- Eder L (1917) Eine neue Schweizer Helicide. *Revue Suisse de Zoologie* 25(15): 442–452.
- Folmer O, Black M, Hoe W, Lutz R, Vrijenhoek R (1994) DNA primers for amplification of mitochondrial cytochrome c oxidase subunit I from diverse metazoan invertebrates. *Molecular Marine Biology and Biotechnology* 3(5): 294–299.
- Gittenberger E, Piel WH, Groenbergh DSJ (2004) The Pleistocene glaciations and the evolutionary history of the polytypic snail species *Arianta arbustorum* (Gastropoda, Pulmonata, Helicidae). *Molecular Phylogenetics and Evolution* 30(1): 64–73. [https://doi.org/10.1016/S1055-7903\(03\)00182-9](https://doi.org/10.1016/S1055-7903(03)00182-9)
- Hartmann JDW (1840–1844) Erd- und Süßwasser-Gasteropoden der Schweiz. Mit Zugabe einiger merkwürdigen exotischen Arten. Scheitlin und Zollikofer, St. Gallen, [i–xx,] 36 pp. [pls 1, 2 [30-06-1840]; 37–116, pls 13–36 [1841]; 117–156, pls 37–60 [1842]; 157–204, pls 61–72 [1843]; 205–227, pls 73–84 [1844]]
- Hewitt GM (2004) Genetic consequences of climatic oscillations in the Quaternary. *Philosophical Transactions of the Royal Society of London. Series B, Biological Sciences* 359(1442): 183–195. <https://doi.org/10.1098/rstb.2003.1388>
- Huelsenbeck JP, Ronquist F (2001) MRBAYES: Bayesian inference of phylogeny. *Bioinformatics (Oxford, England)* 17(8): 754–755. <https://doi.org/10.1093/bioinformatics/17.8.754>
- Ivy-Ochs S (2015) Glacier variations in the European Alps at the end of the last glaciation. *Cuadernos de Investigación Geográfica* 42(2): 295–315. <https://doi.org/10.18172/cig.2750>
- Kerney MP, Cameron RAD, Jungbluth JH (1983) Die Landschnecken Nord- und Mitteleuropas. Parey-Verlag, Hamburg/Berlin, 384 pp.

- Kohler T, Wehrli A, Jurek M (2014) Mountains and climate change: a global concern. Sustainable Mountain Development Series. Centre for Development and Environment (CDE), Swiss Agency for Development and Cooperation (SDC) and Geographica Bernensia, Bern, 136 pp. <https://doi.org/10.1659/mrd-journal-d-09-00086.1>
- Kruckenhauser L, Duda M, Bartel D, Sattmann H, Harl J, Kirchner S, Haring E (2014) Paraphyly and budding speciation in the hairy snail (Pulmonata, Hygromiidae). *Zoologica Scripta* 43(3): 273–288. <https://doi.org/10.1111/zsc.12046>
- Kumar S, Steche G, Li M, Knyaz C, Tamura K (2018) MEGA X: Molecular Evolutionary Genetics Analysis across computing platforms. *Molecular Biology and Evolution* 35(6): 1547–1549. <https://doi.org/10.1093/molbev/msy096>
- Neiber MT, Razkin O, Hausdorf B (2017) Molecular phylogeny and biogeography of the land snail family Hygromiidae (Gastropoda: Helicoidea). *Molecular Phylogenetics and Evolution* 111: 169–184. <https://doi.org/10.1016/j.ympev.2017.04.002>
- Pfenninger M, Hrabáková M, Steinke D, Dépraz A (2005) Why do snails have hairs? A Bayesian inference of character evolution. *BMC Evolutionary Biology* 5(1): e59. <https://doi.org/10.1186/1471-2148-5-59>
- Pročków M (2009) The genus *Trochulus* Chemnitz, 1786 (Gastropoda: Pulmonata: Hygromiidae) – a taxonomic revision. *Folia Malacologica* 17(3): 101–176. <https://doi.org/10.2478/v10125-009-0013-0>
- Pročków M, Kuznik-Kowalska E, Pienkowska JR, Zeromska A, Mackiewicz P (2021) Speciation in sympatric species of land snails from the genus *Trochulus* (Gastropoda, Hygromiidae). *Zoologica Scripta* 50(1): 16–42. <https://doi.org/10.1111/zsc.12458>
- Ronquist F, Huelsenbeck JP (2003) MRBAYES 3: Bayesian phylogenetic inference under mixed models. *Bioinformatics (Oxford, England)* 19(12): 1572–1574. <https://doi.org/10.1093/bioinformatics/btg180>
- Shileyko AA (2012) On the origin of *Cochlopupa* (= *Cylindrus* auct.) *obtus*a (Gastropoda, Pulmonata, Helicidae). *Ruthenica: Rossiiskii Malakologicheskii Zhurnal = Russian Malacological Journal* 22: 93–100.
- Stamatakis A (2014) RAxML Version 8: A tool for Phylogenetic Analysis and Post-Analysis of Large Phylogenies. *Bioinformatics* 30(9): 1312–1313. <https://doi.org/10.1093/bioinformatics/btu033>
- Turner H (1991) Die Nidwaldner Haarschnecke gibt es sonst nirgends auf der Welt: ein kleines zoologisches Geheimnis lebt auf der Bannalp. *Nidwaldner Volksblatt* 240(17 Oktober): 13.
- Turner H, Kuiper JGJ, Thew N, Bernasconi R, Rüetschi J, Wüthrich M, Gosteli M (1998) Atlas der Mollusken der Schweiz und Lichtensteins. *Fauna Helvetica* 2. Center Suisse de cartographie de la faune, Schweizerische Entomologische Gesellschaft, Eidg. Forschungsanstalt für Wald, Schnee und Landschaft, Neuchâtel, 527 pp.
- Veron S, Haevermans T, Govaerts R, Mouchet M, Pellens R (2019) Distribution and relative age of endemism across islands worldwide. *Scientific Reports* 9(1): e11693. <https://doi.org/10.1038/s41598-019-47951-6>

- Wade CM, Mordan PB (2000) Evolution within the gastropod molluscs; using the ribosomal RNA gene-cluster as an indicator of phylogenetic relationships. *The Journal of Molluscan Studies* 66(4): 565–570. <https://doi.org/10.1093/mollus/66.4.565>
- Wigger F (2007) Der mikroklimatische und zeitabhängige Aktivitätsrhythmus von *Trochulus biconicus*. Eine Feldstudie im Rahmen der Projektarbeit in Biogeographie der Universität Basel in Zusammenarbeit mit der Oekologischen Beratung Markus Baggenstos. Basel, unpublished report Basel, 12 pp.

Supplementary material I

Calculated p-distances of the COI of the investigated specimens.

Authors: Jeannette Kneubühler, Markus Baggenstos, Eike Neubert

Data type: excel file

Explanation note: Calculated p-distances of the COI of the investigated specimens.

Copyright notice: This dataset is made available under the Open Database License (<http://opendatacommons.org/licenses/odbl/1.0/>). The Open Database License (ODbL) is a license agreement intended to allow users to freely share, modify, and use this Dataset while maintaining this same freedom for others, provided that the original source and author(s) are credited.

Link: <https://doi.org/10.3897/zookeys.1104.82866.suppl1>

Taxonomic study on the genus *Stenochironomus* Kieffer from the Baishanzu Nature Reserve, China (Diptera, Chironomidae)

Chao Song^{1*}, Bin-Qing Zhu^{2*}, Joel Moubayed-Breil³, Teng Lei¹, Xin Qi¹

1 College of Life Sciences, Taizhou University, Taizhou, Zhejiang 318000, China **2** Nanjing Institute of Environmental Sciences, Ministry of Ecology and Environment, Nanjing 210042, Jiangsu, China **3** Freshwater & Marine biology, 10 rue des Fenouils, F-34070 Montpellier, France

Corresponding author: Xin Qi (qixin0612@tzc.edu.cn)

Academic editor: F. Laurindo da Silva | Received 29 January 2022 | Accepted 8 May 2022 | Published 9 June 2022

<http://zoobank.org/E19A9296-55A8-4640-8DC0-0F9E34357F1E>

Citation: Song C, Zhu B-Q, Moubayed-Breil J, Lei T, Qi X (2022) Taxonomic study on the genus *Stenochironomus* Kieffer from the Baishanzu Nature Reserve, China (Diptera, Chironomidae). ZooKeys 1104: 93–113. <https://doi.org/10.3897/zookeys.1104.81403>

Abstract

During the summer of July to September 2020, a biodiversity survey on Chironomidae of Baishanzu Nature Reserve, China was made. In total, five *Stenochironomus* taxa/species were discovered, of which two belong to undescribed species and one (*S. okialbus* Sasa, 1990) is reported for the first time from China. The male adults of two new species are described and illustrated. *Stenochironomus annulus* Song & Qi **sp. nov.** is distinguished in having a wing with two dark spots restricted to the fork area of FCu and RM, the mid- and hind-femur each with a brown annulus, and the inferior volsella with two setae and one strong terminal spine. *Stenochironomus baishanzuensis* Song & Qi **sp. nov.** is distinguished by a combination of characters: a single dark spot on the middle part of the wing, fore legs brown to dark brown except for the basal 3/4 of femur, and the inferior volsella with four long setae and one stout terminal spine. The neighbour-joining tree based on public COI barcodes formed distinct clades with clear support for the new species. An updated key to known male adults of *Stenochironomus* from China is also provided.

Keywords

Chironominae, DNA barcode, new species, non-biting midge, *Stenochironomus*, taxonomy

* These authors contributed equally to this work.

Introduction

The genus *Stenochironomus* Kieffer, 1919 has a cosmopolitan distribution in all zoogeographical regions except for Antarctica (Cranston et al. 1989). The larvae are known as miners and occur in different habitats such as dead wood, dead leaves, and floating leaves of lotuses, *Nelumbo* (Borkent, 1984). Male adults are characterized by a combination of characters as documented by Borkent (1984) and Townes (1945): different color patterns of the thorax and legs; short to elongate, variably sausage-shaped superior volsella with several bristles; and long narrow curved inferior volsella with few apical bristles and terminal spines. *Stenochironomus* is composed of two subgenera, *Stenochironomus s. str.* and *Petalopholeus*, which cannot be differentiated on imaginal morphology.

Data on the taxonomy, keys, and geographical distributions for *Stenochironomus* show that there are 110 known valid species recorded worldwide, of which 14 species are reported from China (Qi et al. 2008a, b, 2011, 2015; Dantas et al. 2016; Parise and Pinho 2016; Zhang et al. 2016; Amora et al. 2018; Lin et al. 2021).

DNA barcoding employs sequence diversity in short, standardized, gene regions and has become an important tool for species identification and cryptic species discovery (Hebert et al. 2003). Chironomid researchers also confirmed the effectiveness of a DNA barcode reference library in the discovery of new species using the 658-bp fragment of the mitochondrial gene cytochrome c oxidase I (COI) (Kodama et al. 2018; Lin et al. 2020, Qi et al. 2020; Song et al. 2020).

Baishanzu is a nature reserve, spanning the south Zhejiang and north Fujian provinces of eastern China. It belongs to the tropical to warm temperate transitional zone and is a biodiversity hot spot in Asia with the dominant types of vegetation being evergreen broad-leaved forests and mixed coniferous and broad-leaved forests (Peng et al. 2012). During seasonal surveys of the nature reserve, five *Stenochironomus* taxa/species were discovered, of which two belong to undescribed species and one, *S. okialbus* Sasa, 1990, is reported for the first time from China. In addition, DNA barcodes of the new species were analyzed and clearly supported them as new species. An updated key to male adults of known *Stenochironomus* from China is also provided.

Materials and methods

Morphological study

The examined material was collected using light traps; the specimens were preserved in 75% ethanol at 4 °C in a refrigerator before final slide mounting. Specimens were side-mounted in Euparal after genomic extraction following the procedure described by Sæther (1969). Morphological terminology follows that of Sæther (1980). The photographs of the habitus of each specimen were obtained with a DV500 5MP Digital Camera attached to a stereo microscope (Chongqing Optec SZ680). The photo-

graphs of the body parts were obtained using a Leica DMLS compound microscope. Photograph post-processing was done in Adobe Photoshop and Illustrator version 8 (Adobe Inc., California, USA).

The type material including holotype and paratypes of the two new described species are deposited in the collection of the College of Life Sciences, Taizhou University, Taizhou, China (TZU).

Abbreviations used are as follows:

AR	antennal ratio, length of the 13 th / length of flagellomeres 1–12;
BV	length of (femur + tibia + ta ₁) / length of (ta ₂ + ta ₃ + ta ₄ + ta ₅);
Cu	cubitus;
Dc	dorsocentrals;
Fe	femur;
HR	hypopygium ratio, length of gonocoxite / length of gonostylus;
HV	hypopygium value, total length / 10* length of gonostylus;
IV	inner verticals;
LR	leg ratio; Length of ta ₁ / length of tibia;
M	media;
MCu	cross-vein between media and cubitus;
P1, P2, P3	Fore leg, mid leg, hind leg;
R	radius;
RM	cross-vein between radius and media;
Ta	tarsomere;
Ti	tibia;
VR	venarum ratio, length of Cu / length of M.

Molecular study

Tissues for total genomic DNA extraction were removed from the thorax and head of the adults. The genomic extraction procedure followed Frohlich et al. (1999). The standard barcode region of the 5' portion of the mitochondrial gene cytochrome c oxidase I (COI-5P) was amplified using the universal primers LCO1490 and HCO2198 (Folmer et al. 1994); PCR amplifications followed Song et al. (2018). PCR products were electrophoresed in 1.0% agarose gel, purified, and sequenced using an ABI 3730XL capillary sequencer (Beijing Genomics Institute Co., Ltd., Hangzhou, China). Raw sequences were edited in BioEdit 7.2.5 (Hall 1999).

Public *Stenochironomus* sequences were searched in GenBank, and 32 sequences were returned, of which eleven sequence were mitochondrion complete genomes. We extracted COI-5P barcode segments from those genomes.

The pairwise distances were calculated using the Kimura 2-Parameter (K2P) substitution model in MEGA 7 (Kumar et al. 2016). The neighbour-joining tree was constructed using the K2P substitution model, and 1000 bootstrap replicates and the

“complete deletion” option for missing data were utilized. Automatic Barcode Gap Discovery (ABGD) analysis was implemented on the website (www.wabi.snv.jussieu.fr/public/abgd/abgdweb.html, Puillandre et al. 2012), with K2P model. Sequences, trace-files, and metadata of the new species were uploaded to the Barcode of Life Data Systems (BOLD) (Ratnasingham and Hebert 2013).

Results and discussion

Barcode analysis

All 44 public COI-5P DNA barcodes comprising GenBank accessions and sequences from this study (Table 1) representing 12 species within *Stenochironomus* were used to construct the neighbour-joining tree. The twelve species formed 16 distinct genetic clades; two clades separately presented for the new species *Stenochironomus annulus* sp. nov., and *S. baishanzuensis* sp. nov. (Fig. 1). *Stenochironomus annulus* sp. nov. can be distinguished from other species by more than 11.2%, and *S. baishanzuensis* sp. nov. by more than 14.0% (Table 2). In the barcoded *Stenochironomus* species, there is a gap between 4–6% (Fig. 2), which may be used for the delimitation of *Stenochironomus* species. The thresholds for different Chironomidae groups are not always the same; for

Table 1. GenBank accession data used in the analysis; * data from this study.

Species	Sample ID	GenBank Accession	Species	Sample ID	GenBank Accession
<i>Stenochironomus annulus</i>	ZJCH220, *	ON002477	<i>Stenochironomus linanensis</i>	ZJCH251, *	ON002473
<i>Stenochironomus annulus</i>	ZJCH222, *	ON002475	<i>Stenochironomus okiabbus</i>	ZJCH219, *	ON002483
<i>Stenochironomus annulus</i>	ZJCH223, *	ON002480	<i>Stenochironomus okiabbus</i>	ZJCH244, *	ON002479
<i>Stenochironomus baishanzuensis</i>	ZJCH246, *	ON002482	<i>Stenochironomus okiabbus</i>	ZJCH245, *	ON002474
<i>Stenochironomus baishanzuensis</i>	ZJCH247, *	ON002476	<i>Stenochironomus okiabbus</i>	NC_061972	NC_061972
<i>Stenochironomus baishanzuensis</i>	ZJCH226, *	ON002484	<i>Stenochironomus okiabbus</i>	NIESH0017	LC462301
<i>Stenochironomus fascipennis</i>	ZMUO.025362	MZ657887	<i>Stenochironomus okiabbus</i>	NIESH0026	LC462365
<i>Stenochironomus fascipennis</i>	ZMUO.025363	MZ658663	<i>Stenochironomus okiabbus</i>	NIESH0307	LC462355
<i>Stenochironomus gibbus</i>	JN016848	JN016848	<i>Stenochironomus okiabbus</i>	NIESH0746	LC462364
<i>Stenochironomus gibbus</i>	NC_061971	NC_061971	<i>Stenochironomus okiabbus</i>	OL753645	OL753645
<i>Stenochironomus gibbus</i>	OL742440	OL742440	<i>Stenochironomus</i> sp. 1CZ	OL753646	OL753646
<i>Stenochironomus gibbus</i>	PY-32A	KP902798	<i>Stenochironomus</i> sp. 2CZ	OL742441	OL742441
<i>Stenochironomus gibbus</i>	PY-33A	KP902799	<i>Stenochironomus</i> sp. 3CZ	OL753647	OL753647
<i>Stenochironomus gibbus</i>	PY-34A	KP902800	<i>Stenochironomus</i> sp.1BD	HQ551963	HQ551963
<i>Stenochironomus gibbus</i>	STE-GIB-IM-LIM28VII-254	MT535051	<i>Stenochironomus</i> sp.1BD	HQ928366	HQ928366
<i>Stenochironomus gibbus</i>	STE-HIB-IM-VI29VII-304	MT535060	<i>Stenochironomus</i> sp.1BD	MF718872	MF718872
<i>Stenochironomus gibbus</i>	ZMUO.024239	MZ657365	<i>Stenochironomus</i> sp.1BD	MF721507	MF721507
<i>Stenochironomus gibbus</i>	ZMUO.024238	MZ656608	<i>Stenochironomus</i> sp.1BD	MF723892	MF723892
<i>Stenochironomus hibernicus</i>	ZMUO.025366	MZ660623	<i>Stenochironomus tobaduodecimus</i>	NC_061973	NC_061973
<i>Stenochironomus hibernicus</i>	ZMUO.025367	MZ656796	<i>Stenochironomus tobaduodecimus</i>	OL753648	OL753648
<i>Stenochironomus linanensis</i>	ZJCH224, *	ON002473	<i>Stenochironomus zhengi</i>	NC_061974	NC_061974
<i>Stenochironomus linanensis</i>	ZJCH249, *	ON002478	<i>Stenochironomus zhengi</i>	OL753649	OL753649

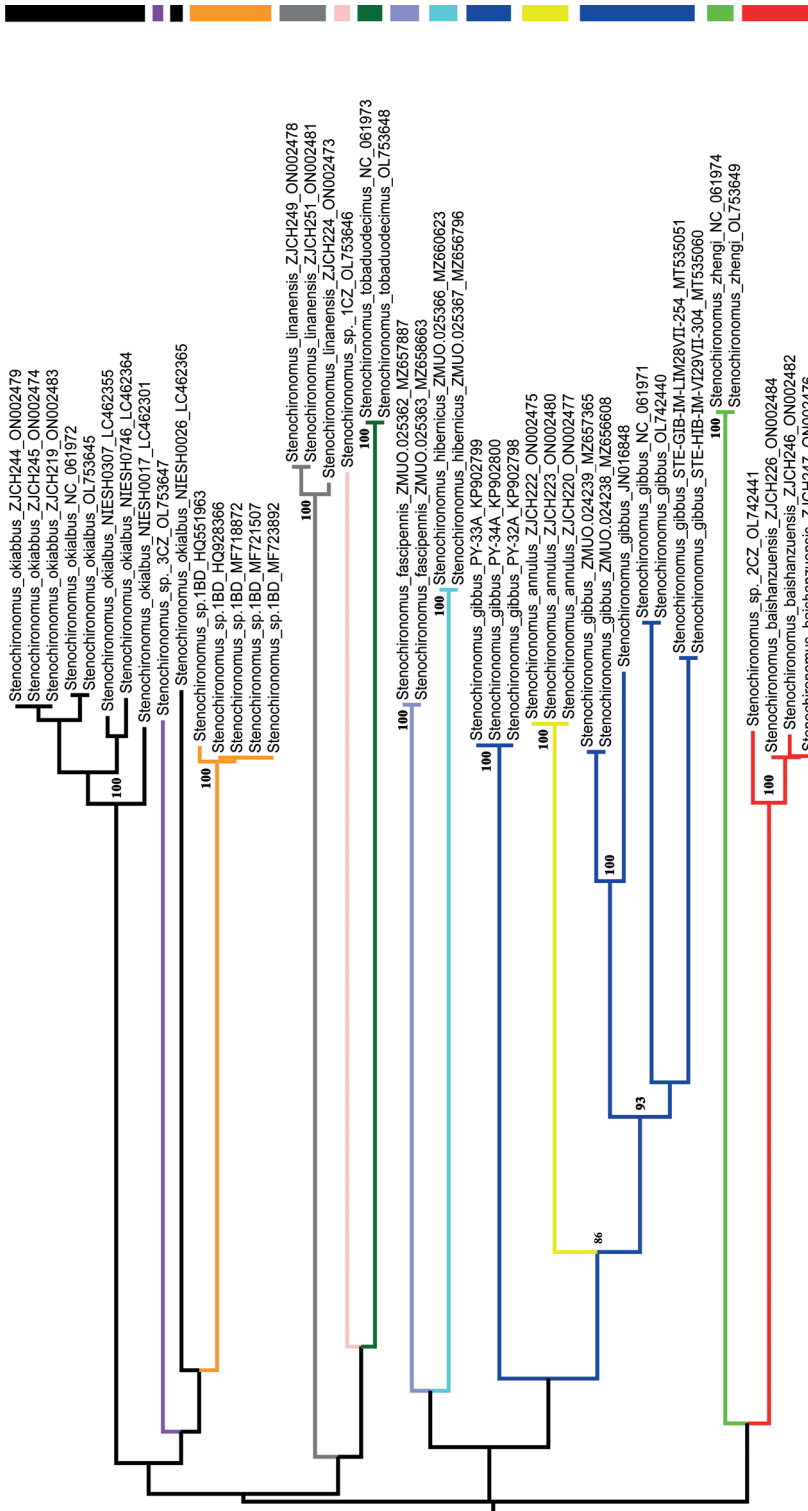


Figure 1. Neighbour-joining tree for twelve species of *Stenochironomus* based on K2P distance in DNA barcodes. Clade in yellow represents *S. annulus* sp. nov., red represents *S. baishanzuensis* sp. nov. Numbers on branches represent bootstrap support (>75%) based on 1000 replicates; scale equals K2P genetic distance.

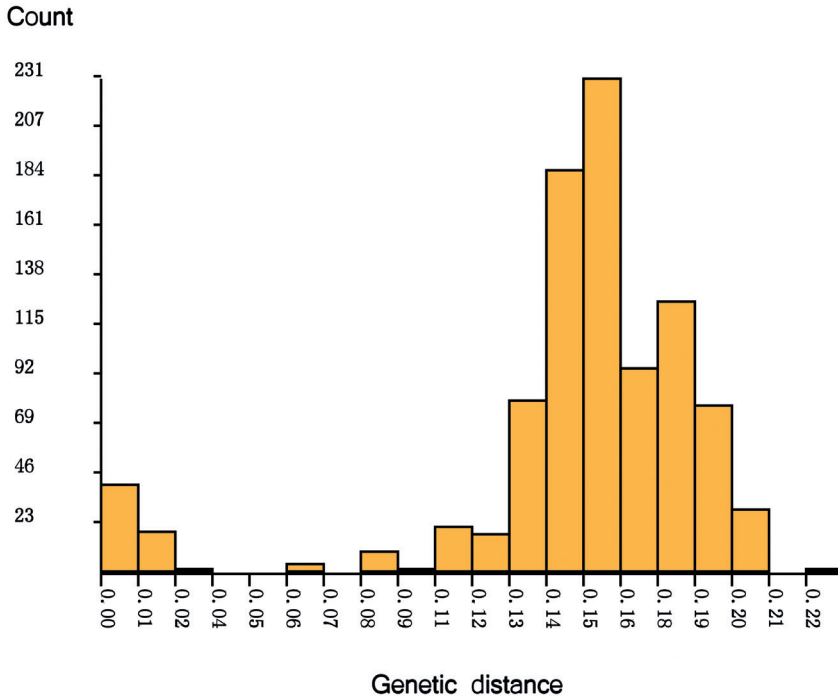


Figure 2. Histogram of pairwise K2P distances of public *Stenochironomus* sequences, generated by web site of ABGD.

Table 2. Kimura 2-parameter pairwise genetic distances based on COI barcodes of twelve known *Stenochironomus* species from GenBank.

Species	Distance										
	1	2	3	4	5	6	7	8	9	10	11
1. <i>S. annulus</i>											
2. <i>S. baishanzuensis</i>	15.13										
3. <i>S. fascipennis</i>	13.74	14.00									
4. <i>S. gibbus</i>	11.17	15.58	15.51								
5. <i>S. hibernicus</i>	16.50	15.36	14.39	14.61							
6. <i>S. linanensis</i>	17.74	18.69	18.29	17.04	18.22						
7. <i>S. okiabbus</i>	15.25	15.03	16.20	15.49	15.66	17.69					
8. <i>Stenochironomus</i> sp.1BD	14.92	14.28	13.91	15.26	15.35	15.92	14.27				
9. <i>Stenochironomus</i> sp.1CZ	18.58	17.11	17.16	18.03	21.01	19.58	19.08	15.80			
10. <i>Stenochironomus</i> sp.3CZ	12.87	14.98	14.20	14.83	17.19	17.69	14.89	14.46	17.39		
11. <i>S. tobaduodecimus</i>	18.11	17.05	18.11	18.32	19.08	19.04	16.12	20.12	17.40	18.83	
12. <i>S. zhengi</i>	17.96	16.59	18.15	19.14	19.32	19.65	18.16	18.43	20.55	17.70	20.09

example, Lin et al. (2015) found a gap of 4–5% for *Tanytarsus* and Song et al. (2016, 2018) found a gap of 5–8% for *Polypedilum*. However, the average genetic distance for *S. gibbus* is up to 9.1% (ranging from 0 to 13.0%), and for *S. okiabbus* is 3.95% (ranging from 0 to 14.4%) clearly larger than the defined threshold. Therefore, the vouchers of the species await to be checked to resolve the problem.

Taxonomy

Stenochironomus annulus Song & Qi, sp. nov.

<http://zoobank.org/793EEC94-E1E4-45F7-906E-13154716B102>

Figs 3–5

Type material. *Holotype* (BOLD & TZU sample ID: ZJCH220; Field ID: BSZ87) 1 male, China, Zhejiang Province, Lishui City, Qingyuan County, Baishanzu National Nature Reserve, 27.76°N, 119.31°E, 11–12. VIII. 2020, light trap, Qi X & Song C.

Paratypes: 2 males, same data as for holotype.

Diagnostic characters. The adult males of *S. annulus* sp. nov. can be separated from known *Stenochironomus* species from China by the following combination of characters: spots on the membrane of wing restricted to RM and FCu areas; posterior portion of median vittae with little pale pigmentation; lateral vittae with stripe markings; postnotum with markings reaching the posterior margin; femur of mid and hind legs with an annulus medially on each; superior volsella cylindrical, with four long setae; inferior volsella extending beyond apex of anal point, with two or three bristles and one well-developed terminal spine.

Etymology. The specific name refers to the circular ring markings of the femur of mid and hind legs of the male adult.

Description. Male imago (N = 3). Total length 3.59–4.17, 3.87 mm. Wing length 1.95–2.03, 2.00 mm. Total length / wing length 1.75–2.05, 1.94. Wing length / length of pro-femur 1.58–1.93, 1.73.

Coloration (Fig. 3). Mature adult mostly brownish. Head yellow. Thorax yellowish except for the lateral vittae, postnotum with dark pigmentation and medial lateral with light pigmentation (sometimes difficult to observe). Membrane with 2 dark spots restricted to RM and FCu areas. Legs. Apical 3/5 of femur of P1 dark brown; apical and annulus of femur, and Ta 5 P2–P3 dark brown; basal 1/2 of tibia of P3 dark brown. Abdomen. Tergites V–IX brown.

Head. AR 1.62–1.88 (2), ultimate flagellomere 680–770 μm long; Temporals 10–13, 12 setae including 5–8 inner, and 2–3 outer, verticals, postorbitals 1–3. Clypeus with 15–22, 19 setae. Tentorium 170–205 μm long, 45–53 μm wide at the widest part. Palp 5-segmented, lengths (in μm) of segments: 60–70, 66; 50–70, 60; 193–220, 203; 140–160, 152; 208–288, 248. Palpomere ratio (5th / 3rd) 1.09–1.31, 1.22.

Thorax. Dorsocentrals 16–17, 18; acrostichals 12–15, 14; prealars 5–6, 6; Scutellum with 11–13 setae in 2 rows.

Wing (Fig. 4A). VR 1.08–1.08, 1.06. Brachiolum with 2–3 setae. Distribution of setae on veins: R, 31–39, 34; R1, 28–40, 34; R4+5, 33–62, 46. Squama with 8–12, 10 setae. Anal lobe normally developed.

Legs (Fig. 4D). Fore leg: width at apex of tibia 43–50, 46 μm , tibia with blunt scale 35–40, 38 μm long. Mid leg: width at apex of tibia 53–65, 59 μm , tibia with 2 apical spurs 35–38, 37 and 40–45, 43 μm long. Hind leg: tibia 60–73 μm width at apex; tibial spurs 40–43, 42 and 40–43, 42 μm long, slightly fused medially. Lengths (in μm) and proportions of legs in Table 3.



Figure 3. Male adult (holotype, in lateral view) of *Stenochironomus annulus* Song & Qi sp. nov.

Hypopygium (Figs 4B, C, 5). Anal point straight and parallel-sided in dorsal view, 103–113, 100 μm long and 30–43, 35 μm wide at base, 8–10, 9 μm wide at apex. Tergite IX with 19–22, 20 long setae medially and posterior margin of tergite IX with 6 strong setae and 5 spines. Laterosternite IX with 4–4, 4 setae. Transverse sternapodeme 43–50, 47 μm long; phallapodeme 78–88, 85 μm long. Gonocoxite 173–185, 181 μm long, gonostylus 205–270, 238 μm long. Superior volsella cylindrical, 40–45, 43 μm long, 20–20, 20 μm wide, with 4–5 long setae (Fig. 4C). Inferior volsella elongate, 203–228 μm long, extending beyond the apex of anal point, with 2–3 long bristles and 1 strong terminal spine. HR 0.64–0.90, 0.77, HV 1.46–1.75, 1.64.

Immature stages and female unknown.

Remarks. Morphologically, *S. annulus* sp. nov. shows high similarity to *Stenochironomus xianjuensis* Zhang, Gu, Qi & Wang, 2016, on the basis of the following similar common characters: membrane of wing with similar spot patterns;

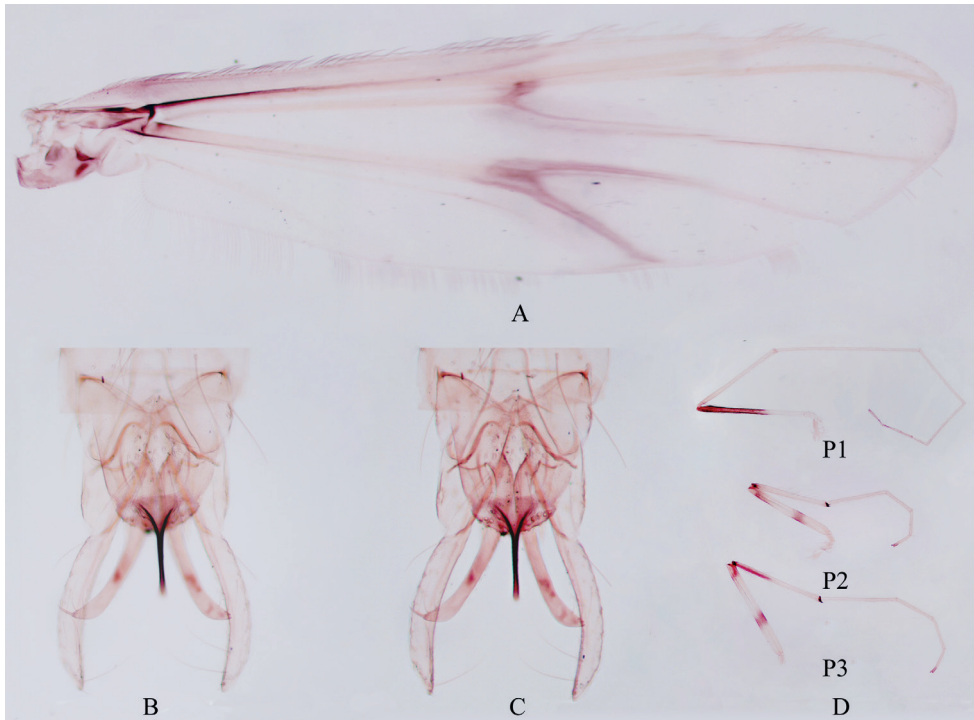


Figure 4. Male adult of *Stenochironomus annulus* Song & Qi, sp. nov. **A** wing **B** hypopygium in dorsal view **C** hypopygium in ventral view **D** legs.

Table 3. Male adult of *Stenochironomus annulus* sp. nov. Length (in μm) and proportions of legs ($N = 3$).

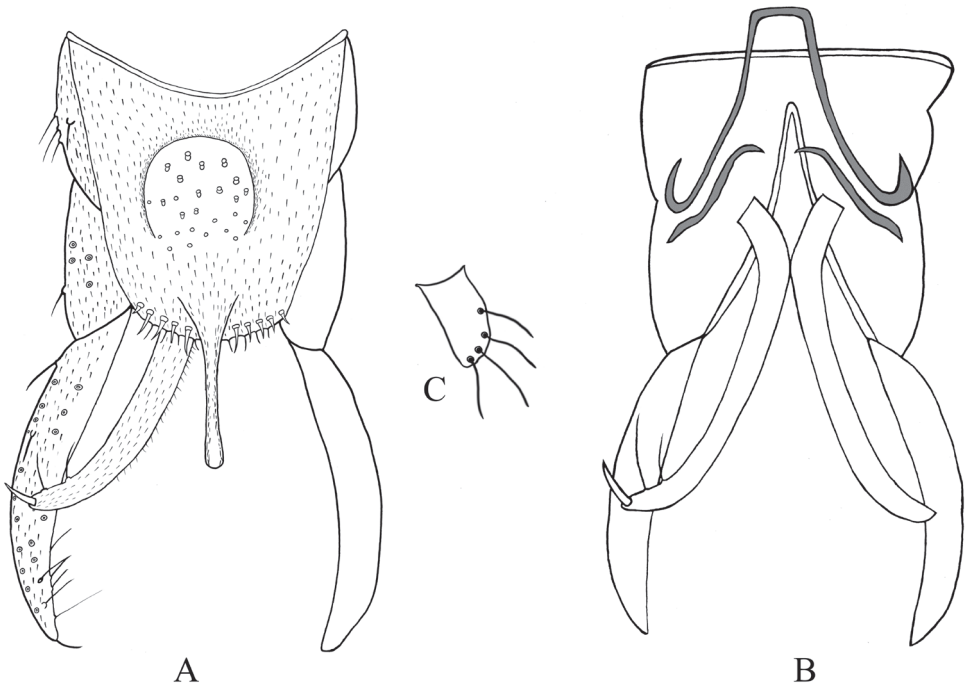
	P1	P2	P3
Fe	1060–1280, 1156	920–1110, 993	1120–1250, 1170
Ti	1050–1150, 1116	850–930, 893	1070–1100, 1060
Ta ₁	1500–1700, 1610	540–720, 656	860–910, 890
Ta ₂	750–820, 796	370–380, 373	460–500, 483
Ta ₃	630–660, 647	270–280, 273	360–380, 370
Ta ₄	440–570, 507	150–160, 156	220–220, 220
Ta ₅	210–240, 230	75–90, 82	80–100, 90
LR	1.42–1.48, 1.44	0.64–0.80, 0.73	0.82–0.85, 0.84
BV	1.75–1.80, 1.78	2.65–3.10, 2.87	2.64–2.78, 2.68
SV	1.35–1.45, 1.41	2.52–3.33, 2.91	2.42–2.61, 2.50

cylindrical superior and inferior volsella. However, the new described species could be distinguished in having a straight and parallel-sided anal point and different leg pigmentation patterns. According to the molecular data, *S. annulus* is sister to *S. gibbus* (Fig. 1), but could be separated by thorax vittate and leg coloration (Table 4).

Distribution. The species is currently known only from Zhejiang Province in Oriental China.

Table 4. Main differences between *S. annulus* sp. nov., *S. baishanzuensis* sp. nov., *S. gibbus*, and *S. xianjuensis*.

	Thorax vittae	Anal point	Legs pattern
<i>S. annulus</i>	Median vittae not obvious; lateral vittae with stripe pigmentation	Anal point straight and parallel-sided	With dark annulus on femur of P2 and P3
<i>S. baishanzuensis</i>	Median vittae with little pigmentation; lateral vittae with stripe pigmentation	Anal point straight and parallel-sided	Entire femur of P2 pale; femur of P3 brown
<i>S. gibbus</i>	Thorax without pigmentation	Apex parallel-sided to slightly bulbous	Nearly 1/2 to entire femur of P2; basal 0.12–0.30 femur of P3 dark brown;
<i>S. xianjuensis</i>	Thorax without median vittae; lateral vittae with stripe pigmentation	Apex of anal point swollen and rounded	Apical 1/4 of P2 and P3 brown

**Figure 5.** Male adult (holotype) of *Stenochironomus annulus* Song & Qi sp. nov. **A** hypopygium in dorsal view **B** hypopygium in ventral view **C** superior volsella.***Stenochironomus baishanzuensis* Song & Qi, sp. nov.**

<http://zoobank.org/16D79540-7339-434A-9662-29D1BB5F360B>

Figs 6–8

Type material. *Holotype* (BOLD & TZU sample ID: ZJCH226; Field ID: BSZ93) 1 male, China, Zhejiang Province, Lishui City, Qingyuan County, Baishanzu National Nature Reserve, 27.76°N, 119.31°E, 11–12. VIII. 2020, Qi X. & Song C., collected by light trap. *Paratypes*: 2 males, same data as for holotype.

Diagnostic characters. Adult males of *S. baishanzuensis* sp. nov. can be distinguished from other related species by the following combination of characters:

membrane of wing with large dark spots on median and apical parts; median vitta, lateral vitta, and postnotum with pigmentation; superior volsella short and broad with four setae; inferior volsella with four long bristles and one stout terminal spine, not overreaching apex of anal point.

Etymology. The specific name refers to the Baishanzu National Nature Reserve, where the holotype was collected.

Description. Male imago (N = 3). Total length 3.98–4.22, 4.07 mm. Wing length 1.90–2.13, 2.05 mm. Total length / wing length 1.87–2.22, 1.99. Wing length / length of pro-femur 1.63–1.65, 1.64.

Coloration (Fig. 6). Head. Antennal hairs dark; palpomeres dark. Thorax almost pale yellow, with posterior portion of media vitta, posterior 3/4 portion of postnotum,



Figure 6. Male adult (holotype, in dorsal view) of *Stenochironomus baishanzuensis* Song & Qi sp. nov. male.

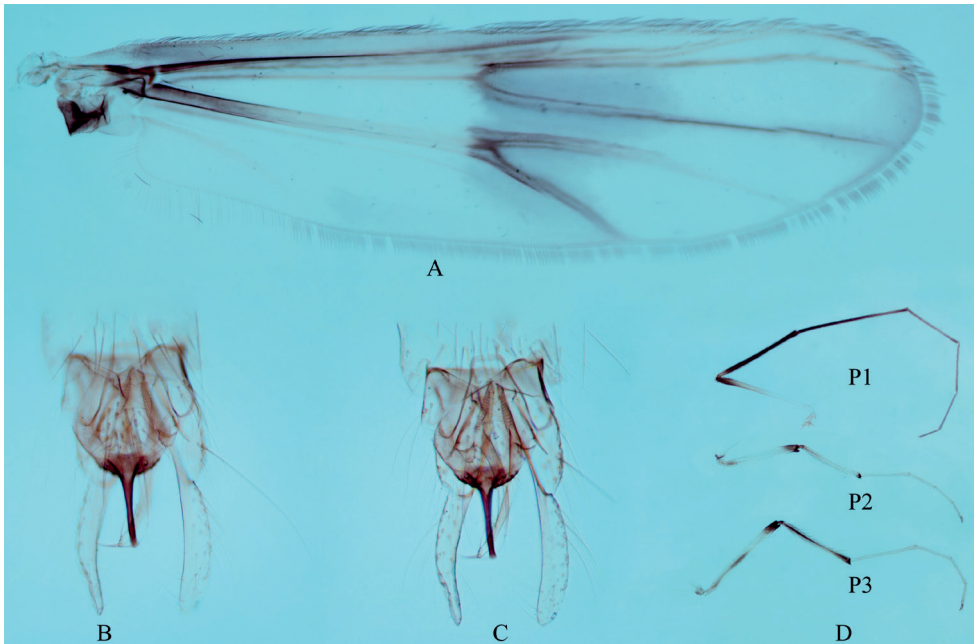


Figure 7. Male adult (holotype) of *Stenochironomus baishanzuensis* Song & Qi, sp. nov. **A** wing **B** hypopygium in dorsal **C** hypopygium in ventral view **D** legs.

and almost the lateral vitta dark brown. Membrane with 2 dark spots located around RM and FCu areas (median spot is darker). Legs. P1: knee, tibia and Ta 1 dark brown, basal 3/4 of femur and Ta 2–5 pale yellowish; P2: yellowish with brownish knee; P3: yellowish with brownish knees and tibia. Abdomen almost light brown with T VI–VII dark brown.

Head. AR 1.93, ultimate flagellomere 810 μm long ($n = 1$); Temporals 12–15, 13 setae, including 5–7, 6 inner and 4–6, 5 outer verticals and 2–3, 3, postorbitals. Clypeus with 14–20, 18 setae. Tentorium 155–193, 170 μm long, 35–53, 44 μm wide. Palp 5-segmented, lengths (in μm) of segments: 42–55, 47; 43–65, 53; 200–223, 214; 130–155, 146; 232–275, 253. Palpomere ratio ($5^{\text{th}} / 3^{\text{rd}}$) 1.13–1.26.

Thorax. Dorsocentrals 15–16, 15; acrostichals 12–15, 14; prealars 6–7, 7. Scutellum with 8–9, 9 setae in 2 rows.

Wing (Fig. 7A). VR 1.05–1.06, 1.06. Brachiolum with 2 setae. Distribution of setae on veins: R, 30–32, 31; R1, 22–26, 25; R4+5, 36–42, 39. Squama with 10–11, 11 setae. Anal lobe normally developed.

Legs (Fig. 7D). Fore leg: apex of tibia 55–61, 58 μm width, tibia with pointed scale 35–38 μm long. Mid leg: apex of tibia 60–68, 65 μm width; tibial spurs 48–55, 51 and 45–55, 49 μm long, completely fused at midline part. Hind leg: apex of tibia 60–68, 64 μm width, tibia with 2 apical spurs 37–50, 47 and 35–47, 41 μm long. Lengths (in μm) and proportions of legs in Table 5.

Hypopygium (Figs 7B, C, 8). Anal point 110–125, 120 μm long, 30–45, 35 μm wide at base, 10–13, 12 μm wide at apex. Tergite IX with 18–23, 20 long setae medially,

and 3–4, 4 setae laterally. Posterior margin of tergite IX with 3–4, 4 spines and 5–7 long setae each side. Transverse sternapodeme 38–53, 44 μm long; phallapodeme 95–113, 105 μm long. Gonocoxite 183–188, 185 μm long. Gonostylus 218–25, 221 μm long. Superior volsella short and broad, 13–15, 14 μm long, 18–25, 21 μm wide, with 4 long setae (Fig. 7C). Inferior volsella elongate, 183–192, 187 μm long, extending at most, to apex of anal point, with 4 setae and 1 strong terminal spine. HR 0.83–0.84, .084, HV 1.77–1.93.

Immature stages and female unknown.

Remarks. The male adult of *S. baishanzuensis* sp. nov. resembles that of *S. gibbus* (Fabricius, 1794) in the structure of the hypopygium and the wing patterns, but can be separated by the following characters: straight and parallel-sided anal point, and legs bearing different patterns (Table 4).

Distribution. The species is currently known only from Zhejiang Province, Oriental China.

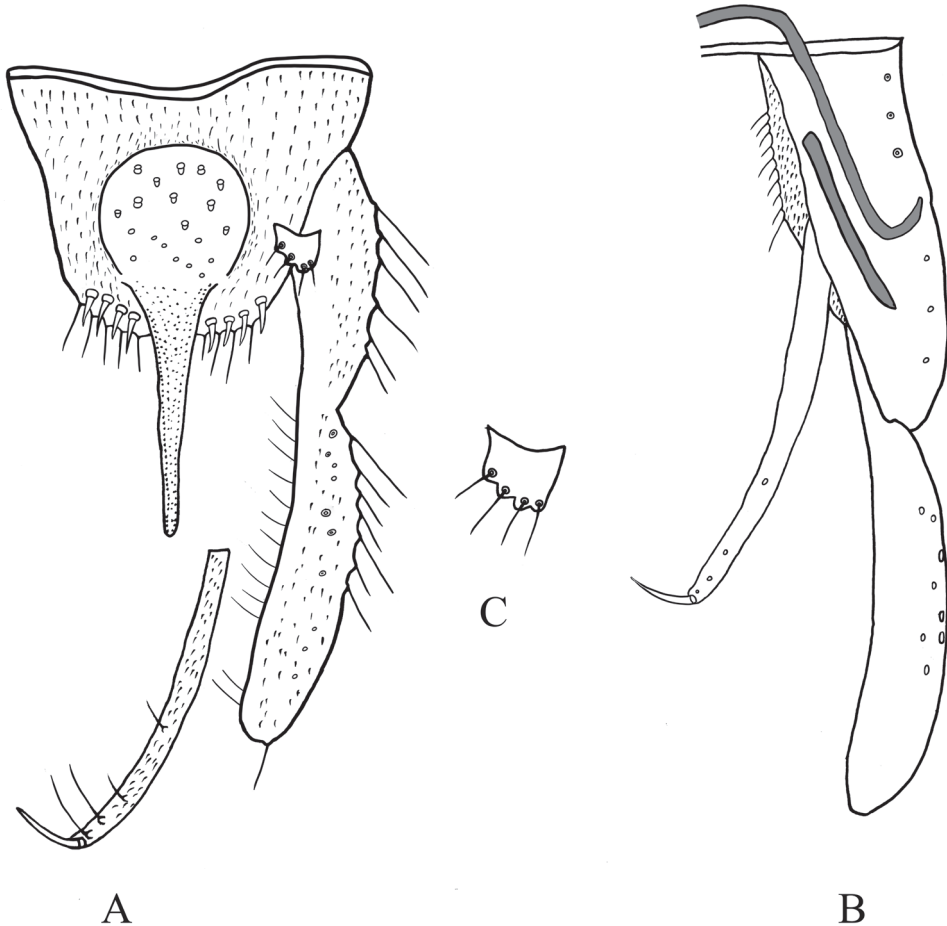


Figure 8. Male adult (holotype) of *Stenochironomus baishanzuensis* Song & Qi, sp. nov. **A** hypopygium in dorsal view **B** hypopygium in ventral view **C** superior volsella.

Table 5. Male adult of *Stenochironomus baishanzuensis* sp. nov. Lengths (in μm) and proportions of legs ($N = 3$, except where otherwise stated).

	P1	P2	P3
Fe	1150–1300, 1250	970–1110, 1053	1140–1310, 1243
Ti	1130–1280, 1230	870–930, 907	1050–1250, 1160
Ta ₁	1250 ($N = 1$)	480–700, 606	820–950, 900
Ta ₂	800 ($N = 1$)	370–400, 387	450–520, 477
Ta ₃	680 ($N = 1$)	300–340, 317	380–410, 397
Ta ₄	560 ($N = 1$)	180–210, 200	230–260, 240
Ta ₅	270 ($N = 1$)	90–100, 95	90–110, 100
LR	0.98 ($N = 1$)	0.52–0.75, 0.67	0.76–0.78, 0.77
BV	2.35 ($N = 1$)	2.46–2.64, 2.57	2.59–2.94, 2.72
SV	2.06 ($N = 1$)	2.91–4.17, 3.31	2.66–2.67, 2.67

Stenochironomus okialbus Sasa, 1990

Figs 9, 10

Stenochironomus okialbus Sasa, 1990: 122, fig. 10.

Material examined. 3 male adults, collected by light trap in Zhejiang Province, Lishui City, Qingyuan County, Baishanzu National Nature Reserve, 27.76°N, 119.31°E, 11–12.VIII.2020, leg. Song C.

Diagnostic characters. *Stenochironomus okialbus* differs from other related species by a combination of characters: wing with dark markings in the middle and apex; superior volsella short and small, spatulate, with four or five long setae; inferior volsella elongate, with 2–4 long setae and a slender terminal spine; posterior margin of tergite IX with 8–10 setae and eight spines.

Description. Male imago ($N = 3$). Total length 2.94–3.98, 3.62 mm. Wing length 1.80–1.85 mm. Total length / wing length 1.85–2.20, Wing length / length of profemur 178–1.88.

Coloration (Fig. 8). Body almost pale yellowish or white, except postnotum with spot area and tergite IV–VII brown; wing with dark pigmentation on median and apical parts; all legs pale yellow with dark knees and apex of tibia.

Head. AR 1.10–1.25, 1.12, ultimate flagellomere 430–660, 580 μm long. Temporal with 12–16, 14 setae, including 7–8, 7 inner verticals, 4–7, 6 outer verticals and 1–2, 2 postorbitals. Clypeus with 12–20, 17 setae. Tentorium 155–220, 190 μm long, 30–53, 44 μm wide. Palpomere lengths (μm): 33–48, 37; 40–65, 55; 123–195, 170; 85–125, 116; 130–218, 194. Palpomere ratio (5th/3rd) 1.05–1.21, 1.13.

Thorax. Dorsocentrals 14–21, 18; acrostichals 9–12, 11; prealars 5–6, 6; Scutellum with 7–12 setae in two rows.

Wings. VR 1.06–1.10, 1.08. Brachiolum with 1–2, 2 setae. Distribution of setae on veins: R, 20–29, 25; R1, 21–39, 31; R4+5, 49–53, 51. Squama with 10–18, 14 setae. Anal lobe normally developed.

Legs. Fore leg: width at apex of tibia 53–63, 58 μm , tibia with blunt scale 35–50, 44 μm long. Mid leg: width at apex of tibia 53–70, 61 μm , tibia with two apical spurs



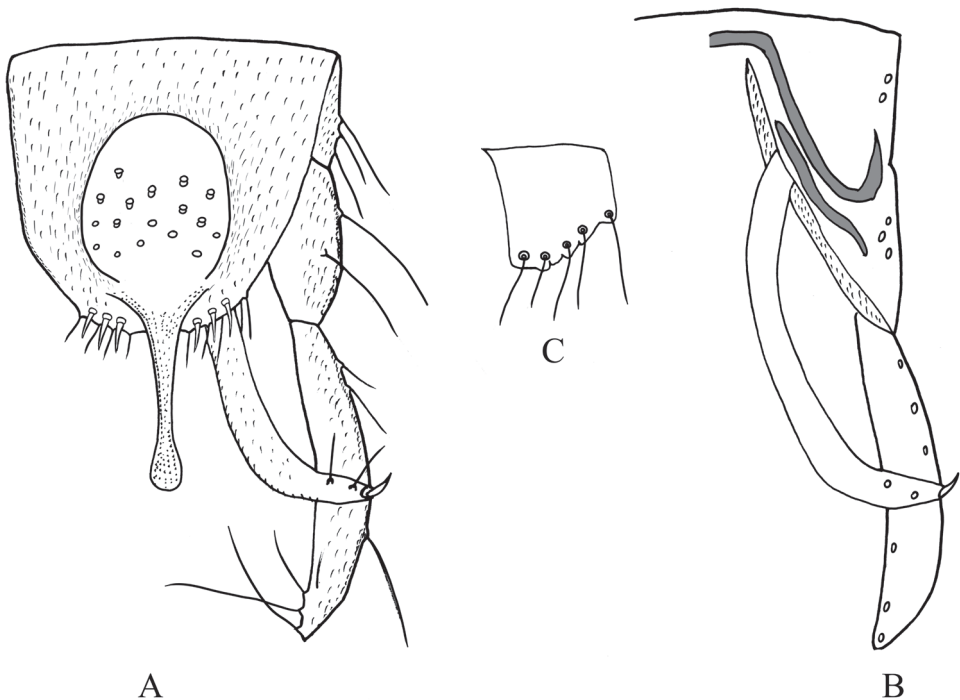
Figure 9. Male adult of *Stenochironomus okialbus* (in lateral view): new record to China

43–53, 48 and 45–58, 52 μm long. Hind leg: width at apex of tibia 58–73, 64 μm , tibia with two apical spurs 45–55, 51 and 45–56, 52 μm long. Lengths (in μm) and proportions of legs as in Table 6.

Hypopygium (Fig. 10). Anal point 110–125, 118 μm long, 43–60; wide, 52 μm width at base, 18–20, 18 μm at apex; slightly swollen and rounded apically. Tergite IX with 19–25, 22 long setae on median part; posterior margin of tergite IX with 6 strong setae

Table 6. Male adult of *Stenochironomus okialbus*. Lengths (in μm) and proportions of legs ($N = 3$, except where otherwise stated).

	P1	P2	P3
Fe	920–1310, 1150	790–1220, 1053	930–1350, 1183
Ti	930–1210, 1050	730–1030, 913	870–1230, 1083
Ta ₁	1200–1640 ($N = 2$)	530–730, 653	710–990, 880
Ta ₂	590–810 ($N = 2$)	290–410, 360	380–520, 470
Ta ₃	500–680 ($N = 2$)	230–310, 277	290–410, 363
Ta ₄	450–650 ($N = 2$)	140–210, 180	180–250, 230
Ta ₅	210–300 ($N = 2$)	60–100, 87	80–110, 97
LR	1.45–1.48 ($N = 2$)	0.70–0.73, 0.72	0.80–0.82, 0.81
BV	1.63–1.69 ($N = 2$)	2.84–2.94, 2.90	2.69–2.75, 2.71
SV	1.42–1.46 ($N = 2$)	2.88–3.08, 3.00	2.53–2.61, 2.57

**Figure 10.** Male adult of *Stenochironomus okialbus*. **A** hypopygium in dorsal view **B** hypopygium in ventral view **C** superior volsella.

and 3 spines. Laterosternite IX with 3–4, 4 setae. Transverse sternapodeme 35–48, 41 μm long; phallapodeme 85–95, 89 μm long. Gonocoxite 138–175, 159 μm long. Gonostylus 185–200, 196 μm long. Superior volsella short, 25–30, 28 μm long, 23–25, 24 μm wide, with 4–5 long setae. Inferior volsella linearly elongate, 183–220, 208 μm long, with 2–3 long setae and 1 stout terminal spine. HR 0.74–0.86, 0.81; HV 1.58–1.97, 1.84.

Remarks. The morphological characters of the Chinese specimens fit well with the original description and illustrations provided by Sasa (1990): wing with two spotted areas; narrow dark rings on knee points; anal point slightly swollen and rounded. However, some relevant differentiating characters were observed within the examined specimens: the inferior volsella have only two or three long setae, while it bears four in the Japanese specimens; average values of the AR 1.10–1.25 are lower than 1.37–1.41 in the Japanese species.

According to the molecular data, specimen (LC462365) of *Stenochironomus okialbus*, shows a large genetic distance to other specimens (up to 14%); as the specimen is not accessible it should be rechecked. The K2P distance between Japanese and Chinese specimens is 1.7%, which well supports them as the same species.

Distribution. Oriental China (Zhejiang) and Japan.

Stenochironomus linanensis Qi, Lin, Liu & Wang

Stenochironomus linanensis Qi et al. (2015): 114.

Material examined. 3 male adults collected by light trap, leg. Qi X.; Zhejiang Province, Lishui City, Qingyuan County, Baishanzu National Nature Reserve, 27.76°N, 119.31°E, 11–12.VIII.2020.

Diagnostic characters. *Stenochironomus linanensis* differs from other related species in having: wing transparent; body yellow; superior volsella finger-like with nine long setae; inferior volsella elongate, with four long setae and one strong terminal spine; tergite IX with 10–15 long setae located medially.

Distribution. Oriental China (Zhejiang).

Stenochironomus satorui (Tokunaga & Kuroda, 1936)

Chironomus (*Stenochironomus*) *satorui* Tokunaga & Kuroda (1936): 2.

Stenochironomus satorui Qi et al. (2011): 226.

Material examined. 2 male adults collected by light trap, leg. Song C., Zhejiang Province, Lishui City, Qingyuan County, Baishanzu National Nature Reserve, 27.76°N, 119.31°E, 11–12.VIII.2020.

Diagnostic characters. Wing with median band; posterior edge of tergite IX with 14–15 long setae; anal point slender parallel-sided, with pointed apex; superior volsella short and finger-like, with four or five setae; inferior volsella with one median seta and three apical setae.

Distribution. China (Zhejiang, Hainan, Guizhou, Xizang); Japan.

Updated key to known adult males of *Stenochironomus* from China

The following key updates Lin et al. (2021) and Qi et al. (2015)

- | | | |
|----|--|--|
| 1 | Inferior volsella with a well-developed terminal spine..... | 2 |
| – | Inferior volsella without a well-developed terminal spine | 12 |
| 2 | Wing membranes with dark pigmentation | 3 |
| – | Wing membranes without any pigmentation | 8 |
| 3 | Legs almost entire brown; wing with dark pigment restricted to a part area..... | 4 |
| – | Legs yellow; entire wing smoky gray..... | <i>S. maculatus</i> Borkent, 1984 |
| 4 | Wing with two dark spots restricted to RM and FCu areas | 5 |
| – | Wing with dark median band | 6 |
| 5 | Anal point straight and parallel-sided | <i>S. annulus</i> Song & Qi, sp. nov. |
| – | Apex of anal point swollen and rounded | <i>S. xianjuensis</i> Zhang et al., 2016 |
| 6 | Anal point bullous, knees of fore femur dark brown..... | 7 |
| – | Anal point almost parallel-sided, fore femur dark brown | <i>S. baishanzuensis</i> Song & Qi, sp. nov. |
| 7 | Mid and hind legs without pigmentation except knees.... | <i>S. okialbus</i> Sasa, 1990 |
| – | Apical 0.23 to entire hind-femur with dark pigmentation | <i>S. gibbus</i> (Fabricius, 1805) |
| 8 | Apex of anal point swollen and rounded | 9 |
| – | Apex of anal point not swollen and rounded | 11 |
| 9 | Superior volsella with 9–12 setae; posterior margin of tergite IX with 10–14 setae and 4–8 spines | 10 |
| – | Superior volsella with four setae; posterior margin of tergite IX with 14–16 setae | <i>S. koreanus</i> Borkent, 1984 |
| 10 | Superior volsella much beyond posterior margin of tergite IX; anal lobe reduced | <i>S. zhengi</i> Lin & Liu, 2021 |
| – | Superior volsella small, finger-like; anal lobe developed..... | <i>S. linanensis</i> Qi, Lin, Liu & Wang, 2015 |
| 11 | Posterior edge of tergite IX with eight long setae and six spines; anal point parallel-sided | <i>S. macateei</i> (Malloch, 1915) |
| – | Posterior edge of tergite IX with 14 long setae, without any spine; anal point roughly triangular, apically pointed..... | <i>S. mucronatus</i> Qi, Shi & Wang, 2008 |
| 12 | Wing membranes with dark pigmentation | 13 |
| – | Wings without any pigmentation or with narrow pigment areas around RM and along veins M_{3+4} and Cu_1 12 | 15 |
| 13 | Abdominal tergites I–IV light yellow, tergites V–VIII light brown, hypopygium dark brown | 14 |
| – | Abdomen and hypopygium light yellow..... | <i>S. inalemeus</i> Sasa, 2001 |
| 14 | Preepisternum with brown spots; anal point apically rounded..... | <i>S. nubilipennis</i> Yamamoto, 1981 |
| – | Preepisternum without any pigmentation; anal point apically pointed..... | <i>S. satorui</i> (Tokunaga & Kuroda, 1936) |

- 15 Posterior margin of tergite IX without spines 16
 – Posterior margin of tergite IX with spines
 *S. brevissimus* Qi, Lin, Liu & Wang, 2015
 16 Entire body yellow, without dark pigmentation; inferior volsella with three long
 setae *S. hainanus* Qi, Shi & Wang, 2008
 – Body yellow, with brown spots on thorax, abdomen, hypopygium and legs; infe-
 rior volsella with six long setae *S. totifuscus* Sublette, 1960

Acknowledgements

The authors are grateful to financial support from the National Natural Science Foundation of China (NSFC, Grant No. 32070481, 32100353), the Zhejiang Provincial Natural Science Foundation of China (Grant No. LY22C040003), the Science & Technology Project of Taizhou (Grant No. 21hb04, 21nya17, 1902gy23), and the Project of Biodiversity Survey in Lishui Municipality, Zhejiang Province of China.

References

- Amora G, Hamada N, Pinho LC (2018) *Stenochironomus munteanpurin* sp n., a new leaf-mining species from Brazil (Diptera: Chironomidae). *Zootaxa* 4382(3): 553–564. <https://doi.org/10.11646/zootaxa.4382.3.6>
- Borkent A (1984) The systematics and phylogeny of the *Stenochironomus* complex (*Xestochironomus*, *Harrisius*, and *Stenochironomus*) (Diptera: Chironomidae). *Memoirs of the Entomological Society of Canada* 128(S128): 1–269. <https://doi.org/10.4039/entm116128fv>
- Cranston PS, Dillon ME, Pinder LCV, Reiss F (1989) The adult males of Chironominae (Diptera: Chironomidae) of the Holarctic region – Keys and diagnoses. In: Wiederholm T (Ed.) *Chironomidae of the Holarctic region. Keys and diagnoses. Part 3 – Adult males.* *Entomologica Scandinavica Supplement* 34: 353–502.
- Dantas GPS, Hamada N, Mendes HF (2016) Contribution to the knowledge of *Stenochironomus* Kieffer (Diptera, Chironomidae) from Brazil: Seven new species and description of females and immatures of some previously known species. *Zootaxa* 4117(1): 1–47. <https://doi.org/10.11646/zootaxa.4117.1.1>
- Folmer O, Black M, Hoeh W, Lutz R, Vrijenhoek R (1994) DNA primers for amplification of mitochondrial cytochrome c oxidase subunit I from diverse metazoan invertebrates. *Molecular Marine Biology and Biotechnology* 3: 294–299.
- Frohlich DR, Torres-Jerez I, Bedford ID, Markham PG, Brown JK (1999) A phylogeographical analysis of the *Bemisia tabaci* species complex based on mitochondrial DNA markers. *Molecular Ecology* 8(10): 1683–1691. <https://doi.org/10.1046/j.1365-294x.1999.00754.x>
- Hall TA (1999) BioEdit: A user-friendly biological sequence alignment editor and analysis program for Windows 95/98/NT. *Nucleic Acids Symposium Series* 41: 95–98. <https://doi.org/10.1021/bk-1999-0734.ch008>

- Hebert PDN, Cywinska A, Ball SL, deWaard JR (2003) Biological identifications through DNA barcodes. *Proceedings of the Royal Society of London. Series B, Biological Sciences* 270(1512): 313–321. <https://doi.org/10.1098/rspb.2002.2218>
- Kodama A, Kawai K, Saito H (2018) A new species of *Tanytarsus* van der Wulp, 1874 (Diptera: Chironomidae) and the first Japanese record of *Tanytarsus ovatus* Johannsen, 1932 with DNA barcodes. *Zootaxa* 4422(4): 591–599. <https://doi.org/10.11646/zootaxa.4422.4.9>
- Kumar S, Stecher G, Tamura K (2016) MEGA7: Molecular Evolutionary Genetics Analysis Version 7.0 for Bigger Datasets. *Molecular Biology and Evolution* 33(7): 1870–1874. <https://doi.org/10.1093/molbev/msw054>
- Lin XL, Stur E, Ekrem T (2015) Exploring genetic divergence in a species-rich insect genus using 2790 DNA Barcodes. *PLoS ONE* 10(9): e0138993. <https://doi.org/10.1371/journal.pone.0138993>
- Lin XL, Yu HJ, Wang Q, Bu WJ, Wang XH (2020) DNA barcodes and morphology confirm a new species of *Rheocricotopus* (*Psilocricotopus*) *orientalis* group (Diptera: Chironomidae). *Zootaxa* 4678(2): 282–290. <https://doi.org/10.11646/zootaxa.4768.2.9>
- Lin XL, Yao Y, Yan CC, Liu WB (2021) *Stenochironomus zhengi* sp. nov. from Dawei Mountain National Park, Yunnan, China (Diptera: Chironomidae). *Zootaxa* 4970(2): 385–390. <https://doi.org/10.11646/zootaxa.4970.2.10>
- Parise AG, Pinho LC (2016) A new species of *Stenochironomus* Kieffer, 1919 from the Atlantic Rainforest in southern Brazil (Diptera: Chironomidae). *Aquatic Insects* 37(1): 1–7. <https://doi.org/10.1080/01650424.2015.1115078>
- Peng Z, Li LZ, Zhao MJ (2012) Five new apterous species of the genus *Lathrobium* Gravenhorst (Coleoptera, Staphylinidae, Paederinae) from the Baishanzu Natural Reserve, East China. *ZooKeys* 251: 69–81. <https://doi.org/10.3897/zookeys.251.3953>
- Puillandre N, Lambert A, Brouillet S, Achaz G (2012) ABGD, Automatic Barcode Gap Discovery for primary species delimitation. *Molecular Ecology* 21(8): 1864–1877. <https://doi.org/10.1111/j.1365-294X.2011.05239.x>
- Qi X, Shi SD, Wang XH (2008a) Two new species and new record of the genus *Stenochironomus* (Diptera, Chironomidae). *Dong Wu Fen Lei Xue Bao* 33(3): 526–531.
- Qi X, Shi SD, Wang XH (2008b) One new record of genus *Stenochironomus* Kieffer in China (Diptera, Chironomidae). *Sichuan Journal of Zoology* 27(5): 837–838.
- Qi X, Shi SD, Lin XL, Wang XH (2011) The genus *Stenochironomus* Kieffer (Diptera: Chironomidae) with three newly recorded species from China. *Entomotaxonomia* 33(3): 220–330.
- Qi X, Lin X, Liu YD, Wang XH (2015) Two New species of *Stenochironomus* Kieffer (Diptera, Chironomidae) from Zhejiang, China. *ZooKeys* 479: 109–119. <https://doi.org/10.3897/zookeys.479.8364>
- Qi X, Song C, Ge KX, Wang XH (2020) *Polypedilum* (*Cerobregma*) *paracyclus* sp. n., a new species from Oriental China (Diptera: Chironomidae). *Zootaxa* 4881(1): 189–195. <https://doi.org/10.11646/zootaxa.4881.1.12>
- Ratnasingham S, Hebert PDN (2013) A DNA-based registry for all animal species: The barcode index number (BIN) system. *PLoS ONE* 8(7): e66213. <https://doi.org/10.1371/journal.pone.0066213>

- Sæther OA (1969) Some Nearctic Podonominae, Diamesinae, and Orthocladiinae (Diptera: Chironomidae). Bulletin - Fisheries Research Board of Canada 170: 1–154.
- Sæther OA (1980) Glossary of chironomid morphology terminology (Diptera: Chironomidae). Entomologica Scandinavica (Supplement 14): 1–51.
- Sasa M (1990) Studies on the chironomid midges (Diptera, Chironomidae) of the Nansei Islands, southern. The Japanese Journal of Experimental Medicine 60: 111–165.
- Song C, Wang Q, Zhang RL, Sun BJ, Wang XH (2016) Exploring the utility of DNA barcoding in species delimitation of *Polypedilum* (*Tripodura*) non-biting midges (Diptera: Chironomidae). Zootaxa 4079(5): 534–550. <https://doi.org/10.11646/zootaxa.4079.5.2>
- Song C, Lin XL, Wang Q, Wang XH (2018) DNA barcodes successfully delimit morphospecies in a superdiverse insect genus. Zoologica Scripta 47(3): 311–324. <https://doi.org/10.1111/zsc.12284>
- Song C, Zheng J, Wang X, Qi X (2020) A new species of *Limnophyes* Eaton (Diptera: Chironomidae) from Xizang, China. Zootaxa 4722(3): 295–300. <https://doi.org/10.11646/zootaxa.4722.3.7>
- Townes HK (1945) The Nearctic species of Tendipedini. (Diptera: Tendipedidae (= Chironomidae)). American Midland Naturalist 34(1): 1–206. <https://doi.org/10.2307/2421112>
- Zhang RL, Gu JJ, Qi X, Wang XH (2016) A new species of the genus *Stenochironomus* Kieffer (Diptera: Chironomidae) from Xianju National Park, Zhejiang Province, China. Entomotaxonomia 38(4): 281–284.

Three new species of the spider genus *Liphistius* (Araneae, Mesothelae, Liphistiidae) from Thailand

Yi Zhan¹, Varat Sivayyapram², Fengxiang Liu^{3,4}, Daiqin Li⁵, Xin Xu¹

1 College of Life Sciences, Hunan Normal University, 36 Lushan Road, Changsha 410081, Hunan Province, China **2** Center of Excellence in Entomology and Department of Biology, Faculty of Science, Chulalongkorn University, Bangkok 10330, Thailand **3** State Key Laboratory of Biocatalysis and Enzyme Engineering, School of Life Sciences, Hubei University, 368 Youyi Road, Wuhan 430062, Hubei Province, China **4** Centre for Behavioural Ecology and Evolution (CBEE), School of Life Sciences, Hubei University, 368 Youyi Road, Wuhan 430062, Hubei Province, China **5** Department of Biological Sciences, National University of Singapore, 14 Science Drive 4, 117543, Singapore, Singapore

Corresponding authors: Xin Xu (xuxin@hunnu.edu.cn); Daiqin Li (dbslidq@nus.edu.sg)

Academic editor: Gergin Blagoev | Received 8 March 2022 | Accepted 17 May 2022 | Published 10 June 2022

<http://zoobank.org/400FB403-5624-4BFA-8C17-F12208C3B564>

Citation: Zhan Y, Sivayyapram V, Liu F, Li D, Xu X (2022) Three new species of the spider genus *Liphistius* (Araneae, Mesothelae, Liphistiidae) from Thailand. ZooKeys 1104: 115–128. <https://doi.org/10.3897/zookeys.1104.83264>

Abstract

We diagnose and describe three new species of the primitively segmented spider genus *Liphistius* from Thailand, based on male palp and female genital morphology: *L. hatyai* Zhan & Xu, **sp. nov.** (♂♀), *L. keeratikiati* Zhan & Xu, **sp. nov.** (♂♀), and *L. inthanon* Zhan & Xu, **sp. nov.** (♂♀). The classification of the three new species of *Liphistius* is discussed: *L. hatyai* **sp. nov.** and *L. keeratikiati* **sp. nov.** are assigned to the *trang*-group, and *L. inthanon* **sp. nov.** is placed in the *bristowei*-group according to male palp and female genital morphology.

Keywords

Morphology, Southeast Asia, taxonomy, trapdoor spiders

Introduction

As the sister lineage to all other extant spiders, the primitively segmented spider family Liphistiidae, belonging to the suborder Mesothelae, retains some plesiomorphic characters, such as abdominal tergites (Fig. 1) and spinnerets situated on the median area of the ventral abdomen (Platnick and Gertsch 1976; Coddington and Levi 1991; Haupt 2003). Currently, Liphistiidae contains 166 species belonging to eight genera in two subfamilies, Liphistiinae Thorell, 1869 and Heptathelinae Kishida, 1923 (WSC 2022). The subfamily Liphistiinae containing a single genus, *Liphistius* Schiødte, 1849, occurs in China (Yunnan Province), Indonesia (Sumatra), Laos, Peninsular Malaysia, Myanmar, and Thailand (WSC 2022).

The genus *Liphistius* was erected by Schiødte (1849) based on the type species *Liphistius desultor* found in Malaysia (Schiødte 1849). Since then, an increasing



Figure 1. Microhabitat, burrows, and general somatic morphology of three new *Liphistius* species **A** microhabitat **B** burrow with trapdoor closed **C** same, trapdoor opened **D** male, *L. hatyai* Zhan & Xu, sp. nov. (XUX-2017-492) **E** female, *L. inthanon* Zhan & Xu, sp. nov. (XUX-2017-374) **F** male, *L. keeratikiati* Zhan & Xu, sp. nov. (XUX-2017-435) Scale bars: 5 mm (**D**, **E**, **F**).

number of *Liphistius* species have been described from Asia. Currently, *Liphistius* includes 59 known species, of which 33 are known from Thailand (WSC 2022). Platnick and Sedgwick (1984) presented the first taxonomic revision of the genus by describing 14 species from Indonesia (Sumatra), Peninsular Malaysia, Myanmar, and Thailand. Recently, Schwendinger and colleagues provided taxonomic revisions of *Liphistius* in Peninsular Malaysia (Schwendinger 2017; Schwendinger et al. 2019).

Members of *Liphistius* can be divided into seven species-groups based on male and female genital morphology: the *batuensis*-group, *birmanicus*-group, *bristowei*-group, *linang*-group, *malayanus*-group, *trang*-group, and *tioman*-group (Schwendinger 1990, 2017; Schwendinger et al. 2019). Specifically, the *trang*-group is subdivided into six species complexes (Schwendinger 1990, 1996, 1998; Schwendinger et al. 2019). Out of 33 named *Liphistius* species from Thailand, 32 are assigned to four species-groups, and one (*L. jarujini* Ono, 1988) is an *incertae sedis* species: *trang*-group (25 species), *bristowei*-group (5 species), *birmanicus*-group (1 species), *linang*-group (1 species) (for details see Sivayyapram et al. 2017).

To investigate the species diversity of *Liphistius* in Thailand, we carried out several field trips in the country. After examining specimens collected, here we diagnose and describe three new *Liphistius* species based on the genital morphology of both sexes.

Material and methods

All specimens were collected in Thailand (Fig. 2). We removed the right four legs of adults, preserved in 100% ethanol and kept at -80°C for extracting genome DNA. We preserved specimen in 80% ethanol as the voucher for morphological examination. All the voucher specimens are deposited at the College of Life Sciences, Hunan Normal University, Changsha, Hunan Province, China.

We examined and dissected the specimens using an Olympus SZ51 stereomicroscope. The soft tissues of female genitalia were degraded using 10 mg/ml pancreatin for at least 3 h at room temperature. We used a digital camera CCD mounted on an Olympus BX53 compound microscope to photograph male palp and female genitalia, and then generated compound focused images using Helicon Focus v. 6.7.1. All measurements were carried out under a Leica M205C stereomicroscope using the software of Leica Application Suite v. 4 and are given in millimeters. Palp and leg measurements are given in the following order: leg total length (femur + patella + tibia + metatarsus [absent on palp] + tarsus).

Abbreviations used in the text

ALE	anterior lateral eyes;	CL	carapace length;
AME	anterior median eyes;	OL	opisthosoma length;
PLE	posterior lateral eyes;	CW	carapace width;
PME	posterior median eyes;	OW	opisthosoma width.
BL	body length (excluding chelicerae);		



Figure 2. Map of Thailand showing the localities of three new *Liphistius* species described.

Taxonomy

Family Liphistiidae Thorell, 1869

Subfamily Liphistiinae Thorell, 1869

Genus *Liphistius* Schiødte, 1849

Type species. *Liphistius desultor* Schiødte, 1849.

Diagnosis. *Liphistius* differs from the other seven liphistiid genera by the presence of signal lines radiating from the burrow's entrance (Fig. 1B, C), by the male palp having a tibial apophysis (Figs 3A, 4A, 5A), and by the female genitalia having a sclerotized poreplate and a median receptacular cluster (Figs 3H–I, 4H–M, 5H–J).

Distribution. China (Yunnan Province), Indonesia (Sumatra), Laos, Peninsular Malaysia, Myanmar, and Thailand.

***Liphistius hatyai* Zhan & Xu, sp. nov.**

<http://zoobank.org/0C8153A0-51E6-42A0-A009-BEDA4DB4D77E>

Fig. 3

Type material. *Holotype*: THAILAND • 1 ♂; Songkhla Province, Hat Yai District, Kho Hong, 7.04°N, 100.50°E; alt. 25 m; 13 November 2016; N. Warrit, V. Sivayyapram, N. Chatthanabun, P. Traiyasut leg.; XUX-2017-492. *Paratype*: THAILAND • 1 ♀, same data as for the holotype; XUX-2017-493.

Diagnosis. The male of *L. hatyai* sp. nov. resembles males of *L. albipes* Schwendinger, 1995 and *L. yangae* Platnick & Sedgwick, 1984 in having a rounded, scale-like paraembolic plate (Fig. 3A, E) but can be distinguished in having the tegulum with three transverse ridges in retrolateral view, while the latter two species have only one transverse ridge (Fig. 3C, G); from males of *L. bicoloripes* Ono, 1988, *L. castaneus* Schwendinger, 1995, and *L. niphanae* Ono, 1988 in having the cumulus slightly elevated (Fig. 3A–C); from the male of *L. inthanon* sp. nov. in having the tibial apophysis with fewer and longer setae (Fig. 3A–C), the cumulus slightly elevated (Fig. 3A–C), the subtegular apophysis absent (Fig. 3A, F), and the embolic parts detached (Fig. 3A–G); from the male of *L. keeratikiati* sp. nov. in having the sclerotised embolic part with three longitudinal ridges reaching the apex (Fig. 3A) and the tegulum with three transverse ridges distally (Fig. 3C, G); from males of other *Liphistius* species in having the cumulus slightly elevated, the sclerotised embolic part with three longitudinal ridges in prolateral view, and the subtegular apophysis absent (Fig. 3A, B, E).

The female of *L. hatyai* sp. nov. differs from females of *L. albipes* and *L. castaneus* in having a slightly narrower V-shaped posterior stalk (Fig. 3H, I); from females of *L. bicoloripes* and *L. castaneus* in having poreplate lacking anterolateral lobes (Fig. 3I); from the female of *L. niphanae* in having the anterior margin of the poreplate straight (Fig. 3H, I); from females of *L. yangae*, *L. inthanon* sp. nov., and *L. keeratikiati* sp. nov. in having the poreplate almost squared and with a slightly V-shaped posterior stalk (Fig. 3H, I); from females of other *Liphistius* species in having a hair at the center of posterior stalk dorsally (Fig. 3H).

Description. Male. Carapace reddish-brown, with a few short, scattered bristles; opisthosoma brown, with 12 brown tergites, close to each other, 2–6 larger than others, fifth largest; chelicerae robust, promargin of cheliceral groove with 12 denticles of variable size; labium yellow and fused with sternum; sternum yellow, with a few short setae on the anterior tip and many long setae on the elongated posterior tip; legs yellowish brown, with strong hairs and spines, without distinct annulations, with 3 tarsal claws; 8 spinnerets. Measurements: BL 17.6, CL 8.81, CW 8.42, OL 8.33, OW 7.31; eye sizes and interdistances: AME 0.06, ALE 0.77, PME 0.47, PLE 0.59, AME–AME 0.13, AME–ALE 0.21, PME–PME 0.08, PME–PLE 0.09, ALE–PLE 0.12, ALE–ALE 0.17, PLE–PLE 0.39, AME–PME 0.12. Labium 0.55 long and 0.70 wide. Sternum 3.74 long and 1.04 wide. Leg I 22.55 (7.11 + 2.57 + 4.90 + 5.64 + 2.33), leg II 22.85 (6.76 + 1.73 + 5.56 + 6.06 + 2.74), leg III 26.62 (6.89 + 3.55 + 5.63 + 7.51 + 3.04), leg IV 30.54 (9.07 + 3.83 + 7.50 + 10.25 + 2.63).

Palp: tibial apophysis with four setae of same length, stouter basally and slender distally (Fig. 3A–C); paracymbium with many setae situated at tip (Fig. 3A–C); several tapering spines on slightly elevated cumulus (Fig. 3A–C); contrategulum with a triangular

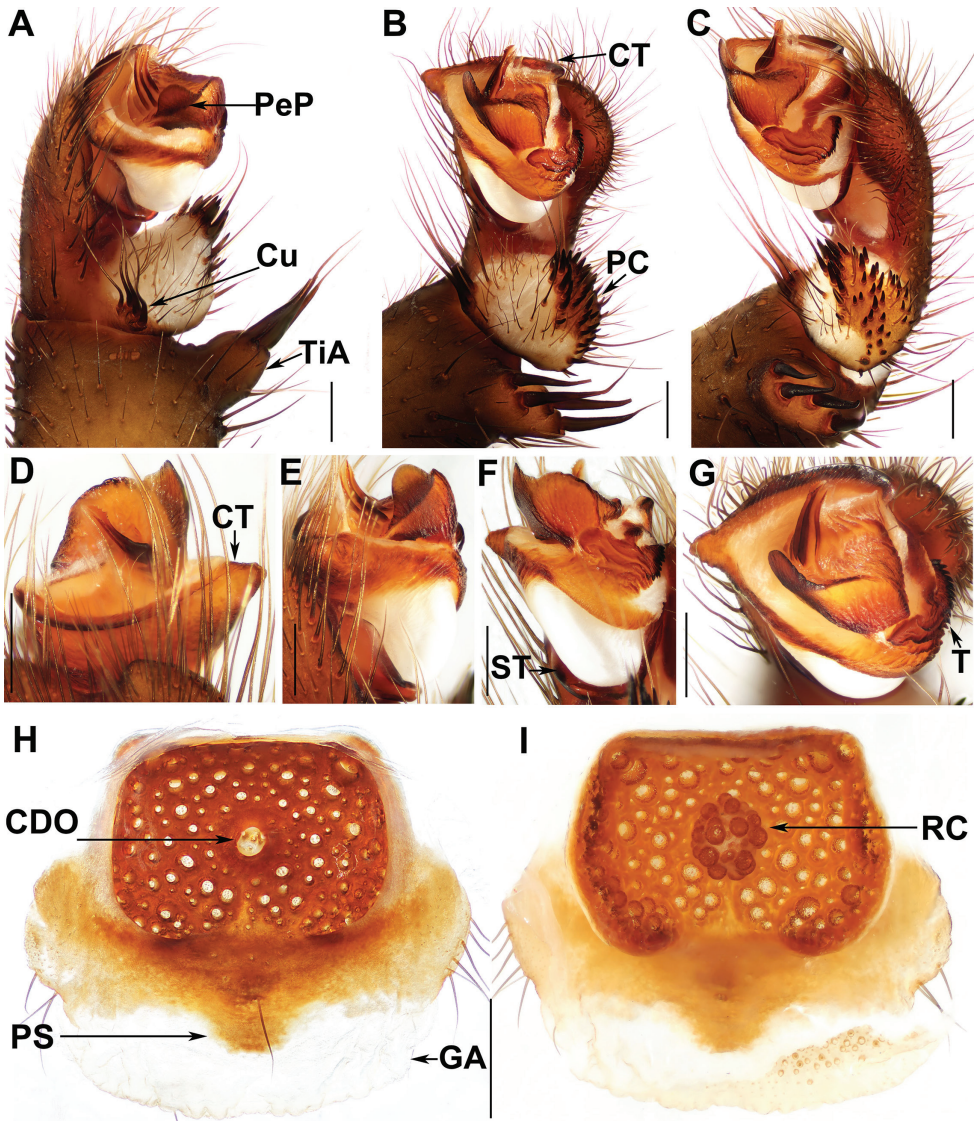


Figure 3. Male palp and female genitalia of *Liphistius hatyai* Zhan & Xu, sp. nov. **A** palp, prolateral view **B** palp, ventral view **C** palp, retrolateral view **D–G** palp, distal views **H, I** vulva, dorsal view **I** vulva, ventral view **A–G** XUX-2017-492 (holotype) **H, I** XUX-2017-493. Abbreviations used: CDO = central dorsal opening; GA = genital atrium; PS = posterior stalk; RC = receptacular cluster; CT = contrategulum; Cu = cumulus; PC = paracymbium; PeP = paraembolic plate; ST = subtegulum; T = tegulum; TiA = tibial apophysis. Scale bars: 0.5 mm.

process, and an arched smooth edge with a sharp projection (Fig. 3B, C, G); tegulum with a serrated edge proximally and 3 transverse ridges distally (Fig. 3B, C, G); embolic parts detached (Fig. 3A–C, G), paraembolic plate semicircular, scale-like (Fig. 3A, E); embolus with 3 distinct longitudinal ridges reaching the tip prolaterally, with a few denticulations on apex, and with a flat membranous opening (Fig. 3A–C, G).

Female. Carapace orange, with few short, scattered bristles; opisthosoma gray, with 12 brown tergites, close to each other, with gray patches, 2–6 larger than others, fifth largest; 8 eyes on dark ocular tubercle; chelicerae robust, reddish brown; promargin of cheliceral groove with 10 denticles of variable size; labium yellow, fused with sternum; sternum yellow with several setae; legs with strong setae and spines, without distinct annulations, with 3 tarsal claws; 8 spinnerets. Measurements: BL 23.8, CL 11.42, CW 10.33, OL 11.03, OW 10.06; eye sizes and interdistances: AME 0.14, ALE 1.00, PME 0.52, PLE 0.61, AME–AME 0.12, AME–ALE 0.25, PME–PME 0.10, PME–PLE 0.12, ALE–PLE 0.15, ALE–ALE 0.10, PLE–PLE 0.60, AME–PME 0.15. Labium 2.45 long and 1.26 wide. Sternum 5.15 long, 1.81 wide. Palp 20.19 (7.41 + 3.65 + 4.72 + 4.41), leg I 25.15 (8.71 + 4.49 + 4.59 + 4.74 + 2.62), leg II 26.62 (9.09 + 4.52 + 4.81 + 5.24 + 2.96), leg III 28.10 (9.25 + 4.28 + 5.56 + 5.89 + 3.12), leg IV 37.53 (11.06 + 4.80 + 7.70 + 9.97 + 4.00).

Genitalia: poreplate almost squared; posterior stalk slightly V-shaped, with a hair situated in the center dorsally; central dorsal opening small, situated in center of poreplate; receptacular cluster spherical (Fig. 3H, I).

Etymology. The species epithet “hatyai” refers to the location of the type locality in Hat Yai District.

Distribution. Southern Thailand (Songkhla Province) (Fig. 2).

Remarks. *Liphistius hatyai* sp. nov. can be assigned to the *trang*-group according to the morphology of male palp and female genitalia. In males, the sclerotised part of embolus has two or three longitudinal ridges reaching the tip, the cumulus is slightly elevated, and the subtegulum is lacking an apophysis (Fig. 3A–G). In females, the poreplate has a small central dorsal opening and a receptacular cluster (Fig. 3H, I).

Specifically, *L. hatyai* sp. nov. belongs to the species complex D of the *trang*-group (sensu Schwendinger 1998; Schwendinger et al. 2019) based on male palp and female genital morphology. In males, the slightly elevated cumulus possesses long, needle-like spines (Fig. 3A–C), and the sclerotised part of embolus carries three longitudinal ridges reaching the tip (Fig. 3A). Female genitalia consist of a nearly squared poreplate, and a narrow, slightly V-shaped posterior stalk (Fig. 3H, I).

Species complex D includes species distributed in southern Thailand, western Peninsular Malaysia, and Sumatra. This species complex in Thailand includes *L. albipes*, *L. bicoloripes*, *L. castaneus*, *L. niphanae*, *L. trang* Platnick & Sedgwick, 1984, and *L. yangae* (for details see Schwendinger 1998; Schwendinger et al. 2019).

***Liphistius inthanon* Zhan & Xu, sp. nov.**

<http://zoobank.org/59FA29B4-17FA-4613-9689-E6F639EBB8A5>

Fig. 4

Type material. Holotype: THAILAND • 1 ♂, Chiang Mai Province, Mae Chaem District, Doi Inthanon National Park, 18.52°N, 98.49°E; alt. 1700 m; 19 November 2017; F.X. Liu, D. Li, X. Xu, V. Sivayyapram leg.; XUX-2017-372A. **Paratypes:** THAILAND • 1 ♂ 7 ♀♀, alt. 1700–1714 m, same data as for the holotype; XUX-2017-373A, XUX-2017-372, 374, 377, 378, 379, 380, 381.

Diagnosis. The male of *L. inthanon* sp. nov. resemble males of *L. bristowei* Platnick & Sedgwick, 1984, *L. lanaiianus* Schwendinger, 1990, *L. maewongensis* Sivayyapram, Smith, Weingdow & Warrit, 2017, *L. marginatus* Schwendinger, 1990 and *L. yamasakii* Ono, 1988 in having adjoining embolic parts (Fig. 4E, G) and a distinctly elevated cumulus (Fig. 4C), but it can be distinguished from the male of *L. bristowei* in having the tibial apophysis with more stouter spines (Fig. 4A–C) and a larger subtegular apophysis (Fig. 4D–G); from males of *L. lanaiianus*, *L. maewongensis*, and *L. marginatus* in having the cumulus more elevated (Fig. 4C); from the male of *L. yamasakii* in having the elevated cumulus longer and with fewer spines (Fig. 4B, C); from males of *L. hatyai* sp. nov. and *L. keeratikiati* sp. nov. in having the tibial apophysis with shorter setae (Fig. 4A–C), the cumulus noticeably elevated (Fig. 4C), and a larger subtegular apophysis (Fig. 4F); from males of other *Liphistius* species in having adjoining embolic parts (Fig. 4E, G) and a strongly elevated cumulus (Fig. 4C).

The female of *L. inthanon* sp. nov. differ from the female of *L. bristowei* in having the poreplate with an arched anterior margin (Fig. 4H–M); from females of *L. lanaiianus* and *L. yamasakii* in having the central dorsal opening larger oval (Fig. 4H–J); from the female of *L. maewongensis* in having the genital atrium with a wider posterior margin (Fig. 4L, M); from females of *L. hatyai* sp. nov. and *L. keeratikiati* sp. nov. in having a wider posterior stalk (Fig. 4I, J), longer oval central dorsal opening (Fig. 4H–J), and larger receptacular cluster (Fig. 4K–M); from females of other *Liphistius* species in having a wider posterior stalk (Fig. 4H–M).

Description. Male (holotype). Carapace reddish brown, with a few short, scattered bristles; opisthosoma olive-green, with 12 dark tergites, close to each other, 2–6 larger than others, fifth largest; chelicerae robust, promargin of cheliceral groove with 9 denticles of variable size; labium yellowish brown, separated from sternum; sternum yellowish brown, with a few weakly setae on the anterior tip and many long setae on the elongated posterior tip; legs dark brown, and with strong setae and spines, without distinct annulations and with 3 tarsal claws; 8 spinnerets. Measurements: BL 17.38, CL 9.25, CW 9.62, OL 7.42, OW 5.66; eye sizes and interdistances: AME 0.18, ALE 0.87, PME 0.49, PLE 0.63, AME–AME 0.09, AME–ALE 0.22, PME–PME 0.12, PME–PLE 0.15, ALE–PLE 0.10, ALE–ALE 0.15, PLE–PLE 0.51, AME–PME 0.13. Labium 1.00 long and 0.51 wide. Sternum 4.49 long and 1.35 wide. Leg I 28.45 (7.56 + 4.16 + 6.37 + 6.50 + 3.86), leg II 31.13 (8.54 + 4.01 + 6.63 + 7.70 + 4.25), leg III 34.09 (8.54 + 4.24 + 6.58 + 9.61 + 5.12), leg IV 42.23 (10.62 + 3.78 + 8.60 + 12.70 + 6.53).

Palp: tibial apophysis with 4 stouter spines, and several strong spines on subterminal ledge (Fig. 4A–C); paracymbium with many short strong setae situated at the tip (Fig. 4B, C); cumulus distinctly elevated with several spines on tip (Fig. 4C); subtegular apophysis large, strongly developed (Fig. 4D, F); proximal edge of contrategulum elevated (Fig. 4F, G); tegulum lunate, with dentate margin (Fig. 4G); embolic parts adjoining (Fig. 4E, F, G); embolus with 2 longitudinal ridges reaching the tip distally (Fig. 4D, E, G).

Female (XUX-2017-372). Carapace reddish brown, with a few short, scattered bristles; opisthosoma olive-green, with 12 dark brown tergites, close to each other, 2–6

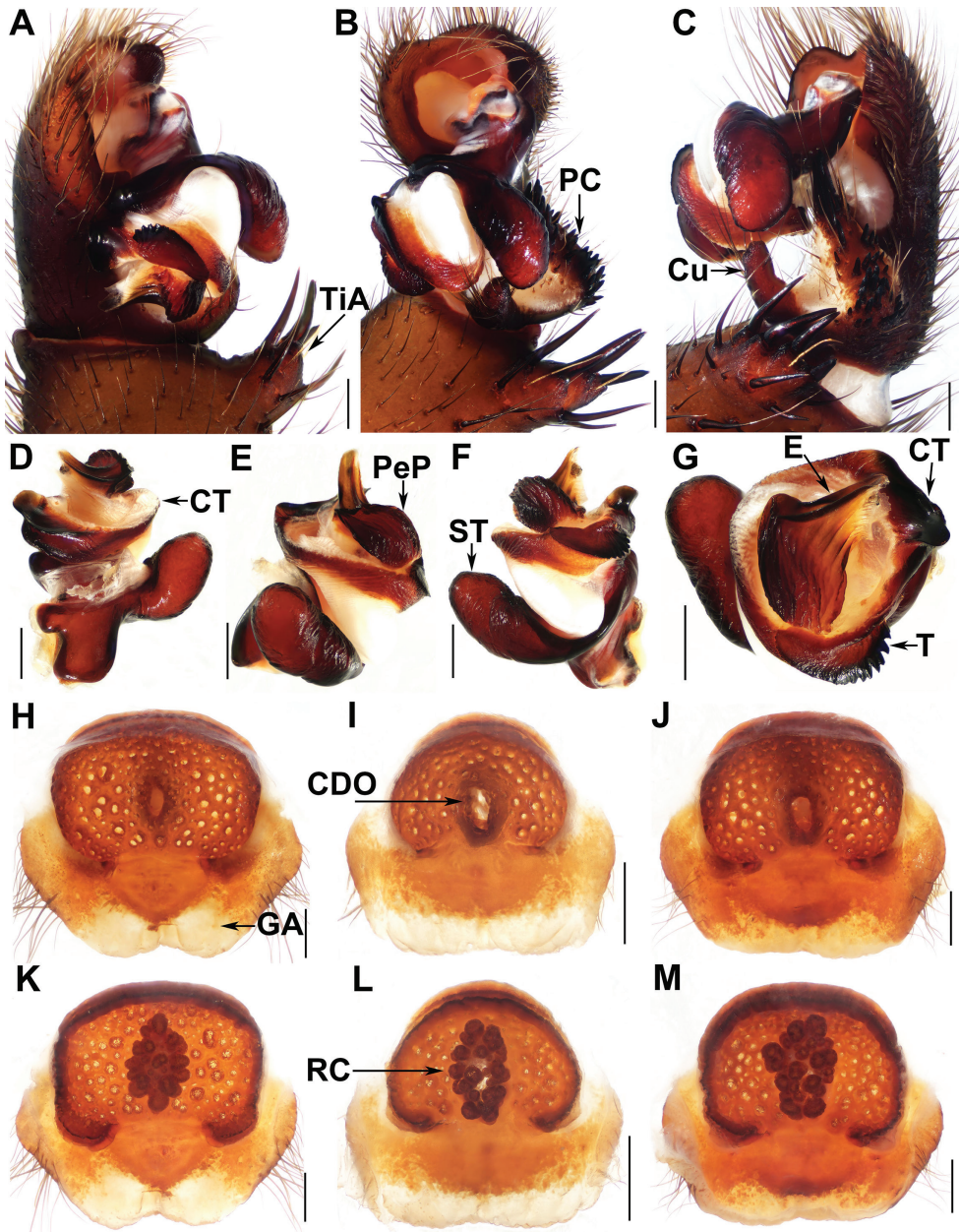


Figure 4. Male palp and female genitalia of *Liphistius inthanon* Zhan & Xu, sp. nov. **A** palp, prolateral view **B** palp, ventral view **C** palp, retrolateral view **D–G** palp, distal views **H–J** vulva, dorsal view **K–M** vulva, ventral view **A–C** XUX-2017-372A (holotype) **D–G** XUX-2017-373A **H, K** XUX-2017-372 **I, L** XUX-2017-379 **J, M** XUX-2017-381. Abbreviations used: CDO = central dorsal opening; GA = genital atrium; RC = receptacular cluster; CT = contrategulum; Cu = cumulus; E = embolus; PC = paracymbium; PeP = paraembolic plate; ST = subtegulum; T = tegulum; TiA = tibial apophysis. Scale bars: 0.5 mm.

larger than others, fifth largest; 8 eyes on dark ocular tubercle; chelicerae robust, reddish brown; promargin of chelicerae groove with 12 denticles of variable size; labium reddish brown, fused with sternum; sternum reddish brown and with several setae; legs reddish brown, with strong setae and spines, without distinct annulations, with 3 tarsal claws; 8 spinnerets. Measurements: BL 30.6, CL 12.18, CW 11.74, OL 17.49, OW 17.38; eye sizes and interdistances: AME 0.14, ALE 1.02, PME 0.52, PLE 0.82, AME–AME 0.19, AME–ALE 0.25, PME–PME 0.09, PME–PLE 0.16, ALE–PLE 0.13, ALE–ALE 0.16, PLE–PLE 0.66, AME–PME 0.12. Labium 2.78 long and 1.85 wide. Sternum 5.15 long, 1.81 wide. Palp 22.82 (7.08 + 4.24 + 5.87 + 5.63), leg I 26.61 (8.27 + 4.51 + 5.71 + 4.80 + 3.32), leg II 26.59 (7.85 + 4.96 + 5.44 + 5.16 + 3.18), leg III 28.88 (8.66 + 4.70 + 5.41 + 6.41 + 3.70), leg IV 33.46 (9.37 + 3.76 + 7.23 + 8.79 + 4.31).

Genitalia: poreplate with a long, oval central dorsal opening, and with projecting posterior corners; receptacular cluster racemose and large; posterior stalk wide, lateral margins of genital atrium with some hairs (Fig. 4H–M).

Etymology. The species epithet “inthanon” is a toponym referring to the type locality, Doi Inthanon National Park.

Distribution. Northern Thailand (Chiang Mai Province) (Fig. 2).

Variation. The range of females’ measurements ($N = 7$): BL 16.92–30.6, CL 7.90–12.18, CW 7.53–11.74, OL 8.5–17.49, OW 6.63–17.38. The number of denticles on the promargin of cheliceral groove varies from 12–14 ($N = 7$). The examined female genitalia were found to differ in that the posterior margin of genital atrium can be narrow, slightly W-shaped (Fig. 4H, K), or wide and straight (Fig. 4I, J, L, M), and the shape of poreplate anterior margin can slightly vary (Fig. 4K–M).

Remarks. *Liphistius inthanon* sp. nov. can be assigned to the *bristowei*-group based on the following characters: the male palp has a pronounced, elevated cumulus (Fig. 4C); the embolic parts are adjoining (Fig. 4D, G), the sclerotised part of the embolus bears two longitudinal ridges reaching the tip (Fig. 4D, G), and, except for *L. marginatus*, all have a large subtegular apophysis (Fig. 4F); the poreplate has a wide posterior stalk and a projecting posterior corner (Fig. 4H–M). The *bristowei*-group contains *L. bristowei*, *L. lannaianus*, *L. maewongensis*, *L. marginatus*, *L. yamasakii* (Schwendinger 1990), and *L. inthanon* sp. nov.

Liphistius keeratikiati Zhan & Xu, sp. nov.

<http://zoobank.org/A45A1921-8728-4095-9496-EBBED27DD903>

Fig. 5

Type material. Holotype: THAILAND • 1 ♂, Chumphon Province, Sawi District, Khao Thalu Subdistrict, Nam Lot Cave. 10.23°N, 98.94°E; alt. 30 m; 25 November 2017; F.X. Liu, D. Li, X. Xu, V. Sivayyapram leg.; XUX-2017-439. **Paratypes:** THAILAND • 1 ♂, 3 ♀, same data as for the holotype; XUX-2017-439, XUX-2017-431, 436, 438.

Diagnosis. The male of *L. keeratikiati* sp. nov. can be distinguished from the male of *L. fuscus* Schwendinger, 1995 in having the paraembolic plate scale-like and

arched (Fig. 5A, E), and the tibial apophysis slightly wider basally (Fig. 5A–C), while in *L. fuscus* the paraembolic plate is broadly rounded; from the male of *L. phuketensis* Schwendinger, 1998 in having the tibial apophysis with four setae (Fig. 5B, C); from the male of *L. schwendingeri* Ono, 1988 in having a longer embolus (Fig. 5A, B, E), the contrategulum with fewer wrinkles proximally (Fig. 5G), and a smaller tegulum (Fig. 5B, C, G); from the male of *L. hatyai* sp. nov. in having the tibial apophysis with longer setae and the paracymbium narrower (Fig. 5A–C); from the male of *L. inthanon* sp. nov. in having the subtegular apophysis absent (Fig. 5B, F) and the paraembolic plate scale-like (Fig. 5E); from males of other *Liphistius* species in having the spines on the cumulus slightly separated from setae on the paracymbium (Fig. 5A–C).

The female of *L. keeratikiati* sp. nov. differs from the female of *L. fuscus* in having the anterior margin of the poreplate slightly curved (Fig. 5H, I); from the female of *L. phuketensis* in having the anterior margin of the poreplate slightly narrower (Fig. 5I); from the female of *L. schwendingeri* in having the receptacular cluster slightly larger (Fig. 5I); from females of other *Liphistius* species in having the arched poreplate lacking lateral edges (Fig. 5I, J) and much wider than long (Fig. 5H, I), and the central dorsal opening situated in the lower center of the poreplate (Fig. 5H).

Description. Male (holotype). Carapace light yellow, with a few short, scattered bristles; opisthosoma yellow, with 12 tergites, with light brown patches; close to each other, 2–6 larger than others, fifth largest; chelicerae robust, promargin of cheliceral groove with 6 denticles of variable size; labium yellow and separated from sternum; sternum yellow, with a few short setae on anterior tip and many long setae on the elongated posterior tip; legs with strong setae and spines; with white annulations, with 3 tarsal claws; 8 spinnerets. Measurements: BL 15.61, CL 6.92, CW 6.72, OL 7.24, OW 5.07; eye sizes and interdistances: AME 0.09, ALE 0.74, PME 0.43, PLE 0.54, AME–AME 0.12, AME–ALE 0.15, PME–PME 0.03, PME–PLE 0.10, ALE–PLE 0.08, ALE–ALE 0.05, PLE–PLE 0.38, AME–PME 0.07. Labium 1.04 long and 0.76 wide. Sternum 3.02 long, 0.95 wide. Leg I 21.60 (5.41 + 1.81 + 4.68 + 4.79 + 4.91), leg II 23.29 (4.97 + 2.19 + 7.68 + 5.96 + 2.49), leg III 14.64 (missing metatarsus and tarsus) (6.17 + 2.87 + 5.60 + NA + NA), leg IV 30.16 (7.69 + 3.08 + 5.97 + 9.31 + 4.11).

Palp: tibial apophysis pronounced elevated, with four tapering spines of similar length (Fig. 5A–C); paracymbium with short, strong setae situated at tip (Fig. 5C), and 5 tapering spines on elevated cumulus (Fig. 5A, B); subtegulum without apophysis (Fig. 5B, F); contrategulum with a process distally, and with several wrinkles proximally (Fig. 5B, G); tegulum with a dentate edge (Fig. 5B, G); embolic parts detached (Fig. 5B), paraembolic plate scale-like, semicircular (Fig. 5A, E); embolus slender, with a few denticulations at the tip (Fig. 5A, B, G).

Female (XUX-2017-431). Carapace light brown, with few short, scattered bristles; opisthosoma gray, with 12 brown tergites, close to each other, 2–6 larger than others, fifth largest; eight eyes on darkened ocular tubercle; chelicerae robust, brown, promargin of chelicerae groove with 11 denticles of variable size; labium yellow, separated from sternum; sternum yellow with several setae; legs with strong hairs and spines; with brown and yellow annulations and 3 tarsal claws; 8 spinnerets. Measurements: BL

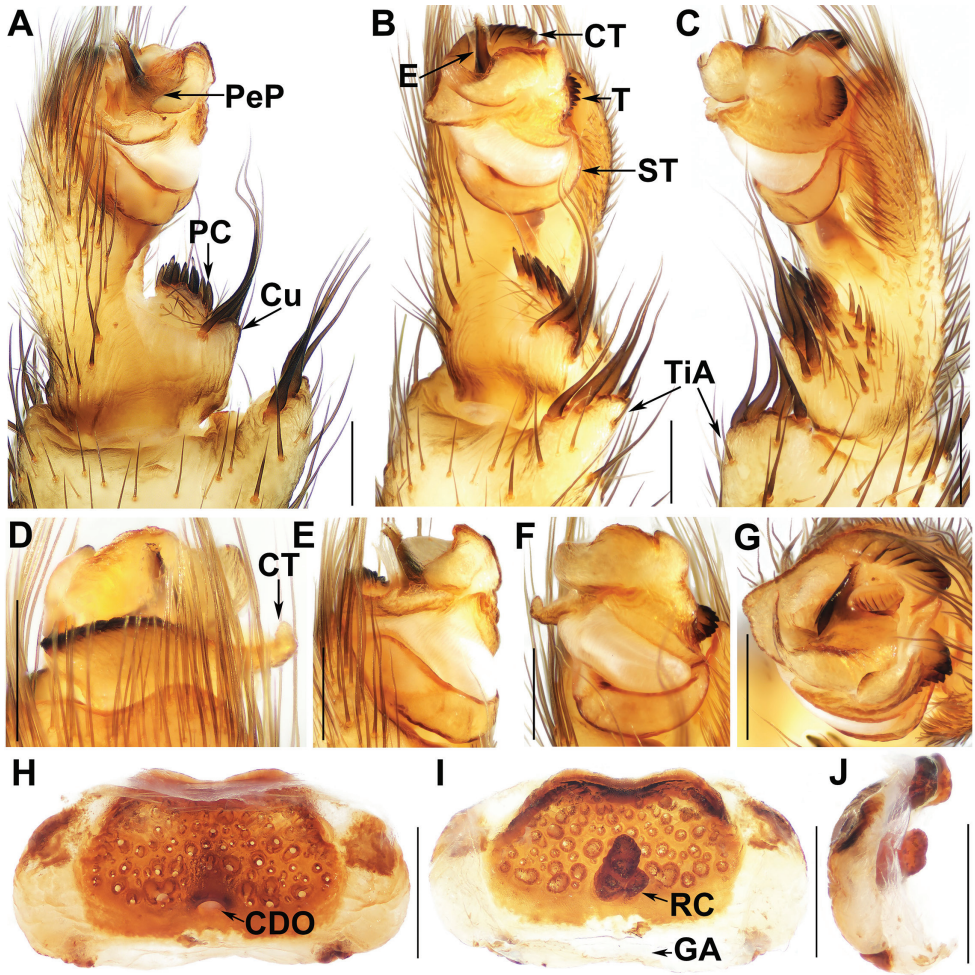


Figure 5. Male palp and female genitalia of *Liphistius keeratikiati* Zhan & Xu, sp. nov. **A** palp, prolateral view **B** palp, ventral view **C** palp, retrolateral view **D–G** palp, distal views **H** vulva, dorsal view **I** vulva, ventral view **J** vulva, lateral view **A–G** XUX-2017-439 (holotype) **H–J** XUX-2017-431. Abbreviations used: CDO = central dorsal opening; GA = genital atrium; RC = receptacular cluster; CT = contrategulum; Cu = cumulus; E = embolus; PC = paracymbium; PeP = paraembolic plate; ST = subtegulum; T = retegulum; TiA = tibial apophysis. Scale bars: 0.5 mm.

16.9, CL 7.21, CW 6.67, OL 9.93, OW 7.57; eye sizes and interdistances: AME 0.07, ALE 0.64, PME 0.30, PLE 0.51, AME–AME 0.08, AME–ALE 0.16, PME–PME 0.06, PME–PLE 0.09, ALE–PLE 0.09, ALE–ALE 0.08, PLE–PLE 0.41, AME–PME 0.09. Labium 1.49 long and 0.76 wide. Sternum 3.40 long, 1.13 wide. Palp 13.37 (4.74 + 2.25 + 3.32 + 3.06), leg I 16.58 (5.65 + 2.72 + 3.62 + 2.92 + 1.67), leg II 19.13 (5.56 + 3.06 + 3.76 + 3.71 + 2.05), leg III 17.14 (4.99 + 2.83 + 3.91 + 3.92 + 2.29), leg IV 24.73 (6.82 + 2.31 + 5.39 + 7.03 + 3.18).

Genitalia: poreplate much wider than long, arched (Fig. 5J), lateral edges absent (Fig. 5I); central dorsal opening situated in the lower center of poreplate (Fig. 5H); receptacular cluster simple (Fig. 5I).

Etymology. The specific name is dedicated to Mr Kaweesak Keeratikiat for providing information on the locality of the species.

Distribution. South-central Thailand (Chumphon Province) (Fig. 2).

Variation. Range in female measurements ($N = 3$): BL 16.45–18.89, CL 7.15–7.49, CW 6.45–7.15, OL 8.79–10.46, OW 6.76–8.99. The number of denticles on the promargin of cheliceral groove varies from 6–13 ($N = 3$).

Remarks. *Liphistius keeratikiati* sp. nov. can be assigned to the *trang*-group according to the morphology of male palp and female genitalia, see the remarks of *hatyai* sp. nov. The new species can be assigned to the species complex C of the *trang*-group. In males, the palp possesses the contrategulum with wrinkles proximally (Fig. 5B, G), the tegulum has a dentate edge (Fig. 5C, F, G), the spines on the elevated cumulus are slightly, distinctly separated from the setae on the paracymbium, and the apex of the embolus bears a few denticulations (Fig. 5A–C, E, G). In females, the poreplate is lacking lateral edges (Fig. 5I), arched (Fig. 5J), wider than long (Fig. 5H–I), and lacking a posterior stalk (Fig. 5H, I). Currently, the species complex C contains *L. fuscus*, *L. phuketensis*, *L. schwendingeri* (Schwendinger et al. 2019), and *L. keeratikiati* sp. nov.

Acknowledgements

We thank Natapot Warrit, Nontawat Chatthanabun, and Prapun Traiyasut for their assistance in the field. We also thank Alireza Zamani, Gergin Blagoev, Mikhail Omelko, and Feng Zhang for helping edit the language and for their constructive comments on the manuscript. This study was supported by the grants from the National Natural Sciences Foundation of China (NSFC) (32070430; 31272324), the Hunan Provincial Natural Science Foundation of China for Excellent Young Scholars (2021JJ20035), and the Singapore Ministry of Education AcRF Tier 1 grant (R-154-000-A52-114).

References

- Coddington JA, Levi HW (1991) Systematics and evolution of spiders (Araneae). Annual Review of Ecology and Systematics 22(1): 565–592. <https://doi.org/10.1146/annurev.es.22.110191.003025>
- Haupt J (2003) The Mesothelae—a monograph of an exceptional group of spiders (Araneae: Mesothelae) (Morphology, behaviour, ecology, taxonomy, distribution and phylogeny). Zoologica 154: 1–102.
- Platnick NI, Gertsch WJ (1976) The suborders of spiders: A cladistic analysis (Arachnida, Araneae). American Museum Novitates 2607: 1–15. <http://hdl.handle.net/2246/5468>

- Platnick NI, Sedgwick WC (1984) A revision of the spider genus *Liphistius* (Araneae, Mesothelae). American Museum Novitates 2781: 1–31. <http://hdl.handle.net/2246/5262>
- Schiødte JC (1849) Om en afvigende Slægt af Spindlernes Orden. Naturhistorisk Tidsskrift 2: 617–624.
- Schwendinger PJ (1990) On the spider genus *Liphistius* (Araneae: Mesothelae) in Thailand and Burma. Zoologica Scripta 19(3): 331–351. <https://doi.org/10.1111/j.1463-6409.1990.tb00262.x>
- Schwendinger PJ (1996) New *Liphistius* species (Araneae, Mesothelae) from western and eastern Thailand. Zoologica Scripta 25(2): 123–141. <https://doi.org/10.1111/j.1463-6409.1996.tb00155.x>
- Schwendinger PJ (1998) Five new *Liphistius* species (Araneae, Mesothelae) from Thailand. Zoologica Scripta 27(1): 17–30. <https://doi.org/10.1111/j.1463-6409.1998.tb00426.x>
- Schwendinger PJ (2017) A revision of the trapdoor spider genus *Liphistius* (Mesothelae: Liphistiidae) in peninsular Malaysia; part 1. Revue Suisse de Zoologie 124: 391–445. <https://doi.org/10.5281/zenodo.893555>
- Schwendinger PJ, Syuhadah N, Lehmann-Graber C, Price L, Huber S, Hashim R, Bhassu S, Monod L (2019) A revision of the trapdoor spider genus *Liphistius* (Mesothelae: Liphistiidae) in Peninsular Malaysia; part 2. Revue Suisse de Zoologie 126(2): 321–353. <https://doi.org/10.35929/RSZ.0017>
- Sivayyapram V, Smith DR, Weingdow S, Warrit N (2017) A new *Liphistius* species (Mesothelae: Liphistiidae: Liphistiinae) from Thailand, with notes on its natural history. The Journal of Arachnology 45(3): 287–295. <https://doi.org/10.1636/JoA-S-17-028.1>
- WSC (2022) World Spider Catalog, Version 23.0. Natural History Museum Bern. <http://wsc.nmbe.ch> [access on 2 May 2022]

Pheidole klaman sp. nov.: a new addition from Ivory Coast to the Afrotropical *pulchella* species group (Hymenoptera, Formicidae, Myrmicinae)

Kiko Gómez¹, Lombart M. Kouakou², Georg Fischer³,
Francisco Hita-Garcia³, Julian Katzke³, Evan P. Economo³

1 Garraf, Barcelona, Spain **2** Station d'écologie de Lamto, Université Nangui Abrogoua, BP 28 N'Douci, Lamto, Ivory Coast **3** Biodiversity and Biocomplexity Unit, Okinawa Institute of Science and Technology Graduate University, 1919-1 Tancha, Onna-son, Okinawa, 904-0495, Japan

Corresponding author: Kiko Gómez (netodejulilla@gmail.com)

Academic editor: Brian Lee Fisher | Received 1 February 2022 | Accepted 1 April 2022 | Published 10 June 2022

<http://zoobank.org/72CC57AE-E3C2-4E41-A519-700D15629476>

Citation: Gómez K, Kouakou LM, Fischer G, Hita-Garcia F, Katzke J, Economo EP (2022) *Pheidole klaman* sp. nov.: a new addition from Ivory Coast to the Afrotropical *pulchella* species group (Hymenoptera, Formicidae, Myrmicinae). ZooKeys 1104: 129–157. <https://doi.org/10.3897/zookeys.1104.81562>

Abstract

In this study the taxonomy of the *Pheidole pulchella* species group is updated for the Afrotropical region and the new species *P. klaman* sp. nov. described. It is integrated into the existing taxonomic system by an updated identification key for the whole group and an update of the known distribution ranges of its members. High quality focus stacking images are provided, with X-ray micro-CT scanned digital 3D representations, of major and minor worker type specimens.

Keywords

Ants, distribution range, identification keys, new species, taxonomy, Taï National Park, X-ray micro-CT, 3D digitalisation

Introduction

The ant genus *Pheidole* has recently been the focus of extensive taxonomic attention in the Malagasy region. Recent work mainly by Salata and Fisher (2020a, b, 2021) improved the taxonomy of the genus, creating eleven new species groups and adding dozens of new species. Much less attention has been paid to the massive undescribed *Pheidole* fauna in the Afrotropical region, remaining poorly known with dozens of species waiting to be described. The only modern attempt to organise the genus in the Afrotropics defined six species groups and assigned 67 valid species and subspecies to these groups based on qualitative morphology of the worker caste (Fischer et al. 2012). Fischer et al. (2012) also revised the *P. pulchella* group containing eleven species, of which seven were newly described. However, despite this work, most of the reorganisation of Afrotropical *Pheidole* taxonomy is still ongoing, since most valid species and many more undescribed ones need to be assigned to groups, and some new groups will need to be defined. More additions to *Pheidole* taxonomy are necessary to structure and catalogue their diversity in Africa to create a better base of understanding for the global radiations of *Pheidole* ants.

Taï National Park (TNP) is the last remaining major intact block of primary forest in West Africa. It was declared a UNESCO World Heritage Site in 1982 due to exceptional richness in fauna and flora. Based on several criteria including species diversity, endemism, presence of rare species and/or endangered and critical habitats, the TNP is considered a priority for the conservation of mammals, birds, amphibians, and invertebrates in West Africa (World Heritage 2022). A recent ant inventory by two of the authors (KG, LMK) in the Taï National Park at Ivory Coast yielded approximately 200 ant species and morphospecies (unpublished data), including undescribed taxa for various genera, including *Bothroponera*, *Carebara*, *Monomorium*, and *Pristomyrmex*, among others.

One of these new species is hereby described as *Pheidole klaman* sp. nov. which we place within the *P. pulchella* group sensu Fischer et al. (2012). Since more material of the group has been sampled since Fischer et al. (2012), we take the occasion to update the illustrated identification key to incorporate the new species, as well as to provide distribution maps with updated distribution ranges for all species. The new species is described based on qualitative morphology of the worker caste, which we illustrate with high quality coloured focus stacking images and 3D models based on x-ray microtomography.

Materials and methods

Terminology follows Bolton (1994). Measurements follow Fischer et al. (2012).

Specimens were examined under a Leica MZ16A stereo microscope and measured at $\times 100$. All images have been modified from originals and edited using GIMP (to compose the figures), IMAGEJ (to scale and add scale bars), and Polarr Photo Editor freeware (to sharpen and improve exposure and contrast). All micro-CT scans were performed at the Okinawa Institute of Science and Technology Graduate University (OIST), Japan, using a Zeiss Xradia 510 Versa 3D X-ray microscope operated with

the Zeiss Scout-and-Scan Control System software (v. 11.1.6411.17883) and saved in DICOM format. 3D reconstructions of the resulting scan projection data were done with the Zeiss Scout-and-Scan Control System Reconstructor (v. 11.1.6411.17883) and saved in DICOM file format. Details on scanning parameters can be found in Table 5. Postprocessing of DICOM raw data was performed with Amira software (version 6.3). Virtual examinations of 3D surface models were performed by using the ‘volren’ function. The desired volume renderings were generated by adjusting colour space range to a minimum so that the exterior surface of specimens remained visible at the highest available quality. The 3D models were rotated and manipulated to allow a complete virtual examination of the scanned specimens in Amira, and in addition, exported in PLY format to be uploaded to the online 3D model platform Sketchfab (<https://sketchfab.com>).

Images of shaded surface display volume renderings were made with the ‘snapshot’ function at the highest achievable resolution (usually at around 1900 × 893 pixels). Surface rendering rotational videos were created in Blender (v. 2.91, Blender Foundation, <https://www.blender.org/>). For optimal display, surface models exported from Amira were shaded ‘smooth’, scaled to ~ 1 m, illuminated with HDRi lighting, and rotated around their own z-axis based on specimens’ lateral views.

All specimens used in this study have been databased, and the data are freely accessible on AntWeb (2022). Each specimen can be traced by a unique specimen identifier attached to its pin. The Cybertype dataset provided in this study consist of the full micro-CT original volumetric datasets (in DICOM format), 3D surface models (in PLY formats), 3D rotation video files (in MKV format), all stacked digital colour images, and all image plates including all important images of 3D models for each species. All data have been archived and are freely available from the Dryad Digital Repository. In addition to the cybertype data on Dryad, we also provide freely accessible 3D surface models of the holotype and two paratypes of the new species on Sketchfab.

Collection references

- NHMUK** Natural History Museum, London, UK;
CASC California Academy of Sciences Collection, California, USA;
FHGC Francisco Hita–García Collection, Okinawa, Japan;
KGAC Kiko Gómez Abal Collection. Barcelona, Spain;
YKPC Yeo Kolo Collection, Lamto Station, Ivory Coast;
RBINS Royal Belgian Institute of Natural Sciences, Brussels, Belgium.

Measurements and indices

Measurements and indices follow Fischer et al. (2012). All linear measurements are in millimetres (mm).

- HL** Head length. Maximum distance from the mid–point of the anterior clypeal margin to the mid–point of the posterior margin of the head,

measured in full–face view; in majors from midpoint of tangent between anteriormost position of clypeus to midpoint of tangent between posteriormost projection of the vertex.

- HW** Head width. Measured at the widest point of the head, in full–face view behind eye–level.
- SL** Scape length. Maximum scape length, excluding basal condyle and neck.
- EL** Eye length. Maximum diameter of compound eye measured in oblique lateral view.
- MF** Metafemur length. Measured from the junction with the trochanter to the junction with the tibia.
- MDL** Mandible length. Maximum length, measured in oblique frontolateral view, from apex to lateral base.
- PW** Pronotal width. Maximum width of pronotum measured in dorsal view.
- WL** Weber’s length. Diagonal length of mesosoma in lateral view from the anterior point of the pronotal slope and excluding the neck, to the posteroventral margin of the propodeum.
- PSL** Propodeal spine length. In dorsocaudal view, with the apex of the measured spine, its base, and the centre of the propodeal concavity between the spines in focus: measurement is taken from apex to base along the one axis of a dual–axis micrometre, which is aligned along the length of the spine, crossing the second axis at the base of the measured spine, and the latter connecting the base with the centre of the propodeal concavity.
- PTL** Petiole length. Maximum diagonal length of petiole, measured in lateral view, from most anteroventral point of the peduncle to most posterodorsal point at the junction to first helcial tergite.
- PTH** Petiolar node height. Maximum height of petiolar node measured in lateral view from the highest (median) point of the node, orthogonally, to the ventral outline of the node.
- PTW** Petiolar node width. Maximum petiolar node width, measured in dorsal view.
- PPL** Postpetiole length. Maximum length of postpetiole, measured in lateral view, from anterior beginning of the dorsal slope to the posterior juncture of postpetiole and second helcial tergite.
- PPH** Postpetiole height. Maximum height of postpetiole, measured in lateral view, from the highest (median) point of the node to the lowest point of the ventral process, often in an oblique line.
- PPW** Postpetiole width. Maximum width of postpetiole, measured in dorsal view
- CI** Cephalic index. $HW / HL * 100$
- EI** Eye index. $EL / HW * 100$
- SI** Scape index. $SL / HW * 100$
- MDI** Mandible index. $MDL / HW * 100$
- PSLI** Propodeal spine index. $PSL / HW * 100$

PWI	Pronotal width index. $PW / HW * 100$
FI	Metafemur index. $MFL / HW * 100$.
PeI	Petiole index. $PTW / PW * 100$
PpI	Postpetiole index. $PPW / PW * 100$
PpWI	Postpetiole width index. $PPW / PTW * 100$
PpLI	Postpetiole length index. $PTL / PPL * 100$

Results

Pheidole pulchella species group

Fischer et al. (2012) provide a diagnosis for the group, which remains unchanged with the minor correction of replacing the erroneous *P. diomandei* (nom. nud.) with *P. heliosa*. A synoptic list of the *P. pulchella* group is provided below.

- Pheidole batrachorum* Wheeler, 1922
Pheidole christinae Fischer, Hita Garcia & Peters, 2011
Pheidole darwini Fischer, Hita Garcia & Peters, 2011
Pheidole dea Santschi, 1921
Pheidole glabrella Fischer, Hita Garcia & Peters, 2011
Pheidole heliosa Fischer, Hita Garcia & Peters, 2011
Pheidole klaman sp. nov.
Pheidole nimba Bernard, 1953
Pheidole pulchella Santschi, 1910
 = *Pheidole niapuana* Wheeler, 1922
 = *Pheidole pulchella* var. *achantella* Santschi, 1939
Pheidole rebecca Fischer, Hita Garcia & Peters, 2011
Pheidole semidea Fischer, Hita Garcia & Peters, 2011
Pheidole setosa Fischer, Hita Garcia & Peters, 2011

Pheidole klaman sp. nov.

<http://zoobank.org/78E38050-CC84-4A26-B882-CEB9FD9B3521>

Material examined. Major worker: Figs 1A–D, 2A–G, 6A, B, Table 1.

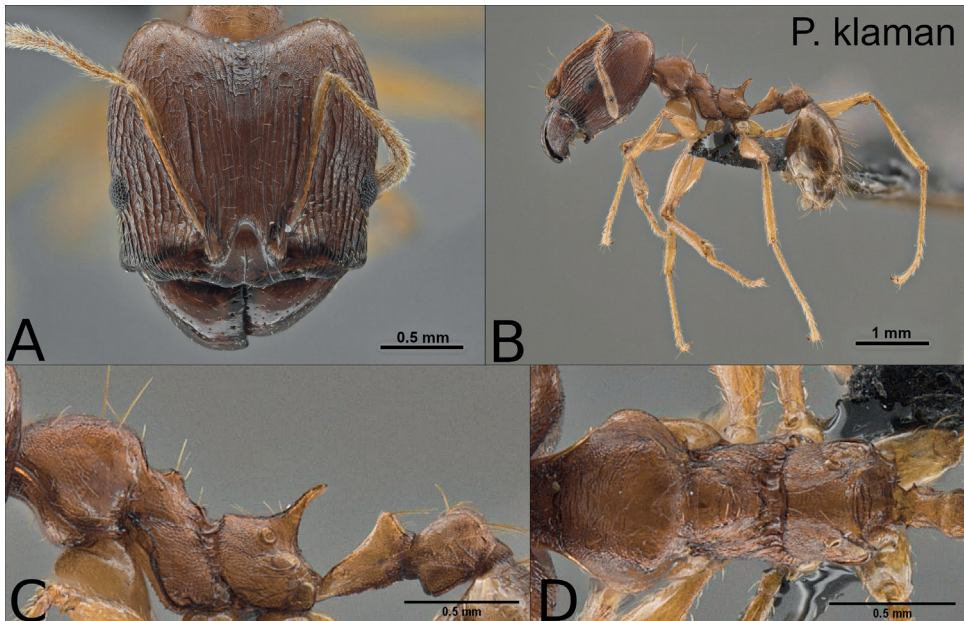
Minor worker: Figs 3A–D, 4A–G, 5A–G, 7A, B, Table 2.

Holotype major worker: IVORY COAST: Montagnes District, Site 05 (Taï N. P.) 200m, 5.8438, -7.3484, 11/11/2019. Hand collected (Gómez, K. & Kouakou, L.). Primary forest, ex. rotten log [CASENT0764691] HNMUK.

Paratype workers: same series, (1 major worker) [KGCOL00585] KGAC; (1 minor worker) [CASENT0745509] FHGC; (1 minor worker) [CASENT0764692] KGAC, (1 minor worker) [KGCOL00587] AFRC; (1 minor worker) [KGCOL00588]

Table 1. Measurements for the major workers of the yellow forms of the *pulchella* species group. Measurements provided as range (mean).

	Yellow species (major workers)		
	<i>P. heliosa</i> (n = 1)	<i>P. klaman</i> (n = 2)	<i>P. pulchella</i> (n = 12)
HL	2.45	1.78–1.98 (1.88)	1.94–2.23 (2.14)
HW	2.35	1.65–1.75 (1.7)	2.0–2.28 (2.16)
MDL	1.30	0.85–0.89 (0.87)	0.90–1.11 (1.02)
EL	0.27	0.22–0.23 (0.22)	0.23–0.26 (0.24)
SL	1.24	1.03–1.08 (1.06)	1.06–1.17 (1.13)
PW	1.07	0.74–0.78 (0.76)	0.81–1.03 (0.95)
PSL	0.27	0.29–0.31 (0.3)	0.24–0.38 (0.32)
PtL	0.61	0.45–0.47 (0.46)	0.53–0.64 (0.59)
PtH	0.42	0.29–0.31 (0.30)	0.33–0.39 (0.36)
PtW	0.31	0.21–0.22 (0.21)	0.20–0.27 (0.24)
PPtL	0.42	0.36–0.38 (0.37)	0.33–0.41 (0.38)
PPtH	0.54	0.4–0.41 (0.41)	0.37–0.5 (0.44)
PPtW	0.70	0.43–0.48 (0.46)	0.42–0.61 (0.52)
WL	2.10	1.47–1.56 (1.51)	1.40–1.74 (1.64)
MFL	1.98	1.44–1.51 (1.47)	1.67–1.84 (1.74)
CI	95	88–93 (90)	98–104 (101)
EI	11	12–14 (13)	11–13 (11)
SI	52	62–62 (62)	51–56 (53)
MDI	55	51–51 (51)	43–50 (47)
PSLI	11	17–18 (17)	11–18 (11)
PWI	45	45–45 (45)	39–47 (39)
FI	84	86–87 (87)	76–90 (81)
PeI	28	28–28 (28)	22–28 (25)
PpI	65	58–62 (60)	47–61 (55)
PpWI	225	210–224 (217)	204–235 (220)
PpLI	145	124–126 (125)	139–166 (157)

**Figure 1.** Holotype of *Pheidole klaman*, major worker (CASENT0764691) **A** head in full-face view **B** habitus lateral view **C** mesosoma, petiole and postpetiole lateral view **D** mesosoma dorsal view.

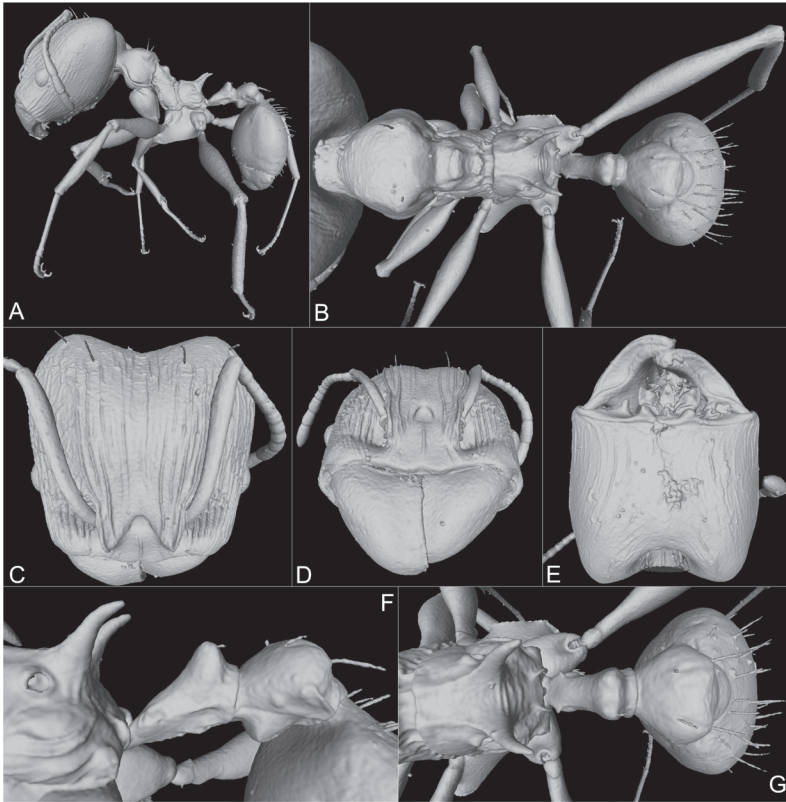


Figure 2. Holotype of *Pheidole klaman*, major worker, 3D model snapshots (CASENT0764691) **A** habitus lateral view **B** habitus dorsal view **C** head dorsal view **D** head frontal view **E** head ventral view **F** propodeum, petiole and postpetiole lateral view **G** propodeum, petiole and postpetiole dorsal view.

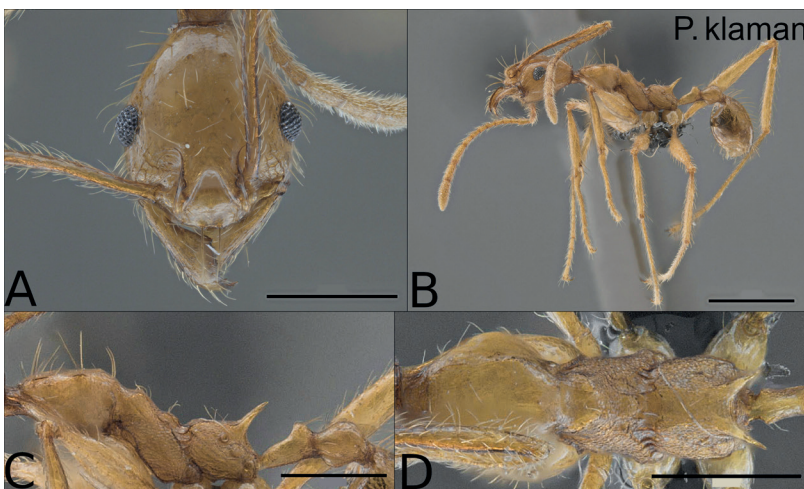


Figure 3. Paratype of *Pheidole klaman*, minor worker (KGCOL00589) **A** head in full-face view **B** habitus lateral view **C** mesosoma, petiole and postpetiole lateral view **D** mesosoma dorsal view. Scale bars: 0.5 mm (**A, C, D**); 1 mm (**B**).

Table 2. Measurements for the minor workers of yellow forms of the *pulchella* species group.

	Yellow species (minor workers)			
	<i>P. christinae</i> (n = 20)	<i>P. heliosa</i> (n = 8)	<i>P. klaman</i> (n = 7)	<i>P. pulchella</i> (n = 12)
HL	0.88–1.02 (0.98)	1.06–1.09 (1.08)	0.77–0.90 (0.81)	0.86–0.93 (0.89)
HW	0.73–0.83 (0.80)	0.78–0.82 (0.80)	0.64–0.71 (0.66)	0.73–0.80 (0.77)
MDL	0.58–0.68 (0.64)	0.64–0.80 (0.69)	0.55–0.62 (0.57)	0.58–0.64 (0.61)
EL	0.16–0.18 (0.17)	0.17–0.20 (0.18)	0.16–0.19 (0.18)	0.17–0.19 (0.18)
SL	1.10–1.35 (1.25)	1.30–1.43 (1.36)	1.17–1.32 (1.21)	1.13–1.24 (1.18)
PW	0.49–0.57 (0.54)	0.57–0.61 (0.60)	0.44–0.51 (0.46)	0.48–0.54 (0.50)
PSL	0.26–0.34 (0.30)	0.29–0.40 (0.32)	0.02–0.23 (0.20)	0.22–0.26 (0.24)
PtL	0.33–0.41 (0.38)	0.37–0.42 (0.39)	0.24–0.27 (0.26)	0.29–0.39 (0.34)
PtH	0.17–0.21 (0.19)	0.19–0.21 (0.20)	0.18–0.20 (0.19)	0.17–0.21 (0.19)
PtW	0.12–0.13 (0.13)	0.12–0.13 (0.13)	0.11–0.14 (0.12)	0.11–0.12 (0.12)
PPtL	0.23–0.28 (0.26)	0.27–0.28 (0.28)	0.23–0.28 (0.26)	0.21–0.26 (0.24)
PPtH	0.22–0.27 (0.25)	0.23–0.28 (0.25)	0.22–0.25 (0.23)	0.21–0.24 (0.22)
PPtW	0.22–0.27 (0.25)	0.26–0.30 (0.27)	0.24–0.27 (0.24)	0.22–0.27 (0.23)
WL	1.14–1.40 (1.30)	1.48–1.54 (1.51)	1.18–1.36 (1.23)	1.16–1.30 (1.25)
MFL	1.33–1.63 (1.49)	1.60–1.74 (1.68)	1.34–1.53 (1.40)	1.37–1.51 (1.43)
CI	79–84 (82)	73–75 (74)	79–83 (81)	84–90 (86)
EI	20–22 (21)	21–24 (22)	26–27 (27)	21–25 (23)
SI	144–165 (156)	163–174 (170)	182–189 (185)	146–159 (154)
MDI	77–84 (80)	79–99 (86)	85–87 (86)	75–82 (79)
PSLI	33–43 (33)	37–49 (37)	30–34 (30)	29–36 (29)
PWI	64–69 (64)	73–75 (73)	68–72 (68)	64–68 (64)
FI	175–197 (187)	205–213 (210)	208–220 (213)	179–194 (186)
Pel	21–25 (24)	20–23 (21)	24–29 (27)	22–24 (23)
Ppl	43–50 (47)	44–49 (46)	50–55 (53)	43–50 (46)
PpWI	183–217 (199)	208–233 (219)	186–209 (197)	183–225 (195)
PpLI	137–171 (149)	132–150 (139)	92–105 (100)	115–177 (146)

NHMUK; (1 minor worker) [KGCOL00590] YKPC; (3 minor workers, in ethanol) [KG04152] KGAC.

Cybertype: we provide virtual 3D data of the major worker holotype (CASENT0764691) and two minor worker paratypes (CASENT0764692 & CASENT0745509) as cybertype dataset, which contains the following data: volumetric raw data (in DICOM format), 3D rotation videos (in mkv format), 3D surfaces (in PLY format), still images of surface volume rendering, and of stacked digital colour images illustrating head in full-face view, profile and dorsal view of the body. The datasets are deposited on Dryad (doi:10.5061/dryad.mpg4f4r1k) and can be freely accessed as virtual representations of the types. In addition, we also provide freely accessible 3D surface models at Sketchfab (holotype: <https://skfb.ly/o68Qw>; paratypes: <https://skfb.ly/o68Qq> & <https://skfb.ly/o68Qo>).

Diagnosis. *Pheidole klaman* is one of the four known yellow to orange species in the *pulchella* group, and appears closest to *P. pulchella*. It is easily separable from the other yellow to orange coloured species in the group as follows:

Minor worker: while *P. pulchella* has appressed scape pilosity, *P. klaman* possesses long erect setae on the scapes that are as long as or longer than the scape width. Sepa-

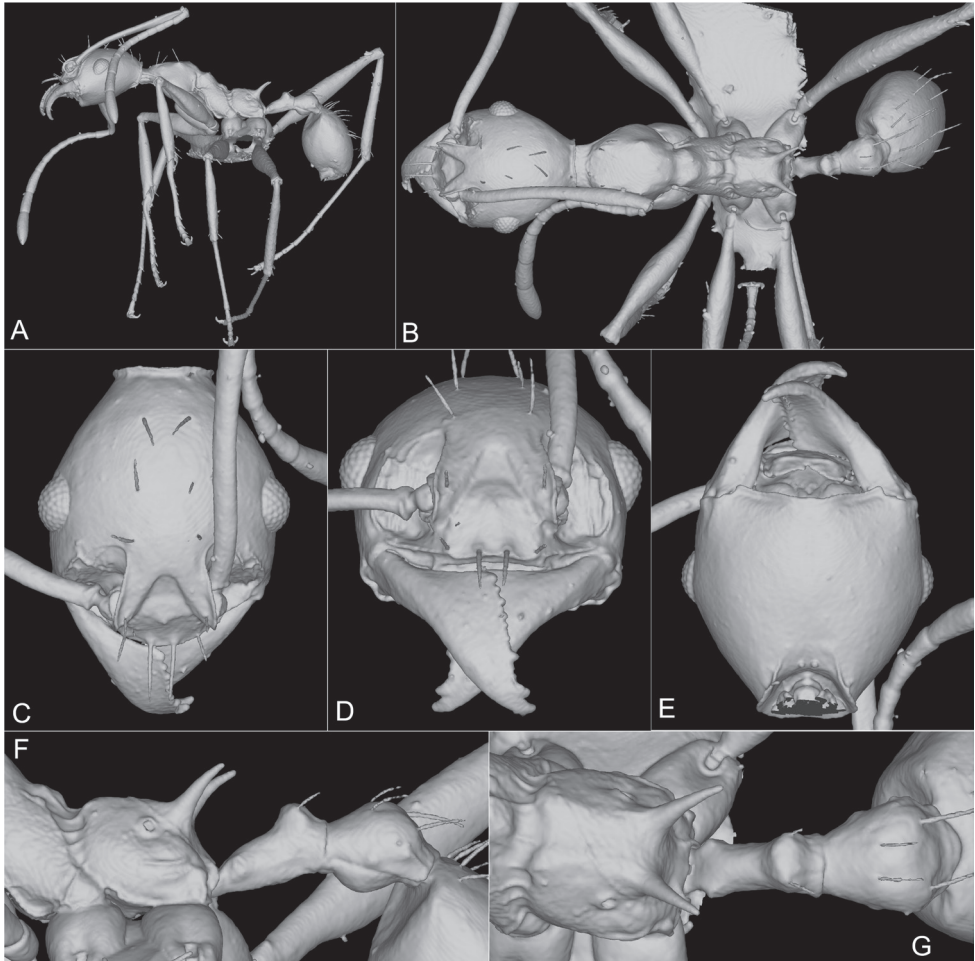


Figure 4. Paratype of *Pheidole klaman*, minor worker, 3D model snapshots (KGCOL00589) **A** habitus lateral view **B** habitus dorsal view **C** head dorsal view **D** head frontal view **E** head ventral view **F** propodeum, petiole and postpetiole lateral view **G** propodeum, petiole and postpetiole dorsal view.

ration from *P. heliosa* and *P. christinae* is based on size, with *P. klaman* clearly smaller (HW: 0.64–0.71) and with relatively longer scapes (SI: 182–189) than the other two species (HW: 0.73–0.83, SI: 143–174).

Major worker: the major of *P. christinae* is unknown. The absence of setae laterally on the head and the presence of clearly demarcated antennal scrobes separates *P. klaman* from *P. heliosa*. Separation from *P. pulchella* is also unambiguous, *P. klaman* clearly being smaller (HW: 1.65–1.75 vs 2.0–2.28 for *pulchella*), with more elongated head (CI: 88–93 vs. 98–104 in *P. pulchella*) and longer scapes (SI: 62–63 vs. 50–56). Sculpture is another separation character, with *P. klaman* being uniformly punctate from mesonotum to propodeum, versus more weakly and irregularly punctate sculpture

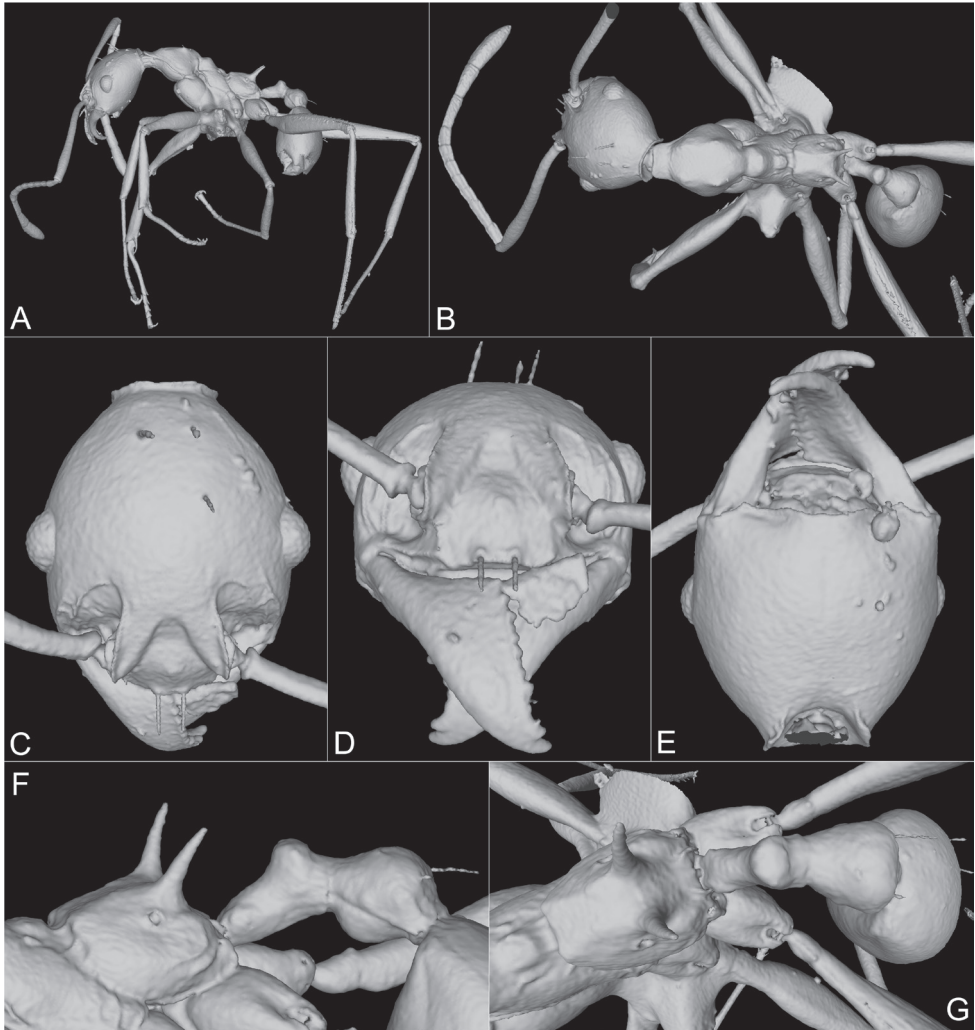


Figure 5. Paratype of *Pheidole klaman*, minor worker, 3D-model snapshots (CASENT0764692). **A** habitus lateral view **B** habitus dorsal view **C** head dorsal view **D** head frontal view **E** head ventral view **F** propodeum, petiole and postpetiole lateral view **G** propodeum, petiole and postpetiole dorsal view.

in *P. pulchella*. In *P. klaman* the posterior third of face has faint incomplete longitudinal rugulae at most, reduced to weak, superficially reticulate punctures posteriorly, while in *P. pulchella* the posterior third of the face is longitudinally rugose and weakly to superficially punctate, changing to obliquely and weakly rugulose towards the posterior head margin.

Description. With the characteristics described for *Pheidole pulchella* species group in Fischer et al. (2012) and:

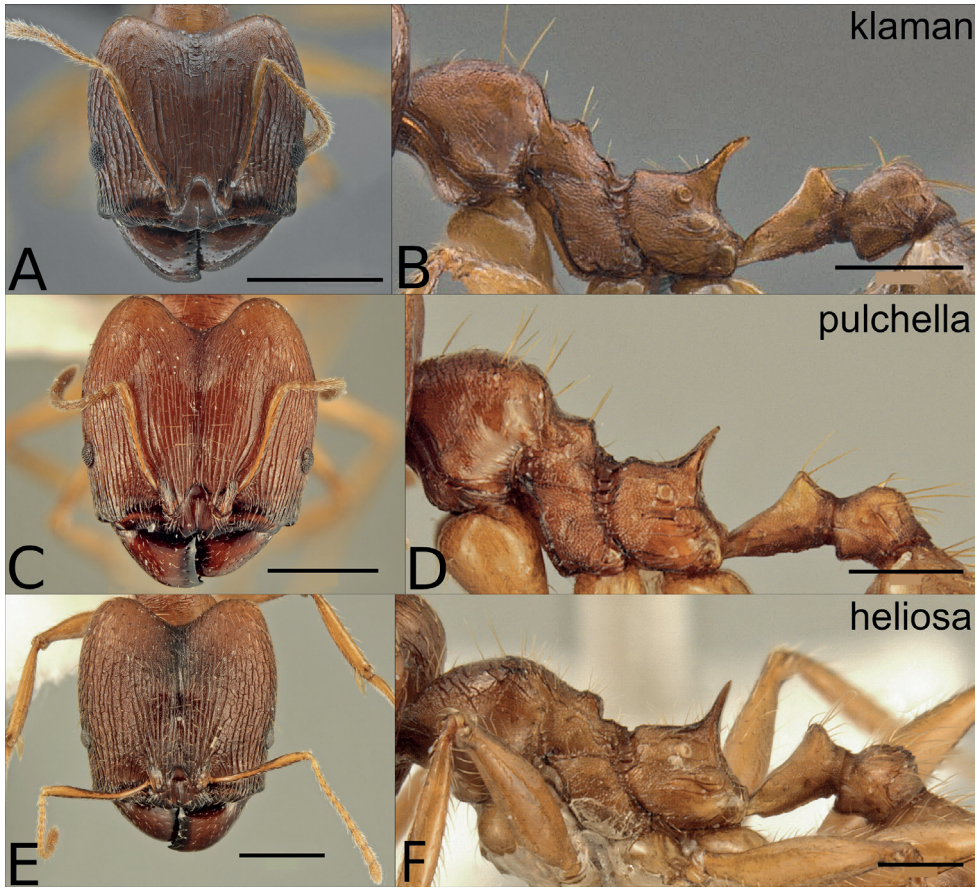


Figure 6. Major workers of the orange species in the *P. pulchella* group: *P. klaman* (**A, B** CASENT0764691), *P. pulchella* (**C, D** CASENT0218336), *P. heliosa* (**E, F** CASENT0227946). The major worker of *P. christinae* is unknown. Scale bars: 0.5 mm **B, D, F**; 1 mm **A, C, E**.

Major worker measurements: Holotype: HL: 1.98; HW: 1.75; MDL: 0.89; EL: 0.22; SL: 1.08; PW: 0.78; PSL: 0.31; PtL: 0.47; PtH: 0.31; PtW: 0.22; PPtL: 0.38; PPtH: 0.41; PPtW: 0.48; WL: 1.56; MFL: 1.51; CI: 88; EI: 12; SI: 62; MDI: 51; PSLI: 18; PWI: 45; FI: 86; Pel: 28; Ppl: 62; PpWI: 224; PpLI: 124

Paratype: HL: 1.78; HW: 1.65; MDL: 0.85; EL: 0.23; SL: 1.03; PW: 0.74; PSL: 0.29; PtL: 0.45; PtH: 0.29; PtW: 0.21; PPtL: 0.36; PPtH: 0.40; PPtW: 0.43; WL: 1.47; MFL: 1.44; CI: 93; EI: 14; SI: 62; MDI: 51; PSLI: 17; PWI: 45; FI: 87; Pel: 28; Ppl: 58; PpWI: 210; PpLI: 126

Head longer than wide (CI: 88–93), frontal carinae and antennal scrobes conspicuous. Scapes relatively long for the group (SI: 61–63). Funicular segments slightly longer than wide, the last three more than twice as long as wide, apical one longer. Pronotum shape in dorsal view rhomboid, with clearly demarcated humeral angles.

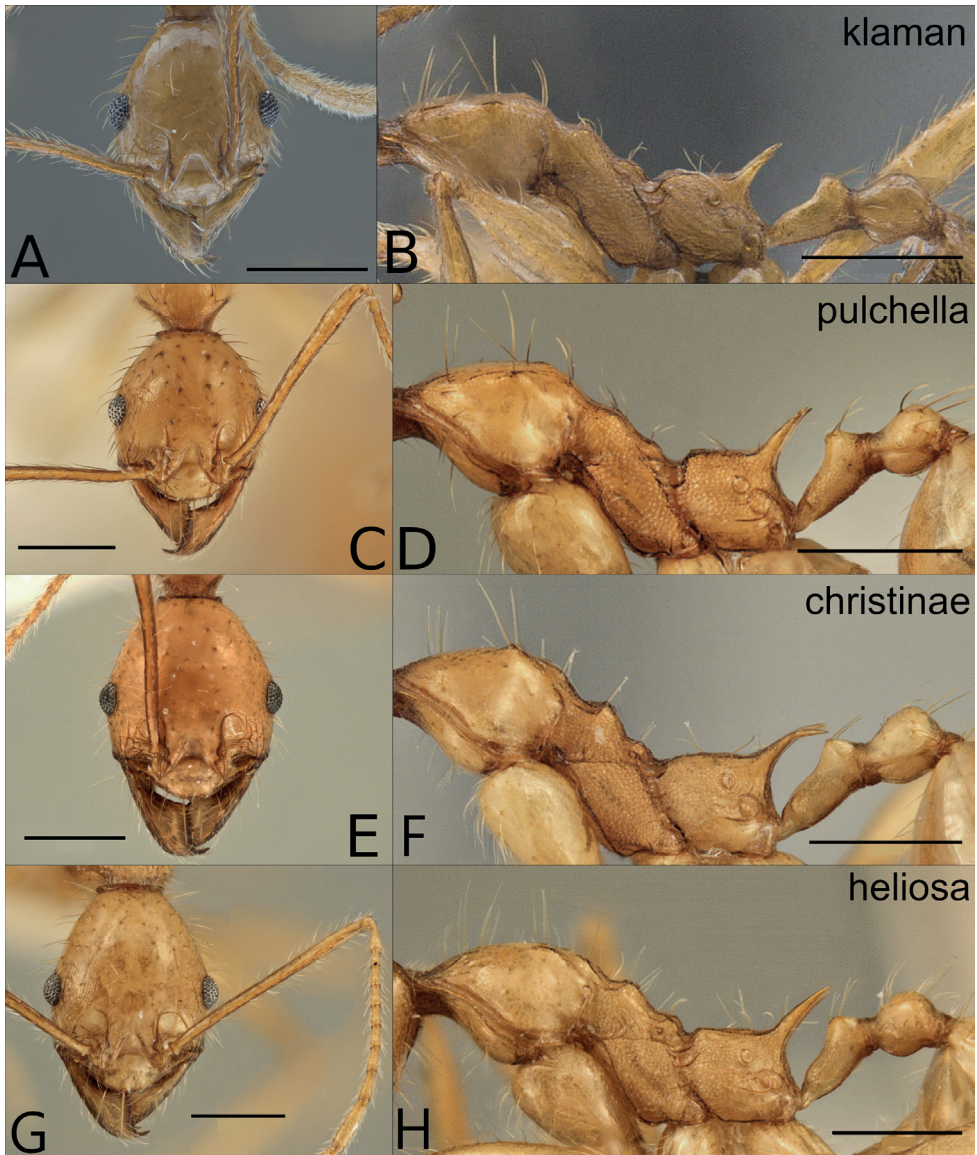


Figure 7. Minor workers of the orange species in the *P. pulchella* species group, head and lateral mesosoma: *P. klaman* (A, B KGCOL00589), *P. pulchella* (C, D CASENT0227963), *P. christinae* (E, F CASENT0227940), *P. heliosa* (G, H CASENT0227945). Scale bars: 0.5 mm.

Promesonotal depression and metanotal groove deep. Primary mesonotal process conspicuous, stepping into a much smaller secondary one. Propodeum dorsally with two rugulae proceeding from the metanotal groove and continuing into the well-developed, long, apically curved spines (PSLI: 17–18). Petiole with very narrow anteroventral laminar process, postpetiole with large, rounded–triangular, anteriorly oriented ventral process, in dorsal view with hexagonal to ellipsoidal shape, and two small translucent flanges extending from medial corners to gaster.

Table 3. Measurements for the major workers of dark forms of the *pulchella* species group.

	Dark species (major workers)					
	<i>P. batrachorum</i> (n = 6)	<i>P. darwini</i> (n = 10)	<i>P. dea</i> (n = 6)	<i>P. glabrella</i> (n = 6)	<i>P. rebecca</i> (n = 4)	<i>P. semidea</i> (n = 3)
HL	1.86–2.04 (1.91)	1.96–2.20 (2.09)	1.76–1.96 (1.83)	1.80–2.13 (1.95)	1.82–1.98 (1.92)	1.70–1.86 (1.79)
HW	1.80–2.0 (1.88)	1.96–2.23 (2.11)	1.78–1.94 (1.84)	1.80–2.15 (1.98)	1.86–1.98 (1.94)	1.70–1.82 (1.76)
MDL	0.89–1.00 (0.95)	0.94–1.06 (1.01)	0.82–0.87 (0.84)	0.78–0.97 (0.86)	0.83–0.91 (0.87)	0.79–0.83 (0.81)
EL	0.23–0.28 (0.25)	0.24–0.27 (0.25)	0.22–0.23 (0.23)	0.22–0.27 (0.24)	0.23–0.27 (0.26)	0.21–0.22 (0.22)
SL	1.01–1.13 (1.07)	1.01–1.13 (1.06)	1.01–1.06 (1.03)	0.94–1.08 (1.02)	0.94–0.98 (0.96)	0.98–1.00 (0.99)
PW	0.80–0.89 (0.83)	0.86–0.98 (0.93)	0.80–0.83 (0.82)	0.74–0.94 (0.86)	0.86–0.90 (0.89)	0.71–0.80 (0.77)
PSL	0.28–0.32 (0.31)	0.33–0.39 (0.36)	0.29–0.33 (0.31)	0.31–0.37 (0.34)	0.24–0.30 (0.28)	0.29–0.31 (0.03)
PtL	0.51–0.57 (0.54)	0.54–0.67 (0.59)	0.46–0.50 (0.49)	0.47–0.57 (0.53)	0.47–0.56 (0.51)	0.49–0.56 (0.52)
PtH	0.30–0.38 (0.33)	0.32–0.38 (0.34)	0.27–0.32 (0.30)	0.30–0.36 (0.33)	0.32–0.34 (0.33)	0.25–0.33 (0.30)
PtW	0.22–0.28 (0.24)	0.21–0.27 (0.23)	0.20–0.24 (0.22)	0.20–0.26 (0.23)	0.21–0.24 (0.23)	0.20–0.22 (0.21)
PPtL	0.33–0.39 (0.37)	0.33–0.39 (0.36)	0.29–0.32 (0.30)	0.30–0.34 (0.32)	0.31–0.36 (0.33)	0.31–0.34 (0.33)
PPtH	0.37–0.46 (0.41)	0.37–0.47 (0.42)	0.32–0.34 (0.33)	0.33–0.44 (0.38)	0.36–0.41 (0.39)	0.34–0.37 (0.36)
PPtW	0.48–0.56 (0.51)	0.47–0.59 (0.54)	0.38–0.43 (0.41)	0.41–0.54 (0.47)	0.46–0.53 (0.50)	0.44–0.47 (0.46)
WL	1.44–1.70 (1.54)	1.48–1.65 (1.56)	1.46–1.56 (1.51)	1.35–1.62 (1.50)	1.44–1.56 (1.50)	1.41–1.48 (1.44)
MFL	1.48–1.70 (1.57)	1.56–1.71 (1.62)	1.46–1.60 (1.49)	1.40–1.63 (1.51)	1.48–1.56 (1.50)	1.41–1.44 (1.43)
CI	97–100 (98)	99–104 (101)	99–102 (101)	99–105 (102)	99–103 (101)	98–100 (99)
EI	12–14 (13)	11–13 (12)	11–13 (12)	11–13 (12)	12–15 (13)	12–13 (12)
SI	55–58 (57)	49–53 (50)	55–58 (56)	49–53 (51)	49–51 (50)	55–58 (56)
MDI	47–53 (50)	42–51 (48)	42–49 (46)	42–45 (43)	44–46 (45)	43–48 (46)
PSLI	15–18 (15)	16–18 (16)	16–19 (16)	16–18 (16)	13–15 (13)	16–18 (16)
PWI	44–45 (44)	43–45 (43)	43–46 (43)	41–44 (41)	45–46 (45)	39–47 (39)
FI	80–85 (83)	75–80 (77)	79–83 (81)	75–78 (77)	75–84 (77)	79–83 (81)
Pel	27–31 (29)	24–28 (25)	25–29 (26)	24–28 (26)	24–27 (26)	25–30 (27)
Ppl	57–67 (62)	55–63 (58)	46–53 (50)	51–59 (55)	53–59 (56)	55–66 (60)
PpWI	182–236 (215)	219–257 (232)	179–200 (190)	192–220 (208)	213–230 (220)	214–224 (219)
PpLI	131–161 (147)	151–176 (163)	156–167 (162)	147–173 (165)	139–165 (153)	148–165 (158)

Mandibles glassy smooth. Frons longitudinally rugose, with irregular pattern of moderately long to shorter rugae, spaces between rugae weakly punctate to almost smooth. Rugae grading weaker posteriorly with transverse incomplete anastomoses between them at vertex, fading from this point being gradually replaced by weaker rugulose–punctate sculpture becoming smooth at some patches. Pronotum smooth, rest of mesosoma strongly punctate, with some incomplete rugulae laterally, continuing at the base of the spines and propodeal declivity. Mesopropodeal suture with strongly demarcated longitudinal short cross–ribs. Petiole and postpetiole with the same punctuation as mesosoma, weaker to smooth dorsally. Anterior half of first gastral tergite superficially punctate, posterior half smooth.

Scape pilosity appressed. In full–face view, head without standing setae laterally. Head, promesonotum, petiole, postpetiole, with several setae that are longer than spine length and with additional short appressed pubescence, long setae more abundant on gaster. Colour orange to darker orange, legs paler. Metatibia with short appressed pilosity.

Minor worker measurements (n = 7): HL: 0.77–0.90; HW: 0.64–0.71; MDL: 0.55–0.62; EL: 0.16–0.19; SL: 1.17–1.32; PW: 0.44–0.51; PSL: 0.20–0.23; PtL: 0.24–0.27; PtH: 0.18–0.20; PtW: 0.11–0.14; PPtL: 0.23–0.28; PPtH: 0.22–0.25; PPtW: 0.24–0.27; WL: 1.18–1.36; MFL: 1.34–1.53; CI: 79–83; EI: 26–27; SI: 182–189; MDI: 85–87; PSLI: 30–34; PWI: 68–72; FI: 208–220; Pel: 24–29; Ppl: 50–55; PpWI: 186–209; PpLI: 92–105

Table 4. Measurements for the minor workers of dark forms of the *pulchella* species group.

	Dark species (minor workers)						
	<i>P. batrachorum</i> (n = 15)	<i>P. darwini</i> (n = 15)	<i>P. dea</i> (n = 28)	<i>P. glabrella</i> (n = 26)	<i>P. rebecca</i> (n = 10)	<i>P. semidea</i> (n = 3)	<i>P. setosa</i> (n = 2)
HL	0.68–0.87 (0.82)	0.77–0.88 (0.84)	0.73–0.94 (0.85)	0.72–0.92 (0.85)	0.93–1.02 (0.97)	0.76–0.81 (0.79)	0.78–0.81 (0.79)
HW	0.59–0.74 (0.68)	0.67–0.76 (0.72)	0.66–0.86 (0.76)	0.67–0.86 (0.78)	0.77–0.82 (0.80)	0.72–0.78 (0.76)	0.69–0.69 (0.69)
MDL	0.46–0.57 (0.54)	0.52–0.61 (0.56)	0.50–0.67 (0.58)	0.51–0.63 (0.58)	0.62–0.64 (0.63)	0.51–0.56 (0.53)	0.53–0.54 (0.54)
EL	0.16–0.19 (0.18)	0.16–0.19 (0.17)	0.17–0.20 (0.18)	0.17–0.19 (0.18)	0.20–0.21 (0.2)	0.17–0.18 (0.17)	0.16–0.19 (0.17)
SL	0.9–1.13 (1.09)	0.99–1.21 (1.08)	0.94–1.16 (1.07)	0.87–1.13 (1.02)	1.27–1.32 (1.30)	0.86–0.9 0 (0.89)	0.97–1.03 (0.99)
PW	0.40–0.51 (0.47)	0.44–0.51 (0.48)	0.42–0.57 (0.49)	0.46–0.57 (0.51)	0.54–0.57 (0.55)	0.46–0.50 (0.48)	0.47–0.48 (0.48)
PSL	0.14–0.24 (0.21)	0.24–0.30 (0.27)	0.20–0.28 (0.24)	0.20–0.36 (0.28)	0.24–0.25 (0.24)	0.19–0.23 (0.22)	0.21–0.23 (0.22)
PtL	0.26–0.37 (0.33)	0.30–0.36 (0.33)	0.26–0.37 (0.32)	0.27–0.37 (0.34)	0.39–0.41 (0.40)	0.28–0.33 (0.31)	0.26–0.29 (0.27)
PtH	0.14–0.19 (0.18)	0.17–0.19 (0.18)	0.16–0.20 (0.18)	0.17–0.21 (0.19)	0.20–0.21 (0.2)	0.17–0.18 (0.17)	0.17–0.17 (0.17)
PtW	0.10–0.13 (0.12)	0.11–0.13 (0.12)	0.11–0.14 (0.12)	0.11–0.13 (0.12)	0.12–0.15 (0.14)	0.11–0.11 (0.11)	0.11–0.12 (0.11)
PPtL	0.18–0.27 (0.23)	0.19–0.24 (0.22)	0.14–0.22 (0.18)	0.18–0.23 (0.2)	0.26–0.28 (0.27)	0.19–0.22 (0.2)	0.19–0.21 (0.2)
PPtH	0.17–0.23 (0.21)	0.19–0.22 (0.21)	0.16–0.24 (0.20)	0.18–0.24 (0.21)	0.24–0.26 (0.25)	0.18–0.21 (0.19)	0.18–0.20 (0.19)
PPtW	0.19–0.24 (0.22)	0.21–0.26 (0.22)	0.17–0.24 (0.21)	0.18–0.27 (0.22)	0.26–0.30 (0.28)	0.19–0.22 (0.20)	0.21–0.22 (0.21)
WL	0.96–1.21 (1.12)	1.08–1.25 (1.16)	1.01–1.33 (1.16)	1.01–1.29 (1.16)	1.32–1.40 (1.36)	1.01–1.08 (1.04)	1.04–1.11 (1.07)
MFL	1.01–1.38 (1.28)	1.13–1.38 (1.28)	1.09–1.44 (1.27)	1.04–1.35 (1.22)	1.44–1.58 (1.51)	0.97–1.07 (1.02)	1.11–1.19 (1.14)
CI	80–87 (83)	84–89 (86)	86–93 (90)	88–95 (91)	81–83 (82)	94–99 (96)	85–88 (87)
EI	24–29 (26)	22–26 (24)	22–27 (24)	22–27 (23)	25–25 (25)	22–24 (23)	23–28 (25)
SI	153–173 (160)	140–159 (149)	133–146 (141)	123–140 (131)	161–165 (163)	114–121 (117)	141–149 (144)
MDI	76–84 (80)	75–82 (78)	73–78 (75)	71–78 (74)	78–80 (79)	68–73 (70)	77–78 (78)
PSLI	24–34 (24)	33–40 (33)	28–36 (28)	30–43 (30)	30–31 (30)	26–30 (26)	30–33 (30)
PWI	65–72 (65)	66–68 (66)	60–68 (60)	61–69 (61)	69–69 (69)	62–65 (62)	68–70 (68)
FI	171–197 (188)	169–190 (177)	158–175 (166)	143–169 (157)	186–192 (189)	133–139 (135)	161–172 (166)
PeL	24–27 (25)	22–27 (24)	22–28 (25)	22–27 (24)	23–27 (25)	22–24 (23)	23–25 (24)
PpL	45–50 (48)	43–52 (46)	39–47 (42)	39–55 (44)	48–53 (50)	41–45 (43)	44–47 (45)
PpWI	175–200 (188)	162–217 (190)	146–192 (169)	162–209 (186)	193–208 (201)	173–200 (185)	175–200 (189)
PpLI	122–164 (141)	136–174 (152)	155–229 (173)	143–206 (171)	148–152 (150)	145–174 (155)	129–145 (137)

Table 5. Summary of micro-CT scanning parameters with resulting voxel sizes (optical magnification was 4 × and image size 1013 × 1013) for all three scanned specimens.

Subcaste	Specimen ID	Magnification	Voxel size (µm)	Exposure (s)	Power (W)	Voltage (kV)	Current (µA)
major	CASENT0764691	4 ×	5,7854	1,2	5,92	70	85
minor	CASENT0745509	4 ×	4,6952	0,6	4,01	50	80
minor	CASENT0764692	4 ×	5,3599	0,6	6,02	70	85

Head longer than wide (CI: 79–83), with sides posterior of eye level weakly convex, slightly rounded towards posterior margin. Occipital carina conspicuous, medially and laterally. Mandibles relatively long (MDI: 85–88). Scapes very long (SI: 182–189), the longest in the whole *pulchella* group. All funicular segments significantly (– 2 ×) longer than wide, apical three segments at least 3 × as long as wide. Mesosoma as described for the group, with moderately long, apically tapering, posteriorly curved spines (PSLI: 30–34). Pronotal humeri slightly peaked in lateral view, first and second mesonotal processes notorious and pronounced, each of these structures weakly marginate, or at least with some feeble rugulae. Metanotal groove broad and deep. Legs very long (FI: 208–220), relative to body size, the longest of all the *pulchella* group.

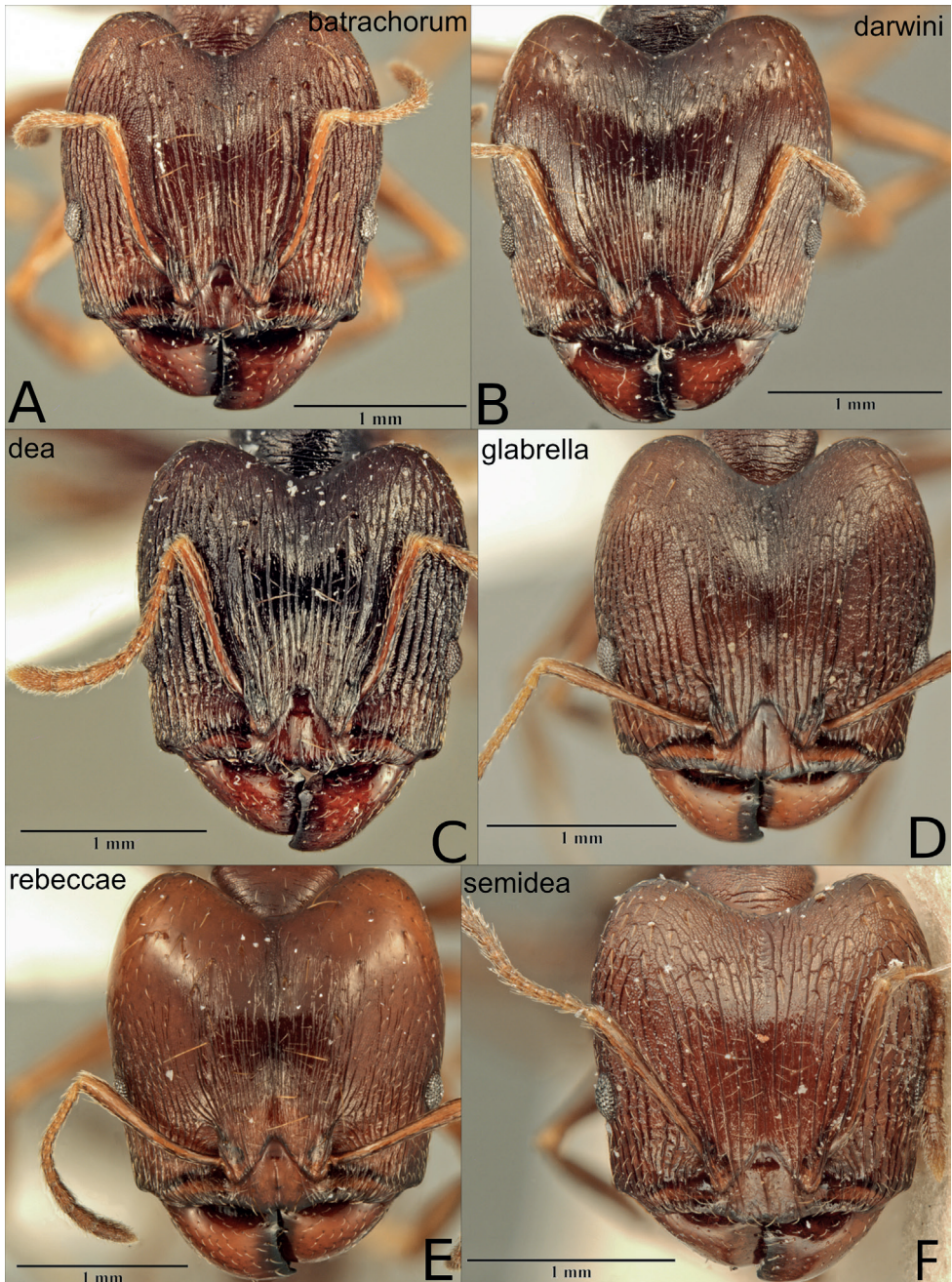


Figure 8. Major workers of the dark species in the *P. pulchella* group, heads in full frontal view **A** *P. batrachorum* (CASENT0415367) **B** *P. darwini* (CASENT0218332) **C** *P. dea* (CASENT0227965) **D** *P. glabrella* (CASENT0227950) **E** *P. rebecca* (CASENT0227954) **F** *P. semidea* (CASENT0227960).

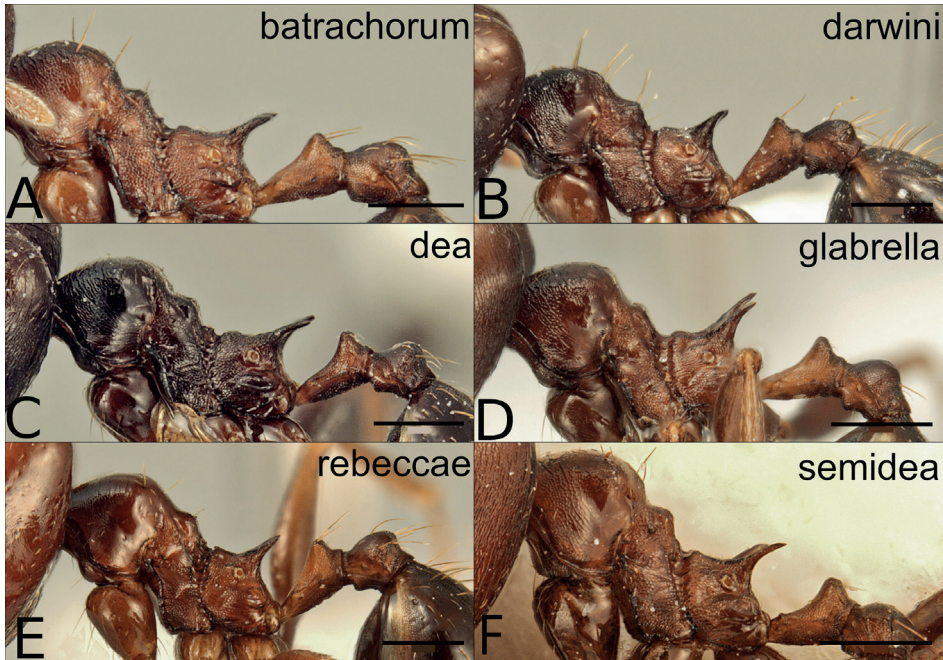


Figure 9. Major workers of the dark species in the *P. pulchella* group, mesosoma in lateral view **A** *P. batrachorum* (CASENT0415367) **B** *P. darwini* (CASENT0218332) **C** *P. dea* (CASENT0227965) **D** *P. glabella* (CASENT0227950) **E** *P. rebecca* (CASENT0227954) **F** *P. semidea* (CASENT0227960). Scale bars: 0.5 mm.

Head, mandibles, pronotum, coxae, legs, postpetiole, and gaster glassy smooth, except for some isolated strong reticulation between eyes and antennal fossae. Mesonotum and propodeum strongly punctate, both laterally and dorsally. Metanotal groove costate. Petiole from micropunctate dorsally to weakly punctate ventrally.

Long, orange erect to semi-erect setae sparsely distributed everywhere, including pro- and mesonotum, propodeum, petiole, postpetiole, and gaster, some longer than spine length. In full-face view, head laterally with semi-erect setae above and below eyes, some longer than eye diameter. Scapes with very abundant semi-erect setae, as long as scape width. Legs also covered with abundant semi-erect to decumbent pilosity.

Colour yellow to pale orange.

Derivatio nominis. The species name *klaman* is a non-Latin noun used in apposition and is the Boualé word for *pulchella* (beauty).

Other material examined. IVORY COAST: Montagnes District, Site 02 (Taï N. P.) 200m, 5.8312, -7.3429 08/11/2019. Winkler sample (Gómez, K. & Kouakou, L.). Primary Forest in leaf litter (1 worker) [KGCOL00507] KGAC

IVORY COAST: Montagnes District, Site 05 (Taï N. P.) 200m, 5.8438, -7.3484 11/11/2019. Winkler sample (Gómez, K. & Kouakou, L.). Primary Forest in leaf litter (1 worker) [KGCOL00443] KGAC

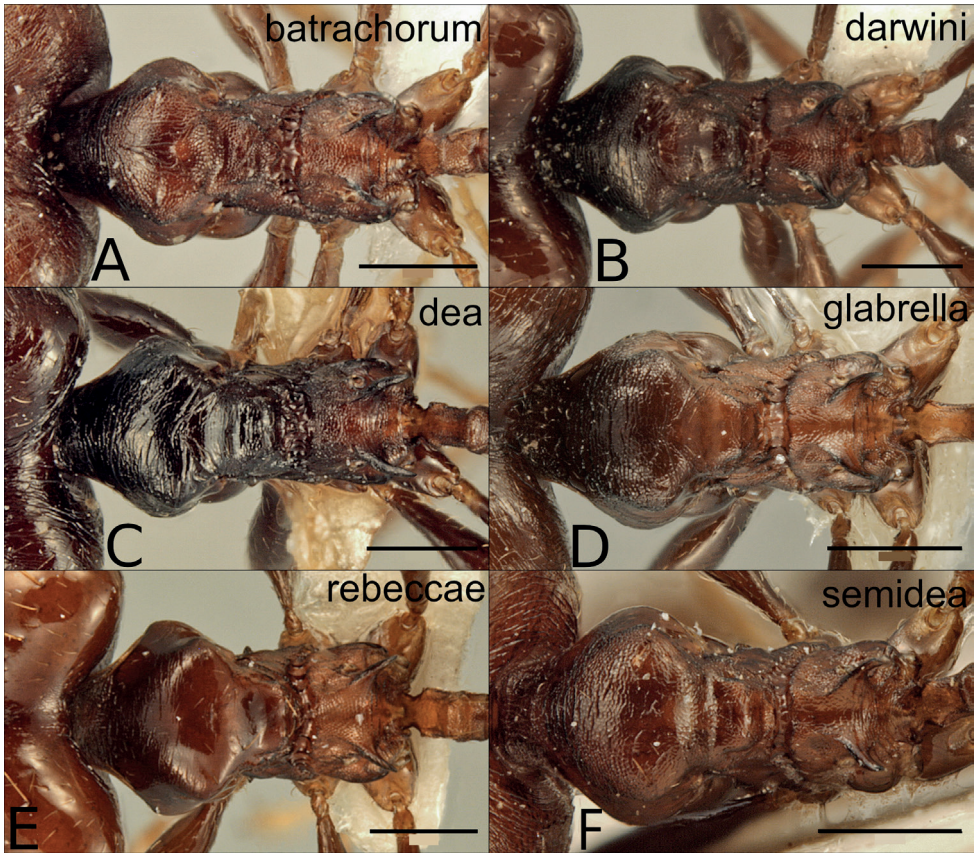


Figure 10. Major workers of the dark species in the *P. pulchella* group, mesosoma in dorsal view **A** *P. batrachorum* (CASENT0415367) **B** *P. darwini* (CASENT0218332) **C** *P. dea* (CASENT0227965) **D** *P. glabrella* (CASENT0227950) **E** *P. rebecca* (CASENT0227954) **F** *P. semidea* (CASENT0227960). Scale bars: 0.5 mm.

Identification key to *P. pulchella* group species

Measurements and indices are sometimes crucial for identification, so we have added detailed comparative measurements and indices for each species separated in yellow forms (Table 1 - minors, Table 2 - majors) and dark forms (Table 3 - minors, Table 4 majors).

Minor workers

- 1 Colour yellow to orange.....2
- Colour reddish brown to black5
- 2 Pilosity on scape and metatibia decumbent (Fig. 7C).....*P. pulchella*
- Pilosity on scape and metatibia suberect to erect (Fig. 7A, E, G).....3

- 3 Smaller species (HW: 0.64–0.71) with relatively longer scapes (SI: 182–189)..... ***P. klaman* sp. nov.**
- Larger species (HW: 0.74–0.83) with relatively shorter scapes (SI: 144–174)..... **4**
- 4 Head, scapes and legs very long (CI: 73–75, SI: 163–174, FI: 205–213); occipital carina broadly extended and collar-like; standing hairs acute and very abundant, present also on lower meso- and metapleuron, visible in dorsal view (Fig. 7G, H) ***P. heliosa***
- Head, scape and legs relatively shorter (CI: 79–84, SI: 144–165, FI: 175–197); occipital carina narrow, not collar-like; standing hairs often apically truncated or split, generally less abundant, absent on lower meso- and metapleuron (Fig. 7E, F) ***P. christinae***
- 5 Head in full frontal view laterally with several relatively long, projecting hairs posterior of eye-level (Figs 11A, B, 12D) **6**
- Head in full frontal view laterally completely without or at most with one or two moderately long projecting hairs near eyes or towards posterior margin (Figs 11C, D, 12A, B, C)..... **8**
- 6 Head shape elliptical (CI: 80–89); posterior margin relatively narrow and evenly convex; occipital carina with weak median impression, scape pilosity uniformly suberect or decumbent (Figs 11A, B, 13A, B)..... **7**
- Head shape broadly rounded, posterior margin not evenly convex (CI: 86–90); occipital carina without median impression; scape pilosity decumbent with additional suberect hairs on outer edge (Figs 12D, 13H) ***P. setosa***
- 7 Head relatively narrow (CI: 80–87); scapes long (SI: 153–173); scape pilosity uniformly decumbent; face almost completely and distinctly punctate (Figs 11A, 13A) ***P. batrachorum***
- Head relatively wider (CI: 84–89); scapes slightly shorter (SI: 140–159); scape pilosity uniformly subdecumbent to suberect; face smooth and shiny to very faintly punctate (Fig. 11B, Fig. 13B) ***P. darwini***
- 8 Sculpture variable, but head and mesosoma never completely and coarsely punctate; at least medially between eyes and on posterior dorsopronotum superficially sculptured to smooth and shiny (Fig. 11C, D, Fig. 12B, C, Fig. 14C, D, F, G) **9**
- Head and mesosoma almost completely and coarsely punctate (Fig. 12A, Fig. 14E)..... ***P. nimba***
- 9 Head longer than wide (CI: 85–95), posterior margin roundly or slightly convex; scapes and mandibles moderately long (SI: 123–149, MDI: 71–78) (Fig. 11C, D, Fig. 12C) **10**
- Head almost as wide as long (CI: 94–99), posterior margin not convex, but almost straight (Fig. 12C); scapes and mandibles shorter (SI: 114–121, MDI: 68–73) (Fig. 12B) ***P. rebecca***

- 10 Long or moderately long hairs completely absent on mesosoma and waist segments; petiole and postpetiole without laterally projecting hairs in dorsal view; metatibia pilosity appressed; second mesonotal process and sculpture on propodeum reduced; metanotal groove wide in profile; spines long (PSLI: 30–43) (Fig. 14D) *P. glabella*
- Moderately long hairs at least present on waist segments, sometimes also on promesonotum; on petiole and/or postpetiole some laterally projecting hairs in dorsal view; metatibia pilosity decumbent; second mesonotal process and sculpture on propodeum not reduced; metanotal groove relatively narrow in profile; spines slightly shorter (PSLI: 28–32) (Fig. 14C, G) **11**
- 11 Posterior head margin roundly convex; face and dorsal promesonotum mostly superficially punctate to punctate; second mesonotal process not raised above the level of dorsopropodeum; postpetiole relatively short (PpLI: 155–229) (Fig. 11C, Fig. 14C) *P. dea*
- Posterior head margin weakly convex, with small median impression; face and promesonotum smooth and shiny, with very few superficial punctures; in lateral view second mesonotal process distinctly raised above the level of dorsopropodeum; postpetiole relatively longer (PpLI: 129–145) (Fig. 12G, Fig. 14G) *P. semidea*

Major workers

Majors of *P. christinae*, *P. nimba*, and *P. setosa* are unknown.

- 1 Colour yellow to orange..... **2**
- Colour reddish brown to black **4**
- 2 Antennal scrobe conspicuous; sides of head without laterally projecting hairs in full-face view (Fig. 6A, E) **3**
- Antennal scrobe absent or inconspicuous; head in full-face view with laterally projecting hairs (Fig. 6C) *P. heliosa*
- 3 Smaller species (HW: 1.65–1.75), with more elongated head (CI: 88–93) and relatively longer scapes (SI: 62). Mesonotum to propodeum strongly punctate. Face sculpture in posterior third with faint incomplete longitudinal rugulae at most, posteriorly reduced to weak, superficially reticulate punctures (Fig. 6B)..... *P. klaman* sp. nov.
- Larger species (HW: 2.0–2.28) with broader head (CI: 98–104) and relatively shorter scapes (SI: 51–56). Mesonotum to propodeum weakly punctate. Face sculpture in posterior third longitudinally rugose and weakly to superficially punctate, posteriorly changing to obliquely and weakly rugulose (Fig. 6D)..... *P. pulchella*
- 4 Posterolateral lobes partly smooth and shiny (Fig. 8B, E) **5**
- Posterolateral lobes variably sculptured, never smooth and shiny, from punctate to longitudinally rugulose (Fig. 8A, C, D, F)..... **6**

- 5 Lateropronotum alutaceous to reticulated, sometimes with transverse rugulae (Fig. 9B). Head above the eyes rugulose, central rugulae between the frontal ridges reaching the occipital line, occipital corners alutaceous to smooth (Fig. 8B, Fig. 10B) ***P. darwini***
- Lateropronotum glassy smooth (Fig. 9B). Head above the eyes faintly sculptured to smooth, central rugulae between the frontal ridges failing to reach the occipital line, occipital corners glassy smooth (Fig. 8E, Fig. 10E) ***P. rebecca***
- 6 Scape and metatibia pilosity fine and inconspicuous, mostly fully appressed; long standing hairs absent on promesonotum (Fig. 9D)..... ***P. glabella***
- Scape and metatibia pilosity conspicuous and decumbent; standing hairs often present on promesonotum (Fig. 9A, C, F)7
- 7 Posterolateral lobes of head longitudinally rugose, the rugulae similar to those in the rest of the head, with spaces between rugae weakly to superficially punctate (Fig. 8C) ***P. dea***
- Posterolateral lobes of head punctate, overlain by superficial rugulae (Fig. 8A, F)..... **8**
- 8 Central rugulae on the head running to occipital line, sometimes broken, separated apart with wide spaces between them, some transverse rugulae may appear on the upper third of the head, but without creating a reticulum (Fig. 8F) ***P. semidea***
- Central rugulae on the head not reaching the occipital line, close together and not leaving wide spaces between them and without transverse rugulae of any kind (Fig. 8A) ***P. batrachorum***

Notes and new distribution data for the *Pheidole pulchella* group

Distribution maps per species can be found at Fig. 15, 16.

Pheidole darwini

Republic of the Congo: Env. De Makaba (par Dimonika) (Mayombe) (L. Matile) (1 worker) [EY19812] MNHN.

Pheidole dea

The label for type locality of this species is “Lugombe” with no additional information and Santschi (1921) cites the locality as “Congo Belgue: Lugombe”. The current official type locality is Lugombe (DRC). Congo Belgue comprised several current countries, and Lugombe is a city in Uganda, close to the capital Entebbe, so, we propose to change the type locality from Lugombe (DRC) to Lugombe (Uganda). Our new citation is the first for DRC.

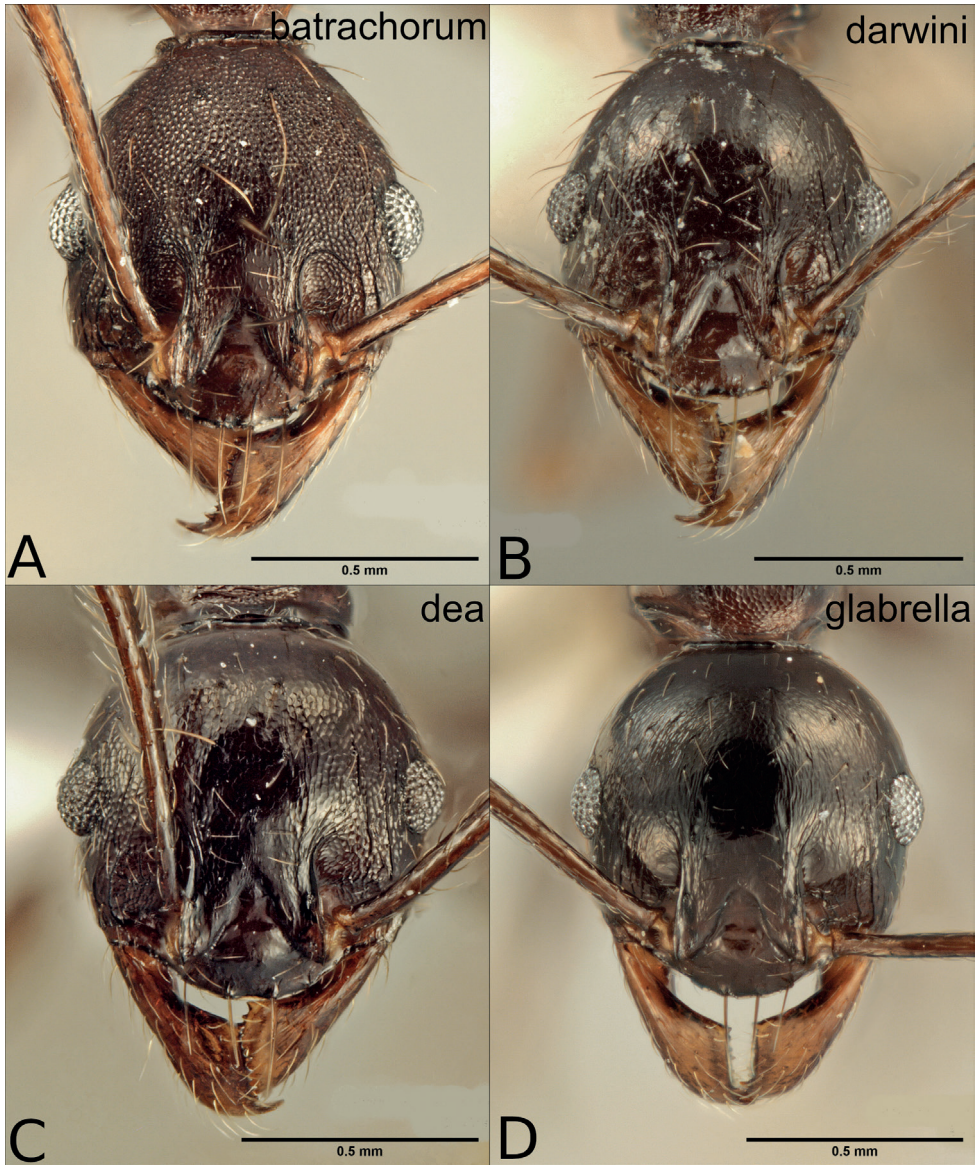


Figure 11. Minor workers of the dark species in the *P. pulchella* group, full frontal view **A** *P. batrachorum* (CASENT0401882) **B** *P. darwini* (CASENT0227962) **C** *P. dea* (CASENT0227964) **D** *P. glabella* (CASENT0227951).

Democratic Republic of Congo: Secteur Nord: Mount Ngulingo, pres Nyamgaleke (Massif Ruwenzori (ex Albert NP)) 2500 m. H. Synave 17-18/08/1953 [RBINS-FOR002196] RBINS

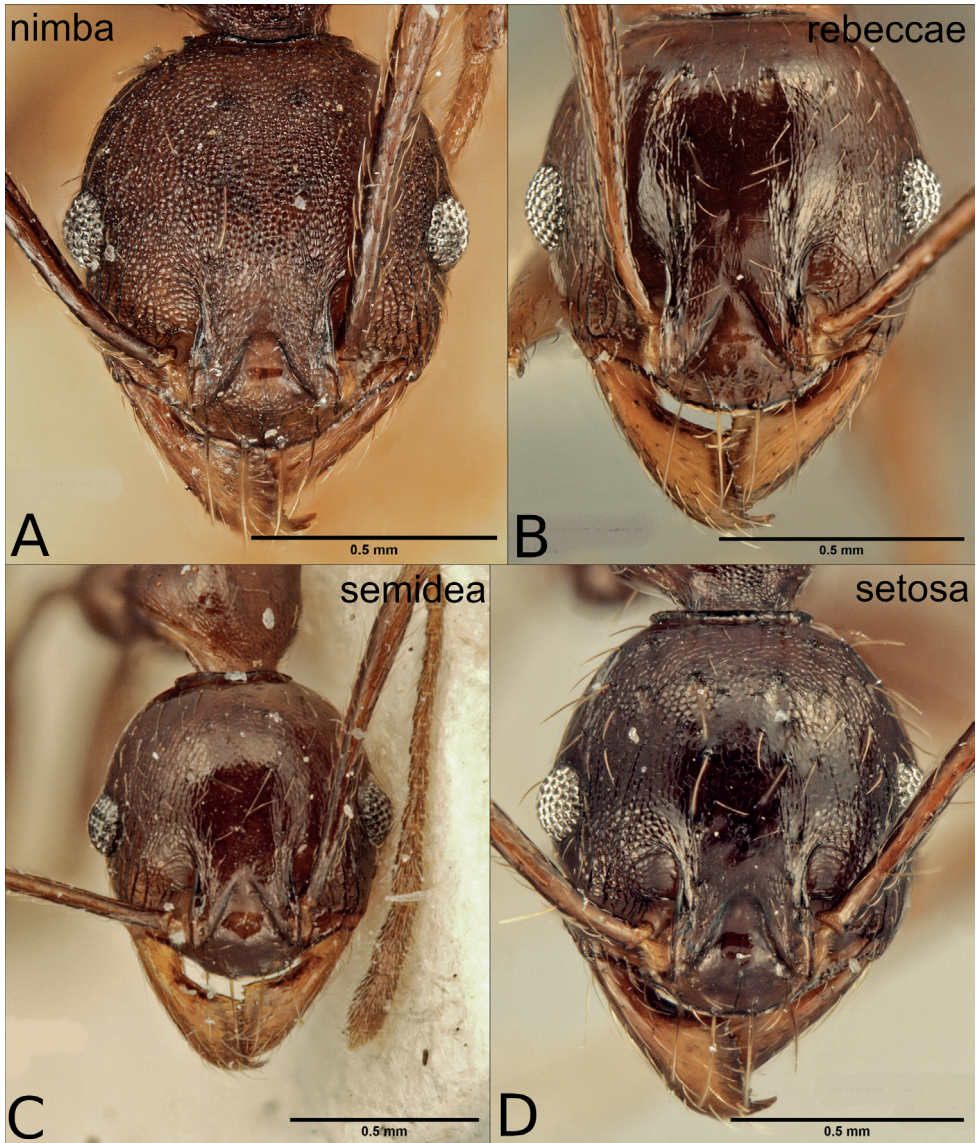


Figure 12. Minor workers of the dark species in the *P. pulchella* group, full frontal view **A** *P. nimba* (CASENT0227967) **B** *P. rebecca* (CASENT0227955) **C** *P. semidea* (CASENT0227960) **D** *P. setosa* (CASENT0218298).

Pheidole glabrella

Previously known from Western Central Africa (Cameroon, Central African Republic, Gabon and the DRC) (Fischer et al. 2012), our findings are first records for the following three countries and expand its distribution from Central to Western Africa:

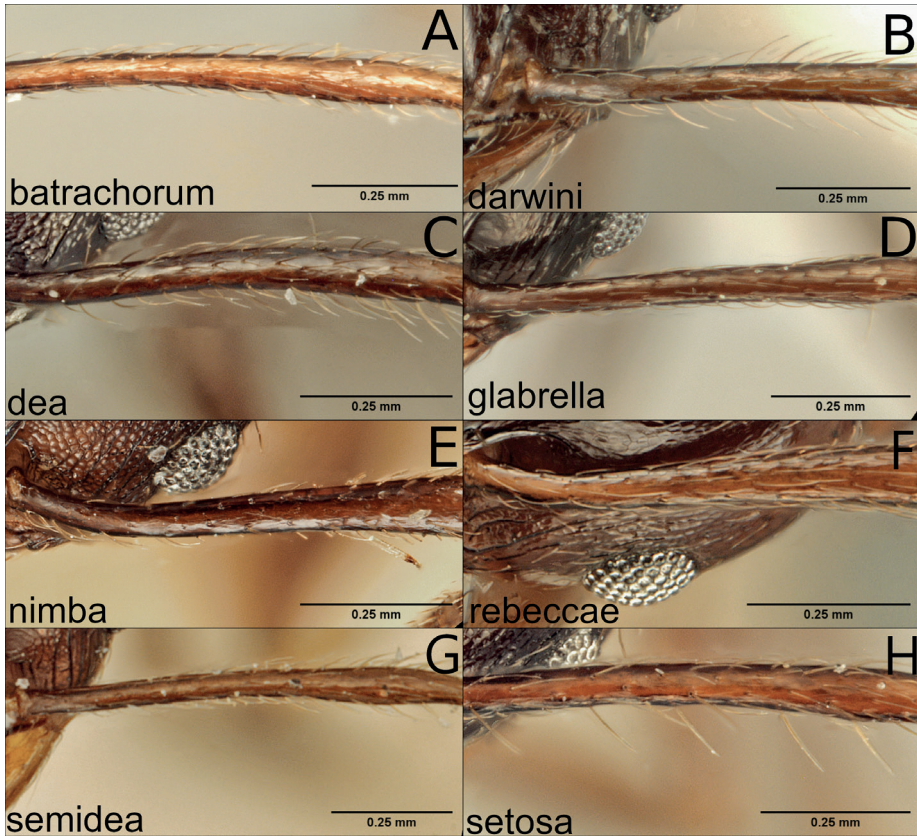


Figure 13. Minor workers of the dark species in the *P. pulchella* group, scapes **A** *P. batrachorum* (CASENT0401882) **B** *P. darwini* (CASENT0227962) **C** *P. dea* (CASENT0227964) **D** *P. glabrella* (CASENT0227951) **E** *P. nimba* (CASENT0227967) **F** *P. rebecca* (CASENT0227955) **G** *P. semidea* (CASENT0227960) **H** *P. setosa* (CASENT0218298).

Ghana: Kumasi, FORIG, near pond, 6.7150, -1.5291, 09/01/2019. Hand collected (Gomez, K.). Fragmented degraded forest (4 workers), ex soil [KG03925C01] KGAC; same data (1 worker), [KGCOL00993] KGAC.

Ivory Coast: Montagnes, Mt. Tonkpi (Man), 1200 m, 7.4542, -7.6372, 23/06–01/07/2018. Malaise (Braet, Y.; Gué, A). Tropical Forest (1 worker) [KGCOL01617] RBINS.

Republic of the Congo: Western Cuvette, Lossi Animal Sanctuary, 0.18, 14.517, 2003. Hand collected (Rodríguez–Teijeiro, J. D.) (2 workers) [KGCOL01013] KGAC.

Pheidole rebecca

Only two series are cited for this species, the type series from Ivory Coast (Abidjan) and a series from the Atewa Forest in Ghana (Fischer et al. 2012). We found it in the

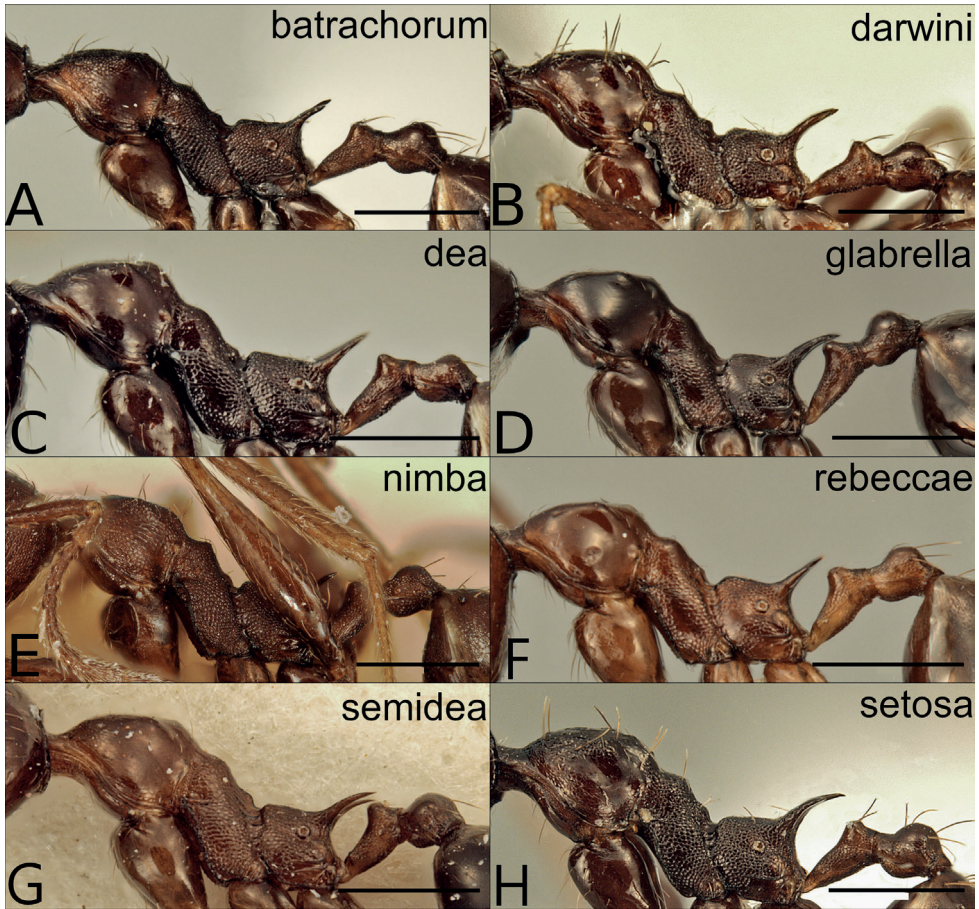


Figure 14. Minor workers of the dark species in the *P. pulchella* group, lateral mesosoma **A** *P. batrachorum* (CASENT0401882) **B** *P. darwini* (CASENT0227962) **C** *P. dea* (CASENT0227964) **D** *P. glabrella* (CASENT0227951) **E** *P. nimba* (CASENT0227967) **F** *P. rebecca* (CASENT0227955) **G** *P. semidea* (CASENT0227960) **H** *P. setosa* (CASENT0218298). Scale bars: 0.5 mm.

Taï Forest National Park in Ivory Coast, where it seems to be abundant, nesting in rotten logs:

Ivory Coast: Montagnes District: Site 02 (Taï N. P.) 200 m, 5.8312, -7.3429 08–10/11/2019. Pitfall (Gómez, K., Kouakou, L.). Primary Forest (2 workers) [KGCOL00346] KGAC; same data, hand collected on tree trunk (1 worker), [KGCOL00725] KGAC; Site 03 (Taï N. P.) 200 m, 5.8389, -7.3452 09/11/2019. Hand collected (Gómez, K., Kouakou, L.). Primary Forest (1 worker, in ethanol), On tree trunk [KG04031C01] KGAC; same data (1 worker, pinned) [KGCOL00287] KGAC; same data, Winkler sample (2 workers, pinned) Primary forest in leaf litter [KGCOL00342] KGAC; Site 05 (Taï N. P.) 200 m, 5.8438, -7.3484 11/11/2019. Winkler sample (Gómez, K., Kouakou, L.). Primary forest in leaf litter (1 worker)

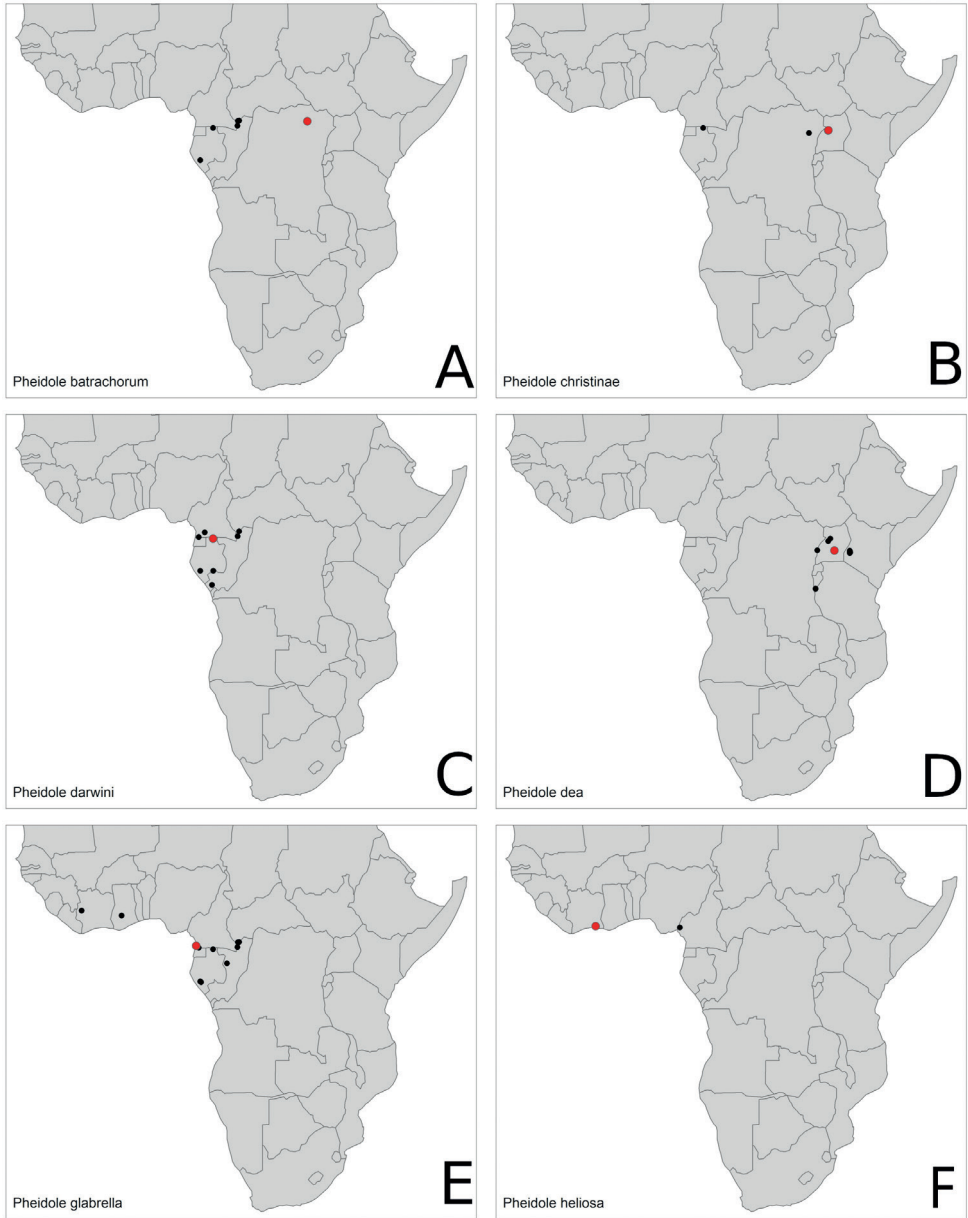


Figure 15. Distribution maps. **A** *P. batrachorum* **B** *P. christinae* **C** *P. darwini* **D** *P. dea* **E** *P. glabrella* **F** *P. heliosa*. Type localities marked in red.

[KGCOL00337] KGAC; Site 06 (Taï N. P.) 200 m, 5.8346, -7.3464 12/11/2019. Hand collected (Gómez, K., Kouakou, L.). Primary Forest (1 dealated queen, 5 majors, > 10w, in ethanol), ex. rotten log [KG04156] KGAC; same series (1 worker, 1 major, pinned), [KGCOL00511] KGAC; Site 09 (Taï N. P.) 200m, 5.8466, -7.3469

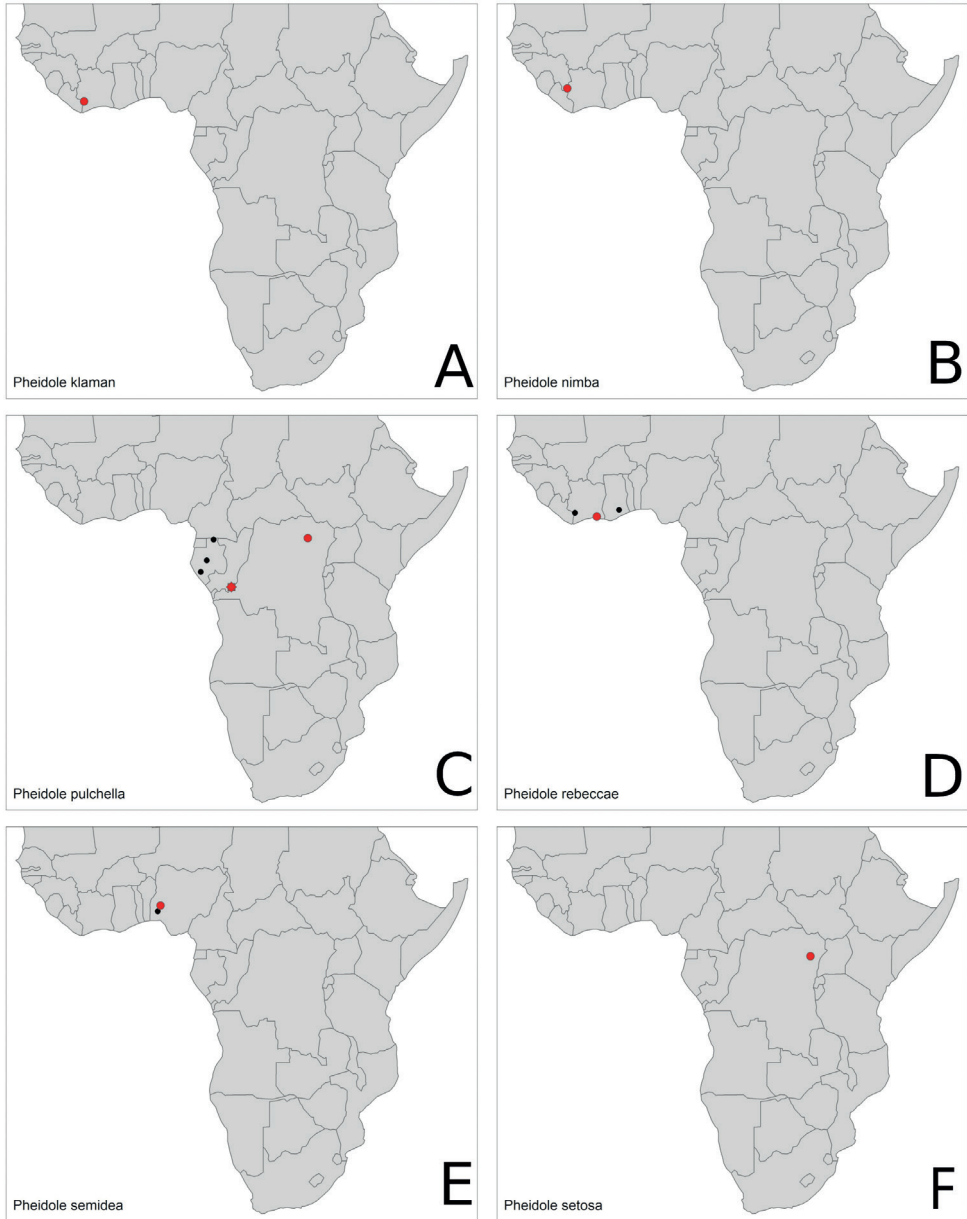


Figure 16. Distribution maps. **A** *P. klaman* **B** *P. nimba* **C** *P. pulchella* **D** *P. rebecca* **E** *P. semidea* **F** *P. setosa*. Type localities marked in red.

15/11/2019. Hand collected (Gómez, K., Kouakou, L.). Primary Forest (1 major, > 10 workers, in ethanol), ex. rotten log [KG04165] KGAC; same series (1 major, 1 worker, pinned) [KGCOL00330] KGAC.

Acknowledgements

Our special thanks to Dr. Soro Kafana, Head of Ecology Research Station of Taï and Prof. Yeo Kolo, Head of Ecology Research Station of Lamto, who helped us through the process of preparing and executing the sampling in Taï Forest. We are also profoundly grateful to our guides in the Taï Forest (Oulaï Laurent and Guei Emmanuel) for their dedication and hard work during the long hours in the forest. Their knowledge of the forest was always a source of amazement.

We thank the Okinawa Institute of Science and Technology Graduate University (OIST) Imaging Section for providing access to the Zeiss Xradia micro-CT scanner and Shinya Komoto for general support. This work was supported by Japan Society for the Promotion of Science (JSPS) grants-in-aid KAKENHI grants [No. 17K15180 to EPE; No. 18K14768 & 21K06326 to FHG].

References

- AntWeb (2022) Version 8.75.4. California Academy of Science. [online at] <https://www.antweb.org> [Accessed 26 May 2022]
- Bolton B (1994) Identification guide to the ant genera of the world. Harvard University Press, Cambridge, 222 pp.
- Fischer G, Hita Garcia F, Peters MK (2012) Taxonomy of the ant genus *Pheidole* Westwood in the Afrotropical zoogeographic region: Definition of species groups and systematic revision of the *Pheidole pulchella* group. *Zootaxa* 3232: 1–43. <https://doi.org/10.11646/zootaxa.3232.1.1>
- Salata S, Fisher BL (2020a) *Pheidole* Westwood, 1839 (Hymenoptera, Formicidae) of Madagascar – an introduction and a taxonomic revision of eleven species groups. *ZooKeys* 905: 1–235. <https://doi.org/10.3897/zookeys.905.39592>
- Salata S, Fisher BL (2020b) Taxonomic revision of the *Pheidole sikorae* species group (Hymenoptera, Formicidae) from Madagascar. *ZooKeys* 949: 1–185. <https://doi.org/10.3897/zookeys.949.51269>
- Salata S, Fisher BL (2021) Taxonomic revision of Madagascan species of the *Pheidole fervens* species-group (Hymenoptera, Formicidae). *PLoS ONE* 16(1): e0244195. <https://doi.org/10.1371/journal.pone.0244195>
- Santschi F (1921) Quelques nouveaux Formicides africains. *Annales de la Société Entomologique de Belgique* 61: 113–122.
- World Heritage (2022) World Heritage. <http://world-heritage-datasheets.unep-wcmc.org/datasheet/output/site/tai-national-park/> [accessed on March 2022]

Supplementary material 1

Video 1

Authors: Kiko Gómez, Lombart M. Kouakou, Georg Fischer, Francisco Hita-Garcia, Julian Katzke, Evan P. Economo

Data type: Video file

Explanation note: 3D rotation video of *Pheidole klaman* sp. nov. holotype major worker (CASENT0764691) based on shaded volumetric surface rendering of full body.

Copyright notice: This dataset is made available under the Open Database License (<http://opendatacommons.org/licenses/odbl/1.0/>). The Open Database License (ODbL) is a license agreement intended to allow users to freely share, modify, and use this Dataset while maintaining this same freedom for others, provided that the original source and author(s) are credited.

Link: <https://doi.org/10.3897/zookeys.1104.81562.suppl1>

Supplementary material 2

Video 2

Authors: Kiko Gómez, Lombart M. Kouakou, Georg Fischer, Francisco Hita-Garcia, Julian Katzke, Evan P. Economo

Data type: Video file

Explanation note: 3D rotation video of *Pheidole klaman* sp. nov. paratype minor worker (CASENT0764692) based on shaded volumetric surface rendering of full body.

Copyright notice: This dataset is made available under the Open Database License (<http://opendatacommons.org/licenses/odbl/1.0/>). The Open Database License (ODbL) is a license agreement intended to allow users to freely share, modify, and use this Dataset while maintaining this same freedom for others, provided that the original source and author(s) are credited.

Link: <https://doi.org/10.3897/zookeys.1104.81562.suppl2>

Supplementary material 3

Video 3

Authors: Kiko Gómez, Lombart M. Kouakou, Georg Fischer, Francisco Hita-Garcia, Julian Katzke, Evan P. Economo

Data type: Video file

Explanation note: 3D rotation video of *Pheidole klaman* sp. nov. paratype minor worker (CASENT0745509) based on shaded volumetric surface rendering of full body.

Copyright notice: This dataset is made available under the Open Database License (<http://opendatacommons.org/licenses/odbl/1.0/>). The Open Database License (ODbL) is a license agreement intended to allow users to freely share, modify, and use this Dataset while maintaining this same freedom for others, provided that the original source and author(s) are credited.

Link: <https://doi.org/10.3897/zookeys.1104.81562.suppl3>

A new species of *Chryxus* Champion, with taxonomic notes on other species of the genus (Hemiptera, Heteroptera, Reduviidae, Chryxinae)

Hélcio R. Gil-Santana¹, John M. Leavengood Jr², Jean-Michel Bérenger^{3,4},
David dos Santos Martins⁵, Jader Oliveira^{6,7}

1 Laboratório de Diptera, Instituto Oswaldo Cruz, Av. Brasil, 4365, 21040-360, Rio de Janeiro, RJ, Brazil
2 United States Department of Agriculture, APHIS, PPQ, 9325 Blay Plaza Blvd, Suite 206, Tampa FL 33619, USA
3 IRD, AP-HM, SSA, Vitrome, IHU Méditerranée Infection, Aix-Marseille Université, Marseille, France
4 Laboratoire d'Entomologie du Muséum National d'Histoire Naturelle, Paris, France
5 Instituto Capixaba de Pesquisa, Assistência Técnica e Extensão Rural, Vitória, ES, Brazil
6 Universidade de São Paulo, Faculdade de Saúde Pública, Laboratório de Entomologia em Saúde Pública, São Paulo, SP, Brazil
7 Laboratório de Parasitologia, Universidade Estadual Paulista "Júlio de Mesquita Filho", Faculdade de Ciências Farmacêuticas UNESP/FCFAR, Rodovia Araraquara Jaú, KM 1, 14801-902, Araraquara, SP, Brazil

Corresponding author: Hélcio R. Gil-Santana (helciogil@uol.com.br; helciogil@ioc.fiocruz.br)

Academic editor: Nikolay Simov | Received 15 December 2021 | Accepted 9 March 2022 | Published 14 June 2022

<http://zoobank.org/402A211F-60D6-4C6A-BFCA-EDBD2962E9AD>

Citation: Gil-Santana HR, Leavengood Jr JM, Bérenger J-M, Martins DS, Oliveira J (2022) A new species of *Chryxus* Champion, with taxonomic notes on other species of the genus (Hemiptera, Heteroptera, Reduviidae, Chryxinae). ZooKeys 1104: 159–175. <https://doi.org/10.3897/zookeys.1104.79411>

Abstract

Chryxus garcetebarretti **sp. nov.** from Paraguay is described, taxonomical notes on *C. bahianus* Gil-Santana, Costa & Marques, 2007 and *C. tomentosus* Champion, 1899 are provided; the latter species is recorded from French Guiana for the first time; a redescription of the genus *Chryxus* Champion, 1899 and an updated key for the genera and species of Chryxinae are presented.

Keywords

Assassin bugs, female and male genitalia, Guyana, Panama

Introduction

Chryxinae currently includes four genera and five species of rarely collected reduviids (Lent and Wygodzinsky 1944; Weirauch 2012; Gil-Santana et al. 2015). Gil-Santana et al. (2007, 2015) summarized the taxonomic history of the group and the scant data available on the biology of this subfamily. Chryxinae can be separated from other Reduviidae by their medium or small size (3–9 mm); the head wide and anteriorly strongly curved downwards; the short, stout and strongly curved labium; and the membrane of hemelytron with only one large cell (Gil-Santana et al. 2007; Weirauch 2012; Weirauch et al. 2014).

The rarity of specimens has made the study of generic limits within the subfamily difficult, posing doubts on the validity of *Wygodzinskyella* Usinger, 1952, for example (Forero 2004; Weirauch 2012).

In the present paper, *Chryxus garcetabarretti* sp. nov. from Paraguay is described, *Chryxus* Champion, 1899 is redescribed, taxonomical notes on *C. bahianus* Gil-Santana, Costa & Marques, 2007 and *C. tomentosus* Champion, 1899 are provided, and an updated key for the genera and species of Chryxinae is presented.

Materials and methods

Photographs of the male holotype of *Chryxus bahianus* (Figs 2–4) were kindly provided by the team of the digitization project of the Entomological Collection of MNRJ (“Projeto Informatização da Coleção Entomológica do Museu Nacional/UFRJ, SIB-BR/CNPq proc. 405588/2015–1”), taken before the fire which destroyed the collection of MNRJ, including this holotype, in 2018 (Escobar 2018). Additional images of the male genitalia of the holotype (Figs 5–9), already dissected previously, were directly produced by the first author (HRG-S).

Photographs of a non-type female specimen of *Chryxus bahianus* (Figs 10, 11) were taken by João Paulo Sales Oliveira Correia (“Laboratório Nacional e Internacional de Referência em Taxonomia de Triatomíneos” (LNIRTT), Instituto Oswaldo Cruz (IOC), Rio de Janeiro, Brazil), with a Leica DMC 2900 camera attached to a Leica M205C stereomicroscope. Several images were stacked using the LAs software version 4.9.

Photographs of *Chryxus garcetabarretti* sp. nov. (Figs 13–28) were taken by the second author (JMLJr.) using a Nikon Digital Sight DS-Fi2 imaging system mounted on a Nikon SMZ-18 stereomicroscope. Photograph layers were stacked using Helicon Focus 6, and composite photographs were edited using Adobe Photoshop 2020. Morphology was measured using a digital Vernier caliper.

Photographs of *Chryxus tomentosus* (Figs 29–31) were taken by the third author (J-MB) using a Canon EOS 5D Mark II digital camera with a Laowa 25 mm ultra-macro lens. Several images were stacked using software combine ZP 1.0. S. A scanning electron microscopy image (Fig. 32) of female genitalia was obtained by the third author (J-MB) using a TM 4000 Plus Hitachi tabletop microscope.

The holotype of *Chryxus garcetebaretta* sp. nov. (Figs 13–28) is deposited at the Florida State Collection of Arthropods (FSCA; Gainesville, Florida, USA). The non-type female specimen of *Chryxus bahianus* (Figs 10–12) will be deposited in the Collection of National Museum of the Federal University of Rio de Janeiro, Rio de Janeiro, Brazil (MNRJ).

The 17 female specimens of *Chryxus tomentosus* examined are deposited in the third author's private collection (J-MB), in France. They were collected by the Société Entomologique Antilles-Guyane (SEAG) during a study on a protected area of French Guyana. The specimens were among some important material caught using interception traps (similar to those described by Lamarre et al. 2012).

General morphological terminology mainly follows general current works on Reduviidae (e.g., Schuh and Weirauch 2020) and Chryxinae (Gil-Santana et al. 2007; Weirauch 2012).

Diagnoses of *Chryxus* and its species were not given because their characteristics are the same as described in the key presented below.

When describing label data, a slash (/) separates the lines and a double slash (//) the different labels.

Results

Taxonomy

Chryxinae Champion, 1899

Chryxus Champion, 1899

Note. Based on two males from Panama, Champion (1899) created *Chryxus* to include a new species, *C. tomentosus*. Because *Chryxus travassosi* Lent & Wygodzinsky, 1944 was transferred to *Wygodzinskyella* by Usinger (1952), *Chryxus* was composed only of its type species and *C. bahianus* Gil-Santana, Costa & Marques, 2007 (Gil-Santana et al. 2007).

Redescription. Total length 3.6–5.2 mm. Integument generally shiny and covered by numerous long and thin setae; membranes of hemelytra glabrous. **Head** wider than long, strongly curved anteriorly; interocular distance in dorsal view about twice the width of an eye; transverse sulcus shallow; a short anterior sulcus arising from middle of transverse sulcus, even shallower; eyes setose, coarsely faceted, widely separated from each other, globose, subhemispherical in dorsal view; clypeus moderately elevated; antennifers small, close to eyes; first two antennal segments stout; scape slightly curved, thicker (except its thinner base) and shorter than other antennal segments; remaining segments progressively thinner, generally covered by long, thin, numerous setae; on scape sparser and shorter. Labium short, stout, very curved; first two visible segments subcylindrical, subequal in length; the last segment shorter, tapering. Gena ventrally

projecting in a short process. Neck well separated from head, relatively thin and short. **Thorax.** Pronotum: anterior collar narrow, clearly marked, lateral angles slightly or largely prominent; fore lobe subrectangular, hind lobe trapezoidal, both separated by a well-defined transverse sulcus; fore lobe shorter and narrower than hind lobe, convexly raised at disc; a median sulcus running from approximately distal portion or distal margin of fore lobe to about distal two-thirds of hind lobe; humeral angles rounded. Scutellum: basal portion with oblique ridges or wrinkled on central portion; lateral margins elevated, running towards distal process; distal process elongated, variably thickened, and obliquely elevated or not elevated at its apex. Supracoxal lobes of propleura somewhat prominent, those of meso- and metapleura progressively less or not prominent. Legs: fore coxae close to each other, separated by a distance shorter than or subequal to width of fore coxa; middle and hind coxae separated by a distance subequal to or larger than the width of respective coxae. Femora variably thickened; fore tibiae thickened towards apex, with a pad at apex; middle and hind tibiae cylindrical, straight or somewhat curved; tarsi three-segmented. Hemelytra ending short or slightly surpassing posterior margin of abdomen; membrane of hemelytron with only one central cell. **Abdomen** oval; connexivum moderately narrow. Sternite II finely canaliculated in both sides of middle of posterior margin.

Distribution. Brazil, French Guiana (new record), Guyana, Panama, Paraguay (new record).

Chryxus bahianus Gil-Santana, Costa & Marques, 2007

Figs 1–12

Note. *Chryxus bahianus* was described based on a single male from the State of Bahia, northeastern Brazil. Unfortunately, the holotype of *C. bahianus* was destroyed on the 2nd of September 2018, during the fire which destroyed most of the zoological collections, including the entire Heteroptera collection of the MNRJ (Escobar 2018). However, images taken before the fire (Figs 2–4) in addition to the drawings presented in the original publication (Gil-Santana et al. 2007), are useful in providing a better knowledge of the holotype. Additionally, a female (Figs 10–12) from the State of Espírito Santo, a neighbouring state of Bahia, was included to this study.

Type material examined. *Chryxus bahianus*, male holotype, **BRAZIL:** Bahia: [handwritten labels]: *Chryxus / bahianus /* Gil-Santana et al // *Chryxus / bahianus /* Gil-Santana et. [sic] al. // [printed labels]: QR CODE / MNRJ-ENT3-1056 // BARRO PRETO - BA / BRASIL - xii. 2004 / O. M. Marques leg. [printed red label bordered with black lines]: HOLOTIPO [= holotype] (previously deposited in MNRJ, now destroyed).

Additional non-type material. *Chryxus bahianus*, female, **BRAZIL:** Espírito Santo: Linhares, Reserva Natural Vale, 19°06'S, 39°45'W, 17.iii.1989, J. S. dos Santos leg., Gil-Santana det. (MNRJ).

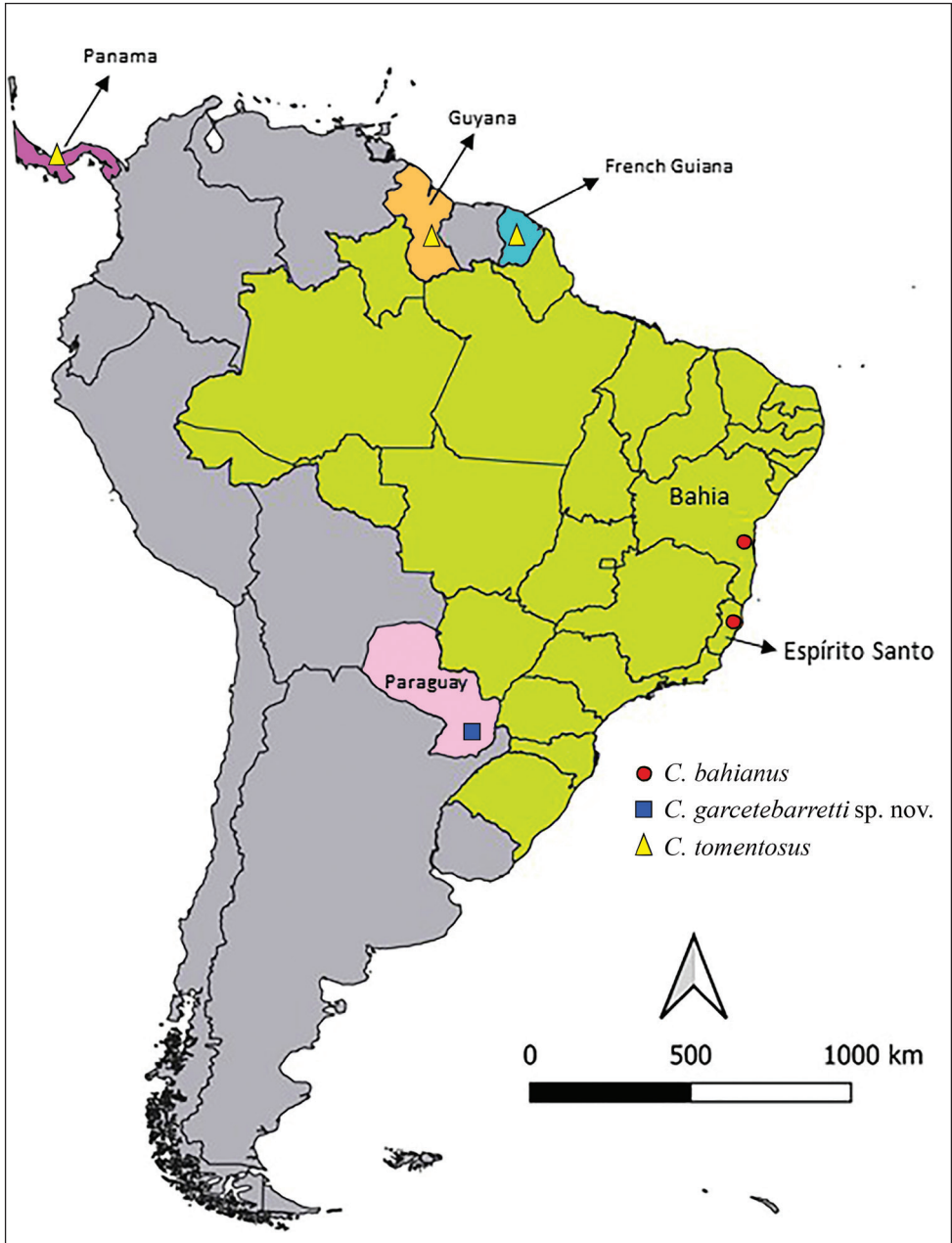
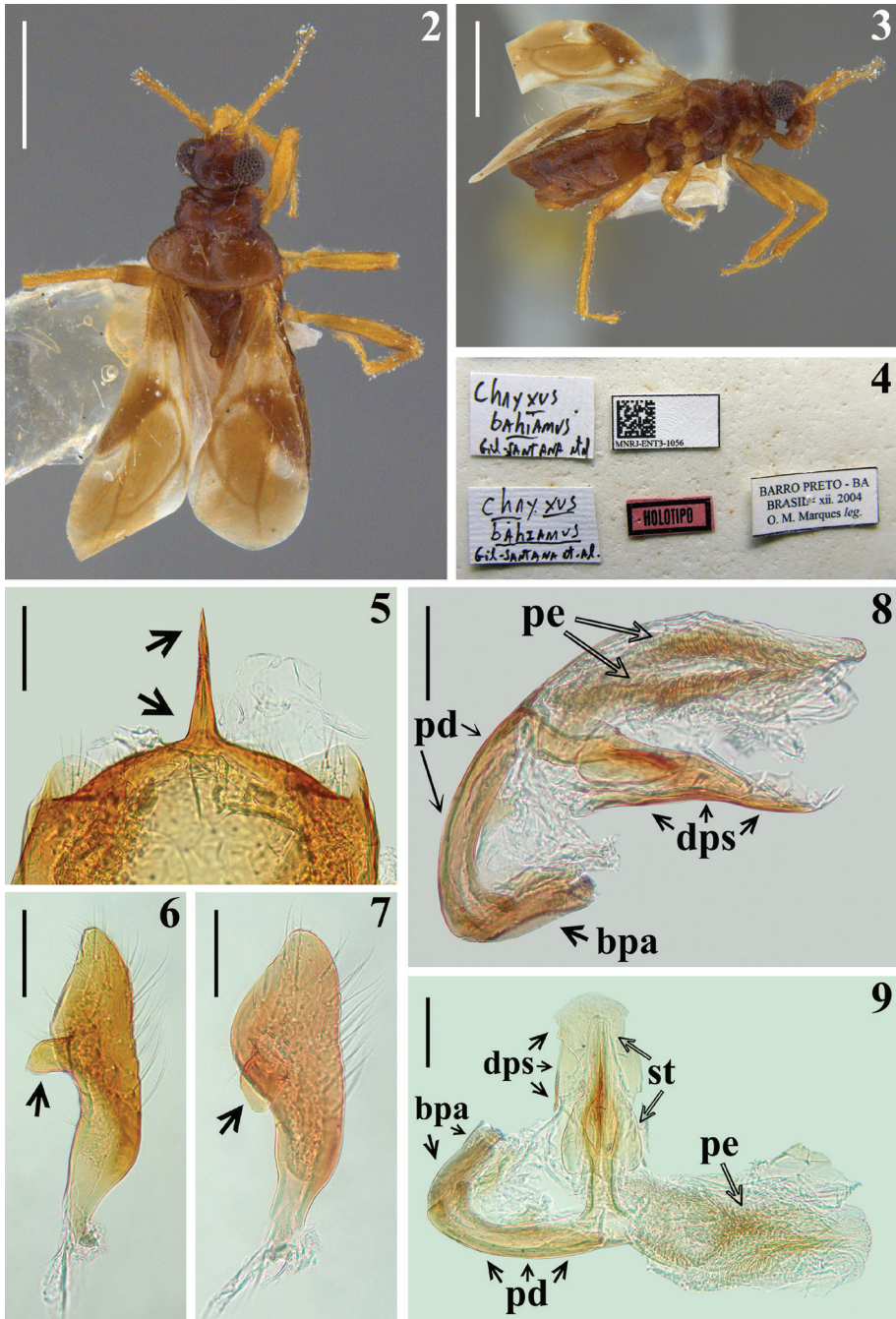


Figure 1. A general map of South America and a small portion of Central America (Panama, purple color) showing occurrence points of species of *Chryxus*: *C. bahianus* (red circles) in the States of Bahia and Espírito Santo of Brazil (pale green color); *C. garcetebarretti* sp. nov. (blue square) in Paraguay (pink color), and *C. tomentosus* (yellow triangles) in French Guiana (blue color), Guyana (orange) (marked randomly in the middle of the country; exactly location not recorded), and Panama (purple).

Morphological remarks. Holotype male. Measurements (mm): total length to tip of hemelytra: 3.6; pronotum length: 0.7; hind lobe maximum width: 1.1; abdomen maximum width: 1.2. **Coloration** (Figs 2, 3): **head** blackish; brownish on clypeus and adjacent portions; second and third visible labial segments pale brownish and dark yellowish, respectively. Scape and pedicel pale brownish; flagellomeres darkened. Neck reddish brown. **Thorax** blackish brown; fore coxae pale brownish; supracoxal lobes and approximately distal two thirds of middle and hind coxae dark yellowish; trochanters pale; remaining portions of legs pale brownish; femora with faint dark narrow rings on subbasal and subapical positions. Hemelytra: clavus dark brownish; corium whitish, with a subbasal dark spot and dark at approximately apical half; membrane pale brownish with two whitish markings, a basolateral spot just after apex of corium and a whitish stripe adjacent to inner margin, contiguous with whitish portion of corium, going from basal portion, shortly invading discal cell, narrowing at midportion, and enlarged at inferodistal portion; veins darkened. **Abdomen.** Connexivum with approximately distal third of segments III–VI darkened. Sternites reddish brown, darkened on lateral portions. **Vestiture** formed by golden long setae, sparse on head and thorax and somewhat more numerous on sternites (Figs 2, 3). Longer curved setae on clypeus and adjacent portion; lateral angles of pronotal collar with a single conspicuous, long, somewhat curved seta inserted in a small elevation. **Structure** (Figs 2, 3). Integument shiny, except dull hemelytra. Pronotum: integument generally smooth; lateral angles slightly prominent; a series of canaliculae behind anterior collar, larger at median portion; median sulcus running from just before transverse furrow to about posterior third of pronotum, larger at basal portion, where it is canaliculated, narrowing towards distal portion; transverse furrow enlarged, formed by canaliculae. Scutellum obliquely elevated and enlarged at its apex. Femora slightly thickened, fore femora a little more thickened than others; hind tibiae straight; hemelytra slightly surpassing posterior margin of abdomen. Connexival segments II–V with posterolateral acute prominences, which are progressively smaller towards distal segments. Sternite II with a shallow keel, on basal portion.

Male genitalia (Figs 5–9). Pygophore covered by numerous setae on exposed portion, in ventral view suboval to subsquare in shape, in lateral view dorsal margin almost straight and ventral margin rounded; medial process of pygophore thin, long, straight, spiniform in anterior and posterior views (Fig. 5), and moderately curved and more thickened in lateral view; parameres symmetrical, generally covered with moderately curved, thin, short to elongate setae (except glabrous basal (inserted) portion), enlarged at approximately middle third, on its inner face medially with a subquadrate laminar process with curved distal margin (Figs 6, 7). Phallus (Figs 8, 9): articulatory apparatus with short basal plate arms (bpa); pedicel (pd) elongated, curved in lateral view. Dorsal phallosclerite (dps) faintly sclerotized, subrectangular; struts (st) fused to each other, quite enlarged at middle portion, narrowed towards distal third. Process of endosoma (pe) formed by a paired subparallel series of faintly sclerotized thickenings.

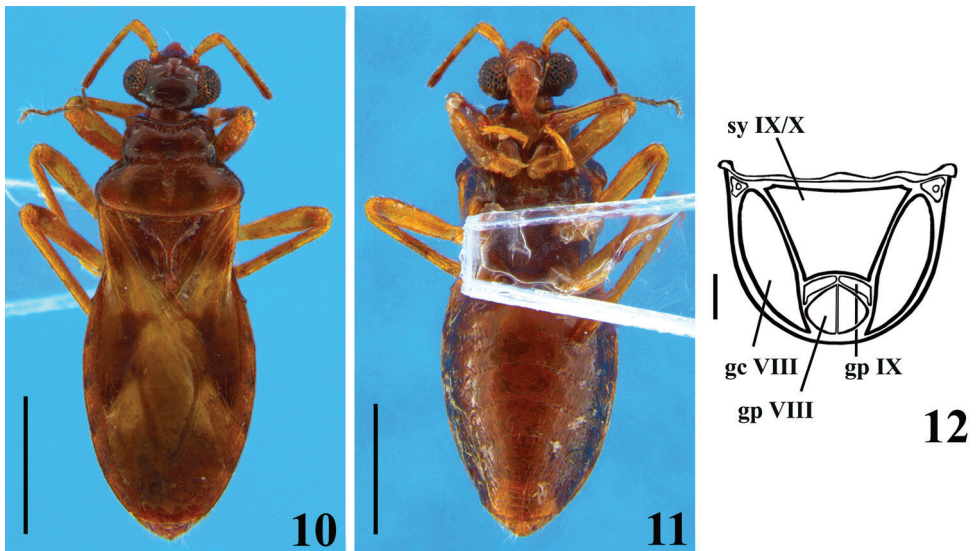
Female. Measurements (mm): total length to tip of abdomen: 3.7, to tip of hemelytra: 3.5; head length (excluding neck): 0.5; length of anteocular portion: 0.15; length of postocular portion: 0.05; width across eyes: 0.7; interocular distance (synthlipsis): 0.4, width of eye: 0.15; length of eye: 0.3; lengths of antennal segments: I: 0.2; II: 0.6;



Figures 2–9. *Chryxus bahianus* Gil-Santana, Costa & Marques, 2007, male holotype, previously deposited in MNRJ **2** dorsal view **3** lateral view **4** labels **5–9** male genitalia **5** apex of pygophore and medial process of pygophore (pointed by arrows), posterior view **6, 7** paramere; laminar process pointed by an arrow **6** lateral view **7** inner surface **8, 9** phallus **8** lateral view **9** with endosoma and dorsal phallosclerite set apart. Abbreviations: **bpa** basal plate arm, **dps** dorsal phallosclerite, **pd** pedicel, **pe** process of endosoma, **st** struts. Scale bars: 1.0 mm (**2, 3**); 0.1 mm (**5–9**).

III: 0.4; IV: 0.3; lengths of labial segments: first visible: 0.17; second visible: 0.15; third visible: 0.17. Thorax: pronotum: fore lobe length (at midline): 0.3, (sublaterally, where it is maximum): 0.32; maximum width: 0.7; hind lobe: length: 0.4; maximum width: 1.1; scutellum, total length: 0.55; width at base: 0.6; length of hemelytra: 2.4. Fore legs: length of femur: 0.7; length of tibia: 0.7; length of spongy fossa: 0.15; length of tarsus (claws excluded): 0.35; middle legs, length of femur: 0.7; length of tibia: 0.8; length of tarsus (claws excluded): 0.3; hind legs: length of femur: 1.0; length of tibia: 1.2; tarsus absent. Abdomen, length: 1.9; maximum width: 1.3. Generally similar to male (Figs 10, 11). Setae generally less numerous and shorter. **Head:** second and third visible labial segments brownish and pale brownish, respectively. **Thorax:** median portion of pronotum somewhat paler; supracoxal lobes pale brownish; pleural and sternal integument generally darker, blackish; coxae dark brownish; subbasal dark ring on hind femora indistinct; fore femora slightly more thickened. Hemelytra not attaining posterior margin of abdomen (Fig. 10); veins generally darkened, except whitish inner vein of corium meeting upper portion of discal cell and respective vein enclosing pale portion of discal cell (Fig. 10). **Abdomen:** intersegmental sutures between sternites very curved at median portion (Fig. 11). Sternite VII quite larger than preceding segments, somewhat more than twice longer at midline than sternite VI (Fig. 11). **Female genitalia.** Posterior view (Fig. 12): light brownish, gonapophysis IX somewhat paler. Syntergite IX/X large, horizontal, as inverted subtrapezoidal; gonocoxa VIII elongate, moderately curved; gonapophysis VIII subrounded; gonapophysis IX arciform.

Distribution (Fig. 1). Brazil, states of Bahia and Espírito Santo.



Figures 10–12. *Chryxus bahianus* Gil-Santana, Costa & Marques, 2007, female specimen from Espírito Santo State, Brazil **10** dorsal view **11** ventral view **12** external genitalia, posterior view, schematic drawing, setation omitted. Abbreviations: **sy IX/X** syntergite IX/X, **gc VIII** gonocoxa VIII, **gp VIII** gonapophysis VIII, **gp IX** gonapophysis IX. Scale bars: 1.0 mm (**10**, **11**); 0.1 mm (**12**).

***Chryxus garcetabarretti* sp. nov.**

<http://zoobank.org/AF7D5827-7DA7-415E-8DC6-B2A7E1ECB4C7>

Figs 1, 13–28

Type material examined. *Chryxus garcetabarretti* sp. nov., female holotype: PARAGUAY: Misiones Dept.: San Ignacio, vic. Hotel Rural, 26°52.508'S, 56°59.355'W, 1.479 m.a.s.l., 5–8.xii.2019, Eger, Tyson & Leavengood leg. (FSCA).

Description. Holotype female. Measurements: total length to tip of abdomen: 4.23; to tip of hemelytra: 4.04; head (excluding neck) length: 0.33; length of anteocular portion: 0.06; length of postocular portion: 0.07; width across eyes: 0.87; interocular distance (synthlipsis): 0.52; width of eye: 0.19; length of eye: 0.30; lengths of antennal segments: I: 0.36; II: 0.76; III: 0.61; IV: 0.67; lengths of labial segments: first visible: 0.29; second visible: 0.23; third visible: 0.09. Thorax: pronotum: fore lobe, length (at midline): 0.33, (sublaterally, where it is maximum): 0.39; maximum width: 0.93; hind lobe: length: 0.54; maximum width: 1.39; scutellum, total length: 0.72; width at base: 0.83; length of hemelytra: 2.88. Fore legs: length of femur: 0.98; length of tibia: 0.77; length of spongy fossa: 0.17; length of tarsus (claws excluded): 0.29; middle legs, length of femur: 1.08; length of tibia: 0.95; length of tarsus (claws excluded): 0.34; hind legs: length of femur: 1.22; length of tibia: 1.47; length of tarsus (claws excluded): 0.36. Abdomen, length: 2.34; maximum width: 1.74. **Coloration** (Figs 13–27): **head** blackish; labium brownish; scape and pedicel pale brownish, apical portion of pedicel darkened; flagellomeres darkened, basal portion of basiflagellomere paler. **Thorax** blackish; posterior margin of pronotum slightly paler; sclerite below basoposterior margins of scutellum reddish brown; meso- and metasterna blackish brown; coxae brown and pale on basal and distal halves respectively; trochanters pale orange to pale yellowish; legs brownish, femora pale at basal portion and largely dark to blackish at median portion; tarsi pale yellowish. Hemelytra: corium mostly blackish, basal third yellowish and whitish on anterior and posterior halves, respectively; membrane dark brownish, veins concolorous; two faint pale rounded spots just around discal cell, one basolateral just after apex of corium and another inferomedial, adjacent to inner margin. **Abdomen.** Connexivum dark brownish with narrow pale distal yellowish bands, which include the respective intersegmental suture; pale band between segments III and IV extending on basal portion of the latter too. Sternites blackish at lateral portion and reddish brown at median portion. **Vestiture.** Conspicuous lateral clusters of setae at each connexival intersegmental suture, ventrally; the most dense of which between segments VI and VII (Figs 14, 26, 27). **Structure** (Figs 13–27). Pronotum: integument generally smooth; lateral angles slightly prominent; median sulcus narrow, margins tortuous, running from transverse furrow to near posterior margin; transverse furrow narrow. Process of scutellum with a narrow sulcus between elevated margins; apex not elevated and slightly thickened. Hind tibiae slightly curved at distal third. Connexivum with a continuous uniform margin. Intersegmental sutures between sternites very curved at median portion. Sternite VII quite larger than preceding segments, somewhat more than four times at midline than sternite VI. **Female genitalia.** Posterior

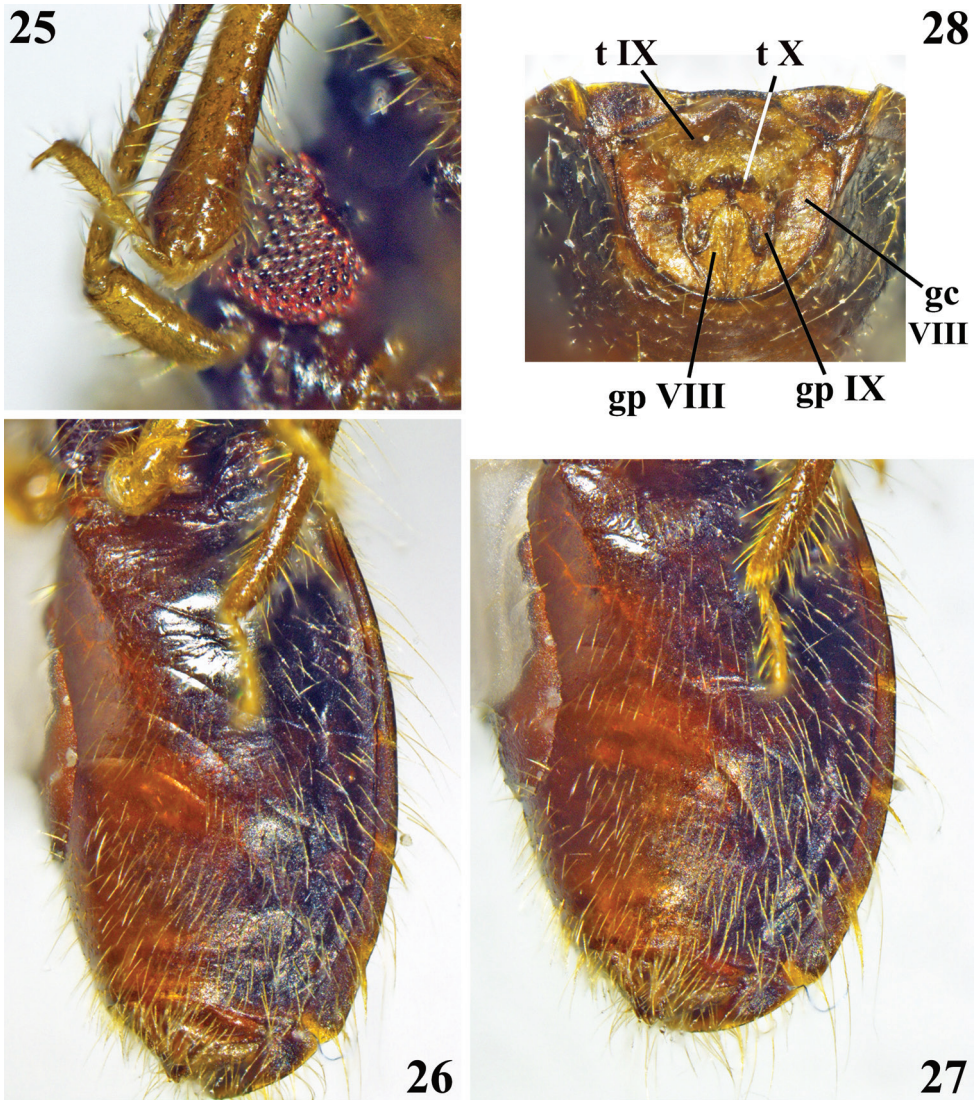


Figures 13–18. *Chryxus garcetebarretti* sp. nov., female holotype **13** dorsal view **14** ventral view **15** lateral view **16** head, pronotum and basal portion of scutellum, dorsal view **17, 18** head and fore lobe of pronotum **17** dorsolateral view **18** frontal view.

view (Fig. 28): pale brownish with scattered darker portions. Tergite IX large, horizontal; tergite X small, surrounded by tergite IX, except posterior margin; gonocoxa VIII elongate, moderately curved; gonapophysis VIII pointed laterally at median portion; gonapophysis IX claviform.



Figures 19–24. *Chryxus garcetebarretti* sp. nov., female holotype **19, 20** head and fore lobe of pronotum **19** dorsolateral view **20** dorsoposterior view **21** head and foreleg, lateral view **22** head and fore coxae, ventral view **23** hind lobe of pronotum, scutellum and basal portion of hemelytra, dorsal view **24** apex of fore tibia, tarsus and a portion of an eye and antennal scape.



Figures 25–28. *Chryxus garcetabarretti* sp. nov., female holotype **25** apex of fore tibia and scape, lateral view **26, 27** abdomen, ventrolateral view **28** external genitalia, posterior view. Abbreviations: **t IX** tergite IX, **t X** tergite X, **gc VIII** gonocoxa VIII, **gp VIII** gonapophysis VIII, **gp IX** gonapophysis IX.

Distribution (Fig. 1). Paraguay, department of Misiones.

Etymology. The new species is named in honor of Dr. Bolívar Rafael Garcete-Barrett (Curator of Entomology of the “Museo Nacional de Historia Natural del Paraguay”, San Lorenzo, Paraguay) for his great contribution to Entomology and specially for his indispensable help which resulted in the collection of the holotype of *C. garcetabarretti* sp. nov.

Comments. The inclusion of *C. garcetabarretti* sp. nov. in *Chryxus* is in accordance with the characteristics assigned to this genus (Champion 1899; Gil-Santana et al.

2007), whereas the diagnostic characteristics recorded (see key below) seem to justify considering it as a species different from its congeners. Besides the general characteristics stated in the key, in regard to *C. bahianus*, the species to which *C. garcetabarretti* sp. nov. seems closer, the coloration of the hemelytra are different between them too. Corium mostly blackish, with basal third yellowish and whitish on anterior and posterior halves, respectively in *C. garcetabarretti* sp. nov. and whitish, with a subbasal dark spot, approximately apical half dark below the whitish area, giving the impression of a transverse pale band in *C. bahianus*. In *C. garcetabarretti* sp. nov., pale markings on membrane faint, that adjacent to the inner margin, just below discal cell, not including a portion of the latter, small and rounded, while in *C. bahianus*, pale markings of membrane more marked, whitish; that adjacent to inner margin, larger, forming a whitish stripe, contiguous with the whitish portion of the corium, going from the basal portion, shortly invading the discal cell, narrowing at midportion and enlarged at the inferodistal portion. Yet, the features of the female genitalia, as seen in posterior view (Fig. 28), are also distinctive in relation to the other species (Figs 12, 32), including *C. bahianus*, whereas the female genitalia of the latter species seems more similar to that of *C. tomentosus*.

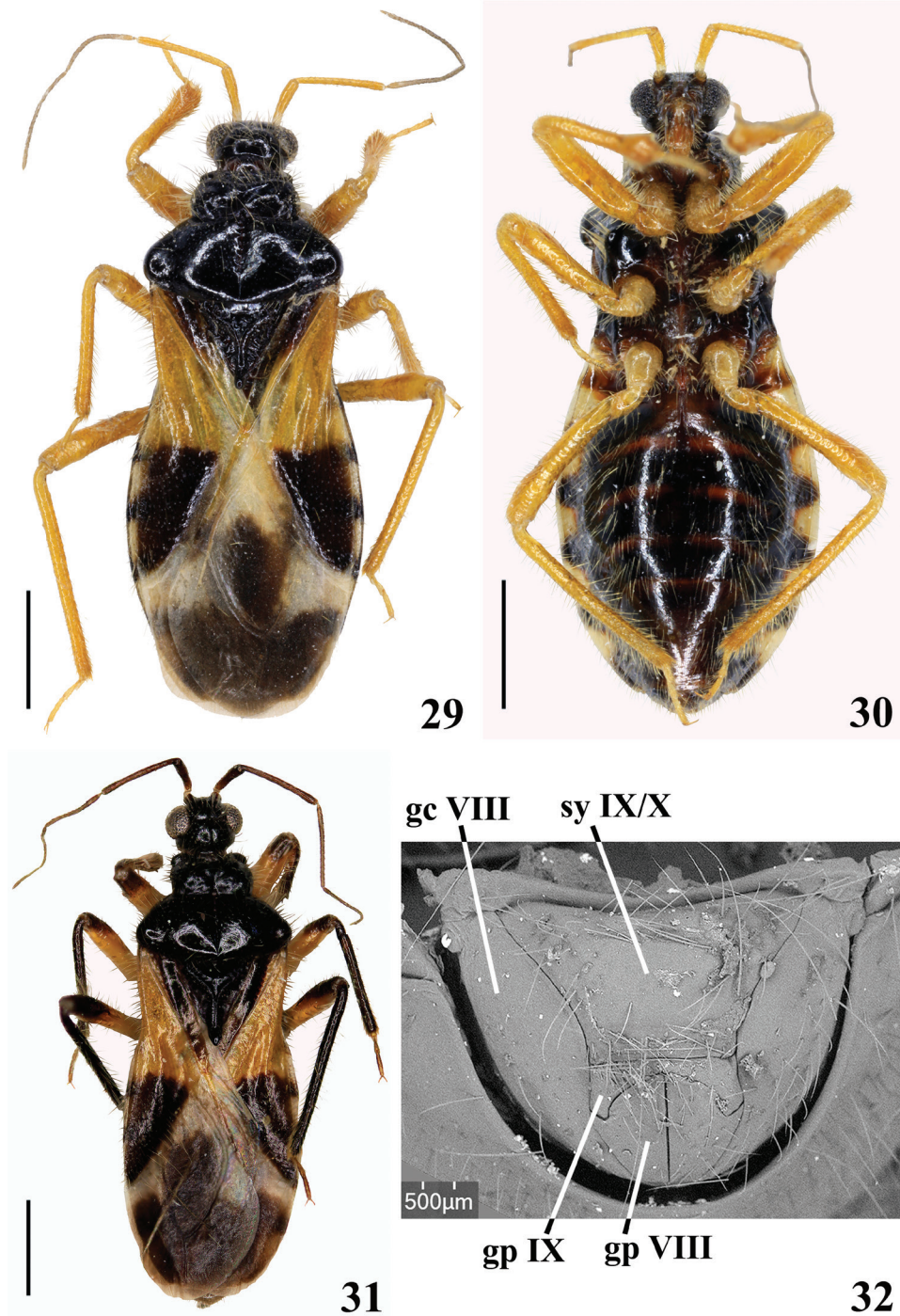
Chryxus tomentosus Champion, 1899

Figs 1, 29–32

Note. Besides the two male syntypes from Panama (Champion 1899), only two other specimens (sex not mentioned) of *C. tomentosus* were recorded in the literature: one as being collected in Guyana (Usinger 1952) and the other in Panama (Lucas et al. 2016).

Non-type material examined. FRENCH GUIANA. Itoupé, 400 m.a.s.l., window trap n°1, 1 female, 31.iii.2010; Saül, window trap, 6 females, 10.xii.2010, 20.xii.2010, 07.iii.2011, 07.iii.2011, 22.iii.2011, 22.iii.2011, SLAM bas (Sea, Land and Air Malaise trap) (SLAM Trap-Standard BugDorm Store), 4 females, 21.iii.2012, 03.vii.2012, 31.x.2012, 27.xi.2012; Saül Belvédère, window trap, 6 females, 09.ix.2010, 17.ix.2010, 06.x.2010, 5.xi.2010, 20.xii.2010, 24.i.2011, SEAG leg. (J–MB).

Morphological remarks. Measurements (mm): total length to tip of hemelytra: 4.75 to 5.2; Pronotum length: 1.25; hind lobe maximum width: 1.75; abdomen maximum width: 2.0. **Coloration** (Figs 29, 30): **head** blackish; apical half of first, second and third visible labial segments pale brownish. Scape and pedicel pale orange to yellowish; flagellomeres darkened, except paler basal portion of basiflagellomere. **Thorax** blackish; legs pale orange to orange yellowish. Hemelytra: corium yellowish with somewhat less than distal half blackish; clavus blackish and pale yellowish on approximately basal and distal halves, respectively; membrane pale whitish with a large blackish spot occupying almost entirely discal cell, except basal portion of discal cell, and another blackish spot in the distal region, which may be partially contiguous to the spot of discal cell. **Abdomen.** Connexivum pale yellow to whitish with distal markings which are larger on the ventral portion of each segment. Sternites generally blackish with some brownish stripes on segments IV–VII. All specimens show



Figures 29–32. *Chryxus tomentosus* Champion, 1899, females from French Guiana **29** dorsal view **30** ventral view **31** specimen from Mont Itoupé, dorsal view **32** external genitalia, posterior view, SEM image. Abbreviations: **sy IX/X** syntergite IX/X, **gc VIII** gonocoxa VIII, **gp VIII** gonapophysis VIII, **gp IX** gonapophysis IX. Scale bars: 1.0 mm (**29–31**).

the same coloration as described above, except one specimen from Mont Itoupé with antennae, distal portion of femora, tibiae and clavus entirely black (Fig. 31). **Structure** (Figs 29–31). Pronotum. Fore lobe: lateral angles largely prominent; shallow faintly defined oblique furrows present along its surface; median sulcus formed by a series of foveae, which may present separately or partially fused along the sulcus and are more or less progressively smaller towards distal portion; median sulcus running from just before transverse sulcus (which is interrupted by the proximal fovea), to somewhat far from posterior margin of pronotum. Transverse furrow narrow. Scutellum with its apex elevated and somewhat thickened. Hind tibiae straight. Connexivum with a continuous uniform margin. **Female genitalia.** Posterior view (Fig. 32): dark blackish, gonapophysis IX paler. Syntergite IX/X large, horizontal, as inverted subtrapezoidal; gonocoxa VIII elongate, moderately enlarged at median portion; gonapophysis VIII pointed laterally at median portion; gonapophysis IX subclaviform.

Distribution (Fig. 1). French Guiana (new record), Guyana, and Panama.

Discussion

The Chryxinae has been considered as being rarely collected reduviids, with only one to about half a dozen specimens known of all species so far (Lent and Wygodzinsky 1944; Weirauch 2012; Gil-Santana et al. 2007, 2015). However, in our study, 17 females of *C. tomentosus*, a species from which only four specimens were previously reported (Champion 1899; Usinger 1952; Lucas et al. 2016), were assembled. They were collected in French Guiana using the windowpane trap similar to that described by Lamarre et al. (2012). It is noteworthy that only females have been collected. Only further collecting with other methods in the same area will help to clarify if the absence of males was caused by the collecting method or other factors. On the other hand, the known apparently limited distributions of species of *Chryxus* (Fig. 1), and also of other Chryxinae, may eventually reveal themselves to be much larger with future study as well as future descriptions of new species if more efficient methods of collecting them are discovered or developed in the future. It would allow a better knowledge of the group as a whole and possibly to solve taxonomic doubts about the validity and limits of their genera such as *Wygodzinskyella* (Forero 2004; Weirauch 2012).

Key to genera and species of Chryxinae, modified from Gil-Santana et al. (2007, 2015) and Weirauch (2012)

- 1 Total length 8.0–9.0 mm; veins on corium indistinct; connexivum with uniform clear coloration..... *Wygodzinskyella travassosi* (Lent & Wygodzinsky, 1944)
- Total length 3.1–5.3 mm; veins on corium distinct, at least basally; connexivum with clear and dark alternate colors 2
- 2 Head with process on frons..... *Petasolettia goellnerae* Weirauch, 2012
- Head without process on frons..... 3

- 3 Head with ocelli and an acute process on its ventral surface; corium of heme-
lytra with a small costal cell.....*Lentia corcovadensis* Wygodzinsky, 1946
- Head without ocelli or an acute process on its ventral surface; corium of
hemelytra without a small costal cell.....*Chryxus* **Champion, 1899**...4
- 4 Fore lobe of pronotum with shallow oblique furrows and anterolateral angles
largely prominent (Figs 29, 31). Connexivum pale with distal dark markings
(Figs 29, 30)*Chryxus tomentosus* **Champion, 1899**
- Fore lobe of pronotum with integument generally smooth, without lateral
furrows and anterolateral angles slightly prominent. Connexivum reddish
brown or dark brownish with darkened or pale markings, respectively.....5
- 5 Transverse and median sulci of pronotum uniformly narrow (Figs 13, 16,
23). Femora largely darkened at median portion (Figs 14, 21). Apex of
scutellum not elevated (Fig. 15). Hind tibiae slightly curved at distal third
(Figs 13, 14). Connexivum dark brownish with narrow pale distal yellowish
bands, which include the respective intersegmental suture, margin conti-
nously uniform (Figs 13, 14, 26–27)
.....*Chryxus garcetebarratti* **sp. nov.**
- Transverse and basal half of median sulci of pronotum enlarged (Fig. 2, 10).
Femora with subbasal and subapical darkened rings (Figs 2, 3, 10). Apex of
scutellum obliquely elevated (Fig. 2). Hind tibiae straight (Fig. 3, 10, 11).
Connexival segments III–VI darkened at their distal thirds (Figs 3, 10); mar-
gins of segments II–V proeminent posterolaterally (Fig. 3)
.....*Chryxus bahianus* **Gil-Santana, Costa & Marques, 2007**

Acknowledgements

We are grateful to João Paulo Sales Oliveira Correia (LNIRTT, IOC) for the photos presented here as Figs 10 and 11; to SEAG members who do an extraordinary job of catching and sorting material by insect orders, and SEAG for donating the specimens of *C. tomentosus* collected by them; to Luiz A.A. Costa (MNRJ) along with the team of the digitization project of the Entomological Collection of MNRJ, for the photos (Figs 2–4) of the holotype of *C. bahianus*. For collecting and export permits prepared for the second author, we are most grateful to Luis Morán (Museum Director), John Kochalka (Chief of the Invertebrates Section) and Dr. Bolívar R. Garcete-Barrett (Museo Nacional de Historia Natural del Paraguay, San Lorenzo, Paraguay). The last author (JO) thanks “São Paulo State Research Support Foundation - FAPESP” and Dr. João Aristeu da Rosa for providing the framework for the work and support. We are also grateful to Valentina Castro-Huertas, Nikolay Simov, and Nathalie Yonow, for their valuable comments and suggestions.

References

- Champion GC (1899) Insecta Rhynchota. Hemiptera-Heteroptera, Fam. Reduviidae, Subfam. Chryxinae [pp. 180–181, pl. XI]. Vol II. In: Godman FD, Salvin O (Eds) *Biologia Centrali Americana*. Taylor and Francis, London, [xvi +] 416 pp. [22 pls]
- Escobar H (2018) In a 'foretold tragedy,' fire consumes Brazil museum. *Science* 361(6406): 960. <https://doi.org/10.1126/science.361.6406.960>
- Forero D (2004) Capítulo 5. Diagnósis de los géneros neotropicales de la familia Reduviidae (Hemiptera: Heteroptera), y su distribución en Colombia (excepto Harpactorinae). In: Fernández F, Andrade G, Amat G (Eds) *Insectos de Colombia Vol. 3*. Universidad Nacional de Colombia, Bogotá DC, 128–275.
- Gil-Santana HR, Costa LAA, Marques OM (2007) Sinopse dos Chryxinae (Hemiptera, Reduviidae). *Revista Brasileira de Zoologia* 24(1): 77–83. <https://doi.org/10.1590/S0101-81752007000100010>
- Gil-Santana HR, Forero D, Weirauch C (2015) Assassin bugs (Reduviidae excluding Triatominae). In: Panizzi AR, Grazia J (Eds) *True bugs (Heteroptera) of the Neotropics, Entomology in Focus 2*. Springer Science+Business Media, Dordrecht, 307–351. https://doi.org/10.1007/978-94-017-9861-7_12
- Lamarre GPA, Molto Q, Fine PVA, Baraloto C (2012) A comparison of two common flight interception traps to survey tropical arthropods. *ZooKeys* 216: 43–55. <https://doi.org/10.3897/zookeys.216.3332>
- Lent H, Wygodzinsky P (1944) Sobre uma nova espécie do gênero “*Chryxus*” Champion, 1898 (Chryxinae, Reduviidae, Hemiptera). *Revista Brasileira de Biologia* 4(2): 167–171.
- Lucas M, Forero D, Basset Y (2016) Diversity and recent population trends of assassin bugs (Hemiptera: Reduviidae) on Barro Colorado Island, Panama. *Insect Conservation and Diversity* 9(6): 546–558. <https://doi.org/10.1111/icad.12191>
- Schuh RT, Weirauch C (2020) *True bugs of the world (Hemiptera: Heteroptera). Classification and natural history*. 2nd edn. Siri Scientific Press, Manchester, 767 pp. [32 pls]
- Usinger RL (1952) A new genus of Chryxinae from Brazil and Argentina (Hemiptera: Reduviidae). *The Pan-Pacific Entomologist* 28(1): 55–56.
- Weirauch C (2012) *Petasolettia goellnerae* gen. nov., sp. nov, a new genus and species of Chryxinae (Heteroptera: Reduviidae). *Entomologische Zeitschrift* 122(3): 119–122.
- Weirauch C, Bérenger J-M, Berniker L, Forero D, Forthman M, Frankenberg S, Freedman A, Gordon E, Hoey-Chamberlain R, Hwang WS, Marshall SA, Michael A, Paiero SM, Udah O, Watson C, Yeo M, Zhang G, Zhang J (2014) An illustrated identification key to assassin bug subfamilies and tribes (Hemiptera: Reduviidae). *Canadian Journal of Arthropod Identification* 26: 1–115. <https://doi.org/10.3752/cjai.2014.26>

Caridina stellata, a new species of atyid shrimp (Decapoda, Caridea, Atyidae) with the male description of *Caridina cavernicola* Liang & Zhou, 1993 from Guangxi, China

Guo-Cai Guo^{1*}, Qing-Hua Chen^{2*}, Wen-Jian Chen³,
Chao-Huang Cai⁴, Zhao-Liang Guo¹

1 Department of animal science, School of Life Science and Engineering, Foshan University (FU), Nanhai 528231, Foshan, Guangdong province, China **2** South China institute of environmental sciences, Ministry of ecology and environment, Guangzhou 510520, Guangdong province, China **3** College of marine sciences, South China agricultural university, Guangzhou 510642, China **4** Hunan Yuanling animal husbandry and fishery affairs center, No. 13, Jinshui Road, Yuanling Town, Yuanling County 419600, Hunan province, China

Corresponding author: Zhao-Liang Guo (zlguo@fosu.edu.cn)

Academic editor: Luis Ernesto Bezerr | Received 8 February 2022 | Accepted 17 May 2022 | Published 14 June 2022

<http://zoobank.org/E5456913-7BBD-4AD8-86E3-E3391913A6E6>

Citation: Guo G-C, Chen Q-H, Chen W-J, Cai C-H, Guo Z-L (2022) *Caridina stellata*, a new species of atyid shrimp (Decapoda, Caridea, Atyidae) with the male description of *Caridina cavernicola* Liang & Zhou, 1993 from Guangxi, China. ZooKeys 1104: 177–201. <https://doi.org/10.3897/zookeys.1104.81836>

Abstract

Caridina stellata **sp. nov.** is described from streams in Guangxi, south-western China. The new species clearly belongs to “*Caridina serrata* group” of the genus and shows a morphological similarity with *C. cantonensis* Yu, 1938, *C. serrata* Stimpson, 1860 and *C. pacbo* Do et al. 2020. *Caridina stellata* is distinguished from congeners, based on differences in its male first pleopod and appendix masculina morphology, along with COI and 16S rRNA molecular evidence. The first pleopod endopod in male is rectangle, about $0.70 \times$ length of exopod, about $3.7\text{--}3.9 \times$ as long as proximally wide, inner margin concave, bearing nearly equal spine setae, outer margin bearing nearly equal long and dense spine setae; appendix interna well developed, arising from distal $1/5$ of endopod, reaching to end of endopod, with cincinuli distally. The new species displays a unique and brightly coloured pattern and, therefore, can be easily recognised in the field. Liang & Zhou, 1993 described *C. cavernicola* from the Lenggu Cave, Du’an County, Guangxi. However, the description was based exclusively on two females. We have collected specimens of both sexes

* These authors contributed equally to this work.

near the type locality and describe herein the previously unknown male and present morphological data on females. Data on the habitat, ecology and levels of threat of the two species are provided and suggest that they should be categorised as vulnerable (VU) under the current IUCN Criteria.

Keywords

COI and 16S rRNA, ecology, habitat, levels of threat, new species, south-western China

Introduction

Caridina H. Milne Edwards, 1837, the largest genus of the family Atyidae, contains more than 300 species and the Indo-West Pacific Region is where the highest diversity is centred (De Grave and Fransen 2011; De Grave et al. 2015; Do VT et al. 2020; De Mazancourt et al. 2021). China harbours more than 100 *Caridina* species (over one-third of the total number of known species), with areas of high species richness in Hunan, Yunan, Guizhou, Guangdong, Taiwan and Guangxi Zhuang Autonomous Region (Liang 2004; Guo and Wang 2005; Liu et al. 2006; Li and Li 2010; Cai 2014; Klotz and von Rintelen 2014; Cai and Ng 2018; Chen et al. 2020; Xu et al. 2020; Feng et al. 2021; Zhou et al. 2021).

Guangxi Zhuang Autonomous Region has 89500 km² of karst landscape, accounting for 37.8% of the total area (Liu et al. 2008). The humid subtropical climate, the diverse karst habitats and the enclosed underground environment provide the conditions for all sorts of organisms. The first records of freshwater atyid shrimps from Guangxi go back to Shen (1948), who listed two species *Caridina elongata* (= *Neocaridina palmata* Shen (1948)) and *C. hofendopoda* (= *N. hofendopoda* Shen (1948)). Since then, only a handful of publications have dealt with the atyids of Guangxi, to date, only four genera and about 22 species known from the region (Liang and Yan 1981; 1983; Liang and Zhou 1993; Liang 2004; Cai and Ng 2018). This may be due to insufficient sampling in the karst areas, especially underground habitats.

A faunal survey for freshwater shrimps from the karst habitats of Guangxi in 2018–2019 yielded numerous specimens referable to the genus *Caridina*. In comparing these specimens, we found that they do not fit the descriptions of any of the currently identified congeneric species and we hereby recognise them as belonging to a new species, *C. stellata* sp. nov.

Caridina cavernicola was described by Liang and Zhou (1993), based on two female specimens collected from a limestone cave in Lenggu Cave, Du'an Yao Autonomous County, Guangxi. Liang (2004), in his monograph of the family Atyidae of China, made an important re-description of *C. cavernicola* with an illustration of the mouthparts. We have collected samples from three sites inside the Chengjiang National Wetland Park, near the type locality of *C. cavernicola*. The opportunity is thus taken to re-describe and provide new figures on the basis of the new material.

Traditional species descriptions primarily utilised morphological differentiation, illustrations and locality data as diagnostic. The incorporation of morphological and molecular data in species delimitation allows a high level of confidence, crucial for both biodiversity and ecological research. Therefore, the molecular analyses and habitat

characterisation of the two species through direct observations are provided. Risk assessments for both are also presented and suggest they both should be categorised as vulnerable (VU) under the current IUCN Criteria.

Materials and methods

Sample collection. The shrimp samples were obtained from the karst habitats of Guangxi (Fig. 1). A sturdy long-handled, fine-meshed dip net (mesh size 0.6 mm) was used to collect the shrimp. The sampling scene was recorded with photographs and video-recordings. Specimens were placed in oxygenated polythene bags, anaesthetised with ice and transported back to the hotel. They were later photographed and fixed in 75% ethanol for further morphological examination and molecular analysis. All collection sites were georeferenced using a GPS.



Figure 1. Map indicating rivers in Guangxi Zhuang Autonomous Region, China, with three red triangles showing the sample sites for *Caridina cavernicola* and five black circles showing the sample sites for *Caridina stellata* sp. nov.

Morphological analysis

Specimens were examined using a dissecting microscope (Olympus SZX7). Morphometric measurements on selected characters and illustrations were made using a digital camera (DP22) mounted on a stereomicroscope (Olympus SZX7) with Olympus CellSens Entry v.1.18 software. The measuring method of morphometric characters follows that of von Rintelen and Cai (2009).

The following abbreviations are used throughout the text: alt (altitude), cl (carapace length, measured from the postorbital margin to the posterior margin of the carapace), rl (rostral length, measured from the rostral tip to the postorbital margin) and tl (total length, measured from the rostral tip to the posterior margin of the telson). All measurements are in millimetres.

Voucher specimens were deposited in the collection of the Department of Animal Science, School of Life Science and Engineering, Foshan University (FU).

Molecular data collection and analysis

An appropriate amount of shrimp abdominal muscle was taken and put in a 1.5 ml centrifuge tube. DNA was extracted according to the instructions of the Easy-Pure Genomic DNA Kit (TransGen Biotech, Beijing, China) and then stored in a -20°C freezer.

Segments of COI and 16S rRNA were amplified by using the primers COI-F-Car and COI-R-Car and 16S-F-Car and 16S-R-Car (von Rintelen et al. 2007). PCRs were conducted in 50 μl volume containing 25 μl 2xEasyTaq PCR SuperMix, 20 μl double distilled H_2O , 2 μl forward primer, 2 μl reverse primer and 1 μl DNA. The reaction conditions for COI and 16S were: 94°C for 3 min, 35 cycles of 30 sec at 94°C , 60 sec at 45°C (COI) or 50°C (16S) and 60 sec (16S) or 90 sec (COI) at 72°C were performed, with a final extension step of 72°C for 5 min. PCR products were forwardly sequenced using primers with an Applied Biosystems 3730 Analyzer (Applied Biosystems, Foster City, CA, USA).

The DNA sequence of *Caridina stellata* sp. nov. has been deposited in GenBank and 59 sequences have been downloaded from GenBank (Table 1). The sequences were aligned with BioEdit software and similarity was searched using the BLAST tool in NCBI. MAFFT 7.313 was used to compare the studied sequences (Katoh and Standley 2013) and the default values were used for each parameter. Finally, a FASTA format file was derived for subsequent analysis. Inter-group mean distance of the shrimps was calculated using MEGA 7.0, based on COI and 16S rRNA, respectively (Kumar et al. 2016). To obtain the best evolutionary model of sequences for Bayesian Inference (BI) and Maximum Likelihood (ML), the best Bayesian Information Criterion (BIC) evolution model selected by ModelFinder (Kalyaana-moorthy et al. 2017) and the BI and ML phylogenetic trees were constructed using MrBayes 3.2.6 (Ronquist et al. 2012) and IQ-Tree 1.6.12 (Nguyen et al. 2015); the best evolutionary models were TIM2+F+G4 (COI) and TPM3u+F+I+G4 (16S rRNA), respectively.

For the ABGD test, we used COI alignment from the phylogenetic analysis, including the outgroup. ABGD was run online (<http://wwwabi.snv.jussieu.fr/public/abgd/abgdweb.html>) with the following settings: Pmin = 0.001, Pmax = 0.1, Steps = 10; X = 1.0; Nb bins = 20 and implemented models: Kimura (K80) TS/TV (2.0).

Results

Taxonomy

Systematic accounts

Family Atyidae De Haan, 1849

Genus *Caridina* H. Milne Edwards, 1837

Caridina stellata sp. nov.

<http://zoobank.org/61D64E94-8898-44A7-AD99-81FF0950ED83>

Figs 2–4A, E

Material examined. *Holotype*: male (FU, 2018-11-05-01), cl 5.4 mm, tl 20.8 mm, rl 2.6 mm, a stream near Liuchacun, Jinxiu Town, Jinxiu Yao Autonomous County, Laibin City, Guangxi Zhuang Autonomous Region, China (24°3'59.63"N, 110°17'43.94"E, alt. 622 m), 5 November 2018. *Paratype*: male (FU, 2018-11-05-02), cl 5.3 mm, *Paratypes*: 15 males (FU, 2018-11-04-03), cl 5.0–6.2 mm; *Paratypes*: 29 females (FU, 2018-11-05-04), cl 4.9–6.6 mm, same collection data as for holotype.

Paratypes: 17 males (FU, 2019-03-20-01), cl 4.7–6.8 mm, three females (FU, 2019-03-20-02), cl 4.5–7.4 mm, a stream near Daxincun, Jinxiu Yao Autonomous County, Laibin City, Guangxi Zhuang Autonomous Region, China (23°57'52.77"N, 110°15'10.91"E, alt. 741 m), 20 March 2019.

Paratypes: Four males (FU, 2019-03-19-01), cl 4.7–6.8 mm, 34 females, one ovigerous (FU, 2019-03-19-02), cl 4.5–7.4 mm, a stream near Ji Jiangcun, Jinxiu Yao Autonomous County, Laibin City, Guangxi Zhuang Autonomous Region, China (24°11'13.18"N, 110°8'36.79"E, alt. 839 m), 19 March 2019.

Paratypes: 31 males (FU, 2019-03-19-03), cl 4.7–6.8 mm, 12 females (FU, 2019-03-19-04), cl 4.5–7.4 mm, a stream near Liupai, Jinxiu Yao Autonomous County, Laibin City, Guangxi Zhuang Autonomous Region, China (24°12'12.76"N, 110°8'25.78"E, alt. 510 m), 19 March 2019.

Paratypes: 10 males (FU, 2018-11-26-01), cl 4.7–6.8 mm, seven females (FU, 2018-11-26-02), cl 4.5–7.4 mm, a stream of Lotus Hill Scenic Spot, Dahua Yao Autonomous County, Hechi City, Guangxi Zhuang Autonomous Region, China (24°3'8.12"N, 107°38'30.5"E, alt. 350 m), 26 November 2018.

Comparative material. *Caridina cantonensis*: 10 females (cl: 4.8–6.9 mm), eight males (cl: 5.5–6.5 mm), Zaomushan, Foshan City, Guangdong Province (22°44'22"N, 112°46'36"E, alt. 56 m), 17 May 2018.

Caridina serrata: 17 females (CL: 3.3–6.7 mm), three ovigerous females (CL: 3.9–5.7 mm), 17 males (CL: 2.8–5.3 mm), Dong'ao Village, Dong'ao Island, Zhuhai City, Guangdong Province (22°01'12"N, 113°42'26"E, alt. 8.4 m), 23 August 2014.

Diagnosis. Rostrum long, straight, slightly sloping downwards, reaching to end of 2nd segment of antennular peduncle, occasionally reaching to end of 3rd segment

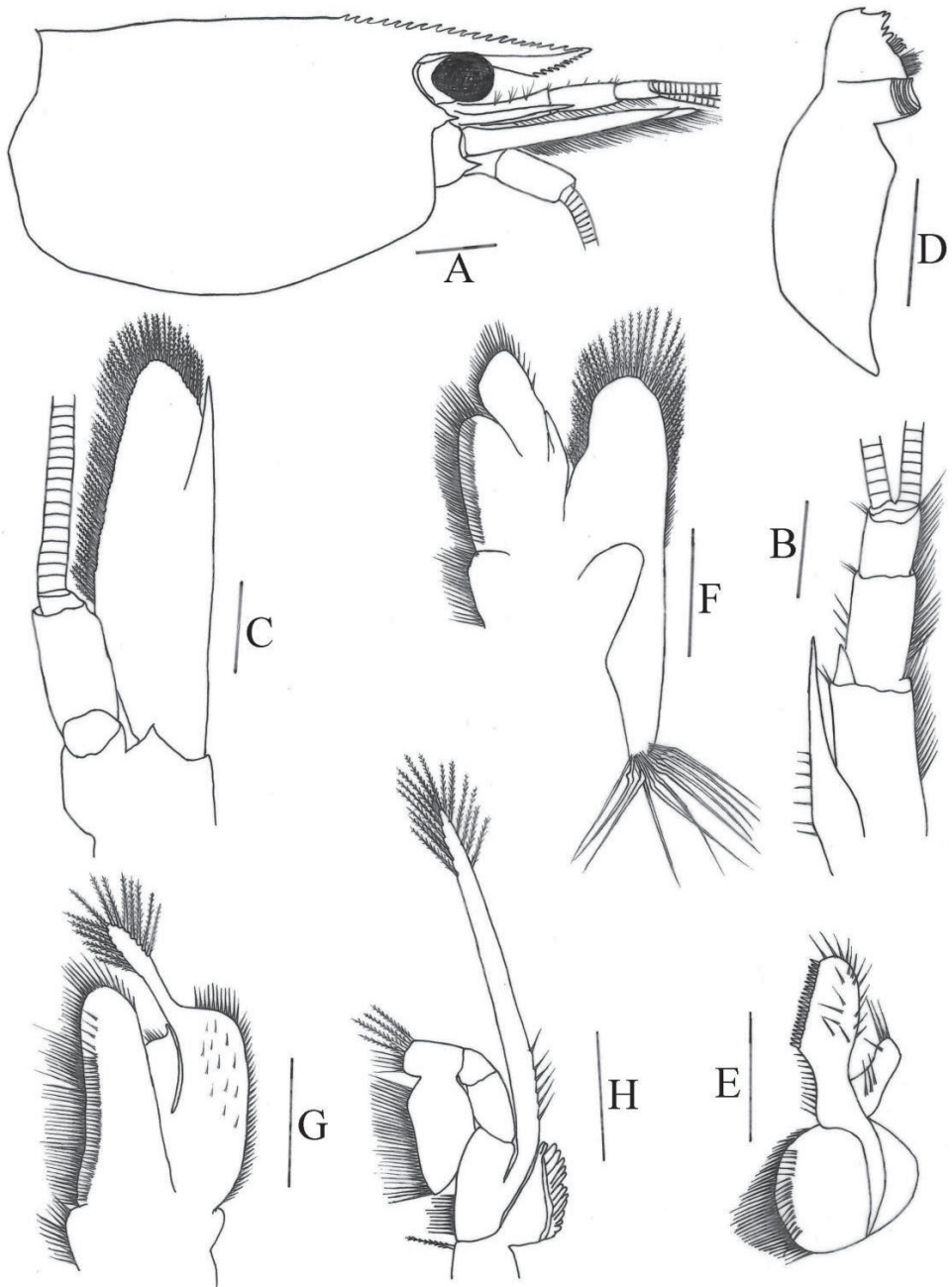


Figure 2. *Caridina stellata* sp. nov. **A** carapace and cephalic appendages, lateral view **B** antennule **C** antenna **D** mandible **E** maxillula **F** maxilla **G** first maxilliped **H** second maxilliped. Scale bars: 1.0 mm (**A**); 0.5 mm (**B–C**); 0.2 mm (**D–H**).

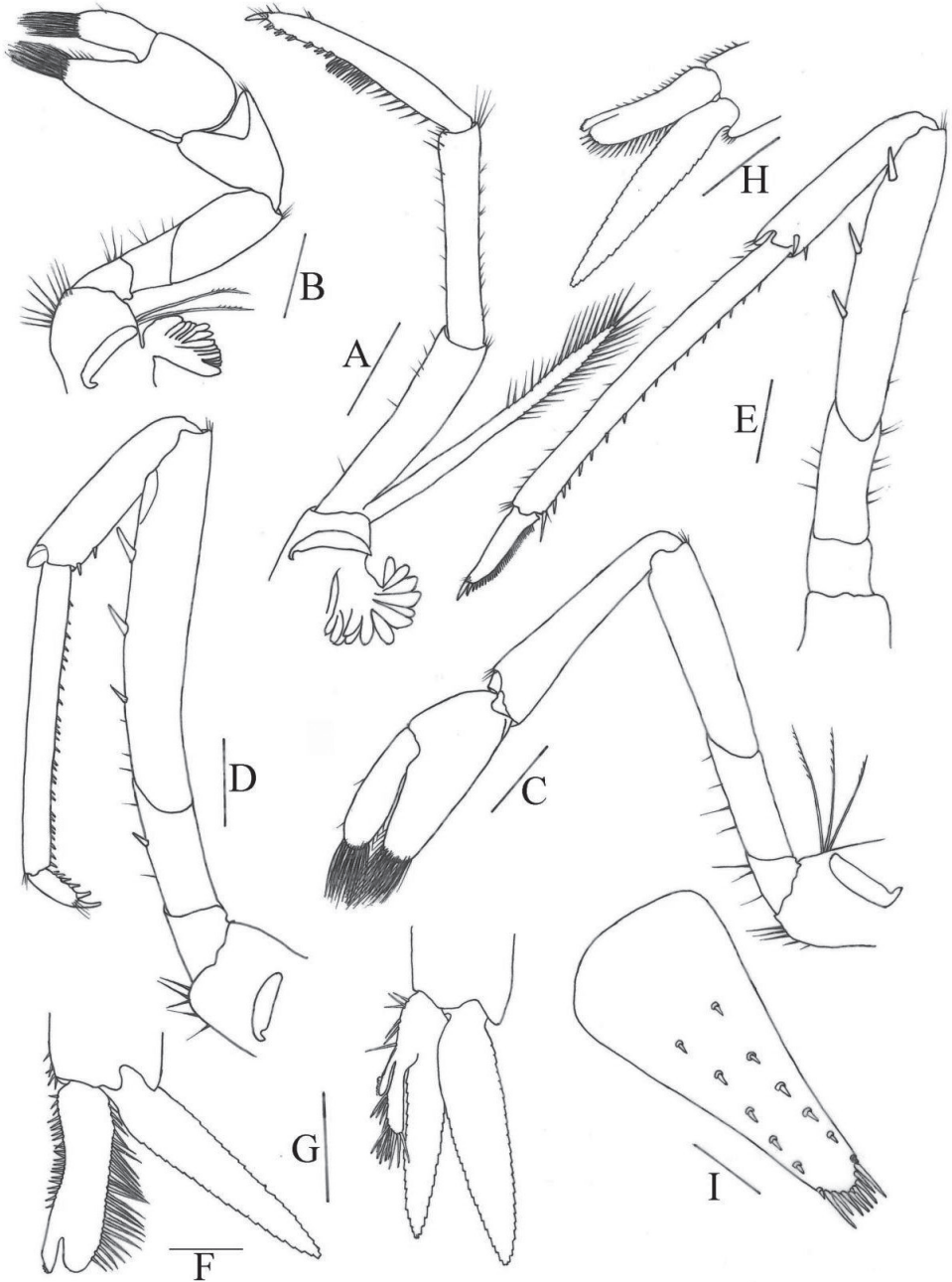


Figure 3. *Caridina stellata* sp. nov. **A** third maxilliped **B** first pereopod **C** second pereopod **D** third pereopod **E** fifth pereopod **F, H** first male pleopod **G** second male pleopod **I** telson. Scale bars: 0.5 mm (**A-E, I**); 0.2 mm (**F-H**).

of antennular peduncle; rostral formula 6-8+7-16/6-13. 1st pereiopod carpus 0.43–0.71 × as long as chela, 1.2–1.4 × as long as high; chela 1.8–2.4 × as long as broad; fingers 0.80–1.1 × as long as palm. 2nd pereiopodcarpus 1.1–1.3 × as long as chela, 4.0–4.8 × as long as high; chela 2.1–2.4 × as long as broad; fingers 1.1–1.4 × as long as palm. 3rd pereiopod propodus 4.0–5.5 × as long as dactylus, with two rows thin spines on the posterior margin, ischium with one spine on the posterior margin. 5th pereiopod propodus 4.2–5.3 × as long as dactylus, with two rows of thin spines on the posterior and lateral margins, dactylus terminating in one claw, with 35–40 spinules on flexor margin. Endopod of male 1st pleopod extending to 0.68 × exopod length, wider proximally, rectangle, about 3.7–3.9 × as long as wide, appendix interna well developed, arising from distal 1/6 of endopod, reaching end of endopod. Appendix masculina of male 2nd pleopod cylindrical, reaching to 0.58 length of endopod, appendix interna reaching to 0.50 length of appendix masculina. Uropodal diaeresis with 17–19 movable spinules. Eggs 0.84–0.89 × 1.27–1.39 mm in diameter.

Description. Body: slender and sub-cylindrical, males up to 30.7 mm tl, females up to 32.5 mm tl.

Rostrum (Fig. 2A): Long, straight, slightly sloping downwards, reaching to end of 2nd segment of antennular peduncle, occasionally reaching to end of 3rd segment of antennular peduncle; 0.39–0.48 of cl; armed dorsally with 13–24 teeth, including 6–9 on carapace posterior to orbital margin, ventrally with 6–13 teeth; rostrum formula 6-9+7-15/6-13; lateral carina dividing rostrum into two unequal parts, continuing posteriorly to orbital margin.

Eyes (Fig. 2A): Well developed, on short ocular peduncle, cornea globular.

Carapace (Fig. 2A): Smooth, glabrous; antennal spine acute, fused with inferior orbital angle; pterygostomian margin rectangular, pterygostomian spine absent.

Antennule (Fig. 2B): Peduncle reaching slightly short of scaphocerite; stylocerite long, reaching 0.40 of 2nd segment; anterolateral angle reaching 0.40 of 2nd segment; basal segment as long as combined length of 2nd and 3rd segments, 2nd segment about 0.60 of 1st segment, about 1.6 of 3rd segments; all segments with marginal plumose setae.

Antenna (Fig. 2C): Peduncle about 0.40 × as long as scaphocerite; scaphocerite about 3.5 × as long as wide, outer margin straight, asetose, ending in a strong sub-apical spine, inner and anterior margins with long plumose setae.

Mandible (Fig. 2D): Without palp; left incisor process with five sharp teeth; two groups of setae medially; molar process ridged.

Maxillula (Fig. 2E): Lower lacinia broadly rounded, with several rows of plumose setae; upper lacinia elongate, medial edge straight, with 20–26 strong spinules and simple setae; palp simple, slightly expanded distally, with seven long simple setae.

Maxilla (Fig. 2F): Scaphognathite tapers posteriorly, distally with regular row of long plumose setae and short marginal plumose setae continuing down proximal triangular process, furnished with numerous long plumose setae; upper and middle endite with marginal simple, denticulate and submarginal simple setae, distally with plumose setae; lower endite with long simple marginal setae; palp slightly shorter than the cleft of upper endite, wider proximally than distally, setose.



Figure 4. Habitats and live colouration of *Caridina stellata* sp. nov. and *C. cavernicola* **A** *C. stellata* sp. nov. **B–D** *C. cavernicola*; **E–H** surrounding environment of *C. stellata* sp. nov. (**E**) and *C. cavernicola* (**F–H**).

First maxilliped (Fig. 2G): Palp broadly triangular ending in fringe-like tip and with terminal plumose setae; caridean lobe broad, with marginal plumose setae; exopodal flagellum well developed, with distally marginal plumose setae; ultimate and penultimate segments of endopod indistinctly divided; medial and distal margins of ultimate segment with marginal and sub-marginal rows of simple, denticulate and plumose setae; penultimate segments with marginal long plumose setae.

Table 1. Species used in the molecular analysis, with details on sampling locations, GenBank accession numbers (COI, 16S rRNA) (a, Klotz W et al. 2014; b, Chen QH et al. 2020; c, Xu DJ et al. 2020; d, Oliveira, C. M. et al. 2019).

Species	Sampling locality	GenBank accession numbers	
		COI	16S rRNA
<i>C. stellata</i> sp. nov.	Jinxiu Guangxi	MZ753496	MZ753799
	Jinxiu Guangxi	MZ753497	MZ753800
<i>C. cavernicola</i>	Hechi Guangxi	MZ753498	MZ753801
	Hechi Guangxi	MZ753499	MZ753802
<i>C. venusta</i>	China, Lixi Town, from type loc.	KP168812 ^a	KP168772 ^a
	China, Lixi Town, from type loc.	KP168813 ^a	KP168773 ^a
<i>C. sp.</i>	China, Gao Zhou Shi	KP168790 ^a	KP168761 ^a
	China, Gao Zhou Shi	KP168791 ^a	KP168762 ^a
<i>C. nanaoensis</i>	China	KP168792 ^a	KP168754 ^a
	China	–	KP168755 ^a
<i>C. breviata</i>	China, from type loc.	KP168788 ^a	KP168718 ^a
	China, from type loc.	KP168789 ^a	KP168719 ^a
<i>C. zhujiangensis</i>	Dong'ao Island, Zhuhai	MN701603 ^b	MT446448 ^c
	Dong'ao Island, Zhuhai	MN701604 ^b	MT446449 ^c
<i>C. trifasciata</i>	Zhuhai China	KP168795 ^a	KP168765 ^a
	Zhuhai China	KP168796 ^a	KP168766 ^a
<i>C. sinanensis</i>	Sinan Guizhou	MT433963 ^c	MT434874 ^c
	Sinan Guizhou	MT433964 ^c	MT434875 ^c
<i>C. serrata</i>	Dong'ao Island, Zhuhai	MN701595 ^b	MT446454 ^c
	Dong'ao Island, Zhuhai	MN701596 ^b	MT446455 ^c
<i>C. mariae</i>	Nankun Mountain, Huizhou	MN701601 ^b	MT446456 ^c
	Nankun Mountain, Huizhou	MN701602 ^b	MT446457 ^c
<i>C. lanceifrons</i>	Dongfang, Hainan	MN701605 ^b	MT446450 ^c
	Dongfang, Hainan	MN701606 ^b	MT446451 ^c
<i>C. huananensis</i>	Yingde, Qingyuan	MN701607 ^b	MT446452 ^c
	Yingde, Qingyuan	MN701608 ^b	MT446453 ^c
<i>C. cantonensis</i>	Qingyuan, China	KP168802 ^a	KP168720 ^a
	Qingyuan, China	KP168803 ^a	KP168721 ^a
<i>N. palmata</i>	Yangshan, Qingyuan	MN701611 ^b	–
	Yangshan, Qingyuan	MN701612 ^b	–
	China	–	KP168779 ^a
<i>A. scabra</i>	Hong Kong, China	–	KP168780 ^a
	Bocas del Toro, Panama	EF489985 ^d	JF810980 ^d
	Bocas del Toro, Panama	EF489986 ^d	JF810981 ^d

Second maxilliped (Fig. 2H): Ultimate and penultimate segments of endopod indistinctly divided, reflected against basal segment; inner margin of ultimate, penultimate and basal segments with long setae of various types; exopod flagellum long, slender with marginal plumose setae distally.

Branchial formula typical for genus.

Third maxilliped (Fig. 3A): Reaches middle of 3rd antennular peduncle segment, endopod three-segmented, penultimate segment as long as basal segment; distal segment 1.1 × as long as penultimate segment, ending in a large claw-like spine surrounded by simple setae, preceded by 12 spines with double arrangement along distal third of posterior margin, a clump of long and short simple, serrate setae proximally; exopod reaches to end of basal segment of endopod, distal margin with long plumose setae.

First pereopod (Fig. 3B): Reaches about end of eye; chela 1.8–2.4 × as long as high; 1.4–2.3 × length of carpus; movable finger 2.4–2.8 × as long as wide, 0.80–

1.1 × length of palm, setal brushes well developed; carpus excavated disto-dorsally, 1.2–1.4 × as long as wide, 0.85–1.0 × length of merus.

Second pereiopod (Fig. 3C): Reaches about end of 2nd antennular peduncle segment, more slender and longer than first pereiopod; chela 2.1–2.4 × as long as high; 0.76–0.94 × length of carpus; movable finger 3.4–4.9 × as long as wide and 1.1–1.4 × as long as palm, setal brushes well developed; carpus 4.0–4.8 × as long as wide, slightly excavated distally, about 1.1 × length of merus.

Third pereiopod (Fig. 3D): Reaches beyond end of scaphocerite; dactylus 2.0–2.9 × as long as wide, ending in prominent claw-like spine surrounded by simple setae, behind which are 4–5 spines; propodus 4.0–5.5 × length of dactylus, bearing two rows of thin spinules on posterior and lateral margin, 8.0–9.9 × as long as wide; carpus 0.57–0.70 × length of propodus; merus 1.7–2.4 × length of carpus, with about 3–4 strong spines on the posterior margin; ischium with a spine on the posterior margin.

Fifth pereiopod (Fig. 3E): Reaches middle of 2nd segment of antennular peduncle; dactylus 1.7–3.0 × as long as wide, ending in prominent claw-like spine surrounded by simple setae, behind which is a comb-like row of 35–40 spines; propodus 4.2–5.3 × length of dactylus, bearing two rows of spinules on posterior and lateral margins, 9.1–13.0 × as long as wide; carpus 0.43–0.58 × length of propodus; merus 1.4–1.5 × length of carpus, with about 3–4 strong spines on the posterior margin.

First four pereiopods with epipod.

First pleopod (Figs 3F and H): Endopod in male is rectangle, about 0.70 × length of exopod, about 3.7–3.9 × as long as proximally wide, tip rounded, inner margin concave, bearing nearly equal spine setae, outer margin bearing nearly equal long and dense spine setae, distally absent (Fig. 3F) or bearing a few sparse thin spine setae (Fig. 3H); appendix interna well developed, arising from distal 1/5 of endopod, reaching to end of endopod, with cincinuli distally.

Second pleopod (Fig. 3G): Appendix masculina rod-shaped, reaching about 0.60 × length of exopod, inner margin bearing and tip bearing nearly equally long and stout spine setae; appendix interna well developed, reaching about 0.50 × length of appendix masculina, with many cincinuli distally.

Telson (Fig. 3I): 0.42–0.55 × length of cl, distinctly longer than sixth abdominal segment, tapering posteriorly, with a projection, dorsal surface with six pairs of stout movable spine setae including the pair at posterolateral angles; posterior margin with four pairs of intermedial plumose setae, the outer one usually strongest and longest. Exopodite of the uropod bears a series of 17–19 movable spinules along the diarsis.

Eggs 0.84–0.89 × 1.27–1.39 mm in diameter.

Colouration. Body semi-transparent, light reddish-brown colour, with small red pigment spots scattered on whole body, several large red-brown dots on the tergum and the posterior margin of the carapace, red-brown vertical stripes on topside of the 1st and 2nd pleon and lower lateral side of 1st, 3rd, 4th and 5th pleon and carapace; appendages transparent, with red-brown stripes in the distal part of each segment; telson and tail fan bright red (Fig. 4A)

Etymology. *Caridina stellata* is named after the Latin word *stellatus*, for dots, alluding to the pigmented pattern of the body.

Remarks. *Caridina stellata* sp. nov. clearly belongs to the “*Caridina serrata* group” of the genus and shows a strong morphological similarity with *C. cantonensis* Yu, 1936 in shape and indentation of the rostrum. *Caridina stellata* sp. nov. can be distinguished from *C. cantonensis* by the broad palp of the 1st maxilliped with a finger-like tip (versus without a finger-like tip in *C. cantonensis*); rostrum with more ventral teeth (6–13 versus 2–6 in *C. cantonensis*); the stouter carpus of the 1st pereopod (1.2–1.4 times as long as wide versus 1.5–1.7 in *C. cantonensis*); the slender endopod of the 1st male pleopod, about 3.7–3.9 × as long as wide, wider proximally (versus 2.5–3.0, wider terminally in *C. cantonensis*); completely different shape of the appendix masculina of male 2nd pleopod (Fig. 3G versus fig. 87r in Liang 2004); and relatively larger eggs, size of developed eggs 0.84–0.89 × 1.27–1.39 mm (versus 0.63–0.72 × 0.99–1.09 mm in *C. cantonensis*). In addition, its distinctive colouration and patterns easily separate the two species when observed in the field.

Caridina stellata sp. nov. resembles *C. pacbo* Do, von Rintelen & Dang, 2020 in colouration and pattern and also in the long stylocerite. Moreover, the type locality, Cao Bang Province, Vietnam, is close to Guangxi, China. However, the new species can be distinguished from *C. pacbo* by the longer rostrum, reaching end of 2nd segment of antennular peduncle, 0.39–0.48 of cl (versus close to end of 1st segment, 0.25–0.36 of cl in *C. pacbo*), with more ventral teeth (6–13 teeth versus 0–3 in *C. pacbo*); the stouter carpus of the 1st pereopod (1.2–1.4 times as long as wide versus 1.3–1.7 in *C. pacbo*); the stouter chela of the 2nd pereopod (2.1–2.4 times as long as wide versus 2.7–3.1 in *C. pacbo*) with carpus as long as the merus (versus longer than merus in *C. pacbo*); and the slender endopod of the 1st male pleopod (3.7–3.9 × as long as wide versus 2.9–3.3 in *C. pacbo*).

Caridina stellata sp. nov. also looks similar to *C. multidentata* Stimpson, 1860 in the colouration and pattern of live individuals. *C. stellata* can be easily distinguished from *C. multidentata* by the longer stylocerite, reaching 0.40 of the 2nd segment of the antennular peduncle (versus 0.70 of the 1st segment of antennular peduncle in *C. multidentata*); with straight rostrum (versus with a crest over orbit in *C. multidentata*), more teeth on carapace posterior to orbital margin (6–9 teeth versus 0 in *C. multidentata*); and large eggs (0.84–0.89 × 1.27–1.39 mm versus 0.23–0.28 × 0.38–0.40 mm in *C. multidentata*).

Ecological notes. *Caridina stellata* appears to be a common atyid species in Guangxi. It was found from four streams in the Jinxiu Yao Autonomous County, Laibin City and also found in Dahua Yao Autonomous County, Hechi City. The environment of the streams is very similar. The streams run through land that is covered by secondary forest, with rocks interspersed with patches of gravel at the bottom (Fig. 4E). The width and depth of the streams were 2.0–3.5 m and 0.3–1.0 m, respectively, with waterfalls and rapids present. The shrimps inhabit vegetation amidst running water, under rocks in lentic environments and even in stagnant water, such as shallow pools. *C. stellata* was found at Jinxiu, in co-existence with the atyid, *Neocaridina palmata* (Shen 1948) and the palaemonid *Macrobrachium nipponense*. At Dahua, this species

was found also living together with *N. palmata*. The majority of the habitats surveyed had a relatively high density of the new species.

Distribution. Known from Guangxi Zhuang Autonomous Region, southwest China.

Molecular phylogenetic results

We analysed a total of 31 COI sequences and 32 16S rRNA sequences, 59 of which were from GenBank. The lengths of the sequences are 638 bp (COI) and 461 bp (16S) for the molecular phylogeny analyses. Based on the Kimura Model, inter-group mean distance of 16 species were calculated (Table 2), the genetic distance between *Caridina stellata* sp. nov. and the other nine *Caridina* ranging from 0.126–1.722 (COI) and 0.065–0.112 (16S). Using *Atya scabra* as the outgroup, the Maximum Likelihood phylogenetic tree and Bayesian phylogenetic tree of 16 species of shrimp were constructed (Figs 5, 6). According to the figures, the genetic variability for COI and 16S rRNA are 0.7 and 0.05, respectively. All species can be clustered into a single branch with a relatively high support rate. The new species described above are all well supported and sufficiently distinct from their sister species.

In addition, the ABGD division results of 31 COI sequences (including outgroups) in this experiment shows that a significant barcode gap can be formed (Fig. 7a), including both initial division and recursive division. Both recursive and initial divisions

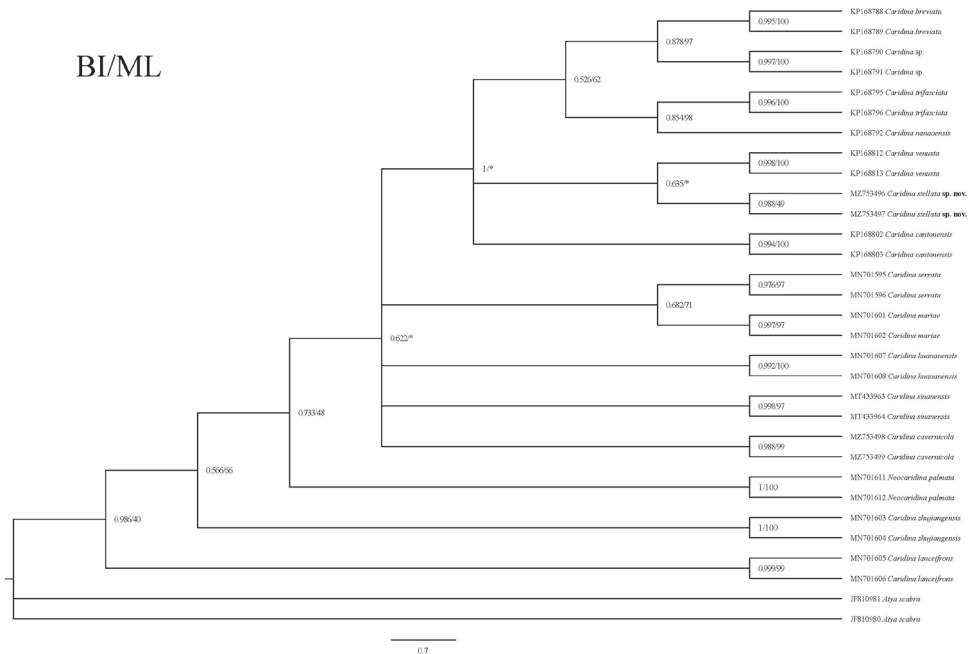


Figure 5. Bayesian Inference (BI) tree and Maximum Likelihood method (ML) tree of 15 atyids and outgroups (*Atya scabra*), based on the COI gene. Support values at the nodes represent posterior probability

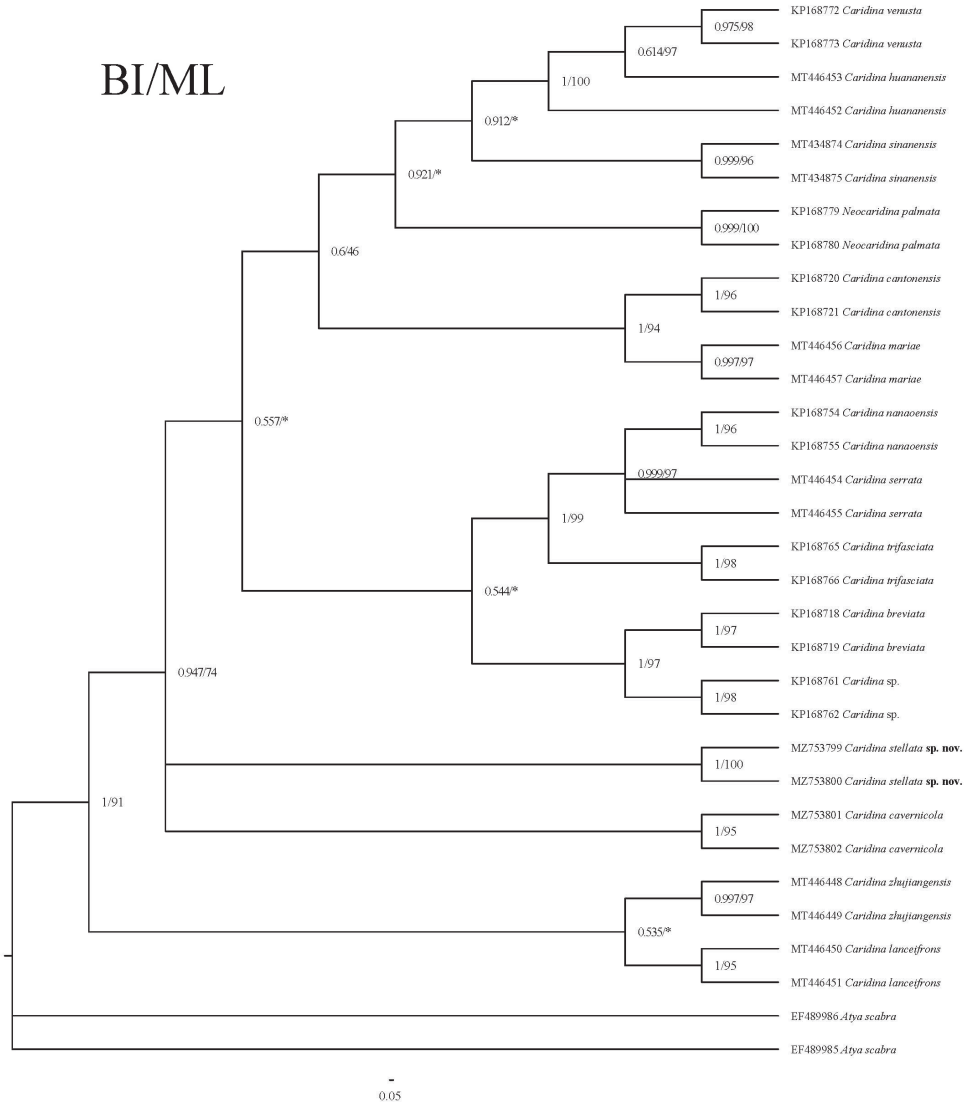


Figure 6. Bayesian Inference (BI) tree and Maximum Likelihood method (ML) tree of 15 atyids and outgroups (*Atya scabra*), based on the 16S rRNA. Support values at the nodes represent posterior probability.

were stable (Fig. 7b). When the Prior maximal distances were 0.001000, 0.001668, 0.002783, 0.004642, 0.007743, 0.012915, 0.021544, 0.035938 and 0.059948, they were divided into 16 groups; when the Prior maximal distance was 0.100000, they were divided into 10 groups (Table 3). Therein, the 16 groups were **Group 1:** *C. stellata* sp. nov.; **Group 2:** *C. cavernicola*; **Group 3:** *N. palmata*; **Group 4:** *C. venusta*; **Group 5:** *C. sp.*; **Group 6:** *C. nanaoensis*; **Group 7:** *C. cantonensis*; **Group 8:** *C. trifasciata*; **Group 9:** *C. trifasciata*; **Group 10:** *C. sinanensis*; **Group 11:** *C. serrata*; **Group 12:** *C. mariae*; **Group 13:** *C. lanceifrons*; **Group 14:** *C. huananensis*; **Group 15:** *C. breviata*

Table 2. Pairwise genetic distance amongst 16 species, based on the COI (bottom left) and 16S rRNA (top right) gene.

	1	2	3	4	5	6	7	8	9	10	11	12	13	14	15	16
1 <i>C. stellata</i> <i>sp. nov.</i>		0.065	0.103	0.098	0.070	0.091	0.080	0.096	0.095	0.095	0.086	0.068	0.112	0.099	0.069	0.236
2 <i>C. cavernicola</i>	1.449		0.099	0.095	0.063	0.073	0.077	0.080	0.082	0.077	0.068	0.078	0.106	0.091	0.047	0.213
3 <i>N. palmata</i>	1.504	0.203		0.086	0.080	0.094	0.077	0.110	0.086	0.080	0.094	0.076	0.121	0.085	0.096	0.214
4 <i>C. Venusta</i>	0.126	1.604	1.770		0.090	0.122	0.088	0.130	0.106	0.070	0.117	0.093	0.133	0.006	0.099	0.235
5 <i>C. sp.</i>	0.163	1.578	1.648	0.145		0.068	0.065	0.100	0.065	0.082	0.063	0.075	0.112	0.091	0.026	0.223
6 <i>C. nanaoensis</i>	0.158	1.588	1.721	0.139	0.129		0.071	0.109	0.039	0.103	0.004	0.008	0.131	0.123	0.069	0.225
7 <i>C. cantonensis</i>	0.144	1.521	1.552	0.134	0.118	0.130		0.086	0.072	0.075	0.071	0.034	0.107	0.086	0.073	0.216
8 <i>C. zhujiangensis</i>	1.703	0.244	0.263	1.754	1.850	1.690	1.672		0.109	0.098	0.104	0.101	0.078	0.128	0.099	0.198
9 <i>C. trifasciata</i>	0.148	1.578	1.689	0.137	0.144	0.075	0.139	1.745		0.090	0.034	0.075	0.130	0.107	0.069	0.218
10 <i>C. sinanensis</i>	1.445	0.143	0.183	1.521	1.525	1.551	1.438	0.240	1.498		0.103	0.070	0.112	0.069	0.081	0.210
11 <i>C. serrata</i>	1.460	0.155	0.223	1.575	1.494	1.515	1.402	0.254	1.483	0.155		0.076	0.125	0.118	0.064	0.222
12 <i>C. mariae</i>	1.462	0.174	0.244	1.593	1.575	1.547	1.409	0.270	1.497	0.185	0.167		0.129	0.092	0.074	0.229
13 <i>C. lanceifrons</i>	1.722	0.268	0.261	1.851	1.742	1.713	1.781	0.239	1.744	0.256	0.261	0.266		0.127	0.115	0.199
14 <i>C. huananensis</i>	1.461	0.200	0.251	1.584	1.599	1.580	1.544	0.268	1.594	0.184	0.195	0.210	0.265		0.100	0.230
15 <i>C. breviata</i>	0.166	1.574	1.601	0.147	0.059	0.115	0.135	1.851	0.120	1.521	1.475	1.536	1.756	1.583		0.226
16 <i>A. scabra</i>	1.823	0.299	0.305	1.785	1.869	1.936	1.970	0.280	1.959	0.278	0.276	0.292	0.266	0.298	1.826	

Table 3. The results of the the ABGD division.

Partition	Groups	Prior maximal distance
1	16	0.001000
2	16	0.001668
3	16	0.002783
4	16	0.004642
5	16	0.007743
6	16	0.012915
7	16	0.021544
8	16	0.035938
9	16	0.059948
10	10	0.100000

and **Group 16:** *A. scabra*. This result had a high degree of agreement with the morphological identification results. The partition results of ABGD correspond to the BI/ML tree and the division results of each ABGD were indicated on the BI/ML tree (Fig. 7c).

Combining all of the above results, the results of the division of phylogenetic trees and the classification of species by ABGD are basically the same; the genetic distance supported the molecular-based description of *C. stellata* sp. nov. as a new species.

***Caridina cavernicola* Liang & Zhou, 1993**

Figs 4B–D, F–H, 8, 9

Caridina cavernicola Liang & Zhou, 1993: 232–234, fig. 2 (1–8). [type locality: Lenggu Cave, Du’an Yao Autonomous County, Guangxi]

Caridina cavernicola Liang 2004: 204–206, fig. 98.

Material examined. Nine males, cl 5.2–7.1 mm, 10 females, cl 5.5–7.8 mm (FU, 2018-11-26-02), Dading Village, Desu Town in the Du’an Chengjiang National Wetland

Rostrum (Fig. 8A): Long, conspicuously high, tip slightly upturned, beyond one-thirds of rostrum and beyond distal end of scaphocerite; 0.91–1.1 of cl; rostrum formula 7-10+21-33/20-29.

Carapace (Fig. 8A): Smooth, glabrous; antennal spine acute, fused with inferior orbital angle; pterygostomian margin rectangularly rounded, pterygostomian spine absent.

Antennule (Fig. 8B): Peduncle reaching distinctly short of scaphocerite; stylocerite reaching 0.91 of 1st segment; anterolateral angle reaching 0.40–0.5 of 2nd segment; basal segment shorter than combined length of 2nd and 3rd segments, 2nd segment about 0.51 of 1st segment, about 1.2 of 3rd segment; all segments with marginal plumose setae.

Antenna (Fig. 8C): Peduncle about 0.32 × as long as scaphocerite; scaphocerite about 3.2–3.4 × as long as wide, outer margin straight, asetose, ending in a strong subapical spine, inner and anterior margins with long plumose setae.

Mouthparts as in figure. **Mandible** (Fig. 8D) without palp; left incisor process with five sharp teeth; with two groups of medial setae; molar process ridged. **Maxillula** (Fig. 8E) with lower lacinia broadly rounded, with several rows of plumose setae; upper lacinia elongate, medial edge straight, with 23–27 strong spinules and simple setae; palp simple, slightly expanded distally, with numerous long simple setae. **Maxilla** (Fig. 8F) with scaphognathite tapering posteriorly, with regular row of long plumose setae distally and short marginal plumose setae continuing down proximal triangular process, furnished with numerous long plumose setae; upper and middle endite with marginal simple, denticulate and submarginal simple setae, with distal plumose setae; lower endite with long simple marginal setae; palp slightly shorter than the cleft of upper endite, wider proximally than distally, setose. **First maxilliped** (Fig. 8G) with broad palp and with terminal plumose setae; caridean lobe broad, with marginal plumose setae; exopodal flagellum well developed, with marginal plumose setae distally; ultimate and penultimate segments of endopod indistinctly divided; medial and distal margins of ultimate segment with marginal and sub-marginal rows of simple, denticulate and plumose setae; penultimate segments with marginal long plumose setae. **Second maxilliped** (Fig. 8H) with ultimate and penultimate segments of endopod indistinctly divided, reflected against basal segment; inner margin of ultimate, penultimate and basal segments with long setae of various types; exopod flagellum long, slender with marginal plumose setae distally. **Third maxilliped** (Fig. 9A) reaches to middle of 3rd antennular peduncle segment, endopod three-segmented, penultimate segment about 1.3 × as long as basal segment; distal segment 0.79 × as long as penultimate segment, ending in a large claw-like spine surrounded by simple setae, preceded by five spines, proximally a clump of long and short simple, serrate setae; exopod long, reaches to half of penultimate segment of endopod, distal margin with long plumose setae. Epipods on first four pereopods.

First pereopod (Fig. 9B): Reaches to about end of eye; chela 1.4–2.2 × as long as high; 1.7–1.9 × length of carpus; movable finger 2.4–2.6 × as long as wide, 0.50–0.67 × length of palm, setal brushes well developed; carpus excavated disto-dorsally, 1.3–1.7 × as long as wide, 1.1–1.2 × length of merus.

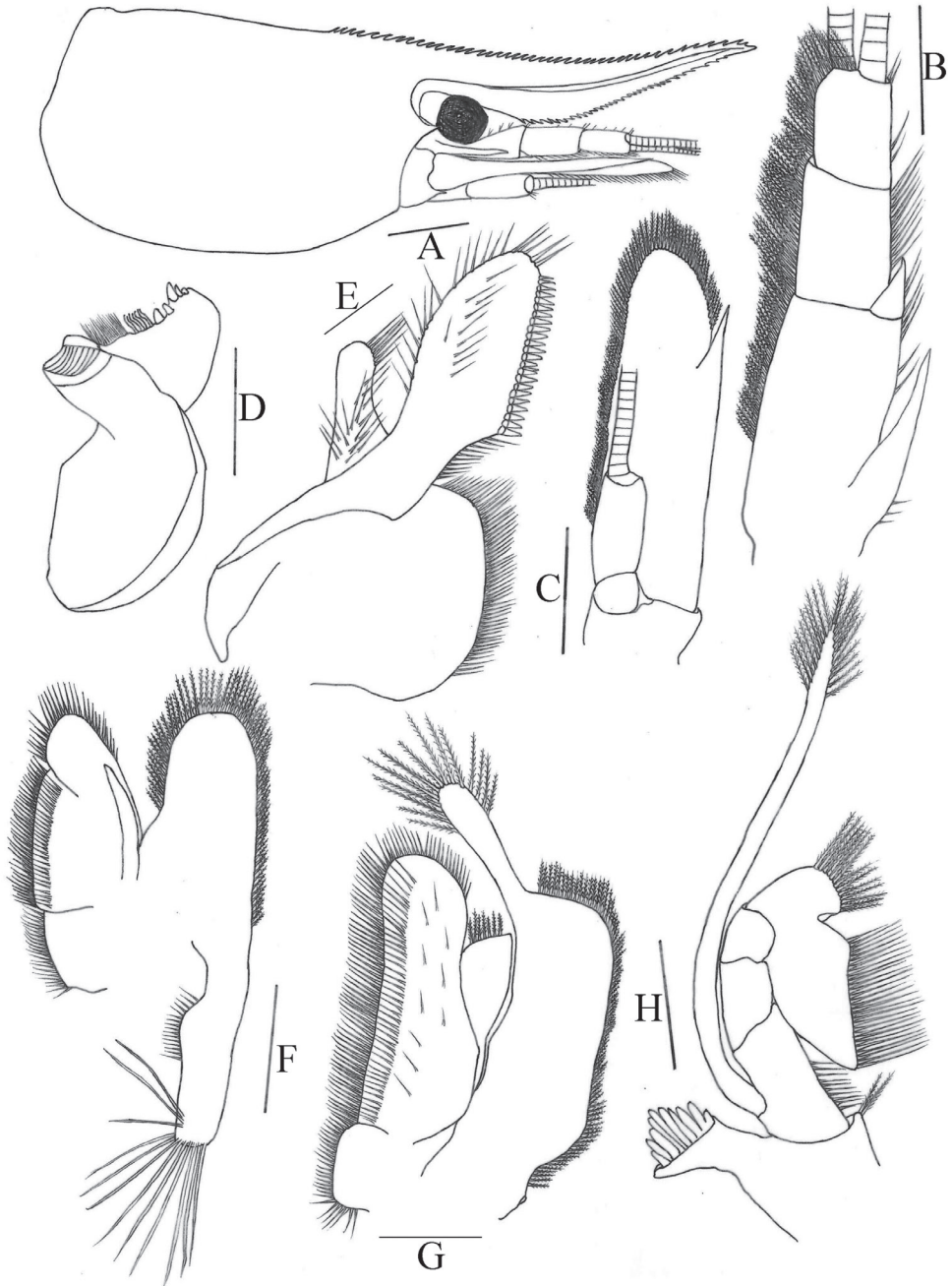


Figure 8. *Caridina cavernicola* **A** carapace and cephalic appendages, lateral view **B** antennule **C** antenna **D** mandible **E** maxillula **F** maxilla **G** first maxilliped **H** second maxilliped. Scale bars: 1.0 mm (**A**); 0.5 mm (**B–C**); 0.2 mm (**D–H**).

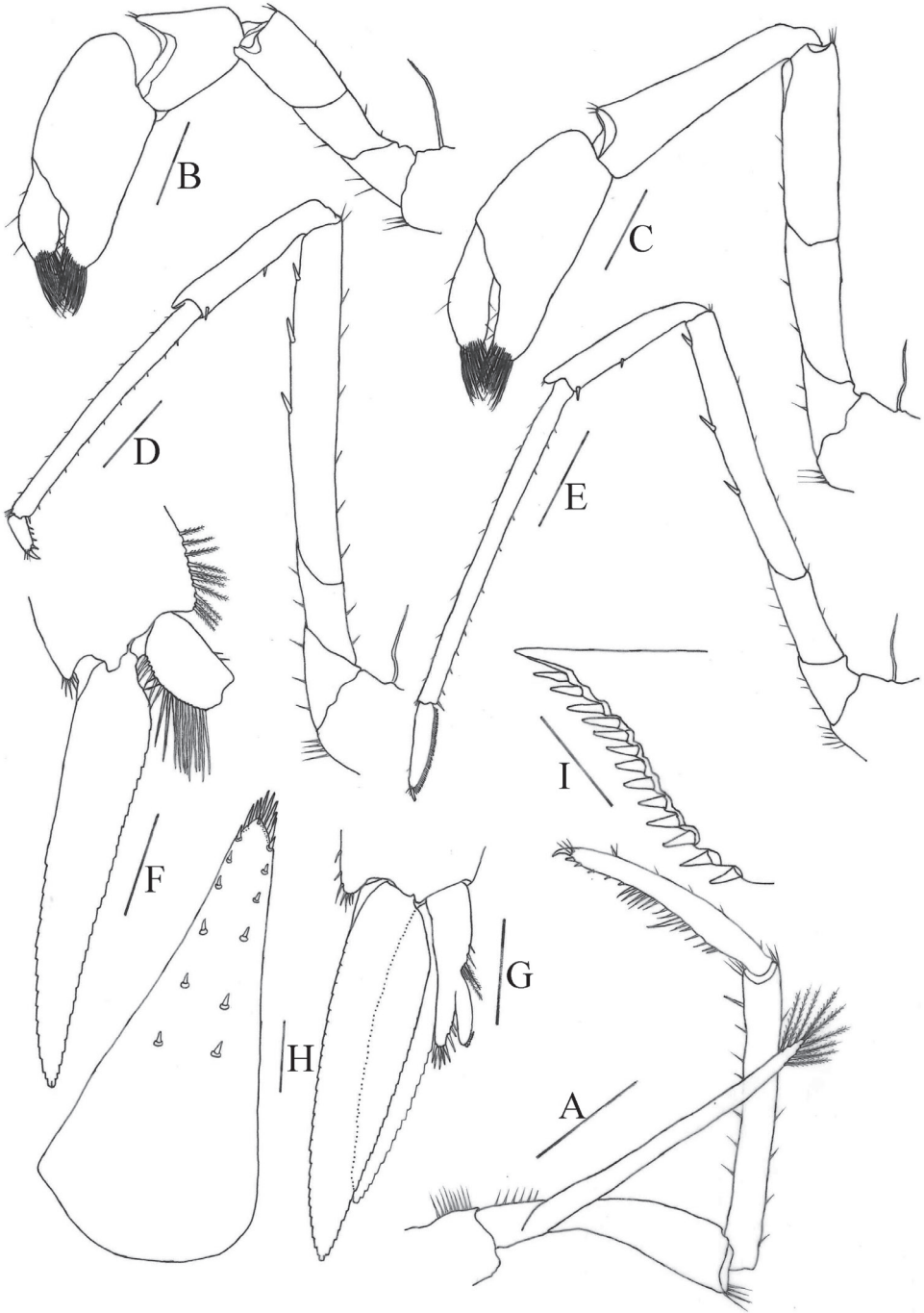


Figure 9. *Caridina cavernicola* **A** third maxilliped **B** first pereopod **C** second pereopod **D** third pereopod **E** fourth pereopod **F** first pleopod **G** second pleopod **H** telson **I** diaeresis of uropodal exopod. Scale bars: 0.5 mm (**A-E, H**); 0.2 mm (**F, G, I**).

Second pereopod (Fig. 9C): Reaches to about end of 2nd antennular peduncle segment, more slender and longer than first pereopod; chela 2.1–2.3 × as long as high; 0.97 × length of carpus; movable finger 2.9 × as long as wide and 0.91 × as long as palm, setal brushes well developed; carpus 3.3–4.2 × as long as wide, excavated distally, about 1.2 × length of merus.

Third pereopod (Fig. 9D): Reaches beyond end of scaphocerite; dactylus about 3.3 × as long as wide, ending in prominent claw-like spine surrounded by simple setae, behind which are 4–5 spines; propodus 4.9–6.4 × length of dactylus, bearing a row thin spinules on posterior and lateral margin, about 12.1 × as long as wide; carpus about 0.68 × length of propodus; merus 1.6–1.9 × length of carpus, with about 3 strong spines on the posterior margin.

Fourth pereopod (Fig. 9E): Reaches middle of 2nd segment of antennular peduncle; dactylus 4.8–5.2 × as long as wide, ending in prominent claw-like spine surrounded by simple setae, behind which is a comb-like row of 61–69 spines; propodus 3.6–4.4 × length of dactylus, bearing a row of spinules on posterior and lateral margins, 16.5–17.1 × as long as wide; carpus 0.50–0.54 × length of propodus; merus 1.3–1.5 × length of carpus, with about three strong spines on the posterior margin.

First pleopod (Fig. 9F): Endopod in male short, rectangle, about 0.26 × length of exopod, about 1.7 × as long as proximally wide, tip concave, inner margin bearing equal two thin spine setae, outer margin bearing nearly equal long and dense spine setae, without an appendix interna.

Second pleopod (Fig. 9G): Endopod about 0.83 × length of exopod; appendix masculina rod-shaped, reaching about 0.49 × length of endopod, inner margin and tip bearing nearly equal spine setae; appendix interna well developed, almost the same size as appendix masculina, reaching about 0.97 × length of appendix masculina, with many cincinnuli distally.

Telson (Fig. 9H): 0.44–0.51 × length of cl, distinctly longer than sixth abdominal segment, posterior margin acutely triangular, with a projection, dorsal surface with 6–7 pairs of stout movable spine setae including the pair at posterior lateral angles; posterior margin with four pairs of intermedial plumose setae, lateral pair of spines subequal to intermedian pairs. Exopodite of the uropod bears a series of 12–15 movable spinules along the diaresis.

Eggs 0.80–0.92 × 1.37–1.40 mm in diameter.

Colouration. Body translucent, rust brown, with small red pigment spots scattered on whole body, with a broad red-brown vertical stripe on each abdominal segment; appendages transparent (Figs 4B–D).

Remarks. *Caridina cavernicola* was known from only two females and one juvenile specimen when it was first collected from a limestone cave in Lenggu Cave, Du'an Yao Autonomous County, Hechi City, Guangxi. Only the name of the cave is mentioned without detailed environmental information and body colour of the shrimps (Liang and Zhou 1993). Attempts to find the Lenggu Cave through enquiring the exact location from local government departments and residents was unfruitful. However, it was most fortunate that we have collected samples from three sites inside the Chengjiang National Wetland Park. This species is abundant amongst leaf litter and the fibrous

roots of riparian trees and plants along the edges of the Chengjiang River. It was also found in small populations in a skylight. No difference was found between individuals collected from the river and skylight sites. We can speculate that the underground water of the skylight may be connected to the Chengjiang River. This also indicates that the shrimp likely only recently invaded the cave environment and can occupy both epigeal and hypogean karst habitats.

Liang (2004) mentioned the status of this species as questionable due to some unusual characters, such as: 1st, 2nd pereopod chela stout; 2nd pereopod carpus disto-dorsally excavated; 3rd, 4th, 5th pereopod propodus posterior margin with numerous long plumose setae. Through this study, however, we have found that the morphological and genetic data are congruent and that this species clearly belongs to the genus *Caridina*.

Ecological notes. Chengjiang National Wetland Park is located in Du'an Yao Autonomous County, Hechi City, Guangxi. It is also a part of the Du'an Subterranean River National Geopark, Guangxi. The Park mainly consists of the Chengjiang River and integrated farming wetland, river wetland and urban wetland, covering a total area of 8.64 km², with a width of 11.7 km and a length of 24.2 km. Chengjiang River originates from two skylights, one is Yantan Pool, located at the foot of Guanyin Mountain in Jiudun Village, Daxing Town, the other is Dongtan Pool, located in Taiyang Village, Daxing Town. Chengjiang River belongs to the Red River system, one of the tributaries of the Pearl River system. The river is 50–80 m wide and 5–10 m deep. Chengjiang River and its associated wetlands are also home to many other rare and endangered endemic species of plants and animals. The seaweed flower, *Ottelia acuminata* is an endangered aquatic plant that is only found in China (Yunnan, Guizhou, Guangxi and Hainan) and can be found in Chengjiang River. Peach blossom jellyfish, *Craspedacusta* sp., appears in skylight 1 at Zhuqing Tun, Dongmiao Village, Dongmiao Township. The teleostean fish, *Metzia formosae* is listed as vulnerable (VU) in the China Red Data of endangered animals: fishes (Yue and Chen 1998) and is also found here. *Yunnanilus pulcherrimus*, *Aphyocypris pulchilineata*, *Metzia longinasus*, *Silurus duanensis* and *Bibarba bibarba* are endemic species of Du'an County (Ye et al. 2016).

Caridina cavernicola were caught alongside *Neocaridina palmata* (Shen 1948) and *Macrobrachium nipponense* in river sites.

Distribution. Know from Guangxi Zhuang Autonomous Region, southwest China.

Discussion

This research was done by comparing DNA barcode sequences, phylogenetic trees were constructed, genetic distances were calculated and ABGD software was applied to classify species. Research results had found that significant barcode gaps can be formed and Automatic partition results of ABGD grouped *Caridina stellata* sp. nov. into a separate group. The results of the division of phylogenetic trees were basically the same as those of ABGD on species. The present results confirmed that the integrated use of DNA barcoding (BI/ML tree, K2P distance and ABGD) are efficient and reliable methods for delineation and

genetic identification of *Caridina stellata* sp. nov. as a new species. At the same time, combined with the research of morphology, this can promote the development of taxonomy.

During the recent sampling along the karst habitats of Du'an County, Guangxi, two species of *Caridina* have been collected. *Caridina cavernicola* was originally found from a subterranean stream near Du'an County, but further surveys have found dense populations in the Chengjiang River.

Narrow distributions, high diversity and a high level of endemism are characteristic of the genus *Caridina*. These isolated and vicariant *Caridina* species occur in karst locations, generally considered as an important part of the natural heritage. They may be particularly vulnerable to anthropogenic activities and face risk of extinction in the future; therefore, more urgent conservation attention may be warranted. Defining potential threats posed by human activities to all *Caridina* species would be the first step in effectively managing their conservation. Guangxi karst landforms have good potential for tourism due to the beautiful natural landscape and ideal climate. *Caridina stellata* sp. nov. is only known from a few hill stream localities. One stream is located in Lotus Hill Scenic Area. The increasing exploitation of tourist resources for human use fails to recognise the needs of the species that live there. Moreover, *C. stellata* has striking colouration and patterns that have received particular attention amongst aquarists. In recent years, it has been collected, reared and traded in commercial aquarium industries. The wild populations will inevitably be threatened by over-harvesting. *Caridina cavernicola* is also facing the same issues due to its distribution in relatively disturbed areas, the Chengjiang National Wetland Park. The population is experiencing considerable stresses and disturbances. The Chengjiang River Basin is surrounded by densely-populated towns. Domestic sewage discharge and wastewater from washing clothes, cleaning vegetables and even people taking showers are problems in many parts of the Chengjiang River (Fig. 4H). Over-exploitation of water for hydroelectricity, agriculture and tourism are also likely to be critical problems. Several hydrotechnical constructions are built along the river, such as irrigation facilities, dams for power generation and landscape. The invasive fish, *Oreochromis niloticus* Linnaeus 1758, can be seen everywhere in the river. In addition, *C. cavernicola* is potentially an ornamental species due to their attractive colour pattern (Figs 4B–D) and may also be impacted by harvesting for the aquarium trade in the future. Given that information, these threats are expected to lead to habitat destruction and fragmentation, resulting in population decline and this situation might be further aggravated by the lack of regulations and active measures for protection. Therefore, the risk of extinction for these two species can be classified into vulnerable (VU) using the IUCN Red List Categories and Criteria (IUCN, 2019, version 4.1).

To deal with the anthropogenic disturbances, regular monitoring of wild population changes should be carried out and campaigns that promote environmental education and raise tourists' awareness of the importance of biodiversity should be encouraged. In addition, developing commercial aquaculture techniques for the captive breeding of ornamental species is urgently needed in order to guarantee a sustainable supply of shrimp for the industry. This can have certain advantages in reducing the risk of extinction if populations can be maintained in captivity in the long term. More

thorough sampling efforts, coupled with molecular identification, will be needed in the future to better understand the diversity and distribution of *Caridina* species in Guangxi. The number of described species will doubtlessly increase dramatically in the near future and more information on their evolution and ecology will be known as more karst habitats are studied. The biodiversity conservation of karst habitats will be greatly strengthened.

Acknowledgements

This study was supported by the “Guangdong Environmental Protection Special Project” (PM-zx555-202106-195) (PM-zx555-202107-208) and the “Key Laboratory of Tropical and Subtropical Fishery Resource Application and Cultivation of Ministry of Agriculture and Rural Affairs” (9020190008) and also the “Demonstration base for joint training of Postgraduates in Guangdong Province in 2021”. Part of this work was funded by the Key projects of the Academic Foundation of Foshan University (Fish fry screening and counting device). Additional support for this project was provided by “Investigation on crustaceans in the priority area of Mangrove Diversity Protection in Guangxi Zhuang Autonomous Region” (kh19051). Funds from the “Foshan University of Science and Technology Graduate Top-notch Innovative Talents Cultivation Program” also supported this project. Additional support for this project was provided by Guangdong College students’ innovation and entrepreneurship (XJ2018247 and XJ2018222). Thanks are also due to subject editor Luis Ernesto Bezerra, two copy editors (Mike Skinner and Zdravka Zorkova) and reviewer Valentin de Mazancourt for providing their valuable suggestions, which greatly improved the manuscript.

References

- Cai Y (2014) Atyid shrimps of Hainan Island, southern China, with the description of a new species of *Caridina* (Crustacea, Decapoda, Atyidae). *Advances in freshwater decapod systematics and biology*, 207–231. https://doi.org/10.1163/9789004207615_013
- Cai YX, Ng PKL (2018) Freshwater shrimps from karst caves of southern China, with descriptions of seven new species and the identity of *Typhlocaridina linyunensis* Li and Luo, 2001 (Crustacea: Decapoda: Caridea). *Zoological Studies [Taipei, Taiwan]* 57(27): 1–33.
- Chen QH, Chen WJ, Zheng XZ, Guo ZL (2020) Two freshwater shrimp species of the genus *Caridina* (Decapoda, Caridea, Atyidae) from Dawanshan Island, Guangdong, China, with the description of a new species. *ZooKeys* 923: 15–32. <https://doi.org/10.3897/zookeys.923.48593>
- De Grave S, Franssen CHJM (2011) Carideorum Catalogus: The recent species of the Dendrobranchiate, Procarididean and Caridean Shrimps (Crustacea: Decapoda). *Zoologische Mededelingen (Leiden)* 85: 195–588.
- De Grave S, Smith KG, Adeler NA, Allen DJ, Alvarez F, Anker A, Cai Y, Carrizo SF, Klotz W, Mantelatto FL, Page TJ, Shy J-Y, Villalobos JL, Wowor D (2015) Dead Shrimp Blues:

- A Global Assessment of Extinction Risk in Freshwater Shrimps (Crustacea: Decapoda: Caridea). PLoS ONE 10(3): e0120198. <https://doi.org/10.1371/journal.pone.0120198>
- De Mazancourt V, Klotz W, Marquet G, Mos B, Rogers DC, Keith P (2021) New Insights on Biodiversity and Conservation of Amphidromous Shrimps of the Indo-Pacific islands (Decapoda: Atyidae: *Caridina*). In: Kawai T, Rogers DC (Eds) Recent Advances in Freshwater Crustacean Biodiversity and Conservation, CRC Press, 381–404. <https://doi.org/10.1201/9781003139560-12>
- Do VT, von Rintelen T, Dang VD (2020) Descriptions of two new freshwater shrimps of the genus *Caridina* H. Milne Edwards, 1837 (Crustacea: Decapoda: Atyidae) from northern Vietnam. The Raffles Bulletin of Zoology 68: 404–420. <https://doi.org/10.26107/RBZ-2020-0057>
- Feng S, Chen QH, Guo ZL (2021) Integrative taxonomy uncovers a new stygobiotic *Caridina* Species (Decapoda, Caridea, Atyidae) from Guizhou Province, China. ZooKeys 1028: 29–47. <https://doi.org/10.3897/zookeys.1028.63822>
- Guo ZL, Wang XQ (2005) *Caridina longiacuta*, a new species of freshwater atyid shrimp (Decapoda, Atyidae) from Hunan Province, China. Zootaxa 1008(1): 13–20. <https://doi.org/10.11646/zootaxa.1008.1.2>
- IUCN (2019) The IUCN Red List of Threatened Species. Version 2018-2, 17 January 2019. <http://www.iucnredlist.org>
- Kalyaanamoorthy S, Minh BQ, Wong TKE, Haeseler AV, Jermini LS (2017) ModelFinder: Fast model selection for accurate phylogenetic estimates. Nature Methods 14(6): 587–591. <https://doi.org/10.1038/nmeth.4285>
- Katoh K, Standley DM (2013) MAFFT multiple sequence alignment software version 7: Improvements in performance and usability. Molecular Biology and Evolution 30(4): 772–780. <https://doi.org/10.1093/molbev/mst010>
- Klotz W, von Rintelen T (2014) To “bee” or not to be – on some ornamental shrimp from Guangdong Province, Southern China and Hong Kong SAR, with descriptions of three new species. Zootaxa 3889(2): 151–184. <https://doi.org/10.11646/zootaxa.3889.2.1>
- Kumar S, Stecher G, Tamura K (2016) MEGA7: Molecular evolutionary genetics analysis version 7.0 for bigger datasets. Molecular Biology and Evolution 33(7): 1870–1874. <https://doi.org/10.1093/molbev/msw054>
- Li J, Li S (2010) Description of *Caridina alba*, a new species of blind atyid shrimp from Tenglongdong Cave, Hubei Province, China (Decapoda, Atyidae). Crustaceana 83(1): 17–27. <https://doi.org/10.1163/001121609X12530988607399>
- Liang XQ (2004). Fauna Sinica. Invertebrata: Crustacea: Decapoda: Atyidae. Science Press, Beijing, 375 pp. [in Chinese with English abstract]
- Liang XQ, Yan SL (1981) A new genus and two new species of freshwater prawns (Crustacea Decapoda) from Guangxi, China. Dong Wu Fen Lei Xue Bao 6(1): 31–35. [In Chinese with English abstract]
- Liang XQ, Yan SL (1983) A new species of *Caridina* (Crustacea, Decapoda) from Guangxi, China. Dong Wu Fen Lei Xue Bao 8(3): 252–254. [in Chinese with English abstract]
- Liang XQ, Zhou J (1993) Study on new atyid shrimps (Decapoda, Caridea) from Guangxi, China. Shui Sheng Sheng Wu Hsueh Bao 17(3): 231–239. [In Chinese with English abstract]

- Liu XY, Guo ZL, Yu H (2006) *Caridina xiangnanensis*, a new freshwater atyid shrimp (Crustacea, Decapoda, Atyidae) from Hunan Province, China. *Zootaxa* 1153(1): 43–49. <https://doi.org/10.11646/zootaxa.1153.1.5>
- Liu YS, Wang JY, Deng XZ (2008) Rocky land desertification and its driving forces in the Karst Areas of Rural Guangxi, Southwest China. *Journal of Mountain Science* 5(4): 350–357. <https://doi.org/10.1007/s11629-008-0217-6>
- Nguyen LT, Schmidt HA, von Haeseler A, Minh BQ (2015) IQ-TREE a fast and effective stochastic algorithm for estimating maximum-likelihood phylogenies. *Molecular Biology and Evolution* 32(1): 268–274. <https://doi.org/10.1093/molbev/msu300>
- Oliveira CM, Terossi M, Mantelatto FL (2019) Phylogeographic structuring of the amphidromous shrimp *Atya scabra* (Crustacea, Decapoda, Atyidae) unveiled by range-wide mitochondrial DNA sampling. *Marine and Freshwater Research* 70(8): 1078–1093. <https://doi.org/10.1071/MF18272>
- Ronquist F, Teslenko M, van der Mark P, Ayres DL, Darling A, Höhna S, Larget B, Liu L, Suchard A, Huelsenbeck JP (2012) MrBayes 3.2: Efficient Bayesian phylogenetic inference and model choice across a large model space. *Systematic Biology* 61(3): 539–542. <https://doi.org/10.1093/sysbio/sys029>
- Shen CJ (1948) On three new species of *Caridina* (Crustacea Macrura) from south-west China. *Contributions from the Institute of Zoology, National Academy of Peiping* 4(3): 119–123.
- Stimpson W (1860) *Prodromus descriptionis animalium everttebratorum, quae in Expeditione ad Oceanum Pacificum Septentrionalem, a Republica Federata missa, Cadwaladaro Ringgold et Johanne Rodgers Ducibus, observavit et descripsit. Pars VIII. Crustacea Macrura.* *Proceedings of the Academy of Natural Sciences of Philadelphia* 22–47(97–116).
- von Rintelen K, Cai Y (2009) Radiation of endemic species flocks in ancient lakes: systematic revision of the freshwater shrimp *Caridina* H. Milne Edwards, 1837 (Crustacea: Decapoda: Atyidae) from the ancient lakes of Sula wesi, Indonesia, with the description of eight new species. *The Raffles Bulletin of Zoology* 57(2): 343–452.
- von Rintelen K, von Rintelen T, von Meixner M, Lüter C, Cai Y, Glaubrecht M (2007) Freshwater shrimp-sponge association from an ancient lake. *Biology Letters* 3(3): 262–264. <https://doi.org/10.1098/rsbl.2006.0613>
- Xu DJ, Li DX, Zheng XZ, Guo ZL (2020) *Caridina sinanensis*, a new species of stygobiotic atyid shrimp (Decapoda, Caridea, Atyidae) from a karst cave in the Guizhou Province, southwestern China. *ZooKeys* 1008: 17–35. <https://doi.org/10.3897/zookeys.1008.54190>
- Ye F, Zhang P, Xiu LH, Yang J (2016) G-F Diversity Indices and Conservation Strategies on Fishes in the Du'an Chengjiang National Wetland Park. *Journal of Nanjing Normal University* 39(2): 78–83. <https://doi.org/10.3969/j.issn.1001-4616.2016.02.015> [Natural Science Edition]
- Yu SC (1938) Studies on Chinese *Caridina* with descriptions of five new species. *Bulletin Fan Memorial Institute of Biology [Zoology]* 8(3): 275–310.
- Yue PQ, Chen YY (1998) *China red data of endangered animals:fishes.* Science Press, Beijing, Hong Kong, New York, 244 pp.
- Zhou GF, Zhang WG, Wong K, Huang JR (2021) Atyid shrimps of the genus *Caridina* (Decapoda, Caridea, Atyidae) of Taipa-Coloane Island, Macau, China, with description of a new species. *Crustaceana*. *Crustaceana* 94(9): 1103–1119. <https://doi.org/10.1163/15685403-bja10146>

Panstrongylus noireai, a remarkable new species of Triatominae (Hemiptera, Reduviidae) from Bolivia

Hélcio R. Gil-Santana¹, Tamara Chavez², Sebastián Pita³,
Francisco Panzera³, Cleber Galvão⁴

1 Laboratório de Diptera, Instituto Oswaldo Cruz, Av. Brasil, 4365, 21040-360, Rio de Janeiro, RJ, Brazil
2 Instituto Nacional de Laboratorios de Salud, Laboratorio de Entomología Médica, La Paz, Bolivia **3** Universidad de la República, Facultad de Ciencias, Sección Genética Evolutiva, Montevideo, Uruguay **4** Laboratório Nacional e Internacional de Referência em Taxonomia de Triatomíneos, Instituto Oswaldo Cruz, Fiocruz, Pavilhão Rocha Lima, Avenida Brasil, 4365, Mangueiras, RJ, Brazil

Corresponding author: Cleber Galvão (clebergalvao@gmail.com)

Academic editor: Jader Oliveira | Received 9 February 2022 | Accepted 24 March 2022 | Published 14 June 2022

<http://zoobank.org/60067924-0516-42DF-85C5-B31E0C01B28C>

Citation: Gil-Santana HR, Chavez T, Pita S, Panzera F, Galvão C (2022) *Panstrongylus noireai*, a remarkable new species of Triatominae (Hemiptera, Reduviidae) from Bolivia. ZooKeys 1104: 203–225. <https://doi.org/10.3897/zookeys.1104.81879>

Abstract

Panstrongylus noireai sp. nov. from Bolivia is described based on male and female specimens. Although morphologically almost indistinguishable from *Panstrongylus rufotuberculatus* (Champion, 1899), the new species shows remarkable chromosome and molecular features, which are very distinctive among all others *Panstrongylus* species. The new species is also separated by some characteristics of the processes of the endosoma of the male genitalia. An updated key for species of *Panstrongylus* is provided.

Keywords

Chagas disease vectors, genitalia, kissing bug, taxonomy

Introduction

The Triatominae are classified as a subfamily of Reduviidae (Hemiptera, Heteroptera), defined by their blood-sucking habit and morphological adaptations associated with host-finding and blood-feeding (Schofield and Galvão 2009). Currently, there are 154 extant and three fossil species distributed in 18 genera and five tribes in Triatominae (Dale et al.

2021; Galvão 2021). All of them are considered as potential vectors of the protozoan *Trypanosoma cruzi* (Chagas, 1909), the causative agent of Chagas disease or American trypanosomiasis, which still is a serious health problem to most Latin American countries (Arias et al. 2021). Among the five tribes included in Triatominae, the tribe Triatomini has ten genera (Galvão 2021), among which *Panstrongylus* Berg, 1879 has several species involved in the transmission of *T. cruzi* in Central and South America (Patterson et al. 2009).

Berg (1879) created the genus *Panstrongylus* for a single new species he was describing, *P. guentheri* Berg, which is the type species of this genus by monotypy. He regarded *Panstrongylus* as being close to *Lamus* Stål, 1859. Champion (1899) described *Lamus rufotuberculatus* based on a single male from Panama. As *Lamus* Stål, 1859 was a preoccupied name by *Lamus* Stål, 1854, a genus of Pentatomidae, Kirkaldy (1904) proposed a new name for it, *Mestor* Kirkaldy. The species was transferred to *Panstrongylus* by Pinto (1931), with the resulting new combination, *P. rufotuberculatus* (Champion). Pinto (1931) argued that *Mestor* should be considered a synonym of *Panstrongylus*. Usinger (1939), however, maintained these two latter genera as valid. Lent and Pifano (1940) strongly defended the synonym of *Mestor* under *Panstrongylus* as proposed by Pinto (1931), which was accepted by subsequent authors so far, with the exception of Usinger (1944), who still considered the validity of both genera. The main novelties involving species of *Panstrongylus*, after the classical taxonomical treatment of the group by Lent and Wygodzinsky (1979), were recently summarized by Monteiro et al. (2018), Costa et al. (2021), Galvão (2021), and Paiva et al. (2022).

Panstrongylus has been considered monophyletic based on morphological features (Lent and Wygodzinsky 1979). However, molecular studies using several nuclear (ITS-2, 18S, 28S, ultraconserved elements), and mitochondrial (16S, coI, coII, cyt b) markers demonstrated a paraphyletic status for *Panstrongylus* (Hypša et al. 2002; Marcilla et al. 2002; Justi et al. 2014; Monteiro et al. 2018; Kieran et al. 2021; Pita et al. 2021).

Panstrongylus rufotuberculatus has been recorded in several countries: Mexico, Panama, Costa Rica, Colombia, Venezuela, French Guiana, Suriname, Ecuador, Peru, Bolivia, Brazil, and Argentina (Galvão et al. 2003; Bérenger et al. 2009; Patterson et al. 2009; Hiwat 2014).

Beginning with the observation of Lent and Pifano (1940), several authors have recorded natural infection of *P. rufotuberculatus* with *T. cruzi* as summarized by Patterson et al. (2009). These latter authors also summarized host observation to this species, which have included different wild and domestic mammals and humans as well.

Panstrongylus rufotuberculatus has been considered as a sylvatic species, which frequently invades human dwellings as it is attracted by electric light (Lent and Wygodzinsky 1979; Salomón et al. 1999; Patterson et al. 2009; Gorla and Noireau 2010). However, truly domestic populations were reported only in some areas of southern Ecuador (Abad-Franch et al. 2001), while breeding colonies have been found inside dwellings in Bolivia and Peru too (Marín et al. 2007; Gorla and Noireau 2010). This species has been incriminated as a vector of Chagas disease in Andean and coastal foci of Ecuador, whereas its presence in the municipality of Amalfi (Antioquia, Colombia) is considered as a major epidemiological risk factor (by being the second most common triatomine caught inside buildings) (Wolff et al. 2001; Patterson et al. 2009; Gorla and Noireau 2010).

Following the description of the male holotype by Champion (1899), Lent and Pifano (1940), Lent and Jurberg (1975) and Lent and Wygodzinsky (1979) provided thorough redescriptions of *P. rufotuberculatus*. These latter authors and some others, e.g., Salomón et al. (1999) and Hiwat (2014), have emphasized the morphological and chromatic variation of this species. Its male genitalia was thoroughly described and figured by Lent and Jurberg (1975), while Lent and Wygodzinsky (1979) commented on some features of it.

Although almost all species of *Panstrongylus* have been recorded as possessing only a paired [lateral] process in the endosoma (Lent and Jurberg 1975; Lent and Wygodzinsky 1979; Jurberg et al. 2001; Papa et al. 2003; Bérenger and Blanchet 2007; Ayala 2014, pers. comm.), *P. rufotuberculatus* has been recorded as the only species of the genus with two paired [lateral] process in the endosoma (Lent and Jurberg 1975; Lent and Wygodzinsky 1979). This latter feature, together with presence of body scalelike setae and an apically bilobed clypeus were all considered the three apomorphies of this species in the phylogenetic scheme proposed by Lent and Wygodzinsky (1979). These authors, however, recorded that these latter two features in *P. rufotuberculatus* were also present as what they considered as plesiomorphic states among *Panstrongylus* spp. (not scalelike setae and not bilobed [unilobed] clypeus, respectively). Salomón et al. (1999), by their turn, recorded scalelike setae but only unilobed clypeus among specimens of *P. rufotuberculatus* from Argentina.

The female genitalia in Triatominae was considered uniform by several authors and, by consequence, without taxonomic significance (Lent and Wygodzinsky 1979; Rodrigues et al. 2018). However, in just over the last decade several works, summarized by Rodrigues et al. (2018), have proven that the study of female genitalia is useful in many cases to the taxonomy in Triatominae, showing that in fact they present characteristics of diagnostic value. Rodrigues et al. (2018) studied, compared, and figured with SEM images the female genitalias of 26 species belonging to seven genera of Triatominae, including *P. rufotuberculatus*.

Pita et al. (2021) through a multidisciplinary approach suggested speciation within populations of *P. rufotuberculatus*. Extensive chromosomal analyses supported that the two chromosomal groups could represent different closely related species. Molecular and morphometric analyses reinforced the marked cytogenetic differences. Therefore, they proposed that Bolivian individuals constituted a new *Panstrongylus* species, which is herewith described as *Panstrongylus noireaui* sp. nov., based on male and female specimens. A detailed morphological description of the new species is provided, comparing its characteristics with extensive previous data from the literature, and examination of specimens of *Panstrongylus rufotuberculatus* from different countries.

Materials and methods

All type specimens of *Panstrongylus noireaui* sp. nov. and non-type specimens of *Panstrongylus rufotuberculatus* examined here are deposited in the “Coleção de Triatomíneos do Instituto Oswaldo Cruz” (CTIOC) of the “Laboratório Nacional e

Internacional de Referência em Taxonomia de Triatomíneos” (LNIRTT) at Oswaldo Cruz Institute, Rio de Janeiro, Brazil.

All the figures were produced by the first author (HRG-S). The photographs were obtained using digital cameras (Nikon D5600 with a Nikon Macro Lens 105 mm, Sony DSC-W830). Drawings were made using a camera lucida. Dissections of the male genitalia were made by first removing the pygophore from the abdomen with a pair of forceps and then clearing it in 20% NaOH solution for 24 hours. The dissected structures were studied and photographed in glycerol. Images were edited using Adobe Photoshop CS6.

General morphological terminology and particularly those of the male genitalia portions used here follows mostly Lent and Wygodzinsky (1979), while to female genitalia Rodrigues et al. (2018) is followed. However, some portions of head terminology follow Schuh and Weirauch (2020), in which “rostrum” is named labium. In this particular, the [visible] segments of the labium are numbered II to IV, given that the first segment is said to be lost or fused to the head capsule (Weirauch 2008). In addition, according to Schuh et al. (2009), for the convention of numbering labial segments in the Reduviidae, the apical segment should be considered as number four and then counted backwards towards the base. Jugum (pl. juga) *sensu* Lent and Wygodzinsky (1979) is named mandibular plate. In male genitalia, “vesica” as recognized by Lent and Jurberg (1975) and Lent and Wygodzinsky (1979) has been considered to be absent in reduviids. The assumed equivalent structure in reduviids is a somewhat sclerotized appendage of the phallosoma or the endosoma (Forero and Weirauch 2012), but not the homologous vesica that occurs in other heteropterans such as Pentatomomorpha (Rédei and Tsai 2011). Thus, this term is not used here for the median process of endosoma, which is named as such.

When describing label data, a slash (/) separates different labels.

Results

Taxonomy

Triatominae Jeannel, 1919

Triatomini Jeannel, 1919

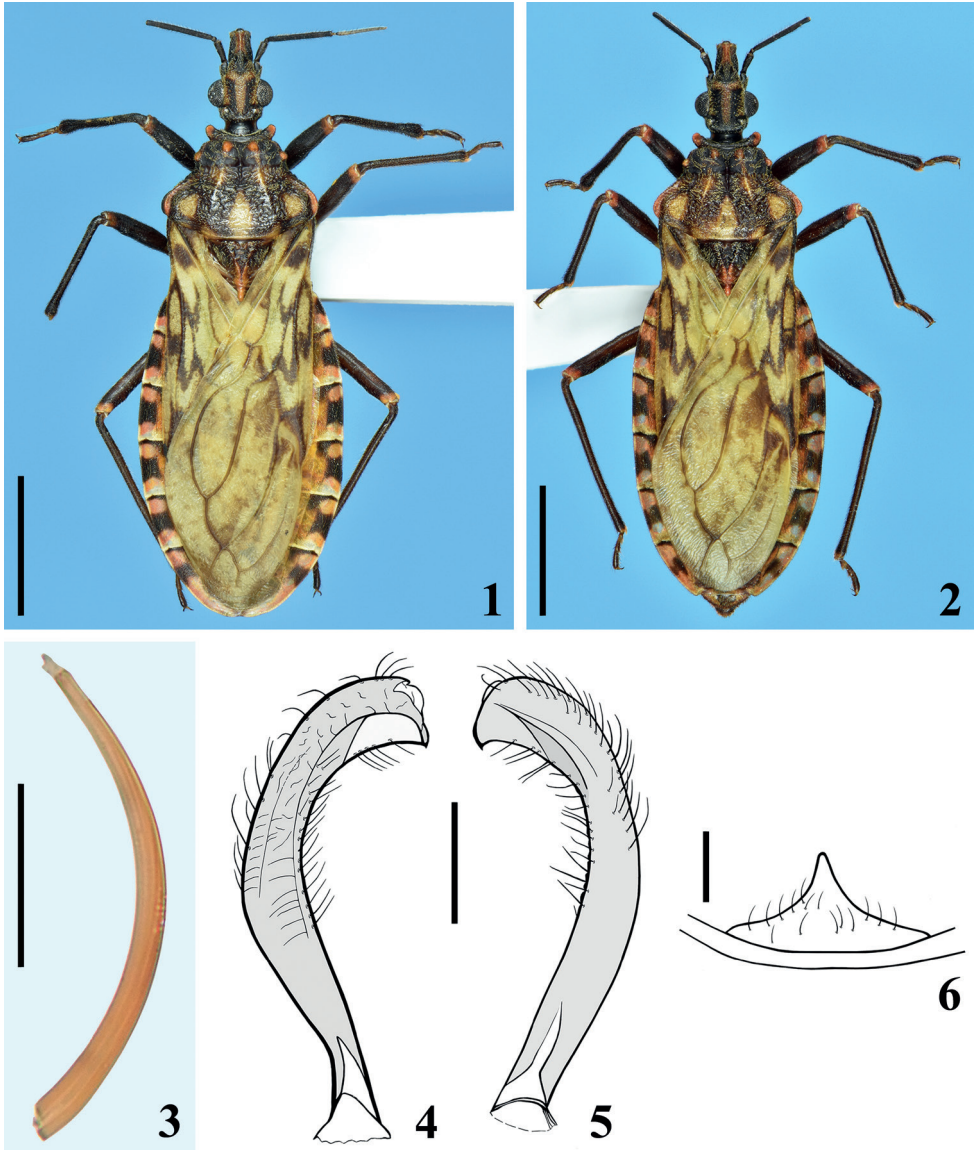
***Panstrongylus* Berg, 1879**

***Panstrongylus noireau* sp. nov.**

<http://zoobank.org/5126A8F8-0FEA-4265-8669-41D03756693E>

Figs 1–11

Type material. BOLIVIA, La Paz Department, Ildefonso de las Muñecas Province, Ayata locality, community of Camata (15°14'22"S, 68°44'52"W), 2004, **Holotype**, male [13177, CTIOC]. **Paratypes** 2 male [13178, 13179, CTIOC], 2 female paratypes [13180, 13181, CTIOC].



Figures 1–6. *Panstrongylus noireai* sp. nov. **1, 2** habitus, dorsal view **1** male holotype **2** female paratype **3** body seta **4, 5** left paramere **4** ventral view **5** dorsal view **6** median process of pygophore, dorsal view. Scale bars: 5.0 mm (**1, 2**); 0.5 mm (**4, 5**); 0.2 mm (**6**); 0.04 mm (**3**).

Diagnosis. *Panstrongylus noireai* sp. nov. can be morphologically separated from *P. rufotuberculatus* mainly by the lateral processes of endosoma, which are smooth in the former and with numerous and delicate teeth at apical portion in the latter species. Additionally, whilst the elongate process which is present on the ventral portion of the lateral flap like prominences of the dorsal phallothecal plate is thinner and almost straight in *P. noireai* sp. nov., it is curved and larger in *P. rufotuberculatus*.

Description. Male. Figs 1, 3–11. Measurements are given in Table 1. **Coloration** (Fig. 1). General coloration brownish black to blackish with orange to yellowish and reddish markings on portions of body, whereas the hemelytra are pale greenish with extensive darkened markings. **Head:** blackish, clypeus reddish on approximately its apical half; a red brownish median longitudinal band, which runs from the space between ocelli to anterior portion, near antennifer tubercles, where it diverges laterally, forming a figure similar to a “T” or a “Y”; area around dorsal portion of eyes with same coloration; mandibular plates, apex of labial segment IV, lateral and ventral portions of collum somewhat paler, red brownish to yellow-brownish, respectively. **Thorax:** blackish; fore lobe of pronotum with anterolateral angles, discal and lateral tubercles and a straight marking above the latter, and dorsal surface of humeral angles reddish; hind lobe of pronotum with the following orange yellowish markings: a pair of small irregu-

Table 1. Measurements (mm) of male specimens ($n = 3$) of *Panstrongylus noireau* sp. nov.

	Holotype	Paratype 1	Paratype 2	Mean
Total length	20.7	19.8	19.6	20.04
Head length	3.4	3.2	3.2	3.27
Anteocular portion	1.8	1.7	1.65	1.72
Postocular portion	0.5	0.5	0.5	0.5
Head width across eyes	2.3	2.4	2.3	2.33
Interocular distance (synthlipsis)	1.2	1.1	1.1	1.17
Right eye: dorsal transverse width	0.6	0.5	0.6	0.57
Right eye: length on dorsal view	1.0	1.0	0.9	0.97
External distance between ocelli	1.3	1.4	1.3	1.33
Antennal segment I	0.7	0.7	0.8	0.73
Antennal segment II	2.3	2.3	2.3	2.3
Antennal segment III ($n = 1$)	1.8	Abs.	Abs.	1.8
Antennal segment IV ($n = 0$)	Abs.	Abs.	Abs.	–
Labium segment II	0.9	0.9	1.0	0.93
Labium segment III	2.4	2.4	2.3	2.37
Labium segment IV	0.7	0.7	0.7	0.7
Pronotum total length	3.7	3.5	3.5	3.57
Pronotum fore lobe length	1.1	1.0	1.0	1.03
Pronotum hind lobe length	2.6	2.5	2.5	2.53
Pronotum maximum width	5.5	5.0	5.0	5.17
Scutellum length	2.2	2.0	1.9	2.03
Fore femur	3.5	3.4	3.5	3.47
Fore femur max. width	0.75	0.7	0.7	0.72
Fore tibia	3.6	3.4	3.4	3.47
Spongy fossa of fore tibia	0.25	0.25	0.3	0.27
Fore tarsus	1.3	1.4	1.5	1.4
Middle femur	3.8	3.5	3.5	3.6
Middle tibia	3.9	3.8	3.7	3.8
Spongy fossa of middle tibia	0.25	0.2	0.2	0.23
Middle tarsus	1.4	1.4	1.4	1.4
Hind femur	5.0	4.7	4.8	4.83
Hind tibia	6.2	5.9	5.7	5.93
Hind tarsus	1.5	1.5	1.5	1.5
Abdomen length	11.2	10.8	11.0	11.0
Abdomen max. width	7.1	6.3	6.0	6.47

lar spots, on anterior portion of submedian carinae, adjacent to transverse sulcus; a somewhat large pair, in which each spot lies between submedian carinae and humeral angle on posterior half, a larger posterior median suboval spot, which ends on posterior margin; a very thin stripe on posterior margin which becomes somewhat larger at the end of submedian carinae on posterior margin and interrupted sublaterally. Rounded reddish to yellow reddish spot on supracoxal lobes, larger on fore lobe and progressively somewhat smaller on middle and hind lobes; a median yellowish marking on posterior margin of mesosternum adjacent to metasternum. Scutellum with posterior process reddish. Legs: blackish to black brownish; trochanters with external portion, mainly adjacent to femora, yellowish; extreme base of femora, adjacent to respective trochanter, somewhat paler; apex of femora reddish on dorsal and lateral surfaces; base of segment II of all tarsi somewhat paler. Hemelytra: greenish or pale green with extensive blackish to brownish markings in a mottled pattern, including larger dark spots on basal, lateral, and apical portions of corium; brownish spots on basal portion of membrane cells and darkened lines and connecting spots over, parallel or between veins of corium. **Abdomen.** Connexivum segments with a reddish tint; each segment with a large median subquadrate to subrectangular blackish spot, which is smaller and subtriangular on segment II, and is located on mid portion of basal half on the last segment; these large median black spots reach outer margin of connexivum and its medial suture on ventral portion, but are far from the medial suture in dorsal portion for a distance approximately the same as transverse width of the spot; portion between the black median spot and medial suture brownish; in the last segment, a small and faint dark spot on its median portion, distally; additionally, each connexival segment with a basal thin blackish stripe and distally pale to yellowish; the basal dark stripe variably enlarged on inner portion, except on segment II. Sternites blackish to brownish black with spiracles and area just around them yellowish. Genital segments darkened. **Vestiture:** body integument covered with numerous adpressed golden, yellowish, or somewhat darkened simple setae (Fig. 3). **Head** with short adpressed golden setae, which are absent or very sparse on dorsal blackish portion between eyes. Antennae: segment I with numerous adpressed darkened setae, sparser on ventral side and more numerous on apical margins of dorsal side of the segment; segment II covered with curved somewhat more elongate setae and very numerous, short, thin, whitish setae on anterior and ventral portions; segment III covered with very numerous, short, thin, whitish setae and sparser long, darkened, almost straight setae; segment IV absent. Labium covered by longer, thin, curved setae, which are progressively more numerous towards apical portion of segment III and segment IV; labial segment IV with scattered longer setae too. Neck glabrous. **Thorax** and **abdomen** covered with short adpressed golden setae, which become somewhat thinner and paler on ventral portions of thorax, sternites and femora; glabrous areas on smooth portions of fore lobe of pronotum, mid and distal portion of clavus of hemelytra, lateral portions of mesosternum and irregular lateral areas of sternites; membrane of hemelytra completely glabrous. Tibiae and tarsi with more numerous, thicker, and darker setae, which become somewhat reddish on apex of tibiae and tarsi, ventrally, where they are a little longer and even more numerous too.

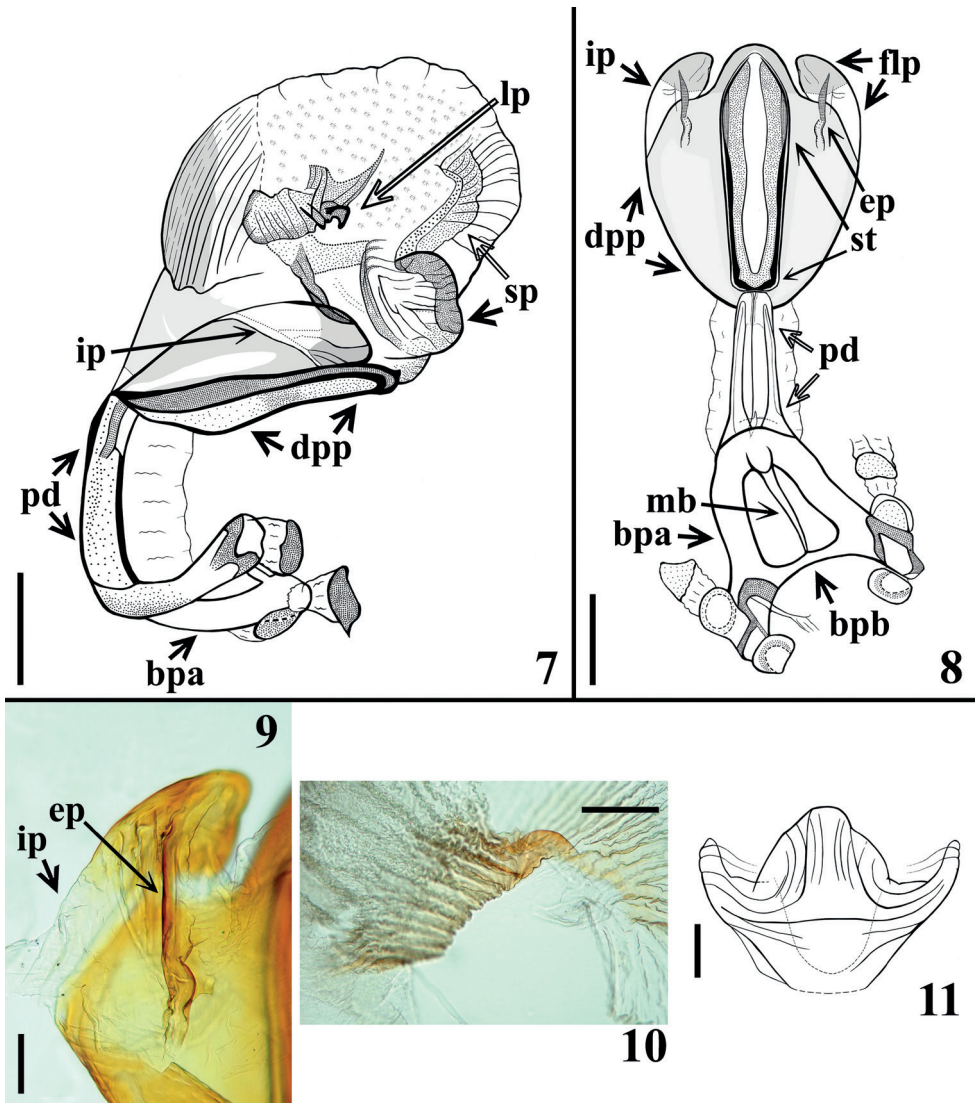
Laterobasal small patches of very thin and numerous short yellowish setae on metasternum and sternite II, just below middle and hind coxae. **Structure: Head:** with rugous integument; slightly shorter than pronotum (ratio head/pronotum length: 1:1.08–1.09); longer than larger (ratio head length/width across eyes: 1: 0.67–0.7); anteocular portion length between 3–4 × the postocular region, with respective ratio: 1:0.28–0.30; eyes globose, in lateral view slightly surpassing level of ventral margin but not reaching dorsal outline of head; ratio width of an eye/interocular transverse distance (synthlipsis): 1:1.84–2.4; clypeus larger on posterior half, with anterior margin almost transversely straight. Antennae: ratio of antennal segments (I–III): 1:2.87–3.3:2.5; segment I not surpassing clypeus, somewhat curved and thickened to the apex; segments II and III subcylindrical, the latter thinner than the former; segment IV absent in all specimens. Dorsal area in which there is a median longitudinal brownish to reddish band, with integument more rugous and somewhat elevated, mainly on the divergent anterior branches. Labium straight, reaching stridulatory sulcus at its anterior half, ratio of segments: 1:2.3–2.7:0.7–0.8. **Thorax:** anterior collar well developed, with integument very finely rugous, subrounded anterolateral angles prominent, compressed dorsoventrally; integument of fore lobe of pronotum almost only rugous on its ridges, on which setae are present; discal and lateral tubercles prominent, rounded; a very shallow crest above lateral tubercles; transverse (interlobar) sulcus large and deep; longitudinal median sulcus linear, extending from anterior margin of fore lobe to approximately basal third of hind lobe of pronotum; hind lobe of pronotum ~ 2.5 × as long as fore lobe, with integument coarsely rugous; submedian carinae shallow, a little larger on basal third; humeral angles prominent somewhat subangular; pleural and sternal integument slightly rugous, completely smooth and shiny on lateral portions of meso- and metasternum; mesosternum with a conical, prominent median protuberance. Scutellum subtriangular with shallow carinae, integument rugous; apex of its process small and rounded. Hemelytra not attaining tip of abdomen by a short distance. Fore trochanter with a basomedial small spine on anterior portion, adjacent to anterior edge of fore coxa. Femora somewhat thickened; fore femora 4.7–4.8 × as long as wide; at apex of all femora, a pair of very small laterodorsal prominences; on ventral submedian distal portion of fore and middle femora, laterally to small shallow glabrous areas, a pair of small prominences variably developed, as small teeth with a terminal seta in the paratypes and sometimes united by a thin shallow ridge. Tibiae straight, thinner; fore tibia thicker at apex, with a mesal distal comb and four to five short spines on distal fifth, ventrally, which may be not easy to distinguish from the very numerous and thicker setae implanted in this portion of the segment; middle tibiae very slightly thicker at apex; spongy fossa very small, with ~ 7–8% (foreleg) to 5–6.5% (middle leg) of respective tibial length. **Abdomen:** sternites somewhat flattened on median portion; integument finely striated transversely; spiracles small, very close to connexival suture. **Male genitalia** (Figs 4–11): pygophore sub-squared; parameres apices close in resting position. Median process of pygophore weakly sclerotized, subtriangular, pointed to apex (Fig. 6). Parameres symmetrical, curved, with a subapical very small sclerotized pointed and curved tooth; several setae on outer and inner surface of distal two thirds (Figs 4, 5). Phallus with articulatory apparatus moderately short, basal plate arms (bpa)

slightly converging towards apex; basal plate bridge (bpb) and median bridge (mb) narrow; pedicel (pd) subretangular (Figs 7, 8). Dorsal phallothecal plate (dpp) somewhat enlarged to the apex, suboval in shape (Fig. 8), with a pair of lateral flap like prominences (flp) at apex; its intermediate portion (ip), between apical half of flap like prominences and main portion of phallothecal plate, much less sclerotized (Figs 7–9); on the ventral portion of the lateral flap like prominence, a moderately elongate process (ep) is present (Figs 8–9); struts (st) subparallel, united at base, somewhat diverging to the apex, in which they are separated (Fig. 8). Endosoma with pair of lateral smooth processes (lp) on approximately median portion (Figs 7, 10) and a subapical median (sp) moderately developed process, which has fine stripes on posterior view (Figs 7, 11).

Female. Fig. 2. Measurements in Table 2. Similar to male. **Coloration** (Fig. 2): mandibular plates darkened; because the last segment of connexivum is shorter than

Table 2. Measurements (mm) of female specimens ($n = 2$) of *Panstrongylus noireau* sp. nov.

	Paratype female 1	Paratype female 2	Mean
Total length	21.8	21.1	21.45
Head length	3.6	3.5	3.55
Anteocular portion	2.0	1.9	1.95
Postocular portion	0.6	0.5	0.55
Head width across eyes	2.5	2.3	2.4
Interocular distance (synthlipsis)	1.3	1.3	1.3
Right eye: dorsal transverse width	0.5	0.5	0.5
Right eye: length on dorsal view	1.0	1.0	1.0
External distance between ocelli	1.4	1.4	1.4
Antennal segment I	0.8	0.7	0.75
Antennal segment II	2.5	2.4	2.45
Antennal segment III ($n = 0$)	Abs.	Abs.	–
Antennal segment IV ($n = 0$)	Abs.	Abs.	–
Labium segment II	0.9	1.0	0.95
Labium segment III	2.6	2.5	2.55
Labium segment IV	0.8	0.7	0.75
Pronotum total length	3.8	3.7	3.75
Pronotum fore lobe length	1.2	1.2	1.2
Pronotum hind lobe length	2.6	2.5	2.55
Pronotum maximum width	5.7	5.2	5.45
Scutellum length	2.0	1.9	1.95
Fore femur	3.9	3.6	3.75
Fore femur max. width	0.8	0.7	0.75
Fore tibia	3.8	3.6	3.7
Spongy fossa of fore tibia	Abs.	Abs.	–
Fore tarsus	1.5	1.5	1.5
Middle femur	3.9	3.8	3.85
Middle tibia	4.2	4.0	4.1
Spongy fossa of middle tibia	Abs.	Abs.	–
Middle tarsus	1.5	1.5	1.5
Hind femur	5.2	5.2	5.2
Hind tibia	6.5	6.5	6.5
Hind tarsus	1.5	1.6	1.55
Abdomen length	12.2	12.0	12.1
Abdomen max. width	7.1	7.0	7.05



Figures 7–11. *Panstrongylus noireau* sp. nov., male genitalia. **7** phallus, lateral view **8** articulary apparatus, dorsal phallothecal plate and struts, dorsal view **9** latero-apical portion of dorsal phallothecal plate (flap like prominence), ventral view **10** lateral process of endosoma, lateral view **11** median process of endosoma, posterior view. Abbreviations: **bpa** basal plate arm, **bpb** basal plate bridge, **dpp** dorsal phallothecal plate, **ep** elongate process, **flp** lateral flap like proeminence, **ip**, intermediate less sclerotized portion, **lp** lateral process of endosoma, **mb** median bridge, **pd** pedicel, **sp** subapical median process of endosoma, **st** struts. Scale bars: 0.5 mm (**7, 8**); 0.2 mm (**10**); 0.1 mm (**9, 11**).

in male, the subquadrate median blackish spot is almost centrally located, similarly to the similar same spots of the other segments. Genital segments darkened, with apical portion paler. **Structure:** ratio head/pronotum length: 1:1.06; antecular portion

length between 3–4 × the postocular region with respective ratio: 1: 0.26–0.30; ratio head length/width across eyes: 1:0.66–0.69; ratio width of an eye/interocular transverse distance (synthlipsis): 1:2.6; antennal segments ratio: 1:3.1–3.4 [segments III–IV absent in all female specimens]; labial segments ratio: 1:2.5–2.9:0.7–0.9; hind lobe of pronotum ~ 2 × as long as fore lobe. Fore femora 4.9–5.1 as long as wide; spongy fossae absent. **Female genitalia:** dorsal view: tergites VII, VIII, IX and X distinctly separated from each other; posterior margins of tergite VII and VIII somewhat concave and slightly curved at median portion, respectively; size of segment X ~ 1/3 that of the preceding segment (IX), both forming a set with subtrapezoidal shape. Ventral view: posterior margin of sternite VII curved backwards on median portion; gonocoxites VIII subtriangular, apical margins rounded; sternites IX barely visible; gonapophysis VIII short, apices rounded. Posterior view: gonocoxites VIII elongate, narrow, slightly wider at median portion; posterior margin of tergite IX well marked, clearly separating it from the following segment (X), these segments combined longer than wide and turned down, perpendicular to the plane of the body.

Distribution. Bolivia.

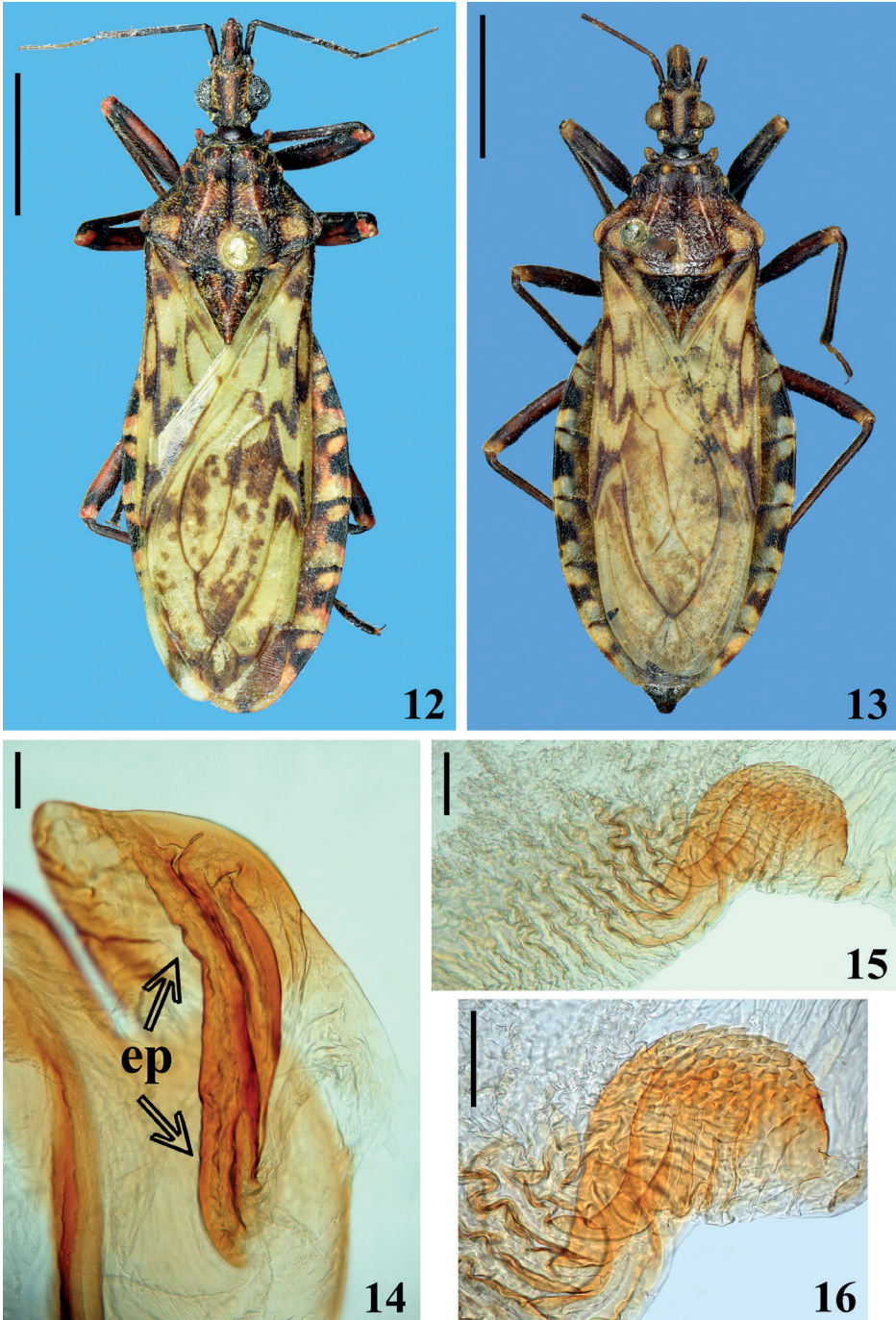
Etymology. The species is named in memory to Dr. François Noireau, a prolific researcher in ecology of Triatominae, who passed away in 2011.

Comments. With exception of the absence of spongy fossa in the female, which is recorded for most species of Triatominae, including *P. rufotuberculatus* (Lent and Wygodzinsky 1979), the subtle differences recorded here between males and females, if attributable to intraspecific or sexual variation, will only be known if (or when) more specimens are examined in the future.

Panstrongylus rufotuberculatus (Champion, 1899)

Figs 12–16

Material examined. *Panstrongylus rufotuberculatus* (Champion, 1899). COSTA RICA, 1 male, Puntarenas, Est. Queb. Bonita, Res. Biol. Carara, 50 m, L–N 194500, 469850, VI.1992, J. C. Saborio [*leg.*], / *Panstrongylus rufotuberculatus* (Champion), R. Carcavallo det., 1997 / Costa Rica INBIO, CR 1000 872011 [barcode] / 3751; PANAMA, 1 male, Barro Colorado, C. Z., 18.III.1936 / collected by Gertsch. Lutz, Wood / *Panstrongylus rufotuberculatus* (Champion, 1899), X-946, H. Lent det. / N° 733, HEMIPTERA, Inst. Oswaldo Cruz; VENEZUELA, 1 male, Cojedes, XI.[19]73, M [?] Irique / Coleção Rodolfo Carcavallo [Green label] / 3760; 1 male, Estado Falcón, municipio Colina, Lugar: Puerto Novo, VII.[19]57 / *Panstrongylus rufotuberculatus* (Champion, 1898), det. M. A. Soares / 3015; ECUADOR, 1 male, Guayaquil, Sta. [?] Liceia, 08.X... / *P. rufotubercul* [...] / Coleção Rodolfo Carcavallo [Green label] / 3749; PERU, 1 male, Cusco, Convención, 5.VIII.[19]70, Coll. F. carrasco / Vivienda / 3014; BOLIVIA, La Paz, 2 males, 4 females, Carrasco, 6/93 [VI.1993], *P. rufotuberculatus* Dom. / 3019 (1 male), 3020, 3026 (2 females); 1 female, Tojima, Licoma, 5/94 [V.1994] / 3025 (CTIOC).



Figures 12–16. *Panstrongylus rufotuberculatus* (Champion, 1899). **12, 13** habitus dorsal view **12** male from Costa Rica **13** female from Bolivia **14–16** male genitalia **14** latero-apical portion of dorsal phallosomal plate (flap like prominence), ventral view, **ep** elongate process **15, 16** lateral process of endosoma, lateral view **16** detail of the portion with denticulate processes. Scale bars: 0.5 mm (**12, 13**); 0.1 mm (**14–16**).

Remarks. Besides reviewing all previous description and thorough redescriptions of *P. rufotuberculatus* (Champion 1899; Lent and Pifano 1940; Lent and Jurberg 1975; Lent and Wygodzinsky 1979), 13 specimens of this species (eight males and five females from different countries) deposited at CTIOC were examined (e.g., Figs 12, 13). Selected measurements of specimens examined in this work are presented in Tables 3 and 4. Data on morphological variation observed to *P. rufotuberculatus* were summarized together with previous synthesis by Salomón et al. (1999) in Table 5. The female genitalia of *P. noireaui* sp. nov. was compared with the female genitalia of specimens of *P. rufotuberculatus* examined and also with the results recorded by Rodrigues et al. (2018) to the latter species, and no difference was found between them. Male genitalia of four males representing extremes of size (as selected by total length) and from different countries (18 mm, 21 mm, Venezuela; 24.5 mm, Panama; 25 mm, Costa Rica, respectively) were dissected in order to ascertain possible intraspecific variation. Although the general morphology of the male genitalia of *P. rufotuberculatus* seemed similar to its description by Lent and Jurberg (1975), three observations deserve to be recorded. Firstly, the presence of a pair of finely and densely denticulate lateral endosoma processes was confirmed (Figs 15, 16). Secondly, bigger males have more sclerotized structures, including, for example, the phallothecal plates. The most striking, indeed is the (subapical) median process of endosoma (“vesica” *sensu* auths.), which although with similar shape definitively was shown to be increasingly larger how much bigger is the male examined. Thirdly, it was verified that, in contrary to Lent and Jurberg (1975) and Lent and Wygodzinsky (1979) assumptions, there is no second or distal pair of endosoma processes. By comparing the figs 1, 203, and 209 of Lent and Jurberg (1975) with all genitalia dissected in this study, it becomes evident that what was interpreted by them as a second or distal pair of lateral endosoma processes are in

Table 3. Selected measurements (mm) of male specimens ($n = 8$) of *P. rufotuberculatus*.

	Maximum	Minimum	Mean	SD
Total length	25.0	18.0	22.7	2.33
Head length (excluding collum)	4.2	3.0	3.7	0.37
Anteocular portion length	2.3	1.6	1.9	0.2
Postocular portion length	0.9	0.5	0.6	0.13
Head width across eyes	2.9	2.2	2.7	0.23
Interocular (synthlipsis)	1.5	1.0	1.28	0.14
Right eye: transverse width	0.8	0.6	0.67	0.08
Antennal segment I	1.1	0.7	0.95	0.13
Antennal segment II ($n = 7$)	4.0	2.5	3.27	0.50
Antennal segment III ($n = 1$)	3.5	3.5	–	–
Antennal segment IV ($n = 1$)	2.5	2.5	–	–
Labium segment II	1.2	0.8	1.1	0.14
Labium segment III	2.7	1.9	2.4	0.27
Labium segment IV	0.9	0.7	0.78	0.09
Pronotum length	5.0	3.5	4.4	0.50
Pronotum maximum width	6.7	4.7	5.9	0.62
Fore femur length	4.9	3.8	4.28	0.4
Fore femur maximum width	1.0	0.7	0.88	0.09
Abdomen maximum width	9.0	5.7	7.73	1.18

Table 4. Selected measurements (mm) of female specimens ($n = 5$) of *P. rufotuberculatus*.

	Maximum	Minimum	Mean	SD
Total length	27.5	25.5	26.3	0.74
Head length (excluding collum)	4.2	4.0	4.14	0.08
Anteocular portion length	2.4	2.3	2.34	0.05
Postocular portion length	0.8	0.7	0.74	0.05
Head width across eyes	2.8	2.7	2.76	0.05
Interocular distance (synthlipsis)	1.6	1.5	1.54	0.05
Right eye: transverse width	0.6	0.6	0.6	0.0
Antennal segment I	1.0	0.9	0.92	0.04
Antennal segment II ($n = 4$)	3.5	3.3	3.4	0.08
Antennal segment III ($n = 0$)	–	–	–	–
Antennal segment IV ($n = 0$)	–	–	–	–
Labium segment II	1.2	1.1	1.18	0.04
Labium segment III	2.8	2.6	2.68	0.10
Labium segment IV	0.9	0.7	0.84	0.89
Pronotum length	5.2	4.4	4.82	0.28
Pronotum maximum width	7.0	6.2	6.6	0.3
Fore femur length	4.9	4.5	4.62	0.18
Fore femur maximum width	1.0	0.9	0.94	0.05
Abdomen maximum width	9.5	8.5	9.0	0.5

Table 5. Comparisons between specimens of *Panstrongylus rufotuberculatus* studied by Lent and Wygodzinsky (1979), Salomón et al. (1999) and present work. Modified from Salomón et al. (1999).

Character	Lent and Wygodzinsky	Salomón et al.	Present work*
Male length	24–27 mm	23.31 mm	18–25 (22.7) mm
Female length	25–28 mm	23.95 mm	25.5–27.5 (26.3) mm
Pronotum width	6–7 mm	6.06–6.11 mm	F: 6.2–7.0 (6.6) mm M: 4.7–6.7 (5.9) mm
Male abdomen width	8–9 mm	8.04 mm	5.0–9.0 (7.73) mm
Female abdomen width	9–10 mm	8.98 mm	8.5–9.5 (9.0) mm
Dorsal setae	Different shapes	Like Panama example (scalelike)	Not scalelike
Head length: width	1: 0.65–0.80	1: 0.73–0.74	F: 1:0.66–1:0.67 M: 1:0.67–1:0.80
Head: Pronotum length	1: 1.15–1.45	1: 1.14–1.23	F: 1:1.11–1:1.24 M: 1:1.11–1:1.31
Anteocular: postocular length	1: 0.25–0.35	1: 0.21–0.24	F: 1:0.29–1:0.35 M: 1:0.26–1:0.39
Apex of clypeus	Uni or bilobed	Unilobed	Bilobed (3 M) Unilobed (5 F / 5 M)
Eye width: synthlipsis	1: 1.30–1.85 1:2.3–3.3*	1: 1.88–1.94	F: 1:2.50–1:2.67 M: 1:1.62–1:2.67
Antennal first segment	Slightly surpassing apex of clypeus (SC)	Not surpassing apex of clypeus (NSC)	NSC: 5 F / 6 M SA: 2 M
Antennal segments	1: 3.0–3.5; 2.2–2.8; 1.9–2.3	1: 2.8–3.1; 2.3–2.4; 1.9–2.0	F: 1:3.5–3.7; --: M: 1:3.2–3.6; 2.9–3.2; 2.2–2.3
Labium segments	1: 1.9–2.2; 0.6–0.7	1: 2.4; 0.8	F: 1:2.3–2.5; 0.6–0.7 M: 1:2.0–2.5; 0.6–0.9
Pronotum color	Dark brown to black	Black	Dark brown: 3 F / 4 M Black: 2 F / 4 M
Humeral angle	Narrowly rounded (NR) to subangular	Subangular (SA)	NR: 4 M SA: 5 F / 4 M
Scutellum posterior process	Apically (AR) or entirely red	Entirely red (ER)	AR: 1 M ER: 5 F / 7 M
Scutellum central carinae	Red or black	Black	Red: 3 M Black: 5 F / 5 M
Scutellum apex	Rounded, suboval or subglobose	Suboval	Rounded: 5 F / 6 M Suboval: 2 M
Fore femora width: length	1: 3.8–4.7	1: 3.8–4.0	F: 1:4.5–5.4 M: 1:4.2–5.2
Connexivum pattern: median spot	Connected or not along outer margin	Not connected	Not connected: 5 F / 6 M Connected: 2M [§]

* data obtained from 13 specimens (see material examined): 05 females (F), 08 males (M); values between parenthesis: median value. α: specimens from Cuzco, Peru; β: connected only on anterior portion of outer margin of segments II–V (one male) or III–IV (one male).

fact the pair of lateral flap-like prominences (flp) of the dorsal phallothecal plate (dpp), including a moderately elongate process (ep) which is present on the ventral portion of these lateral flap like prominences (Fig. 14). It is noteworthy that between these flap-like process and the main portion of phallothecal plate there is an intermediate portion which is much less sclerotized and is prone to be easily broken or fractured in the dissecting process. In this latter case, an artifact can be created, and the observer will possibly misinterpret this flap like portion of phallothecal plate as an independent structure, what it is not. On the other hand, the ventral elongate process is clearly connected to the ventral portion of the dorsal phallothecal plate and is not a part of the endosoma, nor a process of it (Fig. 14).

Table 6. Comparisons between specimens of *P. rufotuberculatus* (Lent and Wygodzinsky 1979, Salomón et al. 1999, and present work) and *P. noireai* sp. nov. Modified from Salomón et al. (1999).

Character	<i>P. rufotuberculatus</i>	<i>P. noireai</i> sp. nov.*
Male length	18–27 mm	19.6–20.7 (20.04) mm
Female length	23.95–28 mm	21.1–21.8 (21.45) mm
Pronotum width	4.7–7.0 mm	F: 5.2–5.7 (5.45) mm M: 5.0–5.5 (5.17) mm
Male abdomen width	5.0–9.0 mm	6.0–7.1 (6.47) mm
Female abdomen width	8.5–10 mm	7.0–7.1 (7.05) mm
Dorsal setae	Simple or scalelike	Simple (Fig. 3)
Head length: width	1: 0.65–0.80	F: 1:0.66–1:0.69 M: 1:0.67–1:0.75
Head: Pronotum length	1: 1.11–1.45	F: 1:1.06 M: 1:1.08–1:1.09
Anteocular: postocular length	1: 0.21–0.39	F: 1:0.26–1:0.30 M: 1:0.28–1:0.30
Apex of clypeus	Uni or bilobed	Unilobed
Eye width: synthlipsis	1: 1.3–3.3	F: 1:2.6 M: 1:1.84–1:2.4
Antennal first segment	Not or slightly surpassing apex of clypeus	Not surpassing apex of clypeus
Antennal segments	1: 2.8–3.7:2.2–3.2:1.9–2.3	F: 1:3.1–3.4 M: 1:2.87–3.3:2.5
Labium segments	1: 1.9–2.5:0.6–0.9	F: 1:2.5–2.9:0.7–0.9 M: 1:2.3–2.7:0.7–0.8
Pronotum color	Dark brown to black	Black
Humeral angle	Narrowly rounded to subangular	Subangular
Scutellum posterior process	Apically or entirely red	Entirely red
Scutellum central carinae	Red or black	Black
Scutellum apex	Rounded, suboval or subglobose	Rounded
Fore femora width: length	1: 3.8–5.4	F: 1:4.9–5.1 M: 1:4.7–5.0
Connexivum pattern: median spot	Connected or not along outer margin	Not connected

*data obtained on 05 type specimens (see material examined): 02 females (F), 03 males (M); values between parenthesis: median value.

Table 7. Comparisons between cytogenetic and molecular characteristics between *P. rufotuberculatus* and *P. noireai* sp. nov. (data from Pita et al. 2021).

Character	<i>P. rufotuberculatus</i>	<i>P. noireai</i> sp. nov.
Diploid chromosome number (2n)	F: 24 chromosomes M: 23 chromosomes	F: 22 chromosomes M: 22 chromosomes
Sex chromosome system	F: X ₁ X ₂ X ₃ X ₄ M: X ₁ X ₂ Y	F: XX M: XY
Chromosome location of 45S ribosomal DNA clusters	One autosomal pair	Both sex chromosomes (X and Y)
Pairwise genetic distance of cyt b sequences among <i>P. rufotuberculatus</i> * and <i>P. noireai</i> sp. nov.		K2p: 10.7–18.7%
Pairwise genetic distance of col sequences among <i>P. rufotuberculatus</i> * and <i>P. noireai</i> sp. nov.		K2p: 10.6–15.8%

*specimens from different localities

Discussion

It is noteworthy that *P. rufotuberculatus* has been considered the only species of *Panstrongylus* to have two paired [lateral] endosoma process (Lent and Jurberg 1975; Lent and Wygodzinsky 1979; Jurberg et al. 2001; Papa et al. 2003; Bérenger and Blanchet 2005; Ayala, pers. comm., 2014). However, as recorded here, the second alleged paired endosoma process described by Lent and Jurberg (1975) was in fact a misinterpretation of the flap like prominence of the dorsal phallothecal plate as well as a moderately elongate ventral process of it. A similar structure was observed in *P. noireaui* sp. nov. Therefore, as in all species of *Panstrongylus* the processes of endosoma have shown to possess only a paired lateral process, it seems that this is a constant feature in this genus. Thus, the consideration of two paired endosoma process as an apomorphy of *P. rufotuberculatus* as proposed by Lent and Wygodzinsky (1979) is not sustainable when confronted with the evidence obtained here. On the other hand, two other apomorphies attributed to *P. rufotuberculatus* by these authors, i.e. presence of body scalelike setae and an apically bilobed clypeus, would need to be confirmed in future more extensive works, given they have been shown not only to be variable but commonly absent (Lent and Wygodzinsky 1979; Salomón et al. 1999; present work).

Because the dissection of the male genitalia is usually carried out on only one specimen of each species (Lent and Jurberg 1985), the variability of these structures may remain unrecorded. Among predatory Reduviidae (Gil-Santana et al. 2013) and particularly Triatominae (Lent and Jurberg 1985; Pires et al. 1998) qualitative differences in some phallic structures of male genitalia have been recorded when more than a male specimen of the same species had its genitalia dissected (e.g., Costa et al. 1997). Therefore, despite not being the main objective of this work, four males of *P. rufotuberculatus* with diverse dimensions and from different localities as well as two males of *P. noireaui* sp. nov. (out of three) were dissected in order to perform a preliminary evaluation of a possible male genitalia variability. While the male genitalia structures of *P. noireaui* sp. nov. were shown to be very similar, in *P. rufotuberculatus* the median process of endosoma (“vesica” *sensu* auths.) was shown to be increasingly larger how much bigger was the male examined. It was strikingly diverse from many previous observations (Lent and Jurberg 1985; Pires et al. 1998; Gil-Santana et al. 2013), which have recorded variations in shape or number of phallic structures but not in their size. Costa et al. (1997), although have recorded that the “vesica” of *Triatoma brasiliensis* Neiva, 1911 was variable in size, did not provide any additional information about other characteristics of the males examined by them possibly related to this variable, such as variation of their body size. The variation in size of the median process of endosoma also contradicts the current evidence to insects in general, which suggests that the allometric slopes of genitalia are lower than those of other body parts, giving rise to the “one size fits all” hypothesis (Eberhard et al. 1998; Schulte-Hostedde and Alarie 2006). Therefore, future studies, possibly including morphometry and dissection

of more specimens of *P. rufotuberculatus* and other triatomine species, should be carried out to clarify the preliminary observations recorded here.

When considering all the morphological and chromatic variation recorded to *P. rufotuberculatus* (Lent and Wygodzinsky 1979; Salomón et al. 1999; Hiwat 2014; this work) (Table 5), almost all features of *P. noireai* sp. nov. lie within part of all variation observed to the former species (Table 6). Yet, while measurements of males of *P. noireai* sp. nov. are comparable to those of smaller males of *P. rufotuberculatus*, females of the new species have been shown to be distinctly smaller (Table 6). However, until more specimens can be examined in order to confirm (or not) possible differences and/or reach a minimal number to allow statistical inference of data, these differences will not be considered to separate these species from each other.

Besides the difference between the ventral process of flap like prominence of phallosomal plate (Figs 9, 14), the smooth lateral endosoma process of *P. noireai* sp. nov. (Fig. 10) in comparison with the finely and densely denticulate lateral endosoma process of *P. rufotuberculatus* (Figs 15, 16) is an objective and reliable morphological feature to separate these species. It is noteworthy that analogous taxonomic situations occur among other species of Triatomini as follows. *Triatoma maculata* (Erichson, 1848) and *T. pseudomaculata* Corrêa & Spínola, 1964 are extremely similar and cannot be easily distinguished from each other based on external characters alone; only the striking structural differences of the endosomal processes of the phallus [lacking apical teeth, with ribbon-shape sclerotizations in *T. maculata* and delicately striate and denticulate in *T. pseudomaculata*] allow secure identification (Lent and Wygodzinsky 1979). Similarly, *Triatoma arthurneivai* Lent & Martins, 1940 and *T. wygodzinskyi* Lent, 1951 are very similar chromatically and in their external morphology, with minor color differences, which may be subject of slight variation. However, the structure of endosoma processes (with ~ 100 teeth in the first species and ~ 20 in the latter) is sufficient to differentiate these species (Lent and Wygodzinsky 1979).

Thereby, although *P. noireai* sp. nov. has proved to be morphologically very similar to *P. rufotuberculatus*, the differences observed in male genitalia are analogous to other cases of close morphological species included in Triatomini as referred just above. Therefore, their separation based in differences of the male genitalia, even if considered by themselves alone, would have good grounds in the taxonomy of Triatominae. At the genetic level, *P. noireai* sp. nov. presents very different chromosomal and molecular characteristics compared to the other *Panstrongylus* species studied so far (Pita et al. 2021) (Table 7). Out of the eight *Panstrongylus* species cytogenetically described, *P. noireai* sp. nov. is the only one that has a simple sex male mechanism (XY), while the other *Panstrongylus* have multiple sex chromosomes (X_1X_2Y or $X_1X_2X_3Y$) (Panzera et al. 2021). In addition, the chromosomal location of the 45S ribosomal DNA clusters is distinctive character of this new species. In *P. rufotuberculatus*, like all *Panstrongylus* species analyzed hitherto, the rDNA clusters are localized on an autosomal pair, while in *P. noireai* sp. nov. are localized in both sex chromosomes (X and Y). Both chromosomal

markers (sex chromosome system and location of ribosomal clusters) are species-specific characters, being their variation within the same species an exceptional event (Pita et al. 2021, 2022). Moreover, mitochondrial DNA markers showed a remarkable genetic diversity between this new species with all others *Panstrongylus* species, higher than the expected for conspecific populations (Pita et al. 2021). Sequence analyses of *cyt b* and *coI* fragments revealed high nucleotide divergence between *P. noireau* sp. nov. with *P. rufotuberculatus* samples from Colombia, Ecuador, and Mexico, showing Kimura 2-parameter distances higher than 10% (10.7–18.7% for *cyt b* and 10.6–15.8% for *coI*) (Pita et al. 2021). Therefore, the morphological evidence presented here is in agreement with previously published genetic data, which reveals that *P. noireau* sp. nov. represents a new species of *Panstrongylus*, morphological and evolutionarily very close to *P. rufotuberculatus*.

Key to the species of *Panstrongylus*, based on Lent and Wygodzinsky (1979), Bérenger and Blanchet (2007), Ayala (2009), and Ayala et al. (2014)

- 1 Process of scutellum elongate, subcylindrical narrowly tapering apically.....2
- Process of scutellum short, rounded, conical or truncate apically 12
- 2 Specimens almost completely black; small red spot on posterolateral angle of connexivum segments and, in some cases, reddish markings on hind lobe of pronotum *chinai* (Del Ponte, 1929)
- Specimens differently colored..... 3
- 3 Abdomen light colored ventrally, generally with longitudinal series of black spots at least laterally..... 4
- Abdomen differently colored, without series of black spots 7
- 4 Femora without markings 5
- Femora with median black annuli or with reddish apex 6
- 5 Integument of postocular lateral portion of head smooth; fore lobe of pronotum without distinct black markings; dorsal connexival segments light colored or with small darkened spots *lenti* Galvão & Palma, 1968
- Integument of postocular lateral portion of head rugous; fore lobe of pronotum with a large mid and smaller lateral darkened markings; connexivum with large dark markings on anterior portion of each segment *martinezorum* Ayala, 2009
- 6 Pronotum with humeral angles flattened; femora light brown with a median black annuli *mitarakaensis* Bérenger & Blanchet, 2007
- Pronotum with humeral angles rounded; femora black with apex reddish..... *geniculatus* (Latreille, 1811)
- 7 Labial segment III [second visible] as long as or shorter than segment II..... *tupynambai* Lent, 1942
- Labial segment III longer than segment II..... 8
- 8 Corium yellow except at base and subapically, contrasting with dark gray membrane; interocular distance (synthlipsis) much less than twice as large as

- width of an eye in dorsal view; femora with slight subapical protuberances...
 *howardi* (Neiva, 1911)
- Corium as dark as membrane, with base and apex light colored; synthlipsis twice or more than twice as large as width of an eye in dorsal view; fore and mid femora with several conspicuous denticles..... **9**
- 9 Fore lobe of pronotum with distinct discal tubercles **10**
- Fore lobe of pronotum with only obsolete or without distinct discal tubercles..... **11**
- 10 Antecular region of head 2.5 × as long as postocular region; general color brownish black with small light markings
 *sherlocki* Jurberg, Carcavallo & Lent, 2001
- Antecular region of head twice as long as postocular region; general color yellowish brown with dark brown markings, particularly on pronotum, corium of hemelytra and connexivum *lutzi* (Neiva & Pinto, 1923)
- 11 Anterolateral processes of pronotum very short, blunt; upper surface of head straight, in lateral view; fore and mid femora with 2–3 denticles; lateral borders of pronotum lobes forming an almost continuous line.....
 *diasi* Pinto & Lent, 1946
- Anterolateral processes of pronotum elongate, salient; upper surface of head convex, in lateral view; fore and mid femora with more than three denticles; lateral borders of pronotum lobes forming a distinct angle.....
 *guentheri* Berg, 1879
- 12 Mandibular plates (juga, auths.) blunt; connexival segments with central dark spot as well as with narrow transverse dark band anteriorly (Figs 1, 2); body integument with numerous golden adpressed setae, mainly dorsally; hemelytra pale greenish (Figs 1, 2) **13**
- Mandibular plates with curved hooklike projection; connexival segments with large anterior dark spot; body integument almost entirely glabrous dorsally; general color of hemelytra not greenish **14**
- 13 Lateral paired process of endosoma of male genitalia with fine and numerous teeth apically (Figs 15, 16) *rufotuberculatus* (Champion, 1899)
- Lateral paired process of endosoma of male genitalia smooth apically, without teeth (Fig. 10) *noireai* sp. nov.
- 14 General color black, with reddish or light reddish brown markings, including four on hind lobe of pronotum; third antennal segment shorter than the second *megistus* (Burmeister, 1835)
- General color yellowish to yellowish brown with dark markings, including one median and two pairs of longitudinal dark markings on hind lobe of pronotum; third antennal segment as long as the second **15**
- 15 Scutellum yellowish with a black median longitudinal stripe; fore lobe of pronotum without sublateral tubercles..... *humeralis* (Usinger, 1939)
- Scutellum black with a yellow median longitudinal stripe; fore lobe of pronotum with sublateral tubercles *lignarius* (Walker, 1873)

Acknowledgements

We thank José Manuel Ayala L. who kindly reexamined the male genitalia of *Panstrongylus martinezorum* by the request of first author (HRG-S) and provided crucial information about the endosoma processes of this species. We are also grateful to an anonymous reviewer, Jane Costa, Jean-Michel Bérenger, and Jader de Oliveira, for their valuable comments and suggestions.

References

- Abad-Franch F, Paucar CA, Carpio CC, Cuba Cuba CA, Aguilar VHM, Miles MA (2001) Biogeography of Triatominae (Hemiptera: Reduviidae) in Ecuador: implications for the design of control strategies. *Memórias do Instituto Oswaldo Cruz* 96(5): 611–620. <https://doi.org/10.1590/S0074-02762001000500004>
- Arias AR, Monroy C, Guhl F, Sosa-Estani S, Santos WS, Abad-Franch F (2021) Chagas disease control-surveillance in the Americas: The multinational initiatives and the practical impossibility of interrupting vector-borne *Trypanosoma cruzi* transmission. *Memórias do Instituto Oswaldo Cruz* 116: e210130.
- Ayala LJM (2009) Una nueva especie de *Panstrongylus* Berg de Venezuela (Hemiptera: Reduviidae, Triatominae). *Entomotrópica* 24: 105–109.
- Ayala LJM, Mattei R, Mattei R (2014) Descripción de la hembra de *Panstrongylus martinezorum* Ayala, 2009 (Hemiptera, Reduviidae, Triatominae) con comentarios sobre la distribución geográfica de la especie en el Estado Amazonas, Venezuela. *Boletín de la SEA* 54: 383–389. <http://sea-entomologia.org/PDF/Boletin54/383389BSEA54HembraPmartinezorumVenezuela.pdf>
- Bérenger J-M, Blanchet D (2007) A new species of the genus *Panstrongylus* from French Guiana (Heteroptera; Reduviidae; Triatominae). *Memórias do Instituto Oswaldo Cruz* 102(6): 733–736. <https://doi.org/10.1590/S0074-02762007000600012>
- Bérenger J-M, Pluot-Sigwalt D, Pagès F, Blanchet D, Aznar C (2009) The Triatominae species of French Guiana (Heteroptera: Reduviidae). *Memórias do Instituto Oswaldo Cruz* 104(8): 1111–1116. <https://doi.org/10.1590/S0074-02762009000800007>
- Berg C (1879) Hemiptera Argentina enumerativ speciesque novas descripsit. Pauli E. Coni, Hamburg, 316 pp. <https://doi.org/10.5962/bhl.title.36493>
- Champion GC (1899) Insecta Rhynchota. Hemiptera-Heteroptera, Fam. Reduviidae, Subfam. Acanthaspidinae. Vol II. In: Godman FD, Salvin O (Eds) *Biologia Centrali Americana*. Taylor and Francis, London, 190–211. [pls. XI–XII] [xvi + 416 pp, 22 pls]
- Costa J, Barth OM, Marchon-Silva V, Almeida CE, Freitas-Sibajev MGR, Panzera F (1997) Morphological Studies on the *Triatoma brasiliensis* Neiva, 1911 (Hemiptera, Reduviidae, Triatominae) Genital Structures and Eggs of Different Chromatic Forms. *Memórias do Instituto Oswaldo Cruz* 92(4): 493–498. <https://doi.org/10.1590/S0074-02761997000400009>
- Costa J, Dale C, Galvão C, Almeida CE, Dujardin JP (2021) Do the new triatomine species pose new challenges or strategies for monitoring Chagas disease? An overview from 1979–

2021. Memórias do Instituto Oswaldo Cruz 116: e210015. <https://doi.org/10.1590/0074-02760210015>
- Dale C, Justi AS, Galvão C (2021) *Belminus santosmalletae* (Hemiptera: Heteroptera: Reduviidae): new Species from Panama, with an updated key for *Belminus* Stål, 1859 species. *Insects* 12(8): e686. <https://doi.org/10.3390/insects12080686>
- Eberhard WG, Huber BA, Rodriguez RL, Briceño RD, Salas I, Rodriguez V (1998) One size fits all? Relationships between the size and degree of variation in genitalia and other body parts in twenty species of insects and spiders. *Evolution; International Journal of Organic Evolution* 52(2): 415–431. <https://doi.org/10.1111/j.1558-5646.1998.tb01642.x>
- Forero D, Weirauch C (2012) Comparative genitalic morphology in the New World resin bugs Apiomerini (Hemiptera, Heteroptera, Reduviidae, Harpactorinae). *Deutsche Zeitschrift Entomologische* 59: 5–41.
- Galvão C (2021) Taxonomy. In: Guarneri A, Lorenzo M (Eds) *Triatominae – The Biology of Chagas Disease Vectors*, *Entomology in Focus* 5. Springer, Cham, 15–38. https://doi.org/10.1007/978-3-030-64548-9_2
- Galvão C, Carcavallo RU, Rocha DS, Jurberg J (2003) A checklist of the current valid species of the subfamily Triatominae Jeannel, 1919 (Hemiptera, Reduviidae) and their geographical distribution, with nomenclatural and taxonomic notes. *Zootaxa* 202(1): 1–36. <https://doi.org/10.11646/zootaxa.202.1.1>
- Gil-Santana HR, Davranoglou L-R, Neves JA (2013) A new synonym of *Graptocleptes bicolor* (Burmeister), with taxonomical notes (Hemiptera: Heteroptera: Reduviidae: Harpactorini). *Zootaxa* 3700: 348–360. <https://doi.org/10.11646/zootaxa.3700.3.2>
- Goñalves D, Noireau F (2010) Geographic distribution of Triatominae vectors in America. In: Telleria J, Tibayrenc M (Eds) *American Trypanosomiasis – Chagas disease, one hundred years of research*. Elsevier, London, Burlington, 209–231. <https://doi.org/10.1016/B978-0-12-384876-5.00009-5>
- Hiwat H (2014) Triatominae species of Suriname (Heteroptera: Reduviidae) and their role as vectors of Chagas disease. *Memórias do Instituto Oswaldo Cruz* 109(4): 452–458. <https://doi.org/10.1590/0074-0276130408>
- Hypša V, Tietz D, Zrzavý J, Rego RO, Galvão C, Jurberg J (2002) Phylogeny and Biogeography of Triatominae (Hemiptera, Reduviidae): A molecular evidence of New World origin of the Asiatic clade. *Molecular Phylogenetics and Evolution* 23(3): 447–457. [https://doi.org/10.1016/S1055-7903\(02\)00023-4](https://doi.org/10.1016/S1055-7903(02)00023-4)
- Jurberg J, Carcavallo RU, Lent H (2001) *Panstrongylus sherlocki* sp. n. do estado da Bahia (Hemiptera, Reduviidae, Triatominae). *Entomología y Vectores* 8: 261–274.
- Justi SA, Russo CM, Mallet JRS, Obara MT, Galvão C (2014) Molecular phylogeny of Triatomini (Hemiptera: Reduviidae: Triatominae). *Parasites & Vectors* 7(1): e149. <https://doi.org/10.1186/1756-3305-7-149>
- Kieran TJ, Gordon ERL, Zaldívar-Riverón A, Ibarra-Cerdeña C, Glenn TC, Weirauch C (2021) Ultraconserved elements reconstruct the evolution of Chagas disease-vectoring kissing bugs (Reduviidae: Triatominae). *Systematic Entomology* 46(3): 725–740. <https://doi.org/10.1111/syen.12485>

- Kirkaldy GW (1904) Bibliographical and nomenclatorial notes on the Hemiptera.-No. 3. The Entomologist 37: 279–283. <https://doi.org/10.5962/bhl.part.2885>
- Lent H, Jurberg J (1975) O gênero *Panstrongylus* Berg, 1879, com um estudo sobre a genitália externa das espécies (Hemiptera, Reduviidae, Triatominae). Revista Brasileira de Biologia 35: 379–438.
- Lent H, Jurberg J (1985) Sobre a variação intra-específica em *Triatoma dimidiata* (Latreille) e *Triatoma infestans* (Klug) (Hemiptera, Reduviidae). Memórias do Instituto Oswaldo Cruz 80(3): 285–299. <https://doi.org/10.1590/S0074-02761985000300004>
- Lent H, Pifano F (1940) Sobre a identidade dos generos *Panstrongylus* Berg, 1879 e *Mestor* Kirkaldy, 1904. Redescricao de *Panstrongylus rufotuberculatus* encontrado, na Venezuela, naturalmente infestado pelo *Schizotrypanum cruzi*. Revista de Entomologia 11(3): 629–639.
- Lent H, Wygodzinsky P (1979) Revision of the Triatominae (Hemiptera: Reduviidae) and their significance as vectors of Chagas' disease. Bulletin of the American Museum of Natural History 163: 123–520. <http://hdl.handle.net/2246/1282>
- Marcilla A, Bargues MD, Abad-Franch F, Panzera F, Carcavallo CU, Noireau F, Galvão C, Jurberg J, Miles MA, Dujardin JP, Mas-Coma S (2002) Nuclear rDNA ITS-2 sequences reveal polyphyly of *Panstrongylus* species (Hemiptera: Reduviidae: Triatominae), vectors of *Trypanosoma cruzi*. Infection, Genetics and Evolution 1(3): 225–235. [https://doi.org/10.1016/S1567-1348\(02\)00029-1](https://doi.org/10.1016/S1567-1348(02)00029-1)
- Marín E, Santillán R, Cuba C, Jurberg J, Galvão C (2007) Hallazgo de *Panstrongylus rufotuberculatus* (Champion, 1899) (Hemiptera, Reduviidae, Triatominae) em ambiente domiciliario en la Región Piura, Perú. Intra-domiciliary capture of *Panstrongylus rufotuberculatus* (Champion, 1899) (Hemiptera, Reduviidae, Triatominae) in Piura, Peru. Cadernos de Saude Publica 23(9): 2235–2238. <https://doi.org/10.1590/S0102-311X2007000900031>
- Monteiro FA, Weirauch C, Felix M, Lazoski C, Abad-Franch F (2018) Evolution, systematics, and biogeography of the Triatominae, Vectors of Chagas Disease. Advances in Parasitology 99: 265–344. <https://doi.org/10.1016/bs.apar.2017.12.002>
- Paiva VF, Belintani T, Oliveira J, Galvão C, Rosa JA (2022) A review of the taxonomy and biology of Triatominae subspecies (Hemiptera: Reduviidae). Parasitology Research 121(2): 499–512. <https://doi.org/10.1007/s00436-021-07414-2>
- Panzera F, Pita S, Lorite P (2021) Chromosome structure and evolution of Triatominae: a review. In: Guarneri A, Lorenzo M (Eds) Triatominae – The Biology of Chagas Disease Vectors, Entomology in Focus 5. Springer, Cham, 65–99. https://doi.org/10.1007/978-3-030-64548-9_2
- Papa AR, Barata JMS, Obara MT, Ceretti Jr W, Jurberg J (2003) Descrição da genitália externa do alótipo macho *Panstrongylus lenti* Galvão & Palma, 1968 (Hemiptera, Reduviidae, Triatominae). Entomología y Vectores 10: 345–352.
- Patterson JS, Barbosa SE, Dora Feliciangeli M (2009) On the genus *Panstrongylus* Berg 1879: Evolution, ecology and epidemiological significance. Acta Tropica 110(2–3): 187–199. <https://doi.org/10.1016/j.actatropica.2008.09.008>
- Pinto C (1931) Valor do rosto e antenas da caracterização dos generos de Triatomídeos. Hemiptera. Reduviídeoidea. Boletín Biológico 19: 45–136.

- Pires HHR, Barbosa SE, Margonari C, Jurberg J, Diotaiuti L (1998) Variations of the external male genitalia in three populations of *Triatoma infestans* Klug, 1834. *Memórias do Instituto Oswaldo Cruz* 93(4): 479–483. <https://doi.org/10.1590/S0074-02761998000400011>
- Pita S, Gómez-Palacio A, Lorite P, Dujardin JP, Chavez T, Villacís AG, Galvão C, Panzera Y, Calleros L, Pereyra-Mello S, Burgueño-Rodríguez G, Panzera F (2021) Multidisciplinary approach detects speciation within the kissing bug *Panstrongylus rufotuberculatus* populations (Hemiptera, Heteroptera, Reduviidae). *Memórias do Instituto Oswaldo Cruz* 116: e210259. <https://doi.org/10.1590/0074-02760210259>
- Pita S, Lorite P, Cuadrado A, Panzera Y, de Oliveira J, Alevi KCCC, Rosa JA, Freitas SPC, Gómez-Palacio A, Solari A, Monroy C, Dorn PL, Cabrera-Bravo M, Panzera F (2022) High chromosomal mobility of rDNA clusters in holocentric chromosomes of Triatominae, vectors of Chagas disease (Hemiptera-Reduviidae). *Medical and Veterinary Entomology* 36(1): 66–80. <https://doi.org/10.1111/mve.12552>
- Rédei D, Tsai J-F (2011) The assassin bug subfamilies Centrocnemidinae and Holoptilinae in Taiwan (Hemiptera: Heteroptera: Reduviidae). *Acta Entomologica Musei Nationalis Pragae* 51: 411–442.
- Rodrigues JMS, Rosa JA, Moreira FFF, Galvão C (2018) Morphology of the terminal abdominal segments in females of Triatominae (Insecta: Hemiptera: Reduviidae). *Acta Tropica* 185: 86–97. <https://doi.org/10.1016/j.actatropica.2018.04.021>
- Salomón OD, Ripoll CM, Rivetti E, Carcavallo RU (1999) Presence of *Panstrongylus rufotuberculatus* (Champion, 1899) (Hemiptera: Reduviidae; Triatominae) in Argentina. *Memórias do Instituto Oswaldo Cruz* 94(3): 285–288. <https://doi.org/10.1590/S0074-02761999000300002>
- Schofield CJ, Galvão C (2009) Classification, evolution, and species groups within Triatominae. *Acta Tropica* 110(2–3): 88–100. <https://doi.org/10.1016/j.actatropica.2009.01.010>
- Schuh RT, Weirauch C (2020) True bugs of the world (Hemiptera: Heteroptera). Classification and natural history. 2nd edn. Siri Scientific Press, Manchester, 767 pp. [32 pls]
- Schuh RT, Weirauch C, Wheeler WC (2009) Phylogenetic relationships within the Cimicomorpha (Hemiptera: Heteroptera): a total-evidence analysis. *Systematic Entomology* 34(1): 15–48. <https://doi.org/10.1111/j.1365-3113.2008.00436.x>
- Schulte-Hostedde A, Alarie Y (2006) Morphological patterns of sexual selection in the diving beetle *Graphoderus liberus*. *Evolutionary Ecology Research* 8: 891–901.
- Usinger RL (1939) Descriptions of new Triatominae with a key to genera (Hemiptera, Reduviidae). *University of California Publications in Entomology* 7: 33–56.
- Usinger RL (1944) The Triatominae of North and Central America and the West Indies and their Public Health significance. *Public Health Bulletin* 288: 1–83.
- Weirauch C (2008) From four- to three- segmented labium in Reduviidae (Hemiptera: Heteroptera). *Acta Entomologica Musei Nationalis Pragae* 48: 331–344.
- Wolff M, Castillo D, Uribe J, Arboleda JJ (2001) Tripanosomiasis americana: Determinación de riesgo epidemiológico de transmisión en el municipio de Amalfi, Antioquia. *Iatreia* 14: 111–121.

